WELDING Journal

November 2006

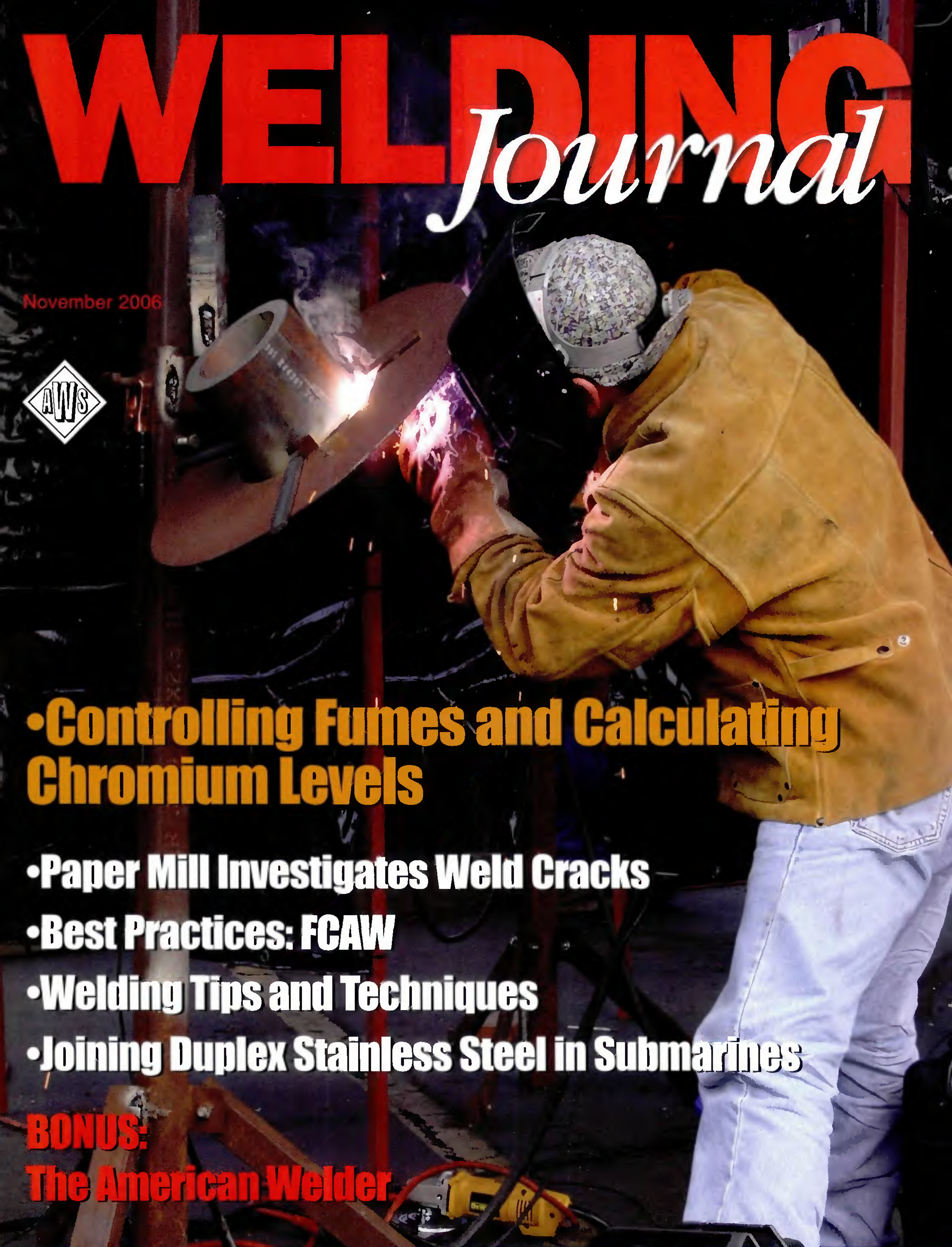

•Controlling Fumes and Calculating Chromium Levels

•Paper Mill Investigates Weld Cracks

•Best Practices: FCAW

•Welding Tips and Techniques

•Joining Duplex Stainless Steel in Submarines

BONUS: The American Welder

PUBLISHED BY THE AMERICAN WELDING SOCIETY TO ADVANCE THE SCIENCE, TECHNOLOGY AND APPLICATION OF WELDING AND ALLIED PROCESSES, INCLUDING JOINING, BRAZING, SOLDERING, CUTTING, AND THERMAL SPRAYING

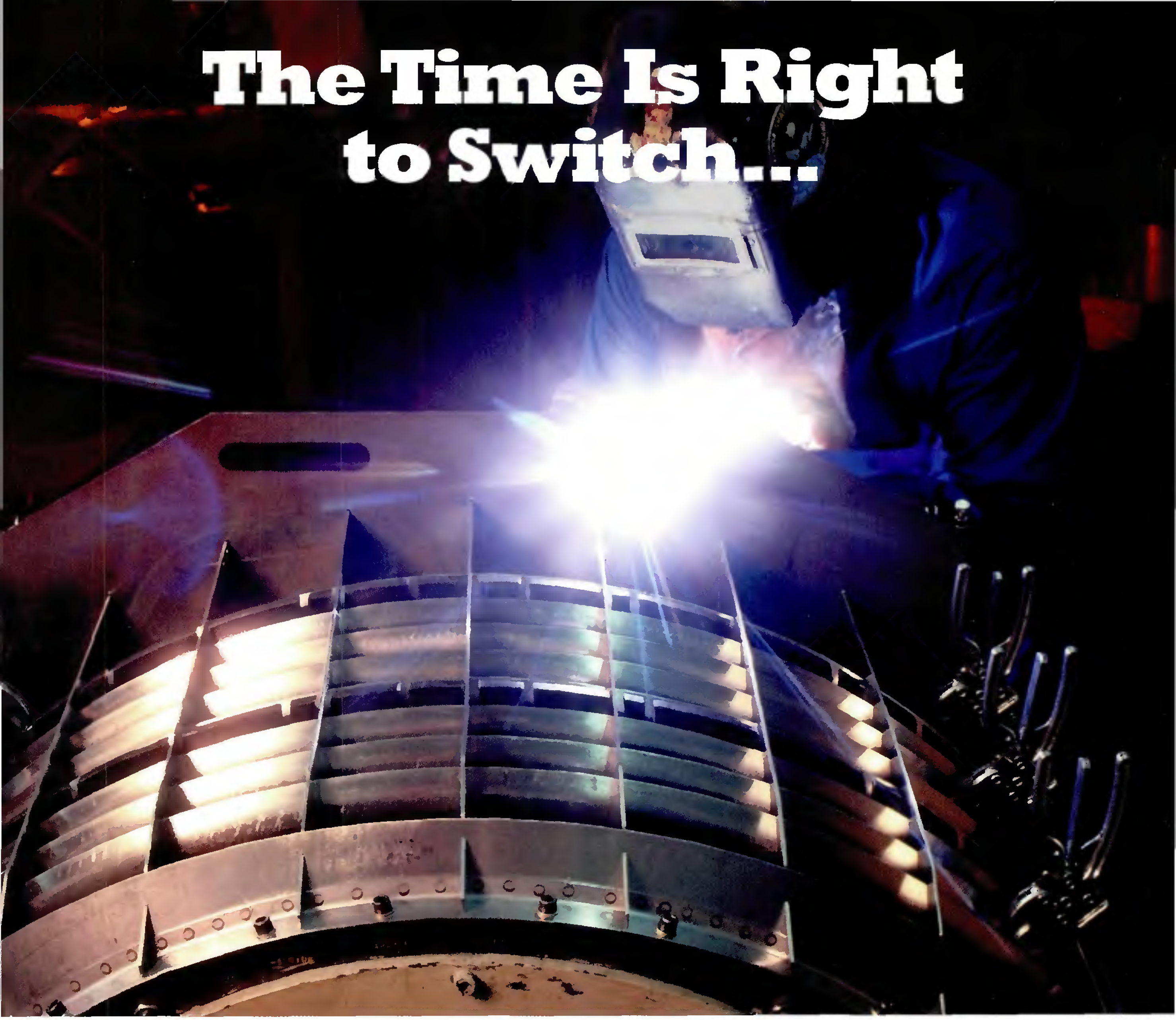

to Select-Arc Metal-Cored Electrodes

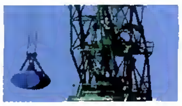

Rising solid wire prices have made specifying Select-Arc's higher productivity metal-cored electrodes an even smarter choice.

Select-Arc metal-cored electrodes have earned their outstanding reputation by delivering an exceptional combination—the efficiencies of solid wire and the high productivity of flux cored. Additional significant benefits include:

- Virtually no spatter emission means reduced cleanup costs
- Very smooth spray transfer
- Low fume generation
- Superb bead geometry
- Faster travel speed for greater productivity

Discover for yourself the many reasons to switch from solid wire to Select-Arc's premium line of metal-cored electrodes. Call us today at 1-800-341-5215.

SELECT ARC INC.®

600 Enterprise Drive
P.O. Box 259
Fort Loramie, OH 45845-0259
Phone: (937) 295-5215
Fax: (937) 295-5217
www.select-arc.com

Circle No. 38 on Reader Info-Card

CONTENTS

November 2006 • Volume 85 • Number 11

AWS Web site http://www.aws.org

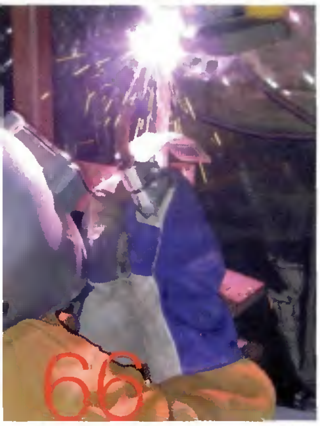

Features

The American Welder

Welding Research Supplement

Cover photo: An Ironworker participating in the union's "Train the Trainer" program practices flux cored arc welding. As part of the program, the trainers for the various locals earn qualifications and learn new skills that they can then pass on to their students. (Photo courtesy of Miller Electric Mfg. Co.)

Departments

Welding Journal (ISSN 0043-2296) is published monthly by the American Welding Society for $120.00 per year in the United States and possessions, $160 per year in foreign countries: $7.50 per single issue for AWS members and $10.00 per single issue for nonmembers. American Welding Society is located at 550 NW LeJeune Rd., Miami, FL 33126-5671; telephone (305) 443-9353. Periodicals postage paid in Miami, Fla., and additional mailing offices. **POSTMASTER:** Send address changes to Welding Journal, 550 NW LeJeune Rd., Miami, FL 33126-5671.

Miller Electric and Hobart Brothers Donate $1 Million to Establish Welder Workforce Development Program

The American Welding Society (AWS), Miami, Fla., recently announced the AWS Foundation has received a $1 million pledge from Miller Electric Mfg. Co. and Hobart Brothers Co. to provide initial funding for the American Welding Society Welder Workforce Development Program.

The AWS Foundation will utilize the donation to fund training for entry-level welders, and specialized training for existing welders in order to address the shortage of trained welders in the United States.

The average age of welders is the mid-fifties. Fewer graduates entering the profession, coupled with the projected retirement of half of the experienced welding workforce, has led to a shortage of skilled welders that could weaken U.S. manufacturing and the overall economy.

The donor companies have selected Bruce Albrecht to represent them on an AWS Foundation committee to help establish the workforce program. Albrecht is an AWS board of directors member and a trustee of the AWS Foundation.

"We hope this unprecedented donation will encourage our other industry partners to join Miller and Hobart Brothers to help us build a stronger welding workforce for America," said Sam Gentry, executive director of the AWS Foundation.

University of New Orleans Lands $3.6 Million Grant for Ship Welding Robot Technology

The University of New Orleans (UNO) has received a $3.6 million grant from the Defense Advanced Research Projects agency to develop automated tools for programming robots to weld ship components. The grant is funded by the Office of NavalResearch.

Much of the work will take place at the UNO Maritime Technology Center of Excellence at Northrop Grumman Ship Systems Avondale Operation.

"This new technology developed by UNO will allow robots to be efficiently and quickly programmed for shipbuilding welding applications," said Russell Trahan, dean of the UNO College of Engineering.

The college will also work with Sandia National Labs in New Mexico and Spatial Corp., a Colorado-based industrial software business that specializes in three-dimensional models, as well as several major shipyards to improve current technology, Trahan said.

Airgas to Build Air Separation Plant in Kentucky

Airgas, Inc., Radnor, Pa., will build an air separation unit in Carrollton, Ky., to supply Dow Corning Corp. and meet increasing demand for bulk and packaged gases in the region.

The company will build the plant on Dow Corning's property located on Four Mile Road with engineering and equipment provided by Universal Industrial Gases, Inc. Also, the company and Dow Corning signed a long-term agreement for gaseous nitrogen. When the plant is completed in late 2008, it will have the capacity to liquefy 350 tons per day of nitrogen, oxygen, and argon.

"We will operate the new plant within our Gas Operations Division, which has the necessary expertise to run the production plant," said Mike Molinini, executive vice president and chief operating officer of Airgas.

The plant will eventually employ more than 20 employees in production and distribution.

WELDING Journal

Publisher *Andrew Cullison*

Editorial
Editor/Editorial Director *Andrew Cullison*
Senior Editor *Mary Ruth Johnsen*
Associate Editor *Howard M. Woodward*
Assistant Editor *Kristin Campbell*
Peer Review Coordinator *Erin Adams*

Publisher Emeritus *Jeff Weber*

Graphics and Production
Managing Editor *Zaida Chavez*
Senior Production Coordinator *Brenda Flores*

Advertising
National Sales Director *Rob Saltzstein*
Advertising Sales Representative *Lea Garrigan Badwy*
Advertising Production *Frank Wilson*

Subscriptions
acct@aws.org

American Welding Society
550 NW LeJeune Rd., Miami, FL 33126
(305) 443-9353 or (800) 443-9353

Do You Have What It Takes to Lead?

It doesn't take long to recognize who the leaders are among us and why. I know that, as a youngster, I observed leadership traits among my peers at school, on the playground, and at a whole lot of other places children gathered. Some kids were bigger, stronger, faster, and were admired for their athleticism; others were (or at least appeared to be) more intellectual, worldly, and could smooze to get their way. No matter which group they came from, they led the pack with little opposition. No one really kept score.

As a teen, the responsibilities and frailties of leadership became more apparent. The good athletes were always on top as long as there was a game to play and the team was winning. Doubt never occurred unless there was an injury, losses were greater than the wins, or scholastic achievement mattered. The intellectual (okay, maybe he or she was only the kid who had the best line or gift of gab) held the teacher's favor — until report cards came. Suddenly, scores were kept.

As adults, we realize leadership comes in many more forms. The reasons why leaders are chosen can be confusing, but one factor is absolute: True leaders have the ability to get things done with and through other people, no matter their leadership style. In civilized society, leadership comes through intellect. Whether in the workplace, social gatherings, or volunteer groups, leaders have to direct, motivate, and challenge to gain favorable results. In the corporate world the score means everything.

So what is the American Welding Society's score? I believe AWS is blessed with a team of great leaders. Its volunteer leadership comes from many disciplines. Scholars, marketers, managers, engineers, and craftsmen all give of their time to work with the Sections or on the board of directors. Their efforts are given for the benefit of the Society, and they challenge themselves and others to maintain the high standards set by previous leaders. Over the years, a proud tradition has been set.

The American Welding Society staff and board of directors work as a team and do an excellent job of managing. The financial statement and membership rolls tell the score: Our Society is in its best financial condition ever and membership continues to grow.

Resources are available from AWS to help you become the type of leader you want to be, one who offers every benefit possible to strengthen your team. Information, resources, direction, and good ethics are some of the tools needed to promote growth within your company. Another tool is to become an AWS Sustaining Member Company, and thereby provide memberships for ten employees. They'll receive information through the monthly *Welding Journal* and you can receive a complete library of standards that are updated as needed. Encourage your members to attend the regular Section meetings. The fellowship and networking adds value to your company. I hope your company will adopt a local Section and sponsor a meeting annually. There's nothing like free food to get people together, and as a guest speaker you'll have the attention of everyone at the meeting. After all, who better to speak about your services or products than you?

My involvement with the American Welding Society came from an invitation to visit a welding school to see if it was teaching skills that would serve my company. During the visit, I met an AWS member who invited me to attend a monthly Section committee meeting. From that one visit I was hooked. Fortunately, in my employment, I had a great manager who allowed us to become a Sustaining Member Company. Three of our employees went on to become Certified Welding Inspectors and four became Section committee members. Everyone gained from our company's involvement with AWS.

Attendance at the first Leadership Symposium solidified my desire to continue to support AWS. I went on to become a board member and eventually to be elected as a vice president for a term that begins in January. All that from a simple visit to look at something I needed and the support of my leader. As a leader, your support can promote positive changes within your company. Please use that gift to help your people benefit from a wonderful organization.

John C. Bruskotter
District 9 Director

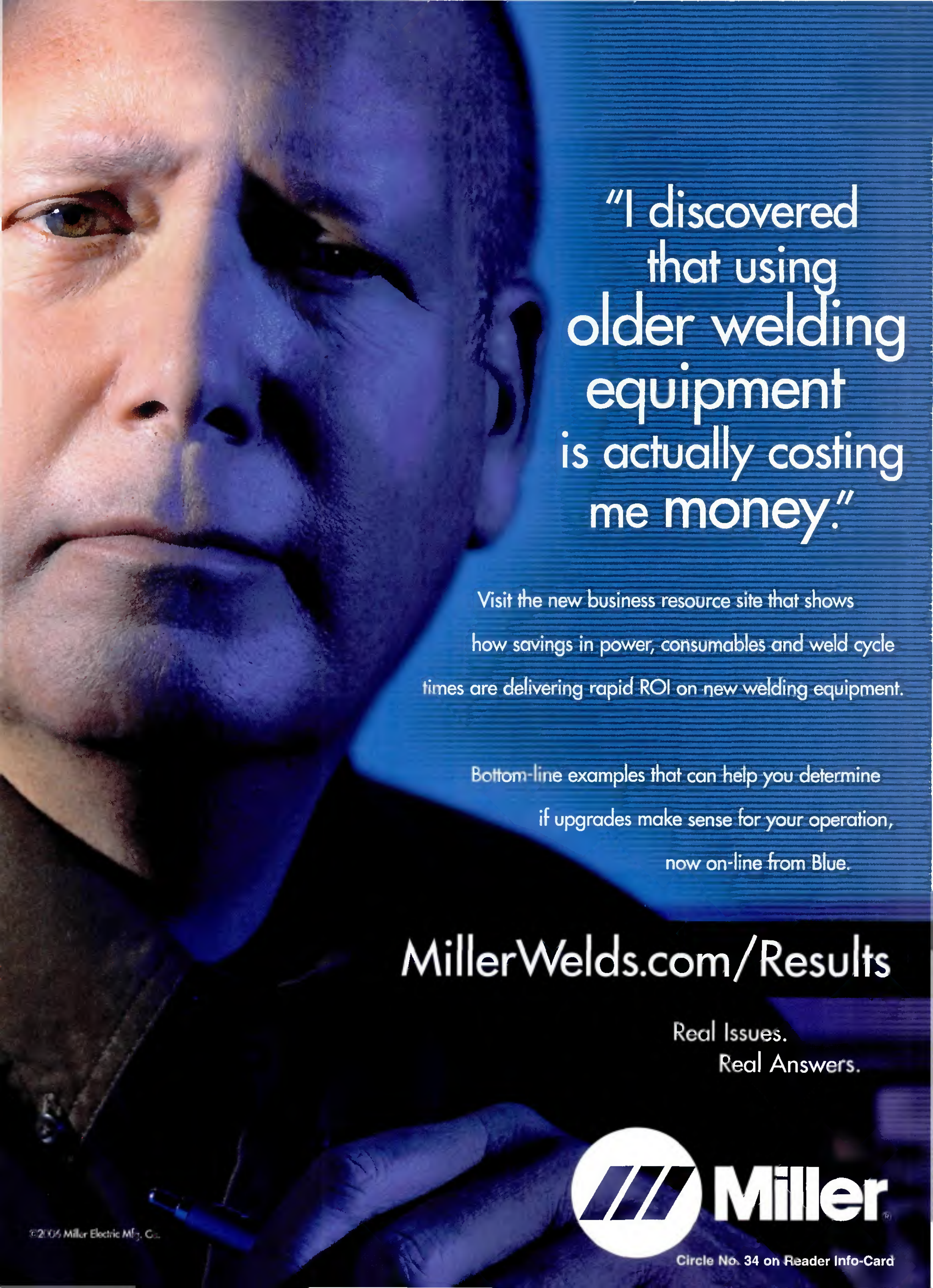

"I discovered that using older welding equipment is actually costing me money."
Visit the new business resource site that shows how savings in power, consumables and weld cycle times are delivering rapid ROI on new welding equipment.
Bottom-line examples that can help you determine if upgrades make sense for your operation, now on-line from Blue.
MillerWelds.com/Results
Real Issues.
Real Answers.
Miller
©2006 Miller Electric Mfg. Co.
Circle No. 34 on Reader Info-Card

Saskatchewan Institute Puts Wheels on Its Training Lab

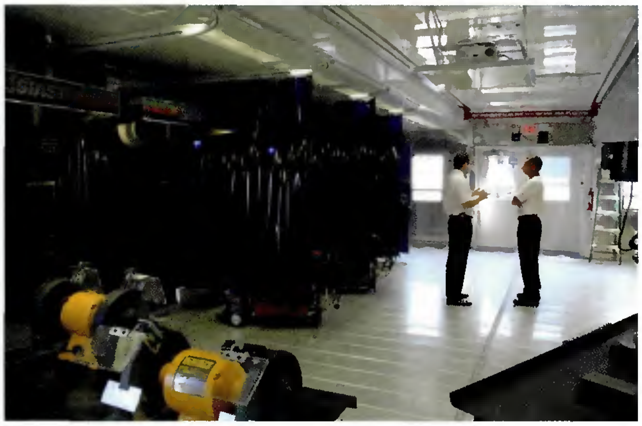

With 1100 sq ft of shop space, the Saskatchewan Institute of Applied Science and Technology's mobile training lab is well equipped to provide training in a number of programs, including welding. It is powered by diesel generators with enough on-board fuel to support a 20-week training session. Supporting the training lab is a supply trailer that connects by walkway to the main unit.

The Saskatchewan Institute of Applied Science and Technology's (SIAST) mobile training lab will expand provincial training capacity and increase access to trades training by taking shop facilities and instructors to remote areas of Saskatchewan, Canada.

The lab includes a tractor trailer unit with pop-out sides that transform it into a 1100-sq-ft training facility. Additionally, it can accommodate a range of programs, including welding, industrial mechanics, and electrical.

Major financial backers of the $1.6-million initiative include the Saskatchewan Apprenticeship and Trade Certification Commission, Cameco, AREVA, SaskTel, and the Northern Apprenticeship Committee. Also, in addition to the tractor-trailer training unit, the mobile training lab includes two supply trailers that contain training aids, materials, and tools, many of which were donated by manufacturers.

Northlands College will play a key role in delivery of training through the lab. The lab will increase college capacity to respond to industry's training needs in a number of the apprenticeship trades as well as increase access for northerners to apprenticeship training and trades-related employment.

Powered by diesel generators, the shop will carry sufficient fuel to operate high-amp equipment and lighting and heating systems for an estimated 20 weeks. Each training session will last 7 to 20 weeks, depending on the program delivered, and the lab can accommodate 12 students at a time.

American Iron and Steel Institute's Summer Internship Yields Concept Vehicles

The American Iron and Steel Institute's summer automotive design internship let college students produce concept vehicles that embody steel technology utilizing a flexible platform. Pictured from left to right are the College for Creative Studies transportation design students Alex Alequin, Carrie Fodor, and Byung Cho with their concept vehicles.

This summer, design and engineering disciplines merged as students from the College for Creative Studies (CCS), Detroit, Mich., and University of Michigan (U-M) unveiled their automotive designs for the 18th annual American Iron and Steel Institute (AISI) summer automotive design internship.

This year's program introduced a real-world twist. Three U-M engineering students joined three CCS transportation design students to produce concept vehicles that targeted Generation X, Baby Boomers, or the Millennial generation.

Throughout the internship, AISI scheduled field trips for the students to demonstrate behind-the-scenes steelmaking and vehicle manufacturing. With guidance from AISI steel-applications specialists and professional automotive designers, students learned the design and engineering potential of steel to increase their understanding of how to work with the metal.

Matrix System Automotive Finishes provided each student with a supply of paint. Each model now boasts a custom-created paint finish.

The three concept vehicles were as follows: the Land Rover Carver, an extreme off-road crossover vehicle, designed by CCS transportation design student Byung Cho and engineered by U-M engineering student Sungchul Choi; the Volvo Stål Concept, a sports car, designed by CCS transportation design student Carrie Fodor and engineered by U-M engineering student Aditya Rajderkar; and the Cadillac Entourage, a sport luxury sedan, designed by CCS transportation design student Alex Alequin and engineered by U-M engineering student Sathish Dhandapani.

Concurrent Technologies Corp. Awarded $1.3 Million for Research and Development

Congressman John P. Murtha and Daniel R. DeVos, president and CEO of Concurrent Technologies Corp. (CTC), Johnstown, Pa., recently announced the U.S. Army Tank Automotive Research, Development and Engineering Center (TARDEC) has awarded the company $1.3 million.

Concurrent Technologies will research, develop, demonstrate, and transfer advanced materials and joining technologies, including aluminum-lithium alloys and friction stir welding, into the U.S. Army's Future Combat Systems' family of vehicles to reduce weight, corrosion, and future maintenance costs while improving vehicle mobility and survivability.

The center, headquartered at the Detroit Arsenal in Warren, Mich., is the nation's laboratory for advanced military ground systems and automotive technology.

Battelle Dedicates Facility for Research into Energetic Materials, High-Speed Events

Battelle officially dedicated a new facility on September 22 at its High Energy Research Laboratory Area in West Jefferson, Ohio, that will give it expanded capabilities to conduct research into materials such as armor. In addition, the laboratory conducts extensive research into energetic materials such as explosives and propellants, and into high-speed events requiring fast data capture equipment.

The facility is 12,500 sq ft. Together with other building and infrastructure improvements, the total cost is about $2.5 million.

The building will give researchers improved meeting and research space, instrumentation labs, and storage facilities and staging areas for setting up experiments before moving them into one of the several test chambers at the facility. Other improvements also include an updated fiber-optic backbone, storage and changing areas for safety equipment, and upgraded chemical lab and storage facilities.

Skyline Steel Opens Mississippi Facility

To open the Skyline Steel Pipe Group's new facility, Mississippi Governor Haley Barbour (right) is shown cutting a ribbon with Skyline Vice President Tom Madison.

Mississippi Governor Haley Barbour officially opened the Skyline Steel Pipe Group facility near Yellow Creek Port in Tishomingo County, Miss., on August 22 during a ribbon cutting ceremony.

The company invested approximately $17 million in the facility to produce spiral welded steel pipe used primarily in heavy construction such as buildings, bridges, and wharves. The facility currently employs 40 workers with 60% working in highly skilled metal trades positions.

Land purchase and the site work, rail spur, water and wastewater systems, access road, and other infrastructure are funded by grants and loans from the Mississippi Development Authority, Appalachian Regional Commission, and Tennessee Valley Authority.

Industry Notes

- IPSCO, Inc., Lisle, Ill., and NS Group, Inc., Newport, Ky., has entered into a definitive agreement pursuant to which IPSCO will acquire NS Group, a manufacturer of seamless and welded oilfield tubular goods. Under the terms of the agreement, approved by both companies' boards of directors, IPSCO will acquire all of the outstanding shares of NS Group for $66 per share in cash, for an aggregate price of approximately $1.46 billion, including NS Group's net cash. The transaction is expected to close by the end of the year.
- Worthington Cylinders is celebrating 35 years of manufacturing. When the company purchased a small cylinder company near Columbus, Ohio, in 1971, creating Worthington Cylinders, the facility produced fewer than 200,000 cylinders a year. Today, it manufactures more than 50 million cylinders a year. In addition, the company has grown from a one-plant operation to employing approximately 2000 workers in eight manufacturing facilities in the United States, Austria, Canada, Portugal, and the Czech Republic.
- Hobart Brothers, Troy, Ohio, has redesigned its Web site at *www.hobartbrothers.com*. To help visitors locate products, it includes a comprehensive database of the company's filler metals. For visitors seeking filler metal recommendations, a step-by-step, interactive search selects filler metals according to base metal, welding process and position, and gas or gasless preferences. The site also includes downloadable welding safety information and helpful reference materials.
- Applied Manufacturing Technologies, Inc. (AMT), Orion, Mich., a supplier of factory automation design, engineering, and process consulting services, has entered into an agreement with DENSO Robotics to provide engineering and support services for the company's robots. Under terms of the agreement, AMT will support DENSO Midwest customers with training, robot programming, and robot rebuild services.
- InnerLogic, Inc., Charleston, S.C., has unveiled a new corporate identity. The company is now KALIBURN, with the tagline, "Plasma Cutting Innovation." Its new logo, from the sword and banner icon symbolizing precision cut, to the bold colors, unites a corporate vision with a graphic identity.
- Sheet Metal Guy, LLC, Cincinnati, Ohio, has opened a new section of its Web site dedicated to AutoCAD users at *www.SheetMetalGuy.com/autocad*. Updated daily, this new section will keep users informed with news and information relative to AutoCAD and the sheet metal industry.
- Cyl-Tec, Inc., Aurora, Ill., a supplier of cylinders, cylinder services, and cylinder accessories for the compressed gas industry, has forged a sales partnership with Fire King of Seattle, Inc., to provide warehousing, servicing, and delivery of Cyl-Tec's new high-pressure cylinders to customers in the Pacific Northwest region of the U.S. By partnering with Fire King, a Seattle company that specializes in cylinder testing and maintenance, the company can service customers in the greater Puget Sound area.
- MQ Power, Rancho Dominguez, Calif., has opened a new

180,000-sq-ft facility in Lewisville, Tex. Additional assembly and modification functions, primarily on the company's Ultra-Silent Series and Super Silent Series portable generators, are performed at the property to supplement MQ Power's existing Santa Fe, Calif., and Danville, Ky., operations. The company's generator trailers will also be assembled at the Lewisville facility.

- Jet Edge, Inc., St. Michael, Minn., a manufacturer of ultra-high-pressure waterjet and abrasivejet systems for precision cutting, surface preparation, and hydrodemolition, has launched its new Web site at *www.jetedge.com*. Featuring an easy-to-navigate contemporary design, it includes a complete product catalog with specifications and drawings, plus an informative waterjet information library and application summaries. Also, the site includes the company's online newsroom and regional sales and service contact information.
- William P. Clark, chairman and CEO of Wall Colmonoy Corp., Madison Heights, Mich., recently announced the acquisition of the assets of HTG Cincinnati, formerly known as The Aerobraze Corp. The facility will be known as Wall Colmonoy Corp., Aerobraze Division. Established in 1955, Aerobraze is now a licensed FAA repair station and continues to serve the aerospace industry.
- Wright Brothers, Inc., Cincinnati, Ohio, an independent gas supplier, plans to expand into the Columbus market. Longtime industry veteran John Congini, previously from Praxair, has been hired to lead the expansion efforts. The company's primary focus will be the service and delivery of packaged gases, laboratory gases, microbulk and bulk, industrial, and specialty gases. Future expansion plans will include a depot for stocking lab and industrial gases as well as additional technical, sales, and service technicians.

Welding Completed for Olympic Bird's Nest' Stadium

Workers finish welding the steel structure of the Bird's Nest.

The supporting structures awaiting removal.

Welding of the steel structure for the main stadium of the 2008 Beijing Olympic Games has been completed, and the temporary support structures are being removed. More than 100 skilled welders were at work during the final structural steel welding stage.

The stadium — 333 m long by 284 m wide by 69 m high — will seat 91,000 spectators during the Olympics and will be used for the opening and closing ceremonies, track and field events, and football (soccer) finals. Construction began in December 2003 and is expected to be completed at the end of 2007. The National Stadium has been nicknamed the "Bird's Nest" because of its shape. The structural elements mutually support each other and converge into a grid-like formation, much like the interwoven twigs of a bird's nest.

The steel structure weighs 42,000 tons, with the roof and hanging parts around it accounting for 11,200 tons. To bear such a heavy load, 78 supporting structures were temporarily installed and different points under stress, with 24 structures along the outer circle, 24 in the middle structure, and 30 in the inner circle. According to the plan, as the supporting structures are removed, the outer circle will drop vertically by 67–70 mm, the middle by 161–178 mm, and the inner by 208–286 mm.

Corus to Build New Rail Welding Facility

Corus recently announced it will build a world-class rail welding facility for its rail manufacturing business at its Scunthorpe, UK, steelworks. The new welding facility will be part of the new rail service center currently under construction. It will replace existing welding facilities at the company's Workington and Castleton sites.

It is anticipated welding will cease at the Castleton site on December 1, 2006, and the new facility begin operation in March 2007.

The new facility is part of an ongoing program to invest £130 million at the Scunthorpe site. This will enable the company to roll longer rail of up to 120 m. Currently, the Castleton site receives 36-m rail from the Workington plant and welds it into 216-m continuous welded strings.

"After reviewing a number of options, we concluded that significant operational and logistics advantages could be gained by having the manufacture and welding of rail on the same site," said Joe Guérin, managing director of Corus's rail businesses. "Our customers will, therefore, benefit from improvements in manufacture, testing, and welding technology with a priority on customer service."

Many Australian Do-It-Yourselfers Fail to Use Eye Protection during Welding, Grinding

More than 70% of Australians do not protect their eyes when doing DIY repairs or improvements, according to a survey by the Optometrists Association Australia. The survey of 1200 people found DIY-ers risked their eyesight by wearing prescription glasses or sunglasses instead of proper eye protection.

Grinding and welding-related activities caused the most eye-related injuries, accounting for 29% of visits to doctors and hospitals. Forty-four percent of all people surveyed said they wore sunglasses or prescription spectacles when welding.

Ian Bluntish, national president of the association, said Australians are underestimating the risk of eye injury when carrying out tasks such as mowing, painting, welding, and pruning.

"People are under the illusion that a pair of sunglasses or prescription spectacles will protect their eyes from damage when they are doing handy work around the home, and this simply isn't true," he said. "In fact, wearing spectacles or sunglasses as protection can be even more dangerous because the lens could shatter when used inappropriately. We urge people to prevent eye injury by wearing the right eye protection for the job."

South African Welding Institute Reports Rising Student Numbers

The Southern African Institute of Welding is experiencing an unprecedented increase in enrollment for its training courses, reported Training Services Manager Etienne Nell.

"What is notable is that 60% to 70% are private students, which includes smaller companies. The increase can be attributed to the fact that people are now beginning to wake up to the career opportunities inherent in the welding sector, ranging from practical welding to nondestructive testing and inspection. Local industry is also beginning to realize the necessity for appropriate certification and testing," Nell said.

South Africa's domestic steel consumption is expected to be around 5.5-million tons in 2006, the highest figure for 30 years, said Peter Dieterich, secretary general of the South African Iron and Steel Institute.

The welding sector in South Africa has been hard hit by a skills shortage in basic welding and welding engineering. Madeleine du Toit, professor, University of Pretoria Department of Materials Science and Metallurgical Engineering, said that, over the last six years, South Africa produced six qualified international welding engineers, of which only three remain in the country. In comparison, Germany produced 2741 welding engineers over the same period.

"There is no better career path for youngsters," Nell said, adding that the demand is such that one local engineering services company has imported 80 Taiwanese welders. He believes South Africa is entering into a period of unprecedented public and private infrastructure development and capital expansion.♦

Reader Praises September Issue

The September issue of the *Welding Journal* is excellent! The brazing topic couldn't have been better planned. Navy brazing certifications are coming up (NAVSEA 0900-LP-001-7000), and the support information in this issue will prove to be very valuable. It's amazing how some welding Q.C. people are so deficient in trade knowledge.

Also, congratulations to AWS on 22,400 CWIs. I just hope some day soon we get the respect we deserve.

Phil Evans
CWI-CWE
Callahan, Fla.

Mother Comments on the Need for Highly Trained Welders, Fabricators

Therese Martin wrote in reference to an article by Ilan Brat titled, 'Where Have All the Welders Gone, As Manufacturing and Repair Boom?' that was published in The Wall Street Journal *on August 15. This spring, her son Phillip graduated from the metal fabrication/welder program at Assabet Valley Regional High School, Marlboro, Mass. Currently, he is employed as a welder/fabricator for Wright Line in Worcester, Mass.*

I would like to address the state of our country and society when it comes to its skilled labor force. It is my belief that without manufacturing and the skilled labor needed to support it, life would be quite different.

Tracing the manufacturing history is as long as our nation's history itself, being an indispensable part of its people's growth, both economically and intellectually, with manufactured goods a base for trade. Fabricating the tools we needed to survive, and to create a modern civilization, manufacturing has become the essence of our society.

Manufacturing, fabrication, and the skilled labor involved to produce the products that are required have become the foundation of our country. This cornerstone of the nation, in my opinion, is in danger, leaving that part of our nation's chain to weaken.

With the advance of technology and the educational demand to fill it, less is thought of for skilled blue-collar workers, causing two to four years of higher education to be a necessity for entry-level jobs. With the cost of higher education, most students do not want to work or can't afford to work in the skilled labor part of the employment ladder, leaving these positions open to outside workers or no replacements at all. This is regretful to me. Working your way up through the ranks is one of the best building blocks of learning in life, and a very necessary part of our society.

Another problem I see is the outsourcing of manufacturing that is done in this country. This, I believe, takes more jobs away from the nation's working class, most in manufacturing, threatening our economy and way of life.

Don't get me wrong; I'm a firm believer in higher education, especially professional development after you have started working to keep you updated in your field of choice. But it is not for every student. More parents need to allow their children to pursue the skilled labor workforce, making this country's foundation strong again by putting the meaning of force back into the nation's vocabulary.

May we see a change soon in our great nation's attitude toward the very needed and proud skilled laborers and the jobs they do supporting this country. It is of the highest importance.

Therese Martin
Boylston, Mass.

Circle No. 24 on Reader Info-Card

BY DAVID BENETEAU

The authors have prepared a comprehensive and sometimes critical review of both accepted resistance welding practice and a broad cross section of modern process research. While the book may not appeal to casual users of the process, it will almost certainly find its way into the library of anyone who needs or wants to understand the physics behind resistance spot welding.

The authors have prepared a detailed analysis of the physics involved in the resistance welding process that is, for the most part, remarkably easy to understand. This astounding feat is achieved through a novel exploitation of the differences in the way that aluminum and steel react during the resistance welding process. By dealing with the two materials in tandem, the authors are able to clearly show unique responses to the same welding variable.

They have also reinforced their methodical explanations with nearly 300 original graphics. This is a pretty substantial number of figures considering there are just over 400 pages in the text. The graphics are far from filler; they work really well with the text to reinforce the concepts presented. Frequently, welding variables or inspection data are correlated to the photograph of the resulting metallographic specimen. The linkage of the theoretical to the observable really allows the book to appeal to a broad range of readers.

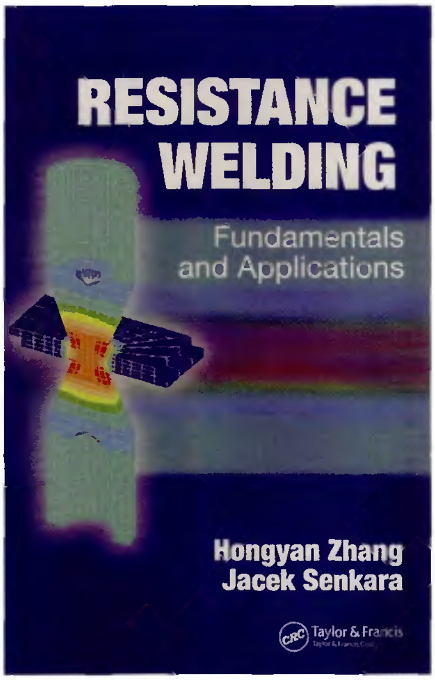

Resistance Welding: Fundamentals and Applications, *by Hongyan Zhang and Jacek Senkara. 448 pages. Published in 2006 by CRC Press, Taylor & Francis Group, 6000 Broken Sound Pky NW, Ste. 300, Boca Raton, FL 33487-2742;* www.crcpress.com; *ISBN 0-8493-2346-0. Price is $99.95.*

More than 250 modern scientific and technical references are cited to address specific variables, material properties, or welding concepts under consideration. In some instances the authors cite references that have drawn conclusions which appear to be quite different — sometimes even conflicting. Usually the differences are explained, but the authors also conducted extensive independent research to fill in the blanks or even propose an alternative approach. Computer simulation is used extensively to help make the dynamic interactions of the process visible.

The ten chapters cover metallurgy; the electrothermal process; discontinuities; mechanical testing; process monitoring and control; quality and inspection; expulsion; the influence of machine mechanics; numerical simulation; and the use of statistics in research. The material is well indexed so the book can be used as a quick reference.

For both the student and process user, there is a lot of basic information presented in an easy to read fashion. For example, in the chapter on expulsion, the authors present a detailed study of expulsion prediction and prevention. They present a concept for an expulsion model then walk the reader through its detailed development. There is a lot of math for those interested in it, but the material is also easy enough to follow if math is not your thing. There are plenty of practical insights and the substantive information that supports them. For instance, you will find out why domed electrodes increase the tendency of spot welds in aluminum sheet metal to crack, and why restraining the aluminum sheets during welding reduces it.

For theoretical studies or laboratory work, there is a bounty of information beyond the excellent compilation of reference materials. Chapter 10 on the application of statistics should give even the most hardcore scientist something to contemplate. In the chapter on mechanical testing, the test specimen specifications from the relevant AWS, Military, and ISO standards are compared and analyzed. The authors use experiments that show the influence of the differences between the standards. They show the instrumentation typically used to analyze the results and propose a design for a new impact testing apparatus and specimen, along with the supporting theory.

My biggest disappointment is that the book lacks a preface or introduction. While the back cover provides the usual promotional overview of the work, there is not a word anywhere to indicate who the authors are. A reasonably large number of editing errors also seems uncharacteristic of the publisher. Hopefully, these issues will be addressed when the book is reprinted. Perhaps the publisher will even consider printing some of the graphics in color so that the data can be interpreted as the authors' intended.

It might be too soon to proclaim this work as historically significant, but it seems a virtual certainty that it will be viewed as such. In any case, the authors have certainly done a great service to the resistance welding industry.◆

DAVID BENETEAU is with CenterLine (Windsor) Ltd.

Hodgson Custom Rolling Inc.

services a wide variety of industries in the ENERGY SECTORS of hydro, petro chemical, atomic, gas, oil, wind, etc. in addition to those in heavy manufacturing, steel, pulp & paper, mining, marine, forestry, etc. Hodgson's commitment to providing customers superior products and personalized professional service has earned itself a reputation for excellence, making the name HODGSON synonymous with "paramount quality and workmanship".

Hodgson Custom Rolling Inc. is one of North America's largest plate rolling, forming, section rolling and fabricating companies.

PLATE ROLLING & FLATTENING

Hodgson Custom Rolling specializes in the rolling and flattening of heavy plate up to 7" thick and up to 12 feet wide. Cylinders and segments can be rolled to diameters ranging from 10" to over 20 feet. Products made include ASME pressure vessel sections. **Crane Hoist Drums**, thick walled pipe, etc.

PRESS BRAKE FORMING & HOT FORMING

Hodgson Custom Rolling's brake department processes all types of steel sections and plate up to 14" thick. Developed shapes such as cones, trapezoids, parabolas, reducers (round to round, square to round) etc.

STRUCTURAL SECTION ROLLING

Hodgson Custom Rolling has the expertise to roll curved structural sections into a wide range of shapes and sizes (angle, wide flange beam, I-beam, channel, bar, tee section, pipe, tubing, rail, etc.). We specialize in **Spiral Staircase Stringers**, flanges, support beams, gear blanks, etc.

FABRICATING

Hodgson Custom Rolling combines expertise in rolling, forming, assembly and welding to produce various fabrications including kiln sections, rope drums, heavy weldments, ladles, pressure vessel parts, multiple **Components for Heavy Equipment** applications etc.

Hodgson
Custom Rolling Inc.

ASME Certified
ISO 9001:2000

5580 Kalar Road
Niagara Falls
Ontario, Canada
L2H 3L1

Telephone: (905) 356-8132
Toll-free: (800) 263-2547
Fax: (905) 356-6025
E-mail: hodgson@hodgsoncustomrolling.com
Website: www.hodgsoncustomrolling.com

U.S. Address:
M.P.O. Box 1526
Niagara Falls, N.Y.
14302 - 1526

HODGSON CAN HELP SOLVE YOUR PROBLEMS

Circle No. 27 on Reader Info-Card

BY DAMIAN J. KOTECKI

Q: We have been repairing cast pump bodies, fittings and valves of CA-15 stainless steel for years, and have been welding attachments of matching 410 wrought stainless steel to the castings using 410NiMo filler metal. We have always used postweld heat treatment (PWHT) at 1100° to 1150°F for several hours, depending upon thickness. These have been very successful products for us. We just received an order from a new customer who insists on PWHT at 1350° to 1400°F. Is it advisable to use the 410NiMo filler metal for this application?

A: CA-15, 410 and 410NiMo are all martensitic stainless steels, with air hardening characteristics. That means that even slow cooling from high temperatures where the metal is austenitic will result in formation of virtually 100% martensite. Filler metal of 410NiMo has a long history of successful application in joining and rebuilding 410 stainless steel base metals. It is lower in carbon content than the 410 base metal, so that the as-welded base metal and HAZ can be substantially harder and stronger than the weld metal. But the addition of about 0.5% Mo retards softening in PWHT so that, after the 1100° to 1150°F (593° to 621°C) PWHT, the 410 base metal and the 410NiMo weld have virtually the same mechanical properties. Table 1 compares the composition of 410 and its cast equivalent (CA-15) with the 410NiMo filler metal composition.

Table 1 — Composition of 410 and CA-15 Base Metals and 410NiMo Filler Metals

Material	UNS Number	%C	%Mn	%P	%S	%Si	%Cr	%Ni	%Mo
410 ASTM A276	S41000	0.08 to 0.15	1.00 max	0.040 max	0.030 max	1.00 max	11.5 to 13.5	N.S.	N.S.
CA-15 ASTM A743	—	0.15 max	1.00 max	0.04 max	0.04 max	1.50 max	11.5 to 14.0	1.00 max	0.50 max
E410NiMo-XX AWS A5.4	W41010	0.12 max	1.0 max	0.04 max	0.03 max	0.90 max	11.0 to 12.5	4.0 to 5.0	0.40 to 0.70
ER410NiMo AWS A5.9	S41086	0.06 max	0.6 max	0.03 max	0.03 max	0.5 max	11.0 to 12.5	4.0 to 5.0	0.4 to 0.7

As-cooled from high temperature, 410 has very high tensile strength, exceeding 190 ksi (1310 MPa). However, it is not often used in this condition. It is normally tempered to soften it and improve ductility. The mechanical properties after tempering (or PWHT) are given in Table 2, along with those for 410NiMo filler metal. Note that the mechanical properties of ER410NiMo are not specified in AWS A5.9, *Specification for Bare Stainless Steel Welding Electrodes and Rods,* because the wire is usable with a number of processes including GMAW, GTAW, and SAW. Instead, AWS A5.9 refers the user to the mechanical properties given in AWS A5.4, *Specification for Stainless Steel Electrodes for Shielded Metal Arc Welding,* for the corresponding covered electrode as those which can be expected from the wire in whatever welding process it is used. From Table 2, you can clearly see that 410NiMo

Table 2 — Mechanical Properties of 410 and CA-15 Base Metals and 410NiMo Weld Metal

Material	Heat Treatment	Tensile, ksi (MPa)	Yield, ksi (MPa)	% Elongation
410	Tempered, temperature not specified	100 (690) min	80 (550) min	15 min
CA-15	Tempered at 1100°F (593°C) min	90 (620) min	65 (450) min	18 min
E410NiMo-XX	Tempered at 1100° to 1150°F (593° to 621°C)	110 (760) min	N.S.	15 min

filler metal is a good match for the base metals after the original PWHT.

The new PWHT at 1350° to 1400°F (732° to 760°C) changes everything. The 410 and CA-15 base metals do not start reforming austenite until the temperature exceeds about 1450°F (790°C), so they will be softened further (tempered) in the new PWHT temperature range as compared to the old PWHT range. The new PWHT will reduce the tensile strength of the 410 or CA-15 to much lower levels. This high temperature treatment will drop the tensile strength of either the 410 or CA-15 base metal to around 70 ksi (480 MPa).

But the effect on the 410NiMo weld metal will be quite different. Note, from Table 1, the high nickel content of 410NiMo filler metal. This nickel depresses the temperature at which austenite starts to form on heating. Austenite will form on heating 410NiMo weld metal above about 1150°F (595°C). When heated into the new PWHT temperature range of 1350° to 1400°F, the weld metal will become almost entirely austenite in the furnace. There will be no tempering of the weld metal in the furnace. Then removal from the PWHT furnace and air cooling will cause the weld metal to transform to new martensite, with tensile strength on the order of 150 ksi (1035 MPa). This means there will then be a very large mismatch between the properties of the base metal and the weld metal, and the weld metal will be quite brittle.

In short, the 410NiMo filler metal is inappropriate for PWHT in the 1350° to 1450°F temperature range. Instead, I suggest you use matching 410 filler metal for the 410 and CA-15 base metals, to obtain matching response to heat treatment and matching properties after this PWHT.

DAMIAN J. KOTECKI is technical director for stainless and high-alloy product development for The Lincoln Electric Co., Cleveland, Ohio. He is president of the American Welding Society, a vice president of the International Institute of Welding, a member of the A5D Subcommittee on Stainless Steel Filler Metals; D1 Committee on Structural Welding, D1K Subcommittee on Stainless Steel Welding; and a member and past chair of the Welding Research Council Subcommittee on Welding Stainless Steels and Nickel-Base Alloys. Questions may be sent to Dr. Kotecki c/o Welding Journal, 550 NW LeJeune Rd., Miami, FL 33126; or e-mail to Damian_Kotecki@lincolnelectric.com.

Welding Wire Delivers High Impact Strength

The Formula XL®-550 gas shielded flux cored wires are for single or multipass welding on ships, storage vessels, earth-moving equipment, structural steel, and offshore oil rigs, as well as for general mild steel applications. Designed for use with 100% CO_2 shielding gas, the wire is available in diameters of 0.045, 0.052, and 1/16 in. Also, these wires offer high impact values at low temperatures (60–70 ft-lb at –40°F). Its low hydrogen level helps eliminate cracking and does not allow worm tracks to form in the weld under normal working conditions. Additionally, the wire features improved wet-in action that produces an aesthetically pleasing, flat or slightly convex bead contour. It has slag release to help reduce downtime for postweld cleanup and to expedite the welding process in multipass applications.

Hobart Brothers Co. **100**
101 Trade Square East, Troy, OH 45373

Power Source Provides Durability

The MultiPower 460-SE is a multiprocess, three-phase power source intended for heavy-duty industrial DC welding applications in harsh coastal environments. Designed for high-performance GMA, pulsed GMA, GTA, flux cored wire, and SMA electrode welding or air carbon arc gouging, it features the company's SuperSwitch technology. Constructed from stainless steel sheet metal parts and hardware, the power source provides durability in tough environments. Its exterior features noncorrosive, high-impact-resistant and nonflammable composite side panels, and top side panels made of Kydex polymer. The 100% solid-state power source offers a rated DC output (constant voltage or constant current) of 450 A at 100% duty cycle at 38 VDC or 500 A at 60% duty cycle at 39 VDC, with a maximum open circuit voltage of 80 VDC. The welding range is 10 A/12 V to 500 A/40 V.

ESAB Welding & Cutting Products **101**
PO Box 100545, 411 S. Ebenezer Rd.
Florence, SC 29501-0545

Gloves Require Less Force to Grip Oily, Wet Objects

The AlphaTEC™ gloves incorporate the company's Grip Technology™. They were designed as a liquid-proof product requiring less force to grip oily or wet objects. The gloves also integrate microscopic channels in a patented ultrathin nitrile layer to direct fluids away from the grip surface, leaving a dry contact area that provides almost the same grip that is possible under fluid-free conditions.

Ansell **102**
200 Schulz Dr., Red Bank, NJ 07701

Weld Monitors Feature Color Display

The MM-370 weld monitor measures current, voltage, force, and displacement, and is capable of setting limits and configuring comprehensive machine input/output. The hand-held MM-380 weld monitor utilizes a weld-through sensor that measures current, voltage, and force simultaneously between the electrodes. They both feature a 5-in. color screen that provides precise graphical displays of waveform time and amplitude, in

addition to numeric peak and average values. Waveforms and data can be output through a built-in printer, which is standard on the MM370 and optional on the MM380, or via a COM port for screen capture and data collection. Also, both monitors can measure single-phase AC, DC, and AC inverter weld controls.

Miyachi Unitek Corp. 103
1820 S. Myrtle Ave., Monrovia, CA 91016

Work Boot Stands up to Extreme Conditions

The PowerWelt work boot features abrasion-resistant Ever-Guard™ leather. This genuine full-grain leather is impregnated with polyurethane, enhancing the leather while retaining its essential characteristics of breathability and flexibility. In addition, this leather is heat resistant up to 346°F and is waterproof. Constructed on the Timberland PRO® TiTAN® last (3D foot form), it provides ample room in the toes. The boot also features the company's PowerFit™ comfort system for ergonomic fit and maximum support, and a dual-density OrthoLite® polyurethane footbed for cushioning that resists compression. The dual-density polyurethane outsole provides cushioned comfort and traction. Sizes include 7–15 M/W.

Timberland PRO 104
200 Domain Dr., Stratham, NH 03885

Torch Contains Insulated Front Housing

The Tough Gun I.C.E. (Integrated Cooling Enhancer) automatic torch provides all of the benefits of a water-cooled torch with the durability of an air-cooled torch. Water circulates to the nozzle, keeping front-end consumables running cooler and lasting longer. It is available in 550- and 650-A models. The torch also features an insulated front housing made from strong, lightweight aluminum tubing and a spring-guard strain relief to prevent kinking and abrasion.

Tregaskiss Ltd. 105
2570 N. Talbot Rd., Oldcastle, ON, Canada N0R 1L0

System Reduces Calibration Times

The SpeedCal system is designed to accurately calibrate up to 12 pipette channels simultaneously. By testing all 12 channels at once, the average time for testing a 12-channel pipette may be reduced to 10 min. A computer records all data and generates a detailed calibration report as well. The system can be used to reduce calibration times for single-channel pipettes and multichannel pipettes up to 12 channels.

Sartorius Corp. 106
131 Heartland Blvd., Edgewood, NY 11717

Manifold System Provides Continuous Gas Flow

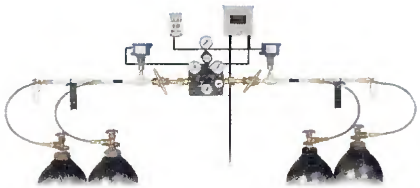

The Gas Manifold and Automatic Changeover Regulator System provides accurate, uninterrupted gas flow. Easy-to-read 2.5-in. chrome-plated gauges allow users to inspect cylinder bank and outlet pressures visually, while an optional audio and visual alarm alerts users when a gas cylinder bank is nearing empty. The company offers its nickel-plated regulator models designed for 15, 40, or 125 lb/in.^{2} outlet pressures. Master header bars attach to the left and right sides of the changeover regulator. Pigtail assemblies are available in 24- and 72-in. lengths, are constructed of stainless steel outer braids, and Teflon® liners for strength and flexibility. Manifold headers include check valves to prevent air from entering the system and gas from escaping from the system. The changeover regulator includes two inlet pressure gauges, an interstage pressure gauge, and an outlet pressure gauge.

Smith Equipment **107**
2601 Lockheed Ave., Watertown, SD 57201-5636

Robots Designed for High-Speed Accuracy

The company's three new robot models are designed for tasks requiring high-speed accuracy including welding, cutting, and measuring applications. The KR 100 HA robot is the basic model with a reach of 2600 mm and payload capacity of 100 kg. The KR 100 L90 HA is an extended model having a reach of 2800 mm, an additional arm extension of 200 mm, and a payload capacity of 90 kg. The KR 100 L80 HA model has a reach of 3000 mm, an additional arm extension of 400 mm, and a payload capacity of 80 kg.

KUKA Robotics Corp. **108**
22500 Key Dr., Clinton Township, MI 48036

Blast Finishing Cabinet Adjusts in Height

The company has extended the capabilities of its Model 8-AH adjustable height blast finishing cabinet. The rigid welded steel base of the cabinet is fitted with an electrically operated jackscrew that raises and lowers the entire blast enclosure. Each individual user can adjust the height with a switch located on its side. Long armholes with attached shoulder-length gloves allow unrestricted movement during use. The finishing enclosure has a full-width side-hinged front door, a top-hinged front door to simplify loading of oversized workpieces, as well as a slam-shut side door for quick access to the cabinet interior. Media and dust extracted from the bottom of the

cabinet are pneumatically conveyed through flexible ducting to a cyclone separator and media reclaimer mounted above the pressure vessel.

Guyson Corp. 109
W. J. Grande Ind. Pk., 13 Grande Blvd.
Saratoga Springs, NY 12866-9090

Saw Offers Speed, Precision

The Titan Model from the FMB Pro Mitre Series of FMB Direct Drive Saws

has precision mitre cuts 0 to 60 deg with a 14-in. cutting capacity. It features a hydraulic control downfeed and rugged variable speed saw drive, allowing it to easily cut a wide range of materials. The saw is useful for thin-wall tubes, profiles as well as heavy steel sections, and hard solid material. Additionally, it features variable blade speeds of 62 to 310 ft/min, 24-in. length stop, heavy-duty clamping vise with quick clamp action, infeed and outfeed roller supports, and offers available recirculating flood coolant system.

Pat Mooney Inc. — The Saw Co. 110
502 S. Westgate St., Addison, IL 60101

Controlling Chromium Fumes

OSHA's lower limits for worker exposure to hexavalent chromium have made providing clean air to the working environment even more important

BY ED RAVERT

Knowing how to calculate the amount of weld fumes and, in turn, how to capture those fumes and provide clean air in the working environment has become especially important in light of the Occupational Safety and Health Administration's (OSHA's) new regulation for employee exposure to hexavalent chromium (Cr(VI)). Hexavalent chromium is a natural metal used in the manufacture of stainless steel.

Even before the new Cr(VI) exposure regulation, OSHA had established limits of 5 mg/m^3 for carbon steel and other types of welding to protect the health of welders and employees in the surrounding area. Hence, knowledge of the weld fume ratios and the calculations provided in this article will be extremely helpful in knowing exactly how much weld smoke is being generated, how much dilution air is required, and the amount of efficiency that will be needed from the dust-collection equipment.

All welding operations, including robotic welding, need careful attention and weld fume monitoring. Consider the example of a plant with a significant number of robotic welding machines. This plant also utilized a number of employees in support of the operation, but, because the equipment was robotic, it was felt there was no initial need for dust and weld smoke control. The company assumed that replacement air for dilution would keep it in compliance with environmental standards. To check, personal monitors were used to see if weld fume exposure was occurring. Indeed it was found that some employees were exceeding the recommended permissible exposure limit (PEL).

The goal of this article is to provide information that will directly help in providing healthful clean air for welders and supporting personnel.

Importance of Weld Fume Particle Size

Weld fume particle size is important because of OSHA and Environmental Protection Agency (EPA) health and environment air quality control aspects. In welding, the intense heat of the arc or flame vaporizes the base metal and/or electrode coating. This vaporized metal condenses into tiny particles called fumes that can be inhaled. Generally, weld fume is submicron in size with average diameters from 0.3 to 0.7 microns. Lung retention is minimal with particles in this size range. However, thermal effects can cause agglomeration of the particles into particle chains and clusters that exceed one micron that can be deposited in the human respiratory tract. Chromium fume, which is created by welding or cutting on stainless steel or other metals coated with a chromium material, is extremely dangerous, hence the new regulations.

Weld Fume Generation

The amount of weld fumes generated will vary depending on the welding process used and the metal being welded. The weight of fumes generated is a percentage of the weight of deposited metal. This percentage can be based on the length of weld electrode used. Table 1 lists the typical ratios by welding process and metal type.

If continuously gas metal arc (GMA) welding on carbon steel at the rate of 10 lb/h, the maximum rate of weld fume produced would be 10 lb × 0.009 (0.9%), or 0.09 lb/h. If, however, the welding is done for only 30 min/h, the fume generation rate will be half, or 0.045 lb/h. By comparison, if continuously GMA welding on stainless steel at the rate of 10 lb/h, the maximum rate of weld fume produced would be 10 lb × 0.07 (0.7%), or 0.7 lb/h.

Air Pollution Control Devices

Electrostatic precipitators (ESP) are ideally suited for collection of weld smoke. The major exception is in dealing with stainless steel and hexavalent chromium. See the two boxed items for more information regarding OSHA's new hexavalent chromium regulations.

ED RAVERT is senior application engineer, United Air Specialists, Inc., Cincinnati, Ohio.

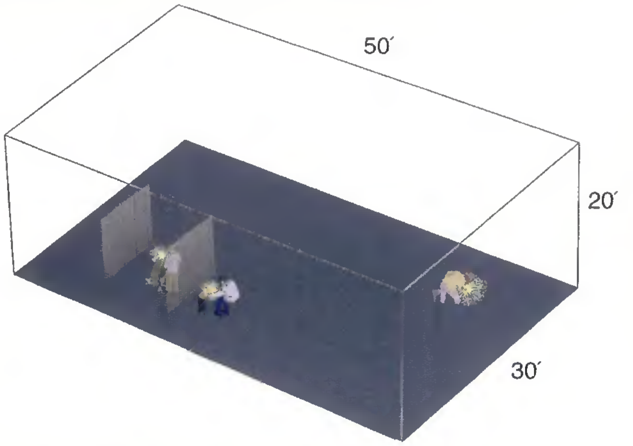

Fig. 1 — A 30,000-sq-ft enclosed welding space. Dilution air assumes continuous welding without the use of air pollution collection devices.

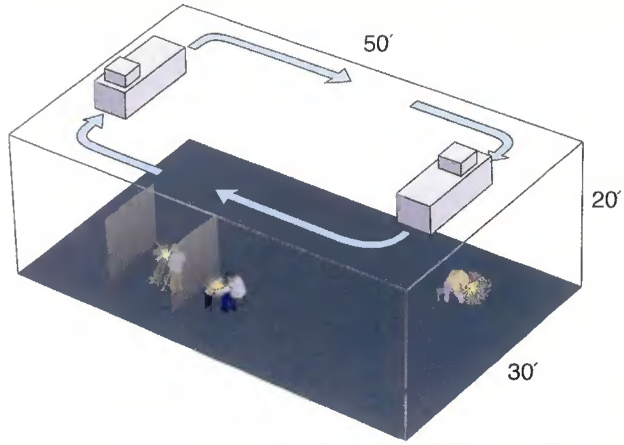

Fig. 2 — Internally filtered air using overhead cartridge dust/fume collectors. Electrostatic precipitators or cartridge dust/fume collectors can be mounted overhead to recirculate the air in a racetrack fashion.

Media filtration units, including cartridge dust collectors, are also ideally suited for collection of weld smoke. Depending on the welding process, source capture systems do the best job of capturing weld fume contaminants using the least amount of cubic feet of air per minute (ft^3/min). Source capture systems include hoods, ducting, air-cleaning devices, and air-moving devices (fans). With separate hoods and ducting, an ESP or cartridge collector can be the recommended method of cleaning air because the weld fume is captured before it can escape into the ambient air.

There are, however, many factors that could render a source capture system impractical. These include the following:

- Where work is done on large parts and the worker has no fixed operating position.
- Where workers are unable to use hooded systems. Some source capture systems may require physical positioning by the worker. If it is unlikely the worker will perform that positioning, the system is rendered ineffective.
- Where there are a large number of small weld smoke producers in a confined area.
- Places in which overhead cranes and process obstructions make ducting installation impossible. Unducted systems, designed properly, can keep the air cleaning units out of the craneways and still achieve effective results.
- Where floor layout revisions are anticipated and could result in expensive duct modifications. Unducted systems are more flexible.

Table 1 — Weld Fume Ratios

Welding Process	Metal Type	Range Weight of Fumes/ Weight of Deposited Metal
FCAW	Carbon Steel Stainless Steel	0.9–2.4%
SMAW	Carbon Steel	1.1–5.4%
SMAW	Stainless High Alloy	0.3–1.4%
GMAW	Carbon Steel	0.3–0.9%
GMAW	Stainless Steel	0.6–7%
GMAW	Copper Aluminum	0.5–1.6%

Air Pollution Control Device Design Considerations

To select the appropriate air pollution control solution for your operation, the following considerations need to be addressed:

- Size and shape of the space where welding operations are performed.
- Containment generation rate and the desired steady-state containment levels.
- Required number of ambient air changes per hour.
- Existing ventilation and replacement air rates, plus all heating, ventilation, and air-conditioning system air volumes and airflow patterns. This applies more to ambient air than with the use of source capture systems.
- Airflow pattern continuity noting seasonal variations.
- Appropriate filtration technology to match room layout, containment generation, and designed steady-state containment levels.

Emissions Control Basics

One way to achieve target room contamination levels without using dust/fume control devices is to simply provide enough dilution (replacement) air into the enclosed space. As shown in Fig. 1 and Table 2, to achieve the 5 mg/m^3 limit normally required by OSHA or the EPA, the enclosed space would require 8.6 air changes per hour with just one welder continuously welding. With three welders continuously welding, 25.8 air changes (AC) per hour would be required. Stricter room contamination levels would require even higher air change schedules.

Weld fumes and gases calculations for the dilution air example shown in Fig. 1 with a 30,000-sq-ft shop size (50 × 30 × 20 ft), and with three welders operating with E7108 electrodes and generating 0.6 g/min of fumes are as follows:

With an allowable room contamination level of 5 mg/m^3

$$\frac{30{,}000 \text{ sq ft} \times 25.8 \text{ AC/h}}{60} = 12{,}900 \text{ ft}^3\text{/min}$$

With an allowable room contamination level of 2 mg/m^3

Overview: New OSHA Regulations For Hexavalent Chromium Exposure

OSHA's new regulation for employee exposure to hexavalent chromium (Cr(VI)) — a natural metal used in the manufacture of stainless steel — has significantly reduced the permissible exposure limit from 52 to 5 micrograms. The regulation (Volume 71, Number 39, 10099–10385) also includes provisions relating to preferred methods for controlling exposure, respiratory protection, protective work clothing and equipment, hygiene, medical surveillance, hazard communication, and recordkeeping. Effective May 30, 2006, the new rule does not require the installation of engineered controls, including air filtration equipment, until May 30, 2010.

This standard applies to all manufacturing processes where hexavalent chromium is present including welding. While all types of welding could be affected, the highest concentration will be from the fumes generated in welding stainless steel. The major health effects associated with exposure to Cr(VI) include lung cancer, nasal septum, ulcerations and perforations, skin ulcerations, and allergic and irritant contact dermatitis.

This new regulation provides for greater employee protection against these health risks by lowering the permissible exposure limit (PEL) for hexavalent chromium, and for all Cr(VI) compounds, from 52 μg to a much more stringent 5 μg of Cr(VI) per cubic meter of air (5 $\mu g/m^3$) as an 8-h time-weighted average.

Welding Specifics in the New OSHA Hexavalent Chromium Regulations

Complete information and a copy of the 287-page regulation (Volume 71, Number 39, 10099-10385) can be found at the OSHA Web site: *www.osha.gov/ SLTC/hexavalentchromium/index.html.*

Following are pertinent quotes from the regulation.

"OSHA concludes that engineering controls, such as local exhaust ventilation (LEV), process control, and process modification or substitution can be used to control exposures in most operations." (Vol. 71, No. 39, 10334)

"OSHA has determined that the primary controls most likely to be effective in reducing employee exposure to Cr(VI) are local exhaust ventilation (LEV) and improving general dilution ventilation. ... This includes installing duct work, a type of hood, and/or a collection system." (Vol.71, No.39, 10262)

"Paragraph (f) of the final rule, Methods of Compliance, establishes which methods must be used by employers to comply with the permissible exposure limit (PEL). It requires that employers institute effective engineering and work practice controls as the primary means to reduce and maintain employee exposures to Cr(VI) to levels that are at or below the PEL ... Engineering controls can be grouped into three main categories: 1) Substitution, 2) isolation; and 3) ventilation, both general and localized." (Vol.71, No.39, 10345)

"Welding: The welding operations OSHA expects to trigger requirements under the new Cr(VI) rule are those performed on stainless steel, as well as those performed on high-chrome-content carbon steel and those performed on carbon steel in confined and enclosed spaces. ... OSHA has determined that engineering and work practice controls are available to permit the vast majority (over 95%) of welding operations on carbon steel in enclosed and confined spaces to comply with a PEL of 5 $\mu g/m^3$. ... OSHA has determined that the PEL of 5 $\mu g/m^3$ is also feasible for all affected welding job categories on stainless steel. ... The two most common welding processes, shielded metal arc welding (SMAW) and gas metal arc welding (GMAW), ... may require the installation or improvement of LEV. ... There are ongoing efforts to reduce the use of SMAW and replace it with GMAW for both efficiency and health reasons. ... OSHA has revised its estimate of the percentage of SMAW welders that can switch to GMAW from 90% to 60%. ... For those stainless steel SMAW operations that cannot switch to GMAW and even some GMAW operations, the installation or improvement of LEV may be needed and can be used to reduce exposures. OSHA has found that LEV would permit most SMAW and GMAW operations to comply with a PEL of 5 $\mu g/m^3$, OSHA recognizes that the supplemental use of respirators may still be necessary in some situations." (Vol.71, No. 39, 10262-10263)

$$\frac{30{,}000 \text{ sq ft} \times 63 \text{ AC/h}}{60} = 31{,}500 \text{ ft}^3\text{/min}$$

Following is the same example with just one welder operating with E7108 electrodes:

With an allowable room contamination level of 5 mg/m^3

$$\frac{30{,}000 \text{ sq ft} \times 8.6 \text{ AC/h}}{60} = 4300 \text{ ft}^3\text{/min}$$

and with an allowable room contamination level of 2 mg/m^3

$$\frac{30{,}000 \text{ sq ft} \times 21 \text{ AC/h}}{60} = 10{,}500 \text{ ft}^3\text{/min}$$

The better way to achieve target room contamination levels is to use dust/fume control devices. Using the same enclosed 30,000-sq-ft workspace, electrostatic precipitator or cartridge collectors can be used — Fig. 2. These units can be hung overhead to clean and recirculate the air in a race track fashion.

With this equipment, 4250 ft^3/min or 8.5 air changes per hour would be pulled in and recirculated. An additional 750 ft^3/min (¼ to ½ ft^3/min/sq-ft of floor space) would be bled in and exhausted. The total volume would be 5000 ft^3/min, or 10 air changes per hour.

If the welders were generating 0.09 lb/h of weld fume, at 99.99% efficiency, all but 0.000009 lb/h would be captured. This amounts to 0.00000021 grains/ft^3 or 0.00048 mg/m^3. This is well within the acceptable levels for any of the weld fume contaminants listed in Table 3.

The following is a calculation example for shielded metal arc welding (SMAW) using E7018 electrodes with internally filtered air:

0.2268 g/min welding operation
0.6804 g/min, 0.0015 lb/min
10.5 grains/min, 0.09 lb/h

$$\frac{5000 \text{ ft}^3 \times 0.0021 \text{ grains/ft}^3 \times 60 \text{ min/h}}{7000 \text{ grains/lb}}$$
$$= 0.09 \text{ lb/h generated}$$

$$\frac{5000 \text{ ft}^3 \times 0.00000021 \text{ grains/ft}^3 \times 60 \text{ min/h}}{7000 \text{ grains/lb}}$$
$$= 0.000009 \text{ lb/h not captured}$$

0.00000021 grains/ft^3 = 0.00048 mg/m^3
= 0.48 $\mu g/m^3$
0.00006804 g/min, 0.00000015 lb/min

If you divide the 7% weld fume weight number by the 0.9% carbon steel number (Table 1), and multiply it by 0.48 $\mu g/m^3$, the micrograms per cubic meter for stainless steel now becomes 3.733 μg.

Table 2 — Dilution Air Requirements

Room Contamination Level		One Welding Operation		Three Welding Operations		
mg/m³	AC/h	std. ft³/min	std. m³/min	std. ft³/min	std. m³/min	AC/h
2.0	21	10,500	297	31,500	892	63
5.0	8.6	4,300	122	12,900	365	25.8
10.0	4	2,000	57	6,000	170	12
20.0	2	1,000	28	3,000	85	6

Table 3 — OSHA Exposure Concentration Limits (mg/m³)

Material	8-h TWA
Beryllium	0.002
Cadmium Oxide (fume)	0.01
Chromium (Cr(VI))	0.005
Copper	0.2
Manganese (fume)	0.2
Molybdenum	0.5
Nickel	1.5
Vanadium Oxide (fume)	0.05
Zinc Oxide (fume)	2.0

The formulas and percentages used in this article can be applied to most welding applications. Robotic welding areas follow the same basic formulas. These areas should be enclosed as much as possible. Strip curtains should be used to prevent weld fumes from migrating into other areas of the facility.

Permit guidance: Even if you can achieve 0.00048 mg/m³ in your facility, do not list that capability on your report. Only list what is required for the permit.

Summary

Depending on the type and quantity of weld fume generated, contaminants can be controlled three different ways:

- Dilution ventilation
- Ambient air collection using dilution air, an air cleaning device (ESP or cartridge collector)
- Source capture using an air cleaning device (ESP or cartridge collector)

Electrostatic precipitators are ideal for the collection of weld fume submicron particles. ESPs are typically used for source capture systems, or ambient air systems on carbon steel welding, and prior to the new OSHA standard, were used for stainless steel welding. ESPs require very little maintenance and are not subject to periodic cartridge filter replacement costs. As ESPs are lower in overall efficiency than cartridge filter collectors, they would not be ideally suited for stainless steel weld fumes, especially if the air is to be returned into the workspace.

If ambient air collection is desired when welding on stainless steel, the welder will be required to wear personal respiratory protection at all times. The source capture system combined with a cartridge collector is the only viable way to deal with stainless weld fumes. Even then, and if the air is to be returned into the workplace, a monitored safety HEPA after filter should be used.◆

Weld Cracking Linked to Wires Containing Boron

Fig. 1 — Cracks were found in the circumferential welds made during the field erection of this carbon steel debarking drum. The 10-ft-diameter drum is fabricated from 1⅜-in.-thick steel.

Field repair welds were studied to determine the causes of cracking and to recommend preventative measures

BY J. J. PERDOMO, T. D. SPRY, J. E. INDACOCHEA, A. POLAR, AND F. RUMICHE

Recently, two paper mills reported cracking in their low-carbon steel welds. One incident occurred during an on-site fabrication of a debarking drum (Fig. 1), and the other resulted from emergency repairs to a lime kiln. The events occurred in different occasions using wires from different manufacturers.

The welding of the low-carbon steel welds was done in the horizontal position using E71T-1, 0.052-in.-diameter, flux cored arc welding (FCAW) wire on ASTM A36 plate shell sections ranging from 1⅜ to 1¼ in. thick.

The welding contractors could not identify a cause or remedy for the cracking, and time was lost as the cracked welds were gouged out and rewelded using different brands of flux cored wire or using the shielded metal arc welding (SMAW) process.

The authors conducted an investigation of the welding parameters that produced these cracking problems then developed methods for avoiding cracked welds on future projects.

The Welding Processes

Flux cored arc welding is a semiautomatic process that provides higher deposition rates than SMAW. It has been used extensively since 1972 for numerous fabrications, including pressure vessels.

The FCAW process is similar to gas metal arc welding (GMAW), where a solid wire is continuously fed through the machine in the presence of a shielding gas. With a FCAW wire, a powdered metal and mineral flux core provides additional shielding by forming a slag layer on top of the deposited weld metal to make sound welds with the appropriate chemistry. De-

JORGE J. PERDOMO (jorge.perdomo@shell.com) was with Smurfit-Stone Container Corp., Carol Stream, Ill., at the time this work was conducted. He is currently with the Downstream Pressure Equipment Integrity Group at Shell Global Solutions, Houston, Tex. THOMAS D. SPRY is with Smurfit-Stone Container Corp., Carol Stream, Ill. J. ERNESTO INDACOCHEA, ALBERTO POLAR, and FRANCISCO RUMICHE are with the University of Illinois, Dept. of Civil and Materials Engineering, Chicago, Ill.

Table 1 — Field Weld Conditions

Equipment	Thickness [in. (cm)]	E71T1 Manufacturer	%w Boron Content	Preheat Temp.	Performance
Debarking Drum	1⅜ (3.5)	No. 1	0.0077	250°F (121°C)	Cracked
Debarking Drum	1⅜ (3.5)	No. 2	0.0034	250°F (121°C)	No Cracks
Kiln Shell	1¼ (3.2)	No. 4 (a)	0.0082	300°F (149°C)	Cracked
Kiln Shell	1¼ (3.2)	No. 3	0.0056	300°F (149°C)	No Cracks

(a) All field welds were carried out with 75% argon and 25% CO_2, with the exception of this particular weld repair, for which the contractor used 100% argon.

pending on the specific type of wire, FCAW can even be used without a shielding gas. This is particularly useful in the field where GMAW may not work well because the shielding gases can be swept away by high winds.

Welding of low-carbon steels is usually straightforward, and most contractors who conduct field repairs are familiar with it. The primary concern with carbon steel welding of thick sections is the presence of moisture, which can produce delayed hydrogen-induced cracking in thick sections. This type of cracking occurs after the welds cool. The cracks are longitudinal. In contrast, the debarking drum and lime kiln weld cracks were transverse to the weld and were detected while the weld metal was still hot — Fig. 2. In both field repairs, the joint design consisted of a double-V where 80% of the weld was performed from the inside. A fair amount of preheat was also used. Table 1 summarizes the conditions under which welding was performed.

Method

Weld samples were analyzed for the chemical composition of deposited welds using optical emission spectroscopy (OES). It was found that both flux cored wires that produced cracks had about 0.008% boron (Table 1). Hardness evaluations of both cracked weld samples showed regions of increased hardness in the weld metal, with hardnesses ranging from 253 to 412 HVN (~23 to 43 HRC), which the authors suspected was caused by the presence of boron, which is known to increase hardenability in low-carbon steels.

A metallographic evaluation of the microstructures showed the presence of bainite and martensite, which is consistent with the hardness measurements obtained (Ref. 1). The cracks were both transgranular and intergranular in nature — Fig. 3.

Boron is used as a microalloying element to improve the strength of low-carbon steels, and its amount is not specified by AWS A5.20/A5.20M:2005, *Specification for Carbon Steel Electrodes for Flux Cored Arc Welding,* that details this wire.

Small amounts of boron can cause localized excessive hardening (Ref. 2). Boron is added to fully killed steels to improve hardenability and it is typically limited to 0.003% max (Ref. 3).

Fig. 2 — Shown is a radiograph of one of the cracks detected in a circumferential weld in the debarking drum shown in Fig. 1.

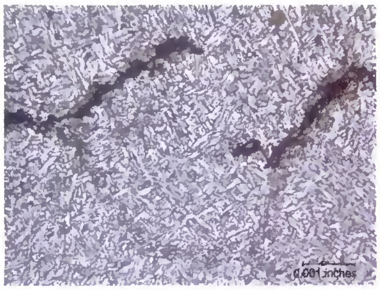

Fig. 3 — Shown is the martensitic and bainitic microstructure of the cracked weld shown in Fig. 2 (manufacurer No. 1). The crack is both transgranular and intergranular.

Table 2 — Welding Voltages and Currents Recommended by Each FCAW Wire Manufacturer Using 75% Argon and 25% CO_2 Shielding Gas Mixture and 0.052-in. (0.13-cm) Diameter Wire

Manufacturer	AWS A5.20	Voltage/[V]	Current/[A]
No. 1	E71-T1	28	300
No. 2	E71-T1	23	220
No. 3	E71-T7(b)	24	400
No. 3	E71-T1	29	295
No. 4	E71-T1	30	325
No. 4-100% Ar(c)	E71-T1	30	325
No. 5	E71-T1	27	225

(b) This wire does not require shielding gas and it was 0.078 in. (0.19 cm) diameter.
(c) This wire was tested with 100% argon as in the cracked field repair.

Follow-up Studies

During follow-up studies, the authors learned that one of the sites had used 100% argon (Ar) as the shielding gas, which is not specified for this wire, in addition to the 0.008% boron present in the weld metal (Table 1).

The chemistry of flux cored wires is balanced for a specific shielding gas — either 75%Ar/25%CO_2 or 100%CO_2 (which is reactive and alters the chemistry). The use of 100%Ar for this type of weld resulted in higher hardness and tensile strength with lower toughness.

The flux cored wires from five different manufacturers were evaluated, including the wires that had been used successfully in other field repairs. The evaluation consisted of welding ASTM A 36, 1½-in.-thick plate using a double-V groove to achieve fusion and a complete penetration weld using 0.052-in.-diameter wire in the flat position. The welds were carried out with a 250°F preheat using 75%Ar/25%CO_2 with the recommended voltages and currents per each wire manufacturer (Table 2). However, one of the wires that had been field welded using 100%Ar was also tested under this condition and the results compared to using 75%Ar/25%CO_2 gas. The chemical compositions of the deposited weld metals were measured using OES.

The Rockwell hardnesses of the welds were also measured. Finally, guided transverse bend tests in accordance to the *ASME Boiler and Pressure Vessel Code,* Section IX, were performed. The results of these tests are summarized in Table 3.

The flux cored wires that did not crack in field repairs contained boron below ~0.006% (Table 1). We found that the traditional transverse bend tests, using the welded coupon approach described, were unable to reproduce the cracking observed in the field welds made with higher-boron-content weld metals.

Considerably softer hardnesses (asso-

Table 3 — Average Weld Hardness (HRB) and Chemical Analysis by Optical Emission Spectroscopy of Deposited Weld Metals in Test Coupons

Manufacturer	AWS A5.20	HRB	C	Si	Mn	B	P	S	Mo	Cr	Al	Ni	Cu
No. 1	E71-T1	91	0.07	0.60	1.60	0.0077	0.009	0.015	0.01	0.05	NA	0.01	0.05
No. 2	E71-T1	90	0.07	0.68	1.51	0.0034	0.014	0.012	0.01	0.05	0.01	0.04	0.03
No. 3	E71-T7(b)	84	0.21	0.27	0.75	0.0005	0.007	0.004	0.01	0.02	1.10	0.01	0.04
No. 3	E71-T1	94	0.08	0.82	1.54	0.0056	0.012	0.012	0.01	0.04	0.01	0.02	0.03
No. 4	E71-T1	92	0.07	0.78	1.45	0.0046	0.013	0.008	0.01	0.05	0.01	0.02	0.05
No. 4-100% AR(c)	E71-T1	96	0.08	1.01	1.85	0.0082	0.009	0.012	0.01	0.04	0.01	0.02	0.01
No. 5	E71-T1	92	0.05	0.01	1.58	0.0050	0.010	0.011	0.01	0.04	0.02	0.02	0.09

(b) This wire does not require shielding gas.
(c) This wire was tested with 100% argon as in the cracked field repair.

ciated with softer microstructures) were obtained as shown in Table 2. The only test weld that actually failed the transverse bend test was the one made with 100%Ar (Manufacturer No. 4). When the chemistry of a flux cored wire is balanced for use with a reactive gas like 75% Ar/25% CO_2 or 100% CO_2 (as for E71T-1), using 100% Ar can lead to higher manganese (1.75% max) and silicon (1.01 max) levels than specified for E711-T1 (AWS A5.20), resulting in higher hardness, tensile strength, and lower toughness. Typically, 75% Ar/25% CO_2 will produce higher hardness welds than with 100% CO_2.

From our discussions with flux cored wire manufacturers, we learned that most weldability tests are conducted in thinner materials. It is only when doing field welds on thicker materials, where the levels of restraint and residual stresses are larger, that the problems of high boron content are encountered. In the case of the test results reported in Table 2, the authors believe that the amount of restraint experienced during the field repairs is considerably larger than that obtained for the welded test coupons.

Conclusions and Recommendations

The authors concluded that the cracking in some of the field repair welds was caused by excessive hardening of the welds promoted by the high levels of boron (> 0.006%), as well as the high degree of restraint, material thickness, shielding gas chemistry, and amount of preheat used. The authors raised their concerns to the weld wire manufacturers as well as to AWS standards-writing committee members so that boron content can be controlled.

The authors suggest that carbon steel flux cored wire be purchased with a maximum boron content of 0.003%. Weld wire spools are identified by a heat number. When requested, the manufacturer for an additional cost, can supply the chemical analysis for the specific spool of weld wire. Higher boron contents can be considered for repairs depending on other factors such as thickness, degree of restraint, and the amount of preheat used. ♦

Acknowledgments

The authors want to express immense gratitude to RICON Welding, Crossett, Ark., for providing the welded coupons for these studies.

References

1. Chaveriat, P. F., Kim, G. S., Shah, S., and Indacochea, J. E. 1987. Low-carbon steel weld metal microstructures: The role of oxygen and manganese. *J. Materials Engineering*, Vol. 9, No. 3, pp. 253–267.

2. Lee, H. W. 2006. The relationship between boron content and crack properties in FCAW deposited metal. *Welding Journal* 85(6): 131-s to 136-s.

3. Davis, J. R. 2001. *Alloying, Understanding the Basics*. ASM Int'l, Metals Park, Ohio, p. 140.

Filtration System Saves by Keeping the Air Inside

Heating and air conditioning efficiency were improved with a system that filters the air and recycles it, rather than exhausting it to the outside

Example of modular air filtration system at F&P Georgia, an automotive parts supplier.

Clean air should be a design consideration for new facilities, and the focus should be at the source of smoke and pollutants. Today, smoke, dust, oil mist, and other production pollutants can be efficiently collected and cleaned through modular air filtration systems that also can suppress fires.

In the past, some facilities that produced airborne pollutants simply collected and exhausted the dirty air to the outside. While acceptable to OSHA standards, this approach is not efficient for it wastes heating, air conditioning, and electric power.

"Most companies today don't have the in-house expertise to spec the kind of air collection and filtration systems they need on the line," said Glen Tuplin, facilities manager at F&P Georgia, a manufacturer of components for Honda and Nissan. A manufacturer of subframe and suspension components, the firm has extensive welding, stamping, and painting operations within its 200,000-sq-ft facilities in Rome, Ga.

Coinciding with plant expansion in 2003, Tuplin decided to install a new modular air filtration system from Clean Air America. That system promised to do a better job of maintaining plant air quality and cutting costs.

Keeping the Air Inside

"Heating and air conditioning costs are about \$2.00 ft^3/min and \$4.00 ft^3/min, respectively," Tuplin explained. "Our exhaust total air volume was 103,000 ft^3." Because the new air filtering system filtered and returned plant air rather than exhausting it to the outside, there was a potential savings of \$200,000 annually.

The configuration of the new air filtration system consists of modular hoods for the welding cells, quick-clamp-style ducting, and patented dust collectors to filter and return the air to the plant. The system is engineered to draw smoke, dust, and aerosols as near as possible to the source.

Fire Suppression

Many different plant operations produce dust, aromatics, oil mists, and other flammable substances. In the presence of sparks, they are an open invitation to internal fires. For that reason, Tuplin had a fire suppression system included with the air filtration system.

"We use a stamping oil during our stamping operation," Tuplin explained. "When the metal is welded, the aerosols mix with the oxides and are drawn up into the smoke handling units. There is the possibility that this 'dust' can be ignited by an uncontrolled welding spark."

Protection is provided with baffling, change of air velocity, and other mechanical means. This system also uses a fire-extinguishing agent Dupont FE-25, which is a very quick suppressant.

Conserve Power and Filters

The air filtration system installed at F&P Georgia uses variable-frequency drive (VFD) to control blowers and help maintain filters.

With VFD, the system uses less power because it only draws the current that is necessary to maintain the desired airflow.

The modularity of the system design and installation enables plants to change their air filtration systems as production operations change.

Tuplin indicated the payback on this system was about one year, and the facility has become a Honda benchmark plant for clean air quality.◆

Information provided by Clean Air America, Inc., Rome, Ga., www.clean-air.com.

Building Submarine Components from Duplex Stainless Steels

BY R. GORDON MURRAY AND
NORMAN COOPER

Fig. 1 — An artist's conception of the UK Astute class submarine.

Exhaustive testing confirmed the value of using a 3%NiCrMo alloy for a specialized marine application

For the UK's *Astute* class submarine (Fig. 1) contract, design changes resulted in the introduction of duplex stainless steel base metal for a certain submarine component. This alloy had to be welded to itself and also welded to Q1N, a quenched and tempered low-alloy steel (derived from the U.S. Alloy HY80). Q1N is a 3%NiCrMo alloy used in the UK for all submarine pressure hull manufacture. This change necessitated the introduction of a duplex stainless welding consumable that is fully compliant to Category 1-4 of UK Naval Engineering Standard NES 770, Part 2, *Approval of Welding Procedures for Submarine Construction* (Ref. 1).

Evaluation of Welding Consumables

Some initial welding development work carried out during the 1990s had

R. GORDON MURRAY (gordon.murray@baesystems.com) *is principal welding engineer, and NORMAN COOPER is TPSD manager at BAE Systems, Barrow-in-Furness, UK.*

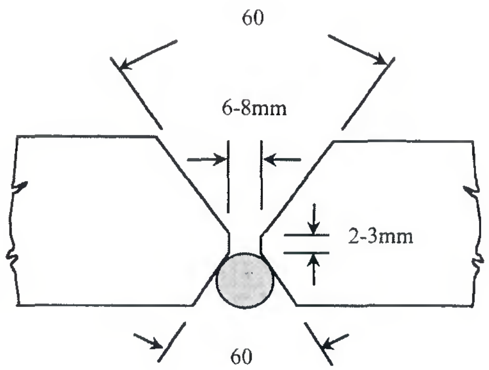

Fig. 2 — Weld preparation used for the test panels.

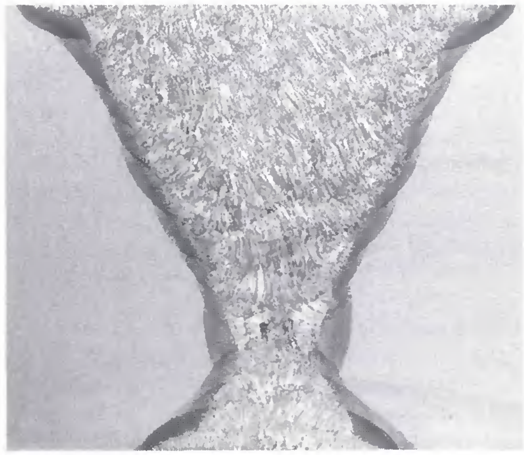

Fig. 3 — A macrosection of a Q1N test panel welded with SAF LEXAL T 22.9.3N consumable.

identified two welding consumables that offered good all-position weldability and excellent mechanical properties with the potential for successfully passing crack tip opening displacement (CTOD) and flawed bulge explosion (FBE) testing to conform to the UK Ministry of Defense MOD(N) standard.

One consumable was a solid wire gas metal arc type; the other was a flux cored arc welding (FCAW) wire.

BAE Systems preferred to use the FCAW process since all of its in-house welding equipment has that capability. Following several weldability trials, the FCAW wire was selected for development and testing purposes. This consumable was supplied by La Soudure Autogène Francaise (SAF), and specified as 1.2-mm-diameter LEXAL T 22.9.3N (nominally 22% Cr-9% Ni-3% Mb) for use with 80% argon-20% CO_2 shielding gas.

Following discussions with QinetiQ (a U.K. research and development agency) and SAF welding engineers, it was concluded that there was no major risk of CTOD failure due to the partly austenitic content of as-deposited weld metal. Similarly, QinetiQ advised that the enhanced austenite content (compared to ferritic Q1N consumables) should indicate a high probability of success in the onerous flawed bulge explosion testing testing. It was agreed with QinetiQ and the Defense Procurement Agency that the standard NES 769 (Ref. 2) minimum Charpy absorbed energy value of 50 J at –50°C required for ferritic Q1N weld consumables was both a) unlikely to be achieved, and b) could be waived as the consumable was partially austenitic. The recorded weld metal Charpy test results were recorded, therefore, for information only.

Also, this was further supported by FCAW duplex welding development initiated by Ministry of Defence (Naval) in the mid-1990s, which provided informal evidence that lower (than traditional ferritic values) Charpy results for FCAW duplex consumables could result in very satisfactory CTOD and FBE results.

The determining factor in weld procedure development was to ensure that the heat input was kept below 1.5 kJ/mm (Ref. 3), as SAF recommended this level to ensure the minimum weld metal 0.2% proof stress value of 550 Mpa was obtained. The root run weld exceeded this heat input value, but was completely removed by backgrinding on the second side.

Table 1 — Typical Welding Parameters Recorded on Test Panels

Side	Run No.	Amps	Volts	Travel Speed mm/min	Heat Input kJ/mm
1	Root	140–150	21–23	60–80	3.5 max typical
1&2	Fill & cap	150–180	22–23	170–220	0.9–1.5

Note: All tests used the FCAW process, 1.2-mm SAF LEXAL T22.9.3 N wire, direct current electrode positive, and shielding gas 80% argon-20% CO_2 with a flow rate of 14–20 L/min.

Weld Procedure Testing

A full welding procedure test program as agreed with QinetiQ was developed. In total two Q1N panels and two 2507 type superduplex stainless steel (UNS S32760, proprietary name Bohler A911SA) panels were welded, prepared as shown in Fig. 2. All welds were completed in the uphill position using the semiautomatic FCAW process. The typical welding parameters recorded during trials are shown in Table 1.

In total, approximately 5 m of weld were made and 55 kg of weld metal were deposited during these trials. The nondestructive examination, which consisted of 100% visual, 100% dye penetrant, and 100% radiography, confirmed that no recordable defects were present in these test panels.

Subsequent to NDE, all panels were sectioned and subjected to mechanical testing as described in NES 770, Part 2, including Charpy V-notch, tensile, static CTOD, and FBE tests.

The standard mechanical tests were done by BAE Systems Technical Production Services Dept., the static CTOD tests were performed by Bodycote; and the FBE tests at QinetiQ, Dunfermline, UK.

The complete mechanical test program for the test panels met NES 770, Part 2, requirements, and the formal Ministry of Defence (Naval) approval of LEXAL T 22.9.3N was obtained.

The welding of duplex to duplex and duplex to Q1N was performed successfully on production components by BAE Systems. The main butt joint welds met the BAE 773 specification (Ref. 4), which is the contractual NDE acceptance standard, with no weld repairs following NDE, which included visual, dye penetrant, and radiographical inspections. Figure 3 shows a macrosection of a Q1N test panel welded with SAF LEXAL T 22.9.3N consumable.

References

1. UK Naval Engineering Standard NES 770, Part 2, *Approval of Welding Procedures for Submarine Construction.*

2. UK Naval Engineering Standard, NES 769, *Welding Consumables for Structural Steels — Approval Procedure.*

3. SAF Technical Report 15157503 LEXAL. La Soudure Autogène Francaise.

4. BAE Specification 773, *Minimum NDE Acceptance Standards for Welds (Astute Class Submarines).*

NOTE: A DIAMOND (♦) DENOTES AN AWS-SPONSORED EVENT.

♦**FABTECH International & AWS Welding Show.** Oct. 31–Nov. 2, Georgia World Congress Center, Atlanta, Ga. This show is the largest event in North America dedicated to showcasing a full spectrum of metal forming, fabricating, tube and pipe, and welding equipment and technology. Contact American Welding Society, (800/305) 443-9353, ext. 462; or visit *www.aws.org*.

♦**Quality Control in Welding Conference.** Nov. 1, Atlanta, Ga., at the FABTECH International & AWS Welding Show. Contact American Welding Society, (800/305) 443-9353, ext. 462; or visit *www.aws.org/conferences*.

♦**Spot Welding Conference.** Nov. 2, Atlanta, Ga., at the FABTECH International & AWS Welding Show. Contact American Welding Society, (800/305) 443-9353, ext. 462; or visit *www.aws.org/conferences*.

16th IAS Rolling Conference and 3rd Conf. on Uses of Steel. Nov. 6–9, Hotel Colonial, San Nicolãs, Buenos Aires, Argentina. Presentations in English. Sponsored by Instituto Argentino de Siderurgia (IAS). Contact *www.siderurgia.org.ar.*

MetalForm Mexico. Nov. 7–9, Centro Banamex, Mexico City, Mexico. Visit *www.metalform.com*, or e-mail *marcela.ordaz@giprex.com*.

Aerospace Testing Expo North America. Nov. 14–16, Anaheim Convention Center, Anaheim, Calif. For information, visit *www.aerospacetesting-expo.com/northamerica/contact.html*.

ShipTech 2007. Jan. 30, 31, Beau Rivage Resort, Biloxi, Miss. Cosponsored by ManTech, ONR Mfg. Technology Program, Nat'l Shipbuilding Research Program. Visit Web site for admission requirements. Contact: *www.nmc.ctc.com*.

Friction Stir Welding and Processing IV Symposium, and TMS Fall Meeting. Feb. 21–March 1, 2007. Orlando, Fla. Sponsored by The Minerals, Metals & Materials Society. Contact *www.tms.org*.

ILSC® 2007, Int'l Laser Safety Conference. March 19–22, Airport Marriott, San Francisco, Calif. Contact *www.laserinstitute.org/conferences/ilsc*.

MetalForm. March 25–28, 2007, Donald E. Stephens Convention Center, Rosemont, Ill. Sponsored by Precision Metalforming Assn. Visit *www.metalform.com*.

World Trade Fair for Industrial Technology. April 16–20, 2007, Hannover Fairgrounds, Hannover, Germany. Organized by Deutsche Messe AG. Visit *www.messe.de*.

ALUMEX 2007, 4th Int'l Aluminum Exhibition. April 22–24, 2007, Dubai Int'l Convention Center, Dubai, U.A.E. Contact *www.alumexdubai.com*.

14th Int'l Conf. on the Joining of Materials (JOM-14), and 5th Int'l Conf. on Education in Welding. April 29–May 2, 2007, LO-Skolen, Helsingör, Denmark. E-mail contact: *jom_aws@post10.tele.dk.*

XXXVIII Int'l Steelmaking Seminar. May 20–23, 2007, Belo Horizonte, Minas Gerais, Brazil. Sponsored by ABM (Associação Brasileira de Metalurgia e Materials). Papers will have simultaneous translations in English and Portugese. Visit: *www.abmbrasil.com.br/seminarios.*

♦8th Int'l Conf. on Brazing, High-Temperature Brazing, and Diffusion Bonding (LÖT 2007). June 19–21, 2007, Aachen, Germany. Cosponsors include American Welding Society and ASM Int'l. Contact the German Welding Society (DVS), *tagungen@dvs-hg.de; www.dvs-ev/loet2007.*

Southeast Asia Wire and Tube Trade Fairs. Oct. 16–18, 2007, Bangkok, Thailand. Contact Messe Düsseldorf North America, *info@mdna.com; www.mdna.com.*

Educational Opportunities

Welding Fabricator Certification Criteria. Dec. 6, 7. **Design of Experiments for the Shop Floor.** February 15, 16. Courses held in downtown Chicago. Contact Atema at (312) 861-3000 or visit *www.atemasolutions.com.*

Boiler and Pressure Vessel Inspectors Training Courses and Seminars. Columbus, Ohio. Contact Richard McGuire, (614) 888-8320, *rmcguire@nationalboard.org, www.nationalboard.org.*

CWI/CWE Course and Exam. This 10-day program prepares stu-

Circle No. 45 on Reader Info-Card

Circle No. 26 on Reader Info-Card

Circle No. 21 on Reader Info-Card

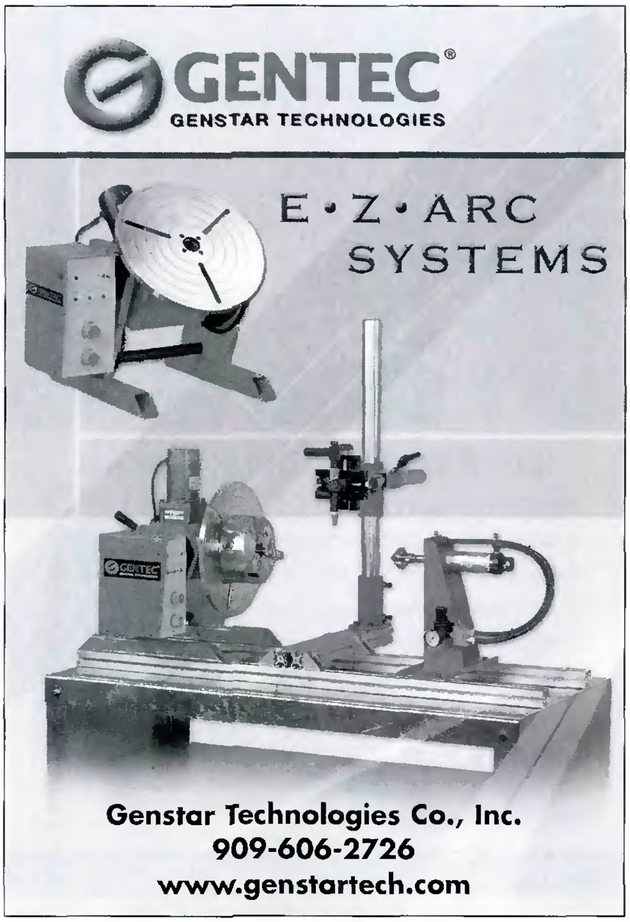

Circle No. 25 on Reader Info-Card

dents for the AWS CWI/CWE exam. For schedule and entry requirements, contact Hobart Institute of Welding Technology (800) 332-9448, *www.welding.org*.

CWI Preparation. Courses on ultrasonic, eddy current, radiography, dye penetrant, magnetic particle, and visual at Levels 1–3. Meet SNT-TC-1A and NAS-410 requirements. On-site training available. T.E.S.T. NDT, Inc., 193 Viking Ave., Brea, CA 92821; (714) 255-1500; *ndtguru@aol.com*; *www.testndt.com*.

CWI Preparatory and Visual Weld Inspection Courses. Classes presented in Pascagoula, Miss., Houston, Tex., and Houma and Sulphur, La. Course lengths range from 40 to 80 hours. Contact Real Educational Services, Inc., (800) 489-2890; *info@realeducational.com*.

EPRI NDE Training Seminars. EPRI offers NDE technical skills training in visual examination, ultrasonic examination, ASME Section XI, and UT operator training. Contact Sherryl Stogner, (704) 547-6174, e-mail: *sstogner@epri.com*.

Fabricators and Manufacturers Assn., and Tube and Pipe Assn. Courses. Contact (815) 399-8775; *www.fmametalfab.org*; *info@fmametalfab.org*.

Hellier NDT Courses. For schedule of courses, contact Hellier, 277 W. Main St., Ste. 2, Niantic, CT 06357, (860) 739-8950, FAX: (860) 739-6732.

Machining and Grinding Courses. Contact TechSolve at *www.TechSolve.org*.

Machine Safeguarding Seminars. Contact Rockford Systems, Inc., PO Box 5525, Rockford, IL 61125, (800) 922-7533; FAX: (815) 874-6144; *www.rockfordsystems.com*.

Circle No. 42 on Reader Info-Card

Circle No. 12 on Reader Info-Card

EWI Facilitates Implementation of Electronic Welding Data Maintenance System at Rock Island Arsenal Technology Center

EWI has recently facilitated the deployment of an electronic welding data management system called *WeldEye*™ at Rock Island Arsenal Joint Manufacturing and Technology Center (RIA JMTC) under the U.S. Army ARDEC Research, Development and Engineering Center (ARDEC) funded program called Advanced Welding Technology Deployment Initiative (AWTDI).

WeldEye™ is a Web-based software application capable of complete documentation of welding procedures, personnel qualifications, quality inspections, and management of welded fabrications by creating full electronic traceability. It has been developed by Weldindustry, Stord, Norway.

The AWTDI focuses on producing lightweight prototype structures to support U.S. Army weapons systems development. As a part of this initiative, Edison Welding Institute (EWI) was asked to work with RIA JMTC to identify a tool to manage (arc) welding procedure specifications (WPSs) supporting the manufacturing of M119 howitzers — Fig. 1.

Although a number of such commercial tools are available, the customizability and Web-accessibility of *WeldEye*™ made it particularly appealing.

The software package is also utilized by defense contractor General Dynamics Electric Boat (GDEB) for tracking WPSs. Electic Boat makes approved versions of procedures available to all trade skills and staff for reference at all of their facilities including Quonset Point, R.I., Norfolk, Va., and Puget Sound, Wash.

After an in-depth training program and pilot testing of *WeldEye*™, EWI deployed the software at RIA JMTC (internally).

With assistance from EWI, the RIA JMTC thoroughly evaluated *WeldEye*™ and selected it as their weld data management software package. As of the date of this article, RIA had inputted 600–700 multipage WPSs into *WeldEye*™ and released approved versions for M119 production.

In February 2006, the Prototype Manufacturing Team at Picatinny Arsenal (PICA) began using *WeldEye*™ through a remote, secure access to EWI's installation of the software. Picatinny Arsenal is interested in tracking gas metal arc welding (GMAW) procedures for fabrication of titanium structures in support of the Future Combat System Program. EWI continues to provide engineering support to RIA JMTC and PICA under the AWTDI program.

The primary benefits of using the *WeldEye*™ welding procedures module are a) simultaneous access to data for multiple users through an intra- or internet, b) producing, publishing, and issuing new welding procedures efficiently (nearly 80% faster), c) ease of revising, publishing, and reissuing existing procedures (nearly 95% faster), d) reduced cost and risk associated with the loss of hard copies of welding procedures or qualification data, e) a means of searching the database for combinations of qualification data that might support the development of a procedure without additional qualification testing, f) customizability of welding procedure templates to meet both commercial and U.S. military welding standards, and g) quality benefits with regard to compliance and audit.

For information on other capabilities of *WeldEye*™, contact Candice Mehmetli at (614) 688-5180, *cmehmetli@ewi.org*, or Suhas P. Vaze at (614) 688-5127, *svaze@ewi.org*.

Fig. 1 — Soldiers from the 7th Field Artillery Regiment, 25th Infantry Division (Light), position an M119 Howitzer near Forward Operating Base Cobra during Operation Crackdown in Afghanistan.

NJC Operated by EWI

The Navy Joining Center
1250 Arthur E. Adams Dr.
Columbus, OH 43221
Phone: (614) 688-5010
FAX: (614) 688-5001
e-mail: *NJC@ewi.org*
Web site: *www.ewi.org*
Contact: Larry Brown

Mark Your Calendar

Friction Stir Welding Technology for Defense Applications Workshop

The third in a series of friction stir welding workshops will be held February 21, 22, 2007, at EWI in Columbus, Ohio. This workshop is sponsored by the Navy Manufacturing Technology Program, Office of Naval Research, and organized by the Navy Joining Center and Navy Metalworking Center.

This workshop will provide industry and the Department of Defense with the latest advancements in the development and implementation of friction stir welding technolgy for defense applications.

Due to ITAR restrictions, workshop participation is limited to U.S. citizens with an approved DD2345.

For further information or to register for this conference, contact Connie Kotula at (614) 688-5156, or email at *connie_kotula@ewi.org*.

SOCIETY NEWS

BY HOWARD M. WOODWARD

IIW Annual Assembly Meets in Québec

The 59th Annual Assembly of the International Institute of Welding (IIW) was held Aug. 27–Sept. 2 at the Convention Centre in Québec City, Canada. The event drew about 400 participants representing 37 countries.

IIW President **Chris Smallbone** opened the meeting. **David E. H. Reynolds** delivered the welcome address on behalf of the Canadian Organizing Committee. The opening ceremony was followed by a folkloric presentation performed by the Painchaud Family and Folk Dancers.

The 11th International Symposium was opened by **Jeffrey Packer** of Canada who presented the Houdremont Lecture, "Tubular brace member connections in braced steel frames." Eighty-three papers were presented in ten sessions. **Vic Matthews,** AWS vice president, presented a well-received paper on the Image of Welding and what AWS has achieved over the years in this important area.

Another highlight of the Assembly was the presentation of awards to the industry's leaders and high achievers in the worldwide welding community.

AWS President and IIW Vice President **Damian J. Kotecki** presented the Thomas Medal to **Detlef von Hofe** of Germany. **Arno Aryus** of Germany received the André Leroy Prize; **Luigi Cimolai** of Italy earned the Ugo Guerrera Prize.

The Henry Granjon Prize winners included (Category A) **Henrikki Pantsar** of Finland, and **Wei Zhang** of the U.S.; (Category B) **Timothy Anderson** of the U.S.; (Category C) **Angelique Lasseigne** of the U.S.; and (Category D) **Jeffrey Sowards,** U.S. The Arthur Smith Award was presented to **Adolf Hobbacher** of Germany. **Taransakar DebRoy,** U.S., received the Yoshiaki Arata Award, and **Bertil Pekkari** of Sweden was presented the Edström Medal.

This year's Paton Prize was awarded to **Allan Sanderson** of the U.K.

The Edison Welding Institute (EWI) was admitted to the IIW as a new Member Society.

Others representing the AWS at the event included Vice Presidents **Jerry Uttrachi** and **Gene Lawson; Tom Mustaleski,** a past president and chairman of the American Council; **Ray Shook,** executive director; **Andrew Davis,** managing director, technical services; and **Steve Hedrick,** manager, safety and health.

The next IIW Annual Assembly will be held July 1–8, 2007, in Dubrovnik/Cavtat, Republic of Croatia. ♦

AWS President Damian Kotecki presented the Thomas Medal at the IIW Assembly.

Aerospace Firm Opts for Sustaining Membership

The TA Aerospace facility, Valencia, Calif., recently joined the Society after discussing and evaluating the benefits of becoming an AWS Sustaining Member Company with **Jack Compton,** District 21 director.

While working at the company's facilities training its welders to use the gas tungsten arc process for joining stainless steels, Compton pointed out to the company's executives how the firm could benefit from acquiring the AWS library of technical literature and standards. He then described how the Sustaining Company level of membership included the 170 standards, ten individual memberships for its employees, plus other perks that make the Sustaining Member program a financially attractive package. The company specializes in engineered high-temperature elastomers and clamps. Its Fastblock® fire-barrier and insulation materials are widely used throughout the aerospace industry. ♦

Shown with their AWS Sustaining Company Member plaque and technical library documents are (standing, from left) TA Aerospace welders Angelica Serrano, Steve Bennett, Jose Euran, and Jose Medina; (front, from left) Production Manager Pete Aguilar, Personnel Director Kelly Ford, and Jack Compton, District 21 director.

Tech Topics

TECHNICAL COMMITTEE MEETINGS

All AWS technical committee meetings are open to the public. To attend a meeting, call (800/305) 443-9353, at the extension listed.

Nov. 1, B1 Committee on Methods of Inspection. Atlanta, Ga. Contact: B. McGrath, ext. 311.

Nov. 1, D15C Subcommittee on Track Welding. Atlanta, Ga. Contact: S. Morales, ext. 313.

Nov. 1, D16 Committee on Robotic and Automatic Welding. Atlanta, Ga. Contact: J. Gayler, ext. 472.

Nov. 2, D10 Committee on Piping and Tubing. Atlanta, Ga. Contact: B. McGrath, ext. 311.

Nov. 2, D10U Subcommittee on Orbital Pipe Welding. Atlanta, Ga. Contact: B. McGrath, ext. 311.

Nov. 2, D10V Subcommittee on Welding High Strength Piping and Tubing. Atlanta, Ga. Contact: B. McGrath, ext. 311.

Nov. 2, 10Y Subcommittee on Duplex Pipe Welding. Atlanta, Ga. Contact: B. McGrath, ext. 311.

Nov. 9, B2F Subcommittee on Plastic Welding Qualifications. Las Vegas, Nev. Contact: S. Hedrick, ext. 305.

Nov. 9, G1A Subcommittee on Hot Gas Welding and Extrusion Welding. Las Vegas, Nev. Contact: S. Hedrick, ext. 305.

Dec. 5, 6, Safety & Health Committee. Miami, Fla. Contact: S. Hedrick, ext. 305.

Standards for Public Review

AWS was approved as an accredited standards-preparing organization by the American National Standards Institute (ANSI) in 1979. AWS rules, as approved by ANSI, require that all standards be open to public review for comment during the approval process. The following standards are submitted for public review. Order draft copies from **Rosalinda O'Neill,** (800/305) 443-9353, ext. 451; *roneill@aws.org.*

A5.30/A5.30M:200X, *Specification for Consumable Inserts. Revised — $25. 10/30/06.*

A10.1M:200X, *Specification for Calibration and Performance Testing of Secondary Current Sensing Coils and Weld Current Monitors Used in Single Phase AC Resistance Welding. New — $35.50. 10/30/06.*

C5.7:2000 (R200X), *Recommended Practices for Electrogas Welding. Reaffirmed — $29.50. 10/16/06.*

D8.8M:200X, *Specification for Automotive Weld Quality — Arc Welding of Steel. Revised — $27.00. 10/23/06.*

Interpretation

AWS D1.1:2002, *Structural Welding Code — Steel*

Subject: Welder Qualification — Pipe Diameters Qualified

Code Edition: D1.1:2002
Code Provision: Tables 4.9 and 4.10
AWS Log: D1.1-02-I06 (INQ-29)

Inquiry: For a welder who is qualified by a plate groove test, what diameter of pipe is the welder qualified to weld fillet welds and PJP welds?

Response: A welder qualified by a plate groove test is also qualified to weld fillet welds on all diameters of pipe and PJP welds over 24-in. diameter within the position and thickness limitations of Tables 4.9 and 4.10.

Standards Approved by ANSI

D9.1M/D9.1:2006, *Sheet Metal Welding Code.* Approved: 7/25/06.

D16.2M/D16.2:2007, *Guide for Components of Robotic and Automatic Arc Welding Installations.* Approved: 8/25/06.

A5.15-90 (R2006), *Specification for Welding Electrodes and Rods for Cast Iron.* Reaffirmed: 9/11/06.♦

Member-Get-A-Member Campaign

Listed are the members participating in the 2006–2007 Campaign for the period June 1, 2006, through May 31, 2007. See page 49 for rules and the prize list. Call the Membership Dept. (800/305) 443-9353, ext. 480, for information about your status as a member proposer.

Winner's Circle

AWS Members who have sponsored 20 or more new members, per year, since 6/1/1999. The superscript denotes the number of times Winners Circle status has been earned if more than once.

J. Compton, San Fernando Valley[6]
E. H. Ezell, Mobile[4]
J. Merzthal, Peru[2]
G. Taylor, Pascagoula[2]
B. A. Mikeska, Houston
R. L Peaslee, Detroit
W. Shreve, Fox Valley
M. Karagoulis, Detroit
S. McGill, NE Tennessee
T. Weaver, Johnstown/Altoona
G. Woomer, Johnstown/Altoona
R. Wray, Nebraska
M. Haggard, Inland Empire

President's Roundtable

Sponsored 9–19 new members.
L. Taylor, Pascagoula — 17
M. Palko, Detroit — 16
J. Compton, San Fernando Valley — 14
R. Myers, L.A./Inland Empire — 10
R. Ellenbecker, Fox Valley — 9

President's Club

Sponsored 3–8 new members.
R. Wilsdorf, Tulsa — 7
J. Bruskotter, New Orleans — 5
T. Ferri, Boston — 4
G. Taylor, Pascagoula — 4
P. Zammit, Spokane — 4
S. Chuk, International — 3
G. Lau, Cumberland Valley — 3

President's Honor Roll

Sponsored 1 or 2 new members.
R. Gollihue, Tri-State — 2
M. Lamarre, Palm Beach — 2
D. Malkiewicz, Niagara Frontier — 2

Student Member Sponsors

Sponsored 3+ new members.
G. Euliano, NW Pa. — 43
B. Lavallee, Northern N.Y. — 18
W. Younkins, Mid-Ohio Valley — 7
J. Angelo, El Paso — 5
A. Dropik, Northern Plains — 4
D. Kowalski, Pittsburgh — 4
C. Schiner, Wyoming — 4
C. Bridwell, Ozark — 3
D. Combs, Santa Clara Valley — 3
R. Hutchison, Long Bch./Or. Cty. — 3
C. Yaeger, NE Carolina — 3♦

Image of Welding Award Winners Announced

The Fourth Annual Image of Welding Awards will be presented November 2 at the FABTECH International and AWS Welding Show in Atlanta, Ga.

Individual Category Award

Christopher Coble was named the recipient of the Individual Category award. Coble is managing director for the welding program at Environmental Air Systems (EAS). He has modernized the company's welding program by creating an automated identification and tracking system to streamline the management of welding data, procedures, qualifications, and techniques.

AWS Section Category Award

The **Indiana Section,** one of the Society's most active Sections, has consistently been committed to encouraging students and others to get involved in the field of welding. This year, the Section conducted the Indiana SkillsUSA, Indiana State, and the Indianapolis Regional Skills Contests. The Indiana Section also hosts its annual Mid-West Team Welding Competition, the Section's largest event. The competition involves 20 high school welding teams from across Indiana, Kentucky, and Illinois. By conducting contests such as these and encouraging members of the community and local schools to get involved, the Indiana Section has been a true leader in communicating the importance of welding in today's world.

Large Business Category Award

This award, presented to companies with 200 or more employees, is presented to the **Hobart Institute of Welding Technology.** Founded in 1930 as a part of the Hobart Brothers Co., based in Troy, Ohio, the Institute has built its reputation as a first-rate educational institution that began training welders during the World War II era. The success of the school's training programs led to its rapid growth over the last 75 years. The Institute has graduated 85,000 students and is recognized internationally. Additionally, the Institute houses the John H. Blankenbuehler Memorial Library, which includes one of the most comprehensive collections of welding books, research, and related subject materials. The Institute's modern 100,000-sq-ft facility includes 150 welding booths, 13 classrooms, and four laboratories. The Institute's 20 instructors, with collectively 400 years of experience, offer a wide range of welding training, including technical continuing education; specialized training; welder qualification and certification; field training; and full-service arc welding training. The Institute is accredited by AWS, Commission of Career Schools, Colleges of Technology, and the Ohio State Board of Career Colleges and Schools.

Small Business Category Award

This award, presented to companies with less than 200 employees, is presented to **Keville Enterprises, Inc.** Established in 1991, Keville is a full-service construction management and inspection services firm. With 95 employees and 12 offices nationwide, Keville provides both quality control and quality assurance welding inspection services to agencies across 20 states, including Amtrak and the U.S. Postal Service. Keville has been featured in *Construction Journal* magazine and recently, one of its employees was honored by AWS with the Certified Welding Inspector of the Year Award. Keville has shown superior dedication to promoting the Image of Welding throughout its communities by encouraging its employees, many of whom hold various AWS certifications, to get involved. One such example of this is the efforts of Keville's Certified Welding Educators, who provide welding training at the Boston Local 7 Ironworkers Union as well as the Local 56 Pile Drivers Union apprentice training programs. Additionally, the company's Certified Welding Engineers have provided weld inspection training to numerous engineering firms and transportation authorities.

Distributor Category Award

This award is presented to the **Indiana Oxygen Co.** Founded in 1915, the company is one of the oldest gas and hard goods distributors in the United States. From its birth as a small family business, the company has evolved into a highly successful network of nearly 50 warehouses and branches throughout Indiana. It is the official gas supplier for the Indianapolis 500, and operates a garage at the Indianapolis Motor Speedway. As the company continues to thrive in Indiana's welding market, its corporate culture is reminiscent of days long ago. Its associates are encouraged to participate and support AWS local Section activities and the company remains heavily involved in community events promoting welding education, Skills USA, and the Indiana Section's Annual Mid-West Team Welding Competitions.

The Educator Category Award

The Educator Category Award is presented to **Leland Vetter**. Vetter said, "It's really about people, not welding," when he reflected on his successful tenure as a welding instructor at Eastern Wyoming College. At the age of 22 he was asked to build the college's first welding program. Vetter recalled, "I was scared, but I knew one thing for sure — I knew how to weld." And he proved it. Over the years, the program has earned him and the school much acclaim, largely due to its success as a training center for a variety of professionals, not only welders. His approach to teaching in the classroom is compared to that of a demanding boss who expects high-quality workmanship and respect for the work. "We take welding very seriously," Vetter said. "We begin early in the morning and go until early evening. There is no room for students who miss class, come in late, or do not put 100% into their training to be competent welders." Now in its 26th year, the program has been expanded to include machine tooling, hydraulics, and a specialized welding curriculum. Enrollment has grown from 13 to more than 50 students, and most of the instructors are graduates of the program. The welding department is an AWS Accredited Testing Facility. The program has attracted more than $400,000 in donations from private individuals and businesses in the community. Vetter continues to regularly visit local high school vocational students to highlight welding as an attractive career and to stimulate the students to consider getting into the field.

Educational Facility Category Award

The Educational Facility Category Award is presented to **Pipe Fitters Local Union 597 Training Center,** Mokena, Ill. The center is a vast state-of-the-art training facility built on the shore of a lake in the Village of Mokena. The spacious facility is equipped with 100 welding booths, each with its own exhaust system, high-quality coupon-holding fixture, and multiprocess welding machine. The training center also features computer rooms with 40 student stations, a modernized lecture hall, 250-seat auditorium, and a complete HVAC instructional and work areas. It presents courses in SMAW, GTAW, GMAW, and orbital and mechanical pipe welding, with training using numerous metals including aluminum, carbon steel, copper, stainless steel, and titanium. The graduation requirements for apprentices and journeymen are challenging, but with a student-to-instructor ratio of 8 to 1, students are never short of attention. The center is cited for raising the bar in welding education. ♦

New AWS Supporters

Sustaining Company

Wabash Steel, LLC
2007 Oliphant Dr.
Vincennes, IN 47591
www.wabashsteel.biz
Representative: Lori Burgett

Wabash Steel has AISC quality certifications for simple and major steel bridges, along with fracture critical and sophisticated paint coating endorsements. The company fabricates steel girders for highway, railroad, and pedestrian bridges, and fabricates structural steel for truss, arch, and bascule bridges. Specialty work by client request includes items such as railway locomotive platforms.

Educational Institutions

Alaain Training & Developing
King Abdul Azis St.
Azizia, Dammam 31453
Saudi Arabia

Aria Azmoon Sanat
Ground Fl., No. 12
2nd St. N. Kargar St.
Tehran 1413696535 Iran

New England Laborers
Training Trust Fund
37 East St.
Hopkinton, MA 01748

Northwest Technology Center
801 Vo-Tech Dr.
Fairview, OK 73731

Rowan Cabarrus Community College
1333 Jake Alexander Blvd.
PO Box 1595
Salisbury, NC 28146

The Fab School
2001 Third St., Unit E
Riverside, CA 92507

U.S. Army Center and School
Weapons Metalworking Services
107 Plumb Pt. Loop
Aberdeen Proving Ground, MD 21005

Supporting Companies

Custom Engineering Co.
2800 McClelland Ave.
Erie, PA 16510

Industrial Supplier Larey, Inc.
3620 E. 14th St.
Brownsville, TX 78521

Kogok Corp.
4011A Penn Belt Pl.
District Heights, MD 20747

Linde BOC Process Plants, LLC
945 Keystone Ave.
Catoosa, OK 74015

Metalsa S. de R. L.
Carr. Miguel Alemán Km. 16.5 #100
Apodaca, Nuevo Leon 66600
Mexico

Zitadel Ltd.
52/54 Trans-Amadi Rd.
Trans Amadi Ind. Layout,
Port Harcourt, Rivers State
Nigeria

Affiliate Companies

Altair Engineering
1820 E. Big Beaver Rd.
Troy, MI 48083

Armonds Welding Service
100 Chapman Ln.
Carlotta, CA 95528

Bowen Engineering
10315 Allisonville Rd.
Fishers, IN 46038

Delgado Erectors, Inc.
14233 S. Dante
Dolton, IL 60419

Gem State Mfg., Inc.
PO Box 987
Caldwell, ID 83606

Shearer & Associates
107 Evangeline Dr.
Slidell, LA 70460

Southernmost Welding & Fabrication
25 Tamarind Dr.
Key West, FL 33040

Tishler Industries, Inc.
1 Barton St.
St Louis, MO 63104♦

Membership Counts

Member Grades	As of 10/1/06
Sustaining	456
Supporting	263
Educational	384
Affiliate	359
Welding distributor	49
Total corporate members	**1,511**
Individual members	44,987
Student + transitional members	4,619
Total members	**49,606**

Nominations Sought for Prof. Koichi Masubuchi Award

Nominations are sought for the 2007 Prof. Koichi Masubuchi Award, sponsored by the Dept. of Ocean Engineering at Massachusetts Institute of Technology. It is presented each year to one person who has made significant contributions to the advancement of materials joining through research and development.

The candidate must be 40 years old or younger, may live anywhere in the world, and need not be an American Welding Society member. The nomination package should be prepared by someone familiar with the research background of the candidate. It should include a résumé and at least three letters of recommendation from researchers familiar with the candidate.

The résumé should include a summary statement of the candidate's research interests and accomplishments, educational background, professional experience, publications, honors, and awards.

This award was established to recognize Prof. Koichi Masubuchi for his contributions to the advancement of the science and technology of welding, especially in the fields of marine and outer space structures.

December 1 is the deadline. Submit your nomination to Prof. John DuPont at *jnd1@lehigh.edu*.♦

SECTION NEWS

DISTRICT 1
Director: Russ Norris
Phone: (603) 433-0855

DISTRICT 2
Director: Kenneth R. Stockton
Phone: (732) 787-0805

DISTRICT 3
Director: Alan J. Badeaux Sr.
Phone: (301) 753-1759

YORK-CENTRAL PA.
August 18
Activity: The Section hosted its annual golf outing at Cool Creek Country Club in Wrightsville, Pa., for 128 golfers. Top prize winners included **Mark Skehan, Joe Redding,** and **Tom Sibol.**

DISTRICT 4
Director: Ted Alberts
Phone: (540) 674-3600, ext. 4314

DISTRICT 5
Director: Leonard P. Connor
Phone: (954) 981-3977

FLORIDA WEST COAST
September 13
Speaker: **Carl Yates,** vice president
Affiliation: InCryo Systems, Inc.
Topic: Cryogenic gases and equipment
Activity: **Bill Machnovitz** raffled a gift certificate to raise money for the Section's scholarship fund.

NORTH FLORIDA
April 20
Activity: The Section toured Hydro Aluminum in St. Augustine, Fla., to study aluminum extrusion. **Scott Johnson,** engineering manager (photo on page 44), conducted the tour and explained the manufacture of tent poles used by the military.

DISTRICT 6
Director: Neal A. Chapman
Phone: (315) 349-6960

Shown are some of the 128 golfers waiting for the shotgun start for the York-Central Pennsylvania Section's annual outing.

First-place winners in the York-Central Pennsylvania golf outing are Mark Skehan (left) and Joe Redding.

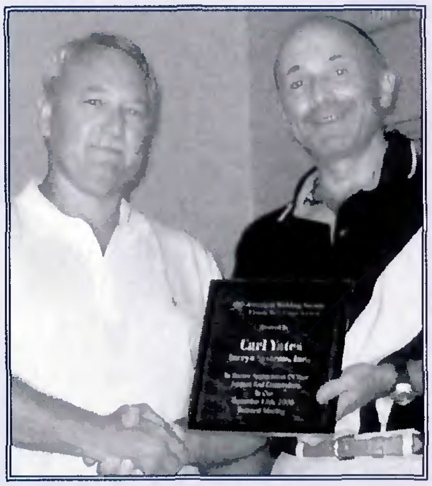

Carl Yates (left) accepts a speaker appreciation gift from Al Sedory, Florida West Coast Section vice chair.

Bill Machnovitz conducted a raffle to benefit the Section's scholarship fund at the Florida West Coast Section program.

Scott Johnson (left) discussed aluminum extrusions for the North Florida Section.

Mike Owens discussed the manufacture of mining equipment for the Pittsburgh Section and Student Chapter members.

Shown at the Mobile Section's program in August are (from left) Marsha Giles, Clyde Singleton, William Harrison Jr., Larry Davis, Mike Barnett, and Lucy Walker.

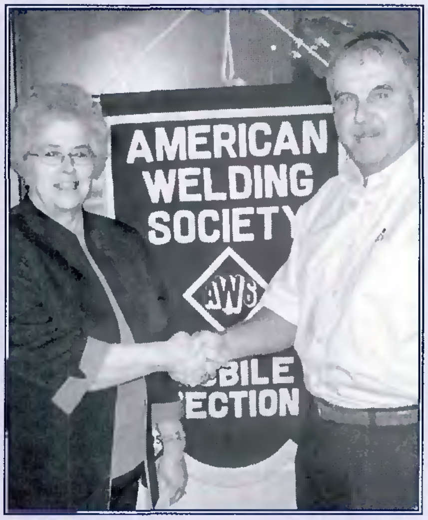

Mobile Section Chair Eleanor Ezell presents a speaker appreciation gift to Jackie Morris at the September program.

The Mahoning Valley golf committee included (from left) Carl Ford, Leon Stitt, and Chuck Moore.

DISTRICT 7

Director: Don Howard
Phone: (814) 269-2895

PITTSBURGH

April 28
Activity: **Mike Owens,** welding engineer, led the Section and its Student Chapter members on a tour of Joy Mining and Manufacturing Co. in Franklin, Pa. About 125 students participated. Following a pizza dinner, awards were presented to the winners in the Section's Student Day Weld-Off Competition held in December.

DISTRICT 8

Director: Wallace E. Honey
Phone: (256) 332-3366

DISTRICT 9

Director: John Bruskotter
Phone: (504) 394-0812

MOBILE

August 14
Activity: The Section members and members of Welding Engineering Supply Co., Prichard, Ala., met with **William H. Harrison Jr.** to celebrate his 87th birthday. Harrison is a charter member of the Section, a past chairman, and works daily as chairman of the board of Harrison Brothers Dry Dock Co., in Mobile, Ala.

September 14
Speaker: **Jackie Morris,** QA manager
Affiliation: Bender Shipbuilding and Repair Co.
Topic: How to prepare a welding procedure specification (WPS)
Activity: The Mobile Section held its election of officers program at The Captain's Table Restaurant on Battleship Causeway in Mobile, Ala.

DISTRICT 10

Director: Richard A. Harris
Phone: (440) 338-5921

MAHONING VALLEY

August 4
Activity: The Section hosted its 31st annual Jim Best golf outing at Tanglewood Golf Course in Pulaski, Pa. The golf committee included **Carl Ford, Leon Stitt, Chuck Moore,** and **Amy Sherwood.** The Columbiana Career Center Student Chapter members assisted with the activities. Hole sponsors included Airgas Great Lakes, Alpha Telecom, Avesta, Brilex Ind., Columbiana Boiler Co., ESAB Welding Products, Falcon Foundry, Hobart Brothers, Hypertherm Inc., Kobelco, Lenox Saw, Lincoln Electric, Linde LLC, Miller Electric, Northeast Fabricators, NortonAbrasives, Prax-

air, RAS Mfg., Reichard Industries, Steel & Alloy Specialists, Stoody Co., Specialty Fab, Spectrochemical Testing, Timkin Inc., Tweco, Valley National Gas, and Youngstown Oxygen & Welding Supply.

DISTRICT 11

Director: Eftihios Siradakis
Phone: (989) 894-4101

DETROIT

SEPTEMBER 14
Speaker: **Timothy Morris,** technical sales manager
Affiliation: Trumpf Inc.
Topic: Unique applications for laser beam welding and cutting
Activity: This student night and scholarship presentation program was held at the Trumpf Laser Technology Center in Plymouth Township, Mich. Following the talk, Morris demonstrated various laser welding processes. The Section presented $26,500 in scholarships to vocational high school and Ferris State University students. The Section's vocational high school welding contest winners were presented their certificates and scholarships. Named were **Adam Ridener, Michael Remer,** and **Brian Peterson.** University scholarships went to **Rod Bereznicki, Kevin Haddix, Zach Woodthorp, Ray Roberts, Larry Kujawski, Amanda D'Arcy, Jeff Lemke, Tim Mikel, Derek Polaikis, Nate Miller, Dan Gipson, Ken Camling, Caleb Haven, Dan Niemela, Jared Fantin, Mike Fitzpatrick, Eric Carlson, Josh Whitford,** and **Jason Ball.**

Shown at the Detroit Section program are (from left) Rod Bereznicki, John Bohr, Kevin Haddix, Zach Woodthorp, Ray Roberts, Larry Kujawski, Amanda D'Arcy, Jeff Lemke, Tim Mikel, Derek Polaikis, Nate Miller, Dan Gipson, Ken Camling, Caleb Haven, Dan Niemela, Jared Fantin, Mike Fitzpatrick, and Jeffrey Carney.

Detroit Section welding contest winners (from left) Adam Ridener and Michael Remer are shown with Steve Slavick, vocational high school program chair.

Speaker Timothy Morris (left) is shown with Mike Karagoulis, Detroit Section technical program chair.

DISTRICT 12

Director: Sean P. Moran
Phone: (920) 954-3828

DISTRICT 13

Director: Jesse L. Hunter
Phone: (309) 359-3063

CHICAGO

AUGUST 20
Activity: The Section held its annual outing at the Brookfield Zoo for a Safari Adventure and family-style buffet dinner.

SEPTEMBER 13
Activity: About sixty Chicago Section members toured the DuPage Manufacturing Research Center at Alion Science and Technology Corp. in St. Charles, Ill., to study its new welding technology. **Valdemar Malin,** director of the center, and **Federico Sciammarella** conducted the tour. Featured was a robotic laser beam welding station for refurbishing worn and corroded shipboard components in development for the Office of Naval Research.

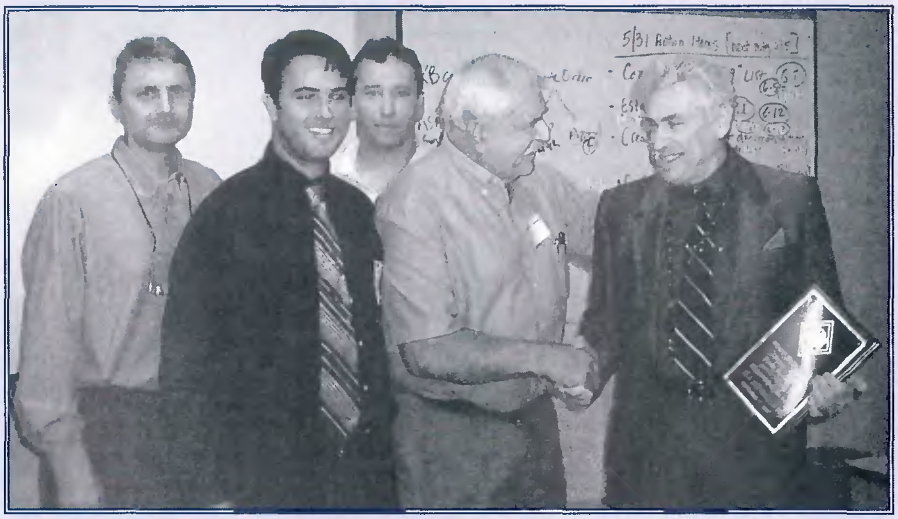

Shown during the Chicago Section's tour of DuPage Manufacturing Research Center are (from left) Robert Wojtas, Federico Sciammarella, Doug Howard, Pete Harris, and Valdemar Malin receiving his speaker's appreciation plaque.

DISTRICT 14

Director: Tully C. Parker
Phone: (618) 667-7744

Shown at the Brookfield Zoo during the Chicago Section's outing are (from left) Chairman Marty Vondra, Hank Sima, Jeff Stanczak, and Craig Tichlar.

4H welding contest contestant Seth Sears (front) awaits the verdict of the Indiana Section judges (from left) Rick Granger, Mike Anderson, Chair Gary Dugger, and Bob Richwine.

Shown are the Indiana Section and Monroe County 4H Welding Club members at their joint meeting in August.

INDIANA

July 17

Activity: The Section participated in the Monroe County 4H Fair Welding Contest in Bloomington, Ind,, headed by **Jason Hollers,** 4H advisor. The welding judges included **Rick Granger,** Treasurer **Mike Anderson,** Chairman **Gary Dugger,** and Secretary **Bob Richwine.**

August 17

Activity: The Indiana Section held a joint meeting with the Monroe County 4H Welding Club to discuss plans for initiating a welding contest at the Indiana State Fair. The primary speakers were Chairman **Gary Dugger** and 4H Advisor **Jason Hollers.** The meeting was held in Bloomington, Ind.

LEXINGTON

August 23

Activity: The Section hosted its District Scholarship Awards presentation program at Hazard Technical College in Lexington, Ky. Welding instructor **Craig Herald** presented $500 scholarships to **Coy Hall** and **Jeff Wilson.** About 40 attended the program.

DISTRICT 15

Director: Mace V. Harris
Phone: (952) 925-1222

DISTRICT 16

Director: Charles F. Burg
Phone: (515) 233-1333

NEBRASKA

May 20

Activity: The Section hosted its annual golf outing.

DISTRICT 17

Director: Oren P. Reich
Phone: (254) 867-2203

NORTH TEXAS

September 19

Speaker: **Susan Anderson,** district sales manager

Affiliation: Harris Product Group

Topic: Oxyfuel safety and a discussion of new welding gases

Activity: About 30 Section and Student Chapter members attended this program held at Spring Creek Barbecue in Dallas, Tex.

Susan Anderson accepts a speaker appreciation gift from Howie Sifford, North Texas Section chairman, in September.

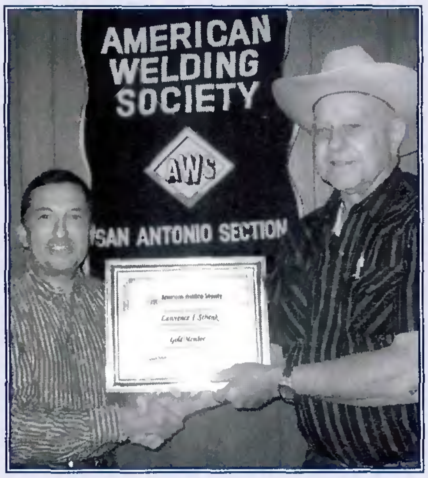

Lawrence Schenk (right) receives his Gold Membership Certificate Award from John Mendoza, District 18 director, during the San Antonio Section program in August.

DISTRICT 18

Director: John L. Mendoza
Phone: (210) 353-3679

SAN ANTONIO

August 26

Activity: District 18 Director **John Mendoza** presented **Lawrence F. Schenk** his AWS Gold Membership Award for 50 years of service to the Society. Schenk, a charter member of the Section since its founding in 1956, recently had a San Antonio Section scholarship named in his honor. The presentation took place during the scholarship picnic held at Braun Hall in San Antonio, Tex.

Shown at the Lexington Section program are (front row, from left) instructor Craig Herald, and scholarship winners Coy Hall and Jeff Wilson. Standing are members of the Hazard Technical College welding class.

The Nebraska Section golfers posed for a group shot during their annual outing in May.

Shown enjoying the Sacramento Valley Section's camping trip are (from left) Angela Hood, Dale Flood, and Debi, Stephanie, and Kerry Shatell.

DISTRICT 19

Director: Phil Zammit
Phone: (509) 468-2310, ext. 120

DISTRICT 20

Director: William A. Komlos
Phone: (801) 560-2353

DISTRICT 21

Director: Jack D. Compton
Phone: (661) 362-3218

Dale Phillips (left) and Mike Urioste (right) are shown with District 22 Director Kent Baucher at the San Francisco program.

Speaker Matt Chia (left) is shown with Richard Hashimoto, San Francisco Section chairman, in September.

San Francisco Section officers are (from left) Secretary Liisa Pine, Treasurer Sharon Jones, Student Affairs Representative Vanessa Barrett, Chairman Richard Hashimoto, Vice Chair Tom Smeltzer, and Past Chair Mike Urioste.

DISTRICT 22

Director: Kent S. Baucher
Phone: (559) 276-9311

SACRAMENTO VALLEY

SEPTEMBER 14
Activity: The Section officers enjoyed a four-day, three-night camping trip and fishing tournament sponsored by the Employee's Association of Tri-Tool, Inc. The outing was held at Wench Creek Campgrounds in the Eldorado National Forest, Calif.

SAN FRANCISCO

SEPTEMBER 6
Speaker: **Matt Chia,** general manager
Affiliation: Ogletree's Welding and Fabrication
Topic: Welding fabrication for the California wine and food industries, and *FEMA-353 Welding Manual* recommendations
Activity:The Section held its past chairmen's night program at Spenger's Restaurant in Berkeley, Calif. **Dave Palfini** received his Silver Certificate for 25 years of membership in the Society. District 22 Director **Kent Baucher** presented the District Director Award to **Mike Urioste,** and the District Educator Award to **Dale Phillips.** ♦

Nominations Sought for Robotic Arc Welding Award

December 31 is the deadline for submitting your nominations for candidates to receive the 2007 Robotic and Automatic Arc Welding Award.

The nomination packet should include a summary statement of the candidate's accomplishments, interests, educational background, professional experience, publications, honors, and awards.

Send the nomination packet to Wendy Sue Reeve, awards coordinator, 550 NW LeJeune Rd., Miami, FL 33126. Contacts: (800/305) 443-9353, ext. 293, or e-mail *wreeve@aws.org*.

In 2004, the AWS D16 Robotic and Automatic Arc Welding Committee, with the approval of the AWS Board of Directors, established the Robotic and Automatic Arc Welding Award.

The award was created to recognize individuals for their significant achievements in the area of robotic arc welding.

This work can include the introduction of new technologies, establishment of the proper infrastructure (training, service, etc.) to enable success, and any other activity having significantly improved the state of a company and/or industry.

The Robotic and Automatic Arc Welding Award is funded by private contributions.

It is presented annually at the AWS Awards/AWS Foundation Recognition Ceremony and Luncheon, held in conjunction with the FABTECH International & AWS Welding Show. ♦

Guide to AWS Services

550 NW LeJeune Rd., Miami, FL 33126
www.aws.org; phone (800/305) 443-9353; FAX (305) 443-7559
(Phone extensions are shown in parentheses.)

AWS PRESIDENT

Damian J. Kotecki
Damian_Kotecki@lincolnelectric.com
The Lincoln Electric Co.
22801 St. Clair Ave.
Cleveland, OH 44117-1199

ADMINISTRATION

Executive Director
Ray W. Shook.. *rshook@aws.org* ....(210)

CFO/Deputy Executive Director
Frank R. Tarafa.. *tarafa@aws.org* ....(252)

Associate Executive Director
Cassie R. Burrell.. *cburrell@aws.org* ....(253)

Associate Executive Director
Jeff Weber.. *jweber@aws.org* ....(246)

Executive Assistant for Board Services
Gricelda Manalich.. *gricelda@aws.org* ..(294)

Administrative Services

Managing Director
Jim Lankford.. *jiml@aws.org* ....(214)

IT Network Director
Armando Campana..*acampana@aws.org* .(296)

Director
Hidail Nunez..*hidail@aws.org*.............(287)

COMPENSATION and BENEFITS

Director
Luisa Hernandez.. *luisa@aws.org* ......(266)

INT'L INSTITUTE of WELDING

Senior Coordinator
Sissibeth Lopez .. *sissi@aws.org* ......(319)
Provides liaison services with other national and international professional societies and standards organizations.

GOVERNMENT LIAISON SERVICES

Hugh K. Webster........ *hwebster@wc-b.com*
Webster, Chamberlain & Bean
Washington, D.C.
(202) 466-2976; FAX (202) 835-0243
Identifies funding sources for welding education, research, and development. Monitors legislative and regulatory issues of importance to the industry.

Brazing and Soldering Manufacturers' Committee

Jeff Weber.. *jweber@aws.org* ....(246)

RWMA — Resistance Welding Manufacturing Alliance

Assistant Manager
Susan Hopkins.. *susan@aws.org* ....(295)

WEMCO — Welding Equipment Manufacturers Committee

Manager
Natalie Tapley.. *tapley@aws.org* ....(444)

CONVENTION and EXPOSITIONS

Associate Executive Director
Jeff Weber.. *jweber@aws.org* ....(246)

Corporate Director, Exhibition Sales
Joe Krall.. *krall@aws.org* ....(297)

Organizes the annual AWS Welding Show and Convention, regulates space assignments, registration items, and other Expo activities.

PUBLICATION SERVICES

Department Information ....(275)

Managing Director
Andrew Cullison.. *cullison@aws.org* ....(249)

Welding Journal

Publisher/Editor
Andrew Cullison.. *cullison@aws.org* ....(249)

National Sales Director
Rob Saltzstein.. *salty@aws.org* ....(243)

Society and Section News Editor
Howard Woodward..*woodward@aws.org* (244)

Welding Handbook

Welding Handbook Editor
Annette O'Brien.. *aobrien@aws.org* ....(303)

Publishes the Society's monthly magazine, *Welding Journal*, which provides information on the state of the welding industry, its technology, and Society activities. Publishes *Inspection Trends*, the *Welding Handbook*, and books on general welding subjects.

MARKETING COMMUNICATIONS

Director
Ross Hancock.. *rhancock@aws.org* ....(226)

Assistant Director
Adrienne Zalkind.. *azalkind@aws.org* ...(416)

MEMBER SERVICES

Department Information ....(480)

Associate Executive Director
Cassie R. Burrell.. *cburrell@aws.org* ....(253)

Director
Rhenda A. Mayo... *rhenda@aws.org* ....(260)
Serves as a liaison between Section members and AWS headquarters. Informs members about AWS benefits and activities.

EDUCATION SERVICES

Director, Education Services Administration and Convention Operations
John Ospina.. *jospina@aws.org* ....(462)

Director, Education and Government Advocacy
Richard J. DePue.. *rdepue@aws.org* ....(237)

Director, Education Product Development
Christopher Pollock.. *cpollock@aws.org* (219)

Tracks effectiveness of programs and develops new products and services. Coordinates in-plant seminars and workshops. Administers the S.E.N.S.E. program. Assists Government Liaison Committee with advocacy efforts. Works with Education Committees to disseminate information on careers, national education and training trends, and schools that offer welding training, certificates, or degrees.
Also responsible for conferences, exhibitions, and seminars on topics ranging from the basics to the leading edge of technology. Organizes CWI, SCWI, and 9-year renewal certification-driven seminars.

AWS AWARDS, FELLOWS, COUNSELORS

Senior Manager
Wendy S. Reeve.. *wreeve@aws.org* .....(293)
Coordinates AWS awards and AWS Fellow and Counselor nominees.

CERTIFICATION OPERATIONS

Department Information ....(273)

Managing Director
Peter Howe.. *phowe@aws.org* ....(309)

Director, Operations
Terry Perez.. *tperez@aws.org* ....(470)

Director, Int'l Business Accreditation and Welder Certification
Walter Herrera.. *walter@aws.org* ....(475)
Provides information on personnel certification and accreditation services.

TECHNICAL SERVICES

Department Information ....(340)

Managing Director
Andrew R. Davis.. *adavis@aws.org* .....(466)
Int'l Standards Activities, American Council of the International Institute of Welding (IIW)

Director, National Standards Activities
John L. Gayler.. *gayler@aws.org* ....(472)
Structural Welding, Machinery and Equipment Welding, Robotic and Automatic Welding, Computerization of Welding Information

Manager, Safety and Health
Stephen P. Hedrick.. *steveh@aws.org* ..(305)
Metric Practice, Personnel and Facilities Qualification, Safety and Health, Joining of Plastics and Composites

Technical Publications

AWS publishes about 200 documents widely used in the welding industry.
Senior Manager
Rosalinda O'Neill.. *roneill@aws.org* ....(451)

Technical Editor
Cynthia Jenney .. *cynthiaj@aws.org* ....(304)
Brazing Handbook, Soldering Handbook, Technical Editing

Staff Engineers/Committee Secretaries
Annette Alonso.. *aalonso@aws.org* .....(299)
Welding in Sanitary Applications, Automotive Welding, Resistance Welding, High-Energy Beam Welding, Aircraft and Aerospace, Oxyfuel Gas Welding and Cutting

Stephen Borrero.. *sborrero@aws.org* ....(334)
Welding Iron Castings, Joining of Metals and Alloys, Brazing and Soldering, Brazing Filler Metals and Fluxes

Rakesh Gupta.. *gupta@aws.org* ....(301)
Filler Metals and Allied Materials, Int'l Filler Metals, Instrumentation for Welding, UNS Numbers Assignment

Brian McGrath . *bmcgrath@aws.org* ....(311)
Methods of Inspection, Mechanical Testing of Welds, Thermal Spray, Arc Welding and Cutting, Welding in Marine Construction, Piping and Tubing, Titanium and Zirconium Filler Metals, Filler Metals for Naval Vessels

Selvis Morales.....*smorales@aws.org* ...(313)
Welding Qualification, Friction Welding, Railroad Welding, Definitions and Symbols

Note: *Official interpretations of AWS standards may be obtained only by sending a request in writing to the Managing Director, Technical Services. Oral opinions on AWS standards may be rendered. However, such opinions represent only the personal opinions of the particular individuals giving them. These individuals do not speak on behalf of AWS, nor do these oral opinions constitute official or unofficial opinions or interpretations of AWS. In addition, oral opinions are informal and should not be used as a substitute for an official interpretation.*

Nominees for National Office

Only Sustaining Members, Members, Honorary Members, Life Members, or Retired Members who have been members for a period of at least three years shall be eligible for election as a director or national officer.

It is the duty of the National Nominating Committee to nominate candidates for national office. The committee shall hold an open meeting, preferably at the Annual Meeting, at which members may appear to present and discuss the eligibility of all candidates.

To be considered a candidate for the positions of president, vice president, treasurer, or director-at-large, the following qualifications and conditions apply:

President: To be eligible to hold the office of president, an individual must have served as a vice president for at least one year.

Vice President: To be eligible to hold the office of vice president, an individual must have served at least one year as a director, other than executive director and secretary.

Treasurer: To be eligible to hold the office of treasurer, an individual must be a member of the Society, other than a Student Member, must be frequently available to the national office, and should be of executive status in business or industry with experience in financial affairs.

Director-at-Large: To be eligible for election as a director-at-large, an individual shall previously have held office as chairman of a Section; as chairman or vice chairman of a standing, technical or special committee of the Society; or as District director.

Interested parties should write a letter stating which office they seek, including a statement of qualifications, their willingness and ability to serve if nominated and elected, and 20 copies of their biographical sketch.

This material should be sent to James E. Greer, Chairman, National Nominating Committee, American Welding Society, 550 NW LeJeune Rd., Miami, FL 33126.

The next meeting of the National Nominating Committee is scheduled for November 2007. The term of office for candidates nominated at this meeting will commence January 1, 2009. ♦

Honorary Meritorious Awards

The Honorary-Meritorious Awards Committee makes recommendations for the nominees presented for Honorary Membership, National Meritorious Certificate, William Irrgang Memorial, and the George E. Willis Awards. These awards are presented during the FABTECH International & AWS Welding Show held each fall. The deadline for submissions is December 31 prior to the year of awards presentations. Send candidate materials to Wendy Sue Reeve, Secretary, Honorary-Meritorious Awards Committee, 550 NW LeJeune Rd., Miami, FL 33126. Descriptions of the awards follow.

National Meritorious Certificate Award: This award is given in recognition of the candidate's counsel, loyalty, and devotion to the affairs of the Society, assistance in promoting cordial relations with industry and other organizations, and for the contribution of time and effort on behalf of the Society.

William Irrgang Memorial Award: This award is administered by the American Welding Society and sponsored by The Lincoln Electric Co. to honor the late William Irrgang. It is awarded each year to the individual who has done the most over the past five-years to enhance the American Welding Society's goal of advancing the science and technology of welding.

George E. Willis Award: This award is administered by the American Welding Society and sponsored by The Lincoln Electric Co. to honor George E. Willis. It is awarded each year to an individual for promoting the advancement of welding internationally by fostering cooperative participation in areas such as technology transfer, standards rationalization, and promotion of industrial goodwill.

International Meritorious Certificate Award: This award is given in recognition of the recipient's significant contributions to the worldwide welding industry. This award reflects "Service to the International Welding Community" in the broadest terms. The awardee is not required to be a member of the American Welding Society. Multiple awards can be given per year as the situation dictates. The award consists of a certificate to be presented at the awards luncheon or at another time as appropriate in conjunction with the AWS president's travel itinerary, and, if appropriate, a one-year membership in the American Welding Society.

Honorary Membership Award: An Honorary Member shall be a person of acknowledged eminence in the welding profession, or who is accredited with exceptional accomplishments in the development of the welding art, upon whom the American Welding Society sees fit to confer an honorary distinction. An Honorary Member shall have full rights of membership. ♦

AWS Publications Sales

Purchase AWS Standards, books, and other publications from World Engineering Xchange (WEX), Ltd.
Toll-free (888) 935-3464 (U.S., Canada)
(305) 824-1177; FAX (305) 826-6195
www.awspubs.com

Welding Journal Reprints

Copies of *Welding Journal* articles may be purchased from Ruben Lara.
Call toll-free
(800/305) 443-9353, ext. 288; *rlara@aws.org*

Custom reprints of *Welding Journal* articles, in quantities of 100 or more, may be purchased from
FosteReprints
Toll-free (866) 879-9144, ext. 121
sales@fostereprints.com

AWS Foundation, Inc.

The AWS Foundation is a not-for-profit corporation established to provide support for educational and scientific endeavors of the American Welding Society. Information on gift-giving programs is available upon request.

Chairman, Board of Trustees
Ronald C. Pierce

Executive Director, AWS
Ray Shook

Executive Director, Foundation
Sam Gentry

550 NW LeJeune Rd., Miami, FL 33126
(305) 445-6628; (800) 443-9353, ext. 293
e-mail: *vpinsky@aws.org*
general information:
(800) 443-9353, ext. 689

AWS Mission Statement

The mission of the American Welding Society is to advance the science, technology, and application of welding and allied processes, including joining, brazing, soldering, cutting, and thermal spraying.

It is the intent of the American Welding Society to build AWS to the highest quality standards possible. The Society welcomes your suggestions. Please contact any staff member or AWS President Damian J. Kotecki, as listed on the previous page.

The AWS Foundation extends a SPECIAL THANK YOU to our 2006 Silent Auction Sponsors for making this year's auction a great success

2006 Silent Auction Sponsors

Your support is being used to help educate welding students!

Plan now to participate in our next Silent Auction. For more information contact the AWS Foundation at 800-443-9353 ext. 250.

Abicor Binzel

Hugh and Wanda Adams

AWS Atlanta Section

AWS Chattanooga Section

AWS Corpus Christi Section

AWS Detroit Section

AWS Drakewell Section

AWS Houston Section

AWS Los Angeles/Inland Empire Section

AWS Mobile Section

AWS Northwest Section

AWS Northwest Pennsylvania Section

AWS San Antonio Section

AWS Siouxland Section

AWS Twin Tier Section

Nancy and Barry Carlson

Sam Gentry

Hypertherm, Inc.

Inweld Corporation

IWDC

Jackson Products

The Lincoln Electric Company

MCD Plastics/Robb Howell

Mathey Dearman, Inc.

John L. Mendoza, District #18 Director

Carole and Tom Mustaleski, AWS Past President

Nelson Stud Welding

Pferd, Inc.

Select-Arc, Inc.

Ray and Sandy Shook

Christine and Jerry Uttrachi, AWS President-Elect

Howard M. Woodward

Donors as of 10/10/06

Welding for the Strength of America

The Campaign for the American Welding Society

Foundation, Inc.

Building Welding's Future through Education

Circle No. 11 on Reader Info-Card

Flux cored arc welding (FCAW) is a process that uses a continuous tubular electrode into which various alloying and fluxing ingredients are deposited. It is an efficient process readily adaptable to semiautomatic or automatic welding operations. Flux cored arc welding offers two major variations, self-shielded (FCAW-S) and gas shielded (FCAW-G).

In the gas-shielded method, the shielding gas (CO_2 or a mixture of argon/CO_2) protects the molten metal from the oxygen and nitrogen present in the air by forming an envelope of gas around the arc and weld pool. With self-shielded flux cored arc welding, the high-temperature decomposition of some electrode core ingredients and their vaporization displace air around the arc to provide the shield. The core ingredients also contain scavengers that combine with undesirable elements that might contaminate the weld pool.

Both variations can be used in most welding applications. The self-shielded method is sometimes chosen for field welding because it can tolerate air currents that might disrupt the shielding envelope of the gas-shielded variety.

FCAW Advantages

High productivity is the chief advantage of FCAW. High travel speeds and deposition rates can be achieved with the process, especially when compared to shielded metal arc welding (SMAW). Flux cored arc welding is more forgiving of minor disparities than gas metal arc welding (GMAW), and it is more flexible and adaptable than submerged arc welding (SAW). The process is also noted for good sidewall fusion, deep penetration, and smooth weld profile.

Some of the disadvantages are the relative high cost of the equipment and complexity of setup, the significant fumes generated must be suitably exhausted, and added time and labor is required to remove the slag cover.

Equipment

The recommended power source is the direct current (DC) constant-voltage type capable of operating at the maximum current required for the specific application. A wire feeder is required to supply the continuous electrode to the arc at a constant preset rate. If the electrode feed rate is changed, the welding machine automatically adjusts to maintain a preset arc voltage. The wire feeder requires drive rolls that will not flatten or distort the tubular electrode.

Welding guns may be either gas cooled or water cooled. Water-cooled guns generally have higher current ratings (up to

Mandatory Classification Designators[1] for FCAW Carbon Steel Electrodes

E X X T -X X -J X HX

- E — Designates an electrode.
- X — Tensile strength designator. For A5.20 this designator indicates the minimum tensile strength (when multiplied by 10,000 psi) of the weld metal when the weld is made in the manner prescribed by this specification. For A5.20M two digits are used to indicate the minimum tensile strength (when multiplied by 10 MPa).
- X — Position designator. This designator is either "0" or "1". "0" is for flat and horizontal positions only. "1" is for all positions (flat, horizontal, vertical with downward progression and/or vertical with upward progression and overhead).
- T — This designator identifies the electrode as a flux cored electrode.
- X — Usability designator. This designator is some number from 1 through 14 or the letter "G" (or "GS"). This designator refers to the usability of the electrode with requirements for polarity and general operating characteristics (see Table 2 in A5.20). The letter "G" indicates that the polarity and general operating characteristics are not specified. An "S" is used after the "G" to indicate that the electrode is suitable only for single pass welding.
- X — Shielding gas designator.[2] Indicates the type of shielding gas used for classification. The letter "C" indicates that the electrode is classified using 100% CO_2 shielding gas. The letter "M" indicates that the electrode is classified using 75-80% Argon/balance CO_2 shielding gas. When no designator appears in this position, it indicates that the electrode being classified is self-shielded and that not external shielding gas was used.

Optional Supplemental Designators[3]

- HX — Optional supplemental diffusible hydrogen designator (see Table 8 in A5.20).
- X — The letter "D" or "Q" when present in this position indicates that the weld metal will meet supplemental mechanical property requirements with welding done using low heat input, fast cooling rate procedures and using high heat input, slow cooling rate procedures as prescribed in Section 17 (see Tables 9 and 10 in A5.20).
- J — The letter "J" when present in this position designates that the electrode meets the requirements for improved toughness and will deposit weld metal with Charpy V-Notch properties of at least 20 ft·lbf at –40°F [27J at –40°C] when the welds are made in a manner prescribed by this specifications.

Notes:
1. The combination of these designators constitutes the flux cored electrode classification.
2. See AWS A5.32/A5.32M.
3. These designators are optional and do not constitute a part of the flux cored electrode classification.

Source: AWS A5.20/A5.20M: 2005, *Specification for Carbon Steel Electrodes for Flux Cored Arc Welding.*

Mandatory Classification Designators[1] for FCAW Low-Alloy Steel Electrodes

E X X T X -X X -J HX

- Designates an electrodes.
- Tensile strength designator. For A5.29 this designator indicates the minimum tensile strength (when multiplied by 10 ksi) of the weld metal when the weld is made in the manner prescribed by this specification. Two digits are used for weld metal of 100 ksi minimum tensile strength and higher. Two digits are used to indicate the minimum tensile strength (when multiplied by 10 MPa). See Table 1M in A5.29.
- Positionality designator. This designator is either "0" or "1." "0" is for flat and horizontal positions only. "1" is for all positions (flat, horizontal, vertical with downward progression and/or vertical with upward progression and overhead).
- This designator identifies the electrode as a flux cored electrode.
- Usability designator. This designator is the number 1, 4, 5, 6, 7, 8, or 11 or the letter "G". The number refers to the usability of the electrode (see Section A7 in Annex A in A5.29). The letter "G" indicates that the polarity and general operating characteristics are not specified.
- Deposit composition designator. Two, three or four digits are used to designate the chemical composition of the deposited weld metal (see Table 7 in A5.29). The letter "G" indicates that the chemical composition is not specified.
- Shielding gas designator.[2] Indicates the type of shielding gas used for classification. The letter "C" indicates a shielding gas of 100% CO_2. The letter "M" indicates a shielding gas of 75–80 % Argon/balance CO_2. When no designator appears in this position, it indicates that the electrode being classified is self-shielded and that no external shielding gas is used.

Optional Supplemental Designators[3]

- Optional supplemental diffusible hydrogen designator (see Table 9 in A5.29).
- The letter "J" when present in this position designates that the electrode meets the requirements for improved toughness and will deposit weld metal with Charpy V-Notch properties of at least 20 ft.lbf (27J) at a test temperature of 20°F [10°C] lower than the temperature shown for that classification in Table 1U (Table 1M)in the specification A5.29.

Notes:
1. The combination of these designators constitutes the flux cored electrode classification. Note that specific chemical compositions are not always identified with specific mechanical properties in the specification. A supplier is required by the specification to include the mechanical properties appropriate for a particular electrode in the classification of the electrode. Thus, for example, a complete designation is E80T5-Ni3. EXXT5-Ni3 is not a complete classification.
2. See AWS A5.32/A5.32M, *Specification for Welding Shielding Gases.*
3. These designators are optional and do not constitute a part of the flux cored electrode classification.

Source: AWS A5.29/A5.29M: 2005, *Specification for Low-Alloy Steel Electrodes for Flux Cored Arc Welding.*

700 A). Current ratings for gas-cooled guns are based on using CO_2. If argon-based gas is used, the gun current rating should be decreased 30%.

Electrode Classifications

The American Welding Society has developed a system of classifications for the various FCAW electrodes. The system is based on electrode type, minimum tensile strength, welding position, chemical composition, usability, impact properties, and diffusible hydrogen tests.

Mild steel electrodes are classified according to AWS A5.20, *Specification for Carbon Steel Electrodes for Flux Cored Arc Welding*; low-alloy electrodes are classified in AWS A5.29, *Specification for Low-Alloy Steel Electrodes for Flux Cored Arc Welding*; and stainless steel flux cored electrodes are classified by the standard AWS A5.22, *Specification for Stainless Steel Electrodes for Flux Cored Arc Welding and Stainless Steel Flux Cored Rods for Gas Tungsten Arc Welding.*

Polarity

Polarity is one of the variables that must be considered when selecting FCAW electrodes. Some FCAW electrodes are designed to be used with direct current electrode positive (DCEP) and others are designed for direct current electrode negative (DCEN). Less base metal penetration results from using DCEN. Determine which polarity the electrode is recommended for before using.

Electrode Extension

The unmelted electrode that extends beyond the contact tube is the electrode extension. This portion of the electrode is resistance heated, which can have an effect on arc energy, deposition rate, and weld penetration. All things being equal, too long an extension produces an unstable arc with excessive spatter, and too short an extension may cause excessive arc length at a particular voltage setting. Most manufacturers recommend ¾ to 1½ in. (19 to 38 mm) for gas-shielded electrodes and ¾ to 3¾ (19 to 95 mm) for self-shielded electrodes.

Gas Shielding

Carbon dioxide (CO_2) and mixtures of argon and CO_2 are the preferred shielding gases for FCAW-G. Carbon dioxide usually provides a globular transfer, good penetration, and low cost in contrast to mixed gases.

Carbon dioxide is relatively inactive at room temperature, but when heated to high temperature by the arc, it dissociates to form carbon monoxide and oxygen.

The gas mixture commonly used in FCAW is 75% argon and 25% CO_2. There can be some variations to the percentages,

Table 1 — Shielding and Polarity Requirements for Mild Steel FCAW Electrodes

AWS Classification	Recommended Weld Passes	External Shielding Medium	Current and Polarity
EXXT-1	Multiple	CO_2	DCEP[c]
EXXT-1M	Multiple	Mixed gas[a]	DCEP
EXXT-2	Single	CO_2	DCEP
EXXT-2M	Single	Mixed gas[a]	DCEP
EXXT-3	Single	None	DCEP
EXXT-4	Multiple	None	DCEP
EXXT-5	Multiple	CO_2	DCEP
EXXT-5M	Multiple	Mixed gas[a]	DCEP
EXXT-6	Multiple	None	DCEP
EXXT-7	Multiple	None	DCEN[d]
EXXT-8	Multiple	None	DCEN
EXXT-9	Multiple	CO_2	DCEP
EXXT-9M	Multiple	Mixed gas[a]	DCEP
EXXT-10	Single	None	DCEN
EXXT-11	Multiple	None	DCEN
EXXT-12	Multiple	CO_2	DCEP
EXXT-12M	Multiple	Mixed gas[a]	DCEP
EXXT-13	Single	None	DCEN
EXXT-14	Single	None	DCEN
EXXT-G	Multiple	Note b	Note b
EXXT-GS	Single	Note b	Note b

Notes:
a. Mixed gas normally refers to 75% to 80% argon/balance CO_2
b. As agreed upon by supplier and user
c. Direct current electrode positive
d. Direct current electrode negative

Table 2 — Typical Parameters for Mild Steel and Low-Alloy Steel Electrodes (EX1T-1 Types) for Welding in All Positions

Diameter mm (in.)	Position	Wire Feed Speed cm/min (in./min)	Current, A	Volts, V
0.9 (0.035)	Flat	1829 (720)	250	32
	Uphill	813 (320)	150	26
	Overhead	813 (320)	150	26
1.2 (0.045)	Flat	953 (375)	250	28
	Uphill	660 (260)	200	25
	Overhead	660 (260)	200	26
1.3 (0.052)	Flat	914 (360)	300	28
	Uphill	610 (240)	225	25
	Overhead	610 (240)	225	26
1.6 (1/16)	Flat	762 (300)	350	29
	Uphill	406 (160)	225	25
	Overhead	406 (160)	225	26
2.0 (5/64)	Flat	635 (250)	400	30
2.4 (3/32)	Flat	457 (180)	450	30
2.8 (7/64)	Flat and horizontal	381 (150)	550	30
3.2 (1/8)	Flat and horizontal	318 (125)	600	33

but this is the most popular. This mixture produces a spray-like transfer and better arc characteristics than straight CO_2.

When gas mixtures are used with electrodes designed for CO_2 shielding, the weld deposit may accumulate excessive amounts of silicon, manganese, and deoxidizing elements since these elements are more readily transferred when high percentages of argon or other inert gases are used. Consult the electrode manufacturer for the recommend shielding gas for a particular electrode.

Inadequate gas flow will result in poor shielding of the weld pool, and excessive gas flow can result in turbulence and mixing in air. Either extreme will increase weld metal impurities. The correct gas flow depends on the type and diameter of gun nozzle, distance of the nozzle to the work, and air movement in the immediate area of the arc.

Handling of Gas Cylinders

Compressed gas cylinders should be handled carefully and should be adequately secured when stored or in use. Cylinders caps should be kept in place (hand tight) to protect the valves unless a regulator is attached to the cylinder.

Before connecting a regulator, the cylinder valve should momentarily be opened slightly then closed immediately to clear the valve of dust or dirt. The valve operator should stand to one side of the regulator gauges, never in front of them.

After the regulator is attached, the pressure adjusting screw should be released by turning it counterclockwise. Open the valve slowly to prevent a surge of high-pressure gas into the regulator. Turn the adjusting screw clockwise until the proper pressure is attained.

The cylinder valve should be turned off if the cylinder is to be left unattended, and the adjusting screw should be in the open position.

Table 3 — Typical Welding Parameters for Mild and Low-Alloy Steel Self-Shielded FCAW Electrodes

AWS Classification	Diameter, mm (in.)	Welding Position	Wire Feed Speed cm/min (in./min)	Volts, V	Current, A
EXXT-3	2.4 (3/32)	Flat	610 (240)	24	510
	3.0 (0.120)	Flat	508 (200)	24	700
	4.0 (5/32)	Flat	330 (130)	23	780
EXXT-4	2.0 (5/64)	Flat	508 (200)	31	275
	2.4 (3/32)	Flat	483 (190)	31	355
	3.0 (0.120)	Flat	406 (160)	30	500
EXXT-6	2.0 (5/64)	Flat	762 (300)	28	450
	2.4 (3/32)	Flat	762 (300)	28	480
EXXT-7	2.0 (5/64)	Flat	508 (200)	26	300
	2.4 (3/32)	Flat	381 (150)	24	350
	2.8 (7/64)	Flat	318 (125)	26	400
EXXT-8	2.0 (5/64)	Flat	305 (120)	21	280
	2.4 (3/32)	Flat	254 (100)	22	340
EXXT-10	2.4 (3/32)	Flat	636 (250)	26	570
EXXT-11	0.9 (0.035)	Flat	330 (130)	17	140
		Uphill	254 (100)	16	90
	1.2 (0.045)	Flat	305 (120)	17	150
		Uphill	241 (95)	16	110
	1.6 (1/16)	Flat	305 (120)	17	230
		Uphill	241 (95)	16	175
	2.0 (5/64)	Flat	305 (120)	20	290
	2.4 (3/32)	Flat	254 (100)	20	365
EXXT-14	1.2 (0.045)	All	254 (100)	16	145
	1.6 (1/16)	All	178 (70)	16	185
	2.0 (5/64)	All	152 (60)	18	210
EXXT-GS	0.8 (0.030)	Flat	572 (225)	16	125
		Uphill	432 (170)	15	100
	0.9 (0.035)	Flat	635 (250)	18	150
		Uphill	635 (250)	18	150
	1.2 (0.045)	Flat	483 (190)	17	200
		Uphill	406 (160)	17	175

Table 4 — Typical Parameters for Gas-Shielded Stainless Steel FCAW Electrodes

AWS Classification	Diameter, mm (in.)	Welding Position	Wire Feed Speed cm/min (in./min)	Current, A	Volts, V
EXXXT0-1/-4	1.2 (0.045)	Flat & horizontal	991 (390)	190	26
EXXXT0-1/-4	1.6 (1/16)	Flat & horizontal	635 (250)	250	29
EXXXT1-1/-4	0.9 (0.035)	Flat	1016 (400)	140	24
		Uphill	699 (275)	95	23
EXXXT1-1/-4	1.2 (0.045)	Flat	546 (215)	390	29
		Uphill	406 (160)	250	26
EXXXT1-1/-4	1.6 (1/16)	Flat	660 (260)	300	29
		Uphill	521 (205)	250	26

Ventilation

The welding fumes generated by FCAW can be hazardous, but they can be controlled by general ventilation, local exhaust ventilation, or by respiratory protective equipment. Consult ANSI Z49.1, *Safety in Welding, Cutting, and Allied Processes*.

Ozone, nitrogen dioxide, and carbon monoxide are toxic gases associated with FCAW. Phosgene gas could also be present as a result of thermal or ultraviolet decomposition of chlorinated hydrocarbon cleaning agents located in the vicinity of welding. Two such solvents are trichlorethylene and perchlorethylene.

Welding with Gas-Shielded FCAW

Joint designs with relatively narrow grooves, small groove angles, and narrow root openings can be used with FCAW-G. The groove angle is properly designed when it provides accessibility for the appropriate gas nozzle and electrode extension.

Adequate gas shielding is required to obtain sound welds. Welding in still air may require gas flow rates of 30 to 40 ft^3/h (14 to 19 L/min). Welding in moving air may require flow rates up to 55 ft^3/h (26 L/min). Regular cleaning of the inside of the gas nozzle and contact tip is recommended to prevent obstruction of gas flow. If there is brisk air movement in the welding area, curtains could be used to restrict the movement and protect the gas shielding.

Welding with Self-Shielded FCAW

The somewhat shallower penetration with FCAW-S means the groove angle needs to be more open than with FCAW-G. Electrode extension introduces a variable that may influence joint design. In making flat position groove weld without backing, care must be taken to obtain sufficient fusion and penetration in the root. Similarly, in grooves with backing, the root opening must be sufficient to permit complete fusion.

Table 5 — Flux Cored Arc Welding Troubleshooting

Problem	Possible Cause	Corrective Action
Porosity	Low gas flow	Increase gas flowmeter setting. Clean spatter-clogged nozzle.
	High gas flow	Decrease to eliminate turbulence.
	Excessive wind drafts	Shield weld zone from draft or wind.
	Contaminated gas	Check gas source.
		Check for leak in hoses and fittings.
	Contaminated base metal	Clean weld joint faces.
	Contaminated filler wire	Remove drawing compound on wire.
		Clean oil from rollers.
		Avoid shop dirt.
		Rebake filler wire.
	Insufficient flux in core	Change electrode.
	Excessive voltage	Reset voltage.
	Excess electrode stickout	Reset stickout and balance current.
	Insufficient electrode stickout (self-shielded electrodes)	Reset stickout and balance current.
	Excessive travel speed	Adjust speed.
Incomplete fusion or penetration	Improper manipulation	Direct electrode to the joint root.
	Improper parameters	Increase current.
		Reduce travel speed.
		Decrease stickout.
		Reduce wire size.
		Increase travel speed (self-shielded electrodes).
	Improper joint design	Increase root opening.
		Reduce root face.
Cracking	Excess joint restraint	Reduce restraint.
		Preheat.
		Use more ductile weld metal.
	Improper electrode	Check formulation and content of flux.
	Insufficient deoxidizers or inconsistent flux-fill in core	Check formulation and content of flux.
Electrode feeding	Excessive contact tip wear	Reduce drive roll pressure.
	Melted or stuck contact tip	Reduce voltage.
		Adjust backburn control.
		Replace worn liner.
	Dirty wire conduit in cable	Change conduit liner. Clean out with compressed air.

When welding in the flat position, techniques similar to those used with low-hydrogen covered electrodes can be followed. When making vertical welds on plates ¾ in. (19 mm) and thicker, the root pass may be deposited downhill for joints without backing and uphill for joints with backing. Subsequent passes are deposited uphill.

Weld Quality

Several types of discontinuities can result from improper procedures or practices. Minor discontinuities may be permitted if they are not objectionable from a design or service standpoint. A few mild steel FCAW electrodes are designed to tolerate a certain amount of mill scale and rust on the base metals. Some deterioration of weld quality should be expected when welding dirty materials. These electrodes are usually designed for single-pass applications. When they are used for multipass welding, cracking caused by accumulated deoxidizing agents in the weld may occur.

The causes and remedies of some discontinuities are listed in the troubleshooting table (Table 5). ♦

Excerpted from *Welding Handbook*, Ninth Edition, Vol. 2, Part 1.

FOR MORE INFORMATION, CIRCLE NUMBER ON READER INFORMATION CARD.

Guide Simplifies OSHA Compliance

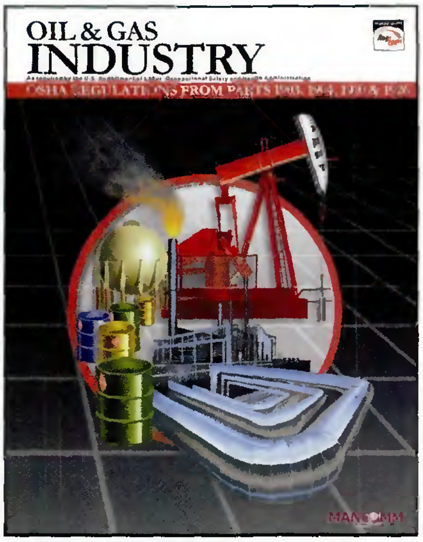

A 720-page, 8½- x 11-in. guide is designed to help companies in the oil and gas industry protect employees and stay compliant with Occupational Safety and Health Administration (OSHA) requirements. The book features a comprehensive index and RegLogic®, a colorful, graphical approach that makes understanding the regulations much easier. The *Oil & Gas Industry: OSHA Regulations from Parts 1903, 1904, 1910, & 1926* covers inspections, citations, and proposed penalties, recording and reporting occupational injuries and illness, general industry, construction, and letters of interpretation. The book may be purchased for $89.95 from MANCOMM. Call (800) 626-2666, or visit *www.mancomm.com.*

Free Handbook Details Gas Metal Arc Welding Process

The 96-page *GMAW Welding Guide* details the gas metal arc welding process and its many applications. Included are a definition of the process, advantages and disadvantages, and its 60-year history. Chapters are devoted to modes of metal transfer, components of the welding arc, list of appropriate shielding gases, advanced welding processes, an overview of welding guns and accessories, an in-depth look at welding carbon and low-alloy steels, stainless steels and aluminum alloys, procedure guidelines for general welding practices, a glossary of welding terms, and a discussion of proper arc welding safety precautions. Visit *www.lincolnelectric.com* to download the document, or request a copy by calling (216) 481-8100.

Catalog Pictures Ovens and Furnaces

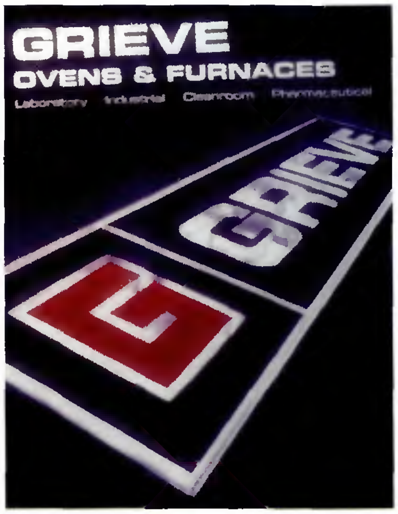

The 100-page, full-color Grieve Ovens & Furnaces catalog details more than 400 standard ovens for laboratory, industrial, Class 100 clean room, and pharmaceutical applications. Also pictured are numerous standard furnaces with operating temperatures to 2700°F. Included are custom heat processing and heat-treating equipment. Each product listing includes complete specifications, workspace dimensions, temperature ranges, air flow circulation diagrams, and optional equipment. Included is an interesting virtual tour of the company's manufacturing facilities.

The Grieve Corp. 111
500 Hart Rd., Round Lake, IL 60073-2898

Force and Torque Measurement Products Illustrated

The company's complete line of digital force- and torque-measurement products, test stands, and gripping fixtures is displayed in a full-color catalog. Included are photographs and descriptions, dimensional drawings for grips and attachments, and product comparison charts. New to this catalog are the Series CT cap torque testers for packaging, Series SJR miniature force sensors, and several new force and torque test stands. The catalog may be downloaded from *www.mark-10.com.*

Mark-10 Corp. 112
11 Dixon Ave., Copiague, NY 11726

OSHA Hearing Safety Bulletin Offered

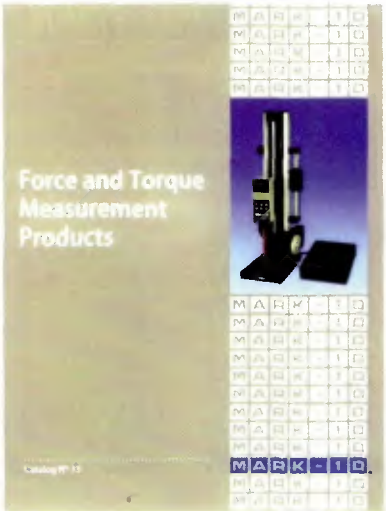

The two-page safety bulletin, Sound Source™ #8A, answers the question, "What parts of OSHA's Hearing Conservation regulations are cited most frequently in compliance inspections." Detailed, in tabular format, are the six industrial noise violations most often cited by OSHA inspectors with complete explanations and the company's recommended solutions. The PDF bulletin may be downloaded from *www.hearingportal.com/hearingconservation/hc-snd-ame.asp.*

Bacou-Dalloz Hearing Safety Group 113
7828 Waterville Rd., San Diego, CA 92154

Circle No. 31 on Reader Info-Card

Rimrock-Wolf Hires Regional Managers


Bruce Anderson


Todd McEllis

Rimrock-Wolf Robotics, Fort Collins, Colo., has named **Bruce Anderson** as its northeast regional manager, and **Todd McEllis** as regional manager for the Great Lakes territory. Anderson has 20 years of experience in industrial sales including more than ten years in the robotic arc welding industry. McEllis has ten years' experience in robotic arc welding sales, service, and project management.

Jet Edge Appoints Int'l Sales Engineer


Antoine Deproost

Jet Edge, Inc., St. Michael, Minn., a manufacturer of ultrahigh-pressure waterjet and abrasive jet systems, has appointed **Antoine Deproost** as international sales engineer. Deproost, in the industry for 20 years, previously held sales and product management positions with Omega Engineering, Thermo-Electron, and Endress-Hauser.

Felco Industries Adds Two Engineers

Felco Industries, Ltd., Missoula, Mont., a manufacturer of construction equipment, roller wheel and vibratory compaction buckets, bedding and backfill conveyor systems, has named **Tim Driscoll** to the post of senior engineer, and **Dylan Johnson** as a mechanical engineer. Driscoll has 20 years' experience as a mechanical designer for the aerospace industries and 15 years as an automotive technician on heavy trucks. Johnson has experience as a machinist, product design engineer, and has interned as a mechanical engineer for an industrial gear box manufacturer.


Tim Driscoll


Dylan Johnson

ABB Automation Names Product Line Manager


Michael Mikolajczak

ABB Automation Products, Low Voltage Drives, New Berlin, Wis., has appointed **Michael Mikolajczak** a product line manager. Previously, Mikolajczak held positions in sales, marketing, and product management at General Electric, Holt Electric, and most recently at Eaton Cutler-Hammer.

Tregaskiss® Reorganizes


Randy Stevens

Tregaskiss® Welding Products, Windsor, Ont., Canada, has announced that its strategic accounts team will report to **Randy Stevens**, director of business development. Stevens will continue to be responsible for the company's China initiatives and Tier One automotive accounts.

Obituary

Heinz Sossenheimer


Heinz Sossenheimer

Heinz Sossenheimer, 81, former executive member of the board of DVS, the German Welding Society, died July 8. He earned his doctorate in welding technology and statics at the University of Darmstadt. From 1956 to 1958, he was an editor for the journal *Schweißen and Schneiden* (Welding and Cutting). He was then assigned as a DVS Executive Member of the Board where he served for more than 30 years. In 1959, Dr. Sossenheimer founded the DVS publishing house where he served as its director. He also served as director of Forschungsvereinigung Schweißen und Schneiden, the DVS research association on welding and cutting, established in 1965. His achievements earned him the title "Dr.-Ing. E. h." (honorary doctor) by the Mechanical Engineering Institute of Dortmund University. Named a Fellow of the International Institute of Welding (IIW), he served as its treasurer, and chairman of the Publications working group. Among his many activities, he served as chairman of the organization committee for the Essen Welding Fair, and was a founding member of the European Welding Federation. In 1991, he was honored with the highest award of the German Welding Society, the DVS-Plakette for his merits and excellent contributions in the field of welding and for the development of the German Welding Society. In 2003, the DVS established a prize with his name in the IIW, the Dr. Sossenheimer Software Innovation Award.

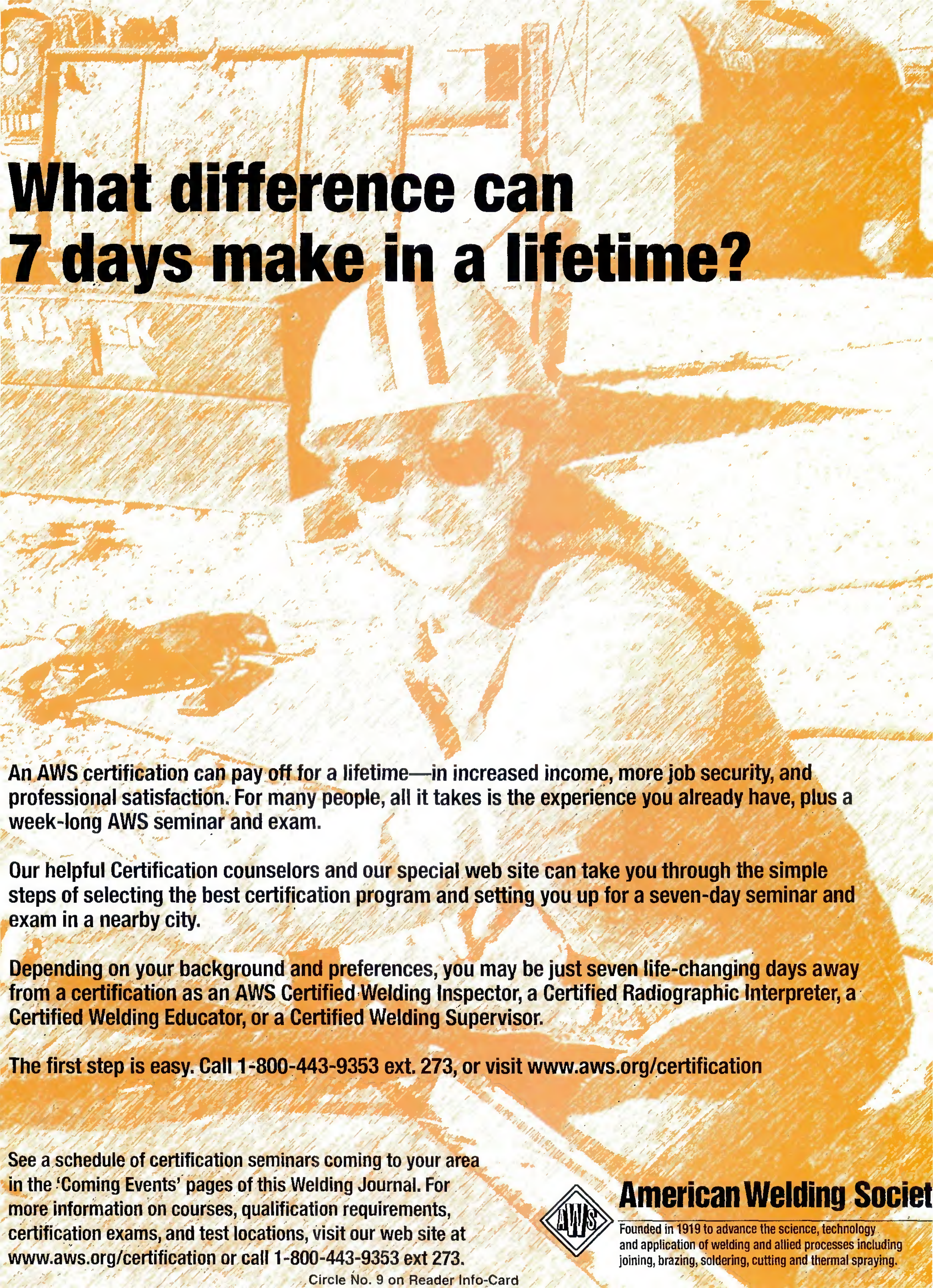
What difference can
7 days make in a lifetime?
An AWS certification can pay off for a lifetime—in increased income, more job security, and professional satisfaction. For many people, all it takes is the experience you already have, plus a week-long AWS seminar and exam.
Our helpful Certification counselors and our special web site can take you through the simple steps of selecting the best certification program and setting you up for a seven-day seminar and exam in a nearby city.
Depending on your background and preferences, you may be just seven life-changing days away from a certification as an AWS Certified Welding Inspector, a Certified Radiographic Interpreter, a Certified Welding Educator, or a Certified Welding Supervisor.
The first step is easy. Call 1-800-443-9353 ext. 273, or visit www.aws.org/certification
See a schedule of certification seminars coming to your area in the 'Coming Events' pages of this Welding Journal. For more information on courses, qualification requirements, certification exams, and test locations, visit our web site at www.aws.org/certification or call 1-800-443-9353 ext 273.
AWS
American Welding Societ
Founded in 1919 to advance the science, technology and application of welding and allied processes including joining, brazing, soldering, cutting and thermal spraying.
Circle No. 9 on Reader Info-Card

Understanding AC GTAW Balance Control

A look at how balance control works, including square wave, traditional, and inverter technologies, its benefits and settings

BY BRENT WILLIAMS

In the 1970s, a new standard was set for AC gas tungsten arc (GTA) welding with the introduction of the first AC/DC welding power source with a square wave AC output and balance control. Today, all professional-grade GTA welding machines feature balance control.

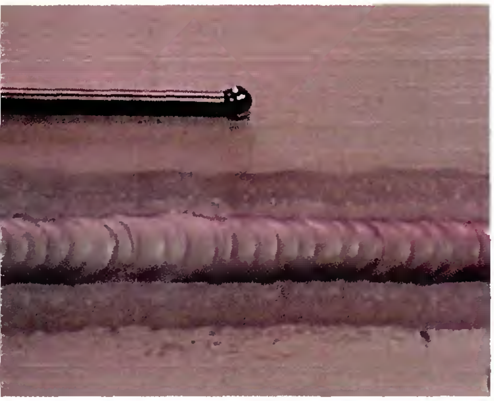

Fig. 1 — Notice the lighter colored "etched zone" or "cleaning action" created by the AC arc.

BRENT WILLIAMS is with Miller Electric Mfg. Co., Appleton, Wis.

Understanding Balance Control

To understand how balance control works, you first need to understand why welding aluminum and magnesium requires an AC welding output. When exposed to air, these metals form oxide layers that melt at much higher temperatures than the base metals. For example, aluminum oxide melts at about 3600°F, while aluminum melts at 1200°F. If not removed, the oxide layer will inhibit the welding process and pool formation.

As opposed to sine waves, squarewave technology allows almost instantaneous transitions between positive and negative polarities, providing a more stable arc and increasing the time spent at maximum amperage values. Traditional technology limits the output frequency to that of the input frequency, typically 60 Hz. Inverter technology allows for much faster switching, up to 50,000 Hz, and can be finely controlled.

Square Wave Technology

Fortunately, the square wave alternating current inherently provides a "cleaning" action. The electrode positive (EP) portion of the cycle — where current flows from the work to the electrode — actually "blasts" off surface oxides. This then allows the electrode negative (EN) portion of the cycle (where the current flows from the tungsten into the work) to melt the base metal and form a weld pool — Fig. 1.

Until the introduction of balance control, the amount of AC "cleaning action" and "weld penetration action" remained balanced at 50% each. Unfortunately, this "one size fits all" approach didn't provide the ideal arc for all applications. Today, however, welders can use balance control to tailor the GTA arc for the job at hand — Fig. 2.

Traditional Technology

A welding machine based on traditional technology, such as Miller Electric's Syncrowave® AC/DC, allows setting balance control on a range from 0 to 10, or from maximum cleaning to maximum penetration, respectively. For the more technically minded, some models using this technology allow fine tuning the duration of the EN portion of the AC cycle from 45 to 68%. In other words, you are spending 68% of the AC cycle (which is $\frac{1}{60}$ of a second) putting energy into the workpiece at the maximum penetration or minimum cleaning setting.

Inverter Technology

Inverter-based GTA welding machines, such as Miller's Dynasty™, extend balance control even further, allowing EN durations from 30 to 99%. On these machines, you actually specify an EN percentage when setting AC balance for greater control and fine tuning of the cleaning action — Fig. 3.

Balance Control Benefits

Making the EN portion of the cycle last longer does the following:

- Achieves greater penetration and faster pool formation
  - May permit increased travel speeds

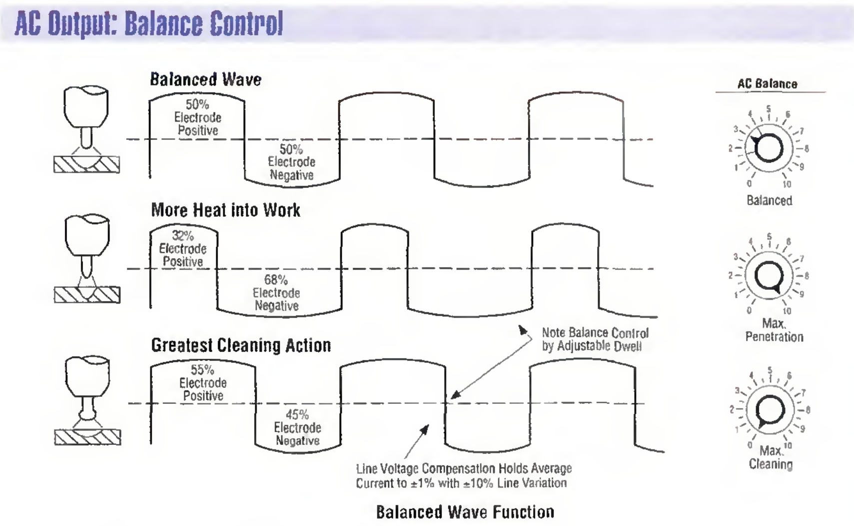

Fig. 2 — Square wave balance control setting.

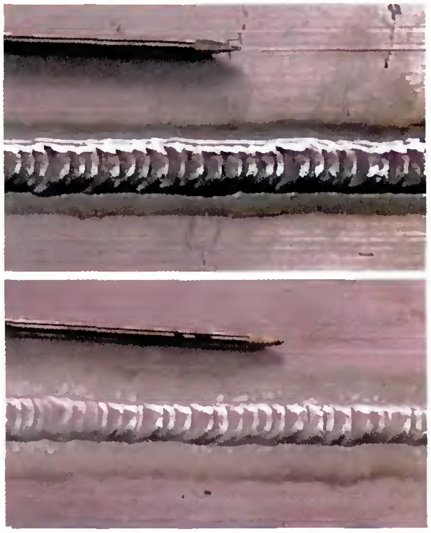

Fig. 3 — A comparison between greater (top) and lesser (bottom) amounts of EN.

- Narrows the weld bead
- Increases tungsten electrode life and reduces balling action
- May permit using a smaller diameter tungsten to more precisely direct the heat or make a narrower weld bead
- Reduces the size of the etched zone for improved cosmetics.

Reducing the EN portion of the cycle does the following:

- Produces greater cleaning action to remove heavier oxidation
- Minimizes penetration, which may help prevent melt-through on thin materials
- Widens the bead profile, such as for catching both sides of a joint
- Decreases tungsten electrode life and increases balling action.

Setting Balance Control

There are no hard rules about setting balance control, but the typical error involves overbalancing the cycle. Too much cleaning action (electrode positive duration) causes excess heat buildup on the tungsten. This creates a large ball on the end of the tungsten. Subsequently, the arc loses stability and you lose the ability to control the direction of the arc and the weld pool. The arc starts begin to degrade as well. Too much penetration (or, more precisely, insufficient cleaning action) results in a "scummy" weld pool. If the pool looks like it has black pepper flakes floating on it, add more cleaning action to "blast" away oxides and other impurities.

For a noninverter machine welding on clean aluminum, a good starting point would be between the 3 and 7 balance control settings. For an inverter, set the EN between 65 and 75%. In all cases, make practice welds on scrap prior to welding to determine the best balance control settings. Lastly, it may help to keep a journal of your favorite balance control and weld parameter settings. Note the material type, thickness, joint configuration, welding position, tungsten type and diameter, and application.◆

Tips for Welding with Self-Shielded Flux Cored Wires

Here's help for better welding with these popular, but difficult-to-use, welding wires

Self-shielded flux cored wires meeting AWS E71T-8 requirements comprise much of the welding wire used for structural steel in buildings, bridges, civil construction, and infrastructure applications. While popular and/or necessary for structural welds, these wires are notoriously difficult to use. Perhaps more than any other tubular electrode, these wires demand special considerations — in both technique and equipment — for obtaining good results.

Greg Metko, a welding engineer with Miller Electric Mfg. Co., has spent thousands of hours training members of the Ironworkers union how to successfully weld with self-shielded flux cored wires. For the past 12 years, he has participated in the Ironworkers Instructor Training Program, which brings together hundreds of instructors who take what they learn and pass it on to thousands of apprentices and journeymen. He is one of the experts dedicated to "training the trainers." Metko took some time out from a recent training effort to offer the following advice.

Floyd Elliff of Local 263 (on right) tests the weld coupon of April Finkbonner from Local 86. This weld shows a slightly convex appearance, so it passes this portion of the weld test.

Q: Why are self-shielded T-8 wires so difficult to weld?

A: Because they operate in a very narrow voltage range. For instance, let's take a look at 5/64-in.-diameter wire, which is fairly common. For an all-position fillet weld, its operating range is just 19 to 22 V. If you make a weld outside of that range, the odds of the weld failing inspection are good.

Q: What happens to the weld if the right voltage isn't used?

A: Excess arc voltage causes porosity, while low voltage causes a convex, "humped" or "ropey" bead and potentially insufficient penetration. Extremely low voltage causes "gun buck" where the wire dives through the molten weld pool and stubs on the plate.

Q: What is the most common cause of voltage variations?

A: There are lots of contributing factors, but the one I see the most during training is improper electrode extension. When using a flux cored welding gun, this is the distance from the end of the contact tip to the arc. With a self-shielded T-8 wire, the operator needs to maintain an electrode extension of 3/4 in. The contact tip to work distance (electrode extension plus arc length) will be about 1 in.

Q: What happens if proper electrode extension isn't maintained?

A: Too little electrode extension doesn't allow enough "preheat" time for the wire to form the proper shielding gas coverage, which leads to porosity. Too great an electrode extension will cause the amperage to drop outside of the proper range and the weld may have insufficient penetration. Also, long electrode extensions may preheat the wire too long, which may change the wire's composition.

Q: How do welders know if they're using the right voltage?

Based on information proved by Miller Electric Mfg. Co., Appleton, Wis.

Fig. 1 — For good results when welding with AWS E71T-8 flux cored wires, maintain a proper electrode extension (¾ in.) and use the proper gun angle (5 to 10 deg toward the direction of travel).

A: The weld will have little to no spatter, no porosity, and a slightly convex appearance. A good way to ensure proper voltage is to use a portable wire feeder with a digital voltage display. It displays voltage during welding and for 5 s after welding is stopped. Note that analog meters aren't very accurate compared to a digital display, and any readout back at the power source won't be accurate because the long cable lengths common in field welding cause voltage drop.

Q: Other than technique, what else causes voltage problems?

A: Poor weld cables are a common culprit of excess voltage drop. Make sure your weld cables are sized properly and that the cable, clamp, and all connections are in good condition.

Q: Should you use a specific type of power source for good voltage control?

A: Yes. To start, welding codes with seismic requirements (e.g., D1.1, *Structural Welding Code — Steel*, and *FEMA 353*) dictate using a constant voltage (CV) power source. Even if procedures don't demand it, Miller always recommends a CV welding machine for wire welding. This type of machine lets the operator set voltage and wire feed speed/amperage, which makes it easy to dial-in optimum welding parameters.

Q: Are some types of CV welding machines better than others for voltage control?

A: Yes. With an electric welding machine, primary power fluctuations can affect weld voltage. Fortunately, some inverters popular for construction work can compensate for voltage spikes and dips, maintaining a steady welding output as long as the primary power remains within a 190–630 VAC range. With some engine-driven machines, drawing on generator power (such as using a grinder) while welding may also affect arc voltage. Some engine drives are specifically designed to overcome this problem.

Q: What's the most common welding advice you give?

A: Maintain proper electrode extension and use the proper gun angle — Fig. 1. Some T-8 wires simply won't run well if you don't use a drag technique. Point the wire into the leading edge of the weld pool and angle the gun toward the direction of travel by 5 or 10 deg. It is also critical to keep the wire directed in the molten slag pool, otherwise the wire will dive into the plate, stub and create a cold spot. Some brands of wire are more forgiving to use than others, so you might want to experiment.

Q: Do welders need to do anything special during arc starts?

A: Yes. Clip or jog the wire so that you start with the proper electrode extension of ¾ in. When starting, hold the contact tip about the same distance away from the work as when you're welding (¾ in.), pull the gun trigger, wait a second or two for the arc to establish and the weld pool to form, and then drag the gun forward. If you experience wire stubbing, start the arc about ¼ in. closer, then move it back once it is established. If your wire feeder has a "soft start" or "run-in control," you can use those features to improve arc starts.◆

A Look at Owning Your Own Weld Shop

Dave Lynnes achieved one of his life's goals when he established Dave's Welding and Metal Fabrication, Inc.

BY KRISTIN CAMPBELL

"It has been a lifetime dream of mine to run my own shop and business," said Dave Lynnes of West Fargo, N.Dak. Through persistence and dedication, he made it happen. Over the past 2½ years, his company has taken off, and he is happy with his decision to start this new endeavor.

Fig. 1 — Dave Lynnes (center) is pictured with his twin sons, Adam (left) and Nathan. The trio enjoys welding together.

Introduction to Welding

Dave Lynnes's father, Earl, worked as a welder at Fargo Tank Co. in Fargo, N.Dak. "I enjoyed going to the shop when I was young and watching everyone welding and fabricating," he said. "I was hooked on welding from the first day of watching it being done."

While attending Agassiz Junior High School and Fargo South High School, both in Fargo, Lynnes took shop classes. In 1987, after he graduated from high school, he started his first welding job at Dakota Fence Co. in Fargo, where he stayed for three years.

To learn more about welding, he attended a 10-month welding program from 1990 to 1991 at the Moorhead campus of Minnesota State Community and Technical College. At that time, his welding instructor was close to retiring and did not want to continue teaching night classes. He asked Lynnes if he was interested in taking over. "Being very interested, I took him up on his offer and started my teaching career," he said.

He taught gas metal arc welding (GMAW), shielded metal arc welding (SMAW), gas tungsten arc welding (GTAW), and oxyacetylene cutting from 1992 through 1995. "I enjoyed teaching welding as it is my passion," Lynnes said. "To teach others who enjoy welding was completely rewarding."

In 1993, he started a five-year pipe trades apprenticeship program at the Plumbers and Pipefitters Local 300 in Fargo to become a pipe welder. After completing the program, Lynnes started teaching pipe welding to the apprentices in 1998. He also received certifications in GMAW, GTAW, SMAW, carbon steel, and stainless in the 6G position.

Additionally, Lynnes has been a member of the American Welding Society (AWS) for 14 years. He has held all officer positions with the Northern Plains Section. In 1999, he became an AWS Certified Welding Inspector and AWS Certified Welding Educator.

How the Company Formed

Lynnes has twin sons, Adam and Nathan, who are now 18 years old — Fig. 1. They have been welding with him since they were 13, and when they were 16, they wanted to start working as welders during the summers, but they were not old enough to do this in a welding shop. "That is when I started contracting work from other shops so my sons could put their welding skills to use," he said.

Lynnes began welding at night with his sons while working as a pipefitter during the day. Their first job consisted of welding mild steel parts for skid steer loaders. After a while, Lynnes chose to quit his job to pursue a welding business full time.

In April 2004, he established Dave's Welding and Metal Fabrication, Inc., in West Fargo. Its Web site is *www.davesweldingmetalfab.com*. The company started out with two employees — his sons.

In the beginning, Lynnes rented space

KRISTIN CAMPBELL (kcampbell@aws.org) *is assistant editor of the* Welding Journal.

Lynnes Welding Training

Instructor Wayne Reitz (center), PhD, is shown teaching metallurgy to a group of students who attended the school from August 21 to September 1, 2006, for the 80-hour gas metal arc welding course.

Dave Lynnes made another dream come true when he opened his welding school, Lynnes Welding Training, Inc., in the fall of 2004. It helped that he could house the school in the large weld shop where his company is located in West Fargo, N.Dak.

At the time, the technical training school in Moorhead, Minn., had shut down its welding program, leaving Fargo without any welder training facilities within a 50-mile radius.

"I love welding and, after having a taste of teaching, I knew I wanted to be independent and offer the community a resource that was needed," Lynnes said.

Courses Offered

Lynnes wanted to offer courses that focused mainly on welding skills. He contacted Dennis Klingman, manager of technical training at The Lincoln Electric Co., Cleveland, Ohio, and told him his ideas. "He didn't hesitate one moment to get involved with our center," Lynnes said.

The school is networked with Lincoln Electric and uses its multiprocess welding machines in the training center. This company assists with training materials, videos, and technical support as well.

Currently, the school offers an 80-hour course in gas metal arc welding (GMAW). It consists of 65 hours for hands-on welding training and 15 hours for classroom theory.

"This class runs from 8 a.m. to 4:30 p.m. Monday through Friday. The students get a break in the morning and afternoon with a ½-hour lunch. We also give 10 minutes at the end of each class for clean up time," Lynnes explained. "We not only want to teach our students how to weld, but also gear them for a regular workday."

In addition, the school offers 40-hour courses in GMAW, gas tungsten arc welding, and shielded metal arc welding; both day and evening classes are available. "We focus primarily on hands-on training for these classes," he said.

Customized training is offered, too.

The school covers theory, safety, blueprint reading, welding symbols, and metallurgy. It takes up about 25% of the weld shop, has eight welding booths, and contains space for discussions and demonstrations. The students also learn in a small classroom that is set up for them. They are provided with handouts on all material covered.

To receive a certificate of completion from a course, the students must pass a written test and weld tests.

There are four instructors at the school — Lynnes, Chad Erickson, Gary Burggraff, and Wayne Reitz. Combined, they have more than 75 years of experience.

There are no more than 10 students per instructor. "We take pride in ourselves that our instructors spend quality time with each student and that our student/teacher ratio is where it is at," Lynnes said.

In 2007, another welding instructor will be added, and Lynnes also hopes to put in two to four more welding booths. Plus, the school will offer an advanced GMAW course and a pipe welding course.

Makeup of Students

More than 250 students have attended the school, including 20 women.

"We have a variety of students from 18 years of age to 62, with the average age being 21 to 30 years old," Lynnes said. "Most of our students have been adults wanting a career change or have taken a course in high school and enjoyed welding...but the majority of them have never welded before."

He mails follow-up surveys to former students every few months to get feedback. About 70% of them respond. "They let us know how their jobs are going, where they're working, and what their wages are," he said. "We want to know what they learned here, and how it benefited them, how the industry is once they leave here, or if we should be offering something else."

Job Placement

The school does not directly place students in a job, but based on results from follow-up surveys, Lynnes estimates job placement is at 90%.

A majority of the students go on to work in the area. "They either start out as a welder's helper or they pass a welding test and they're able to start out welding," he said.

The school is networked with local staffing agencies, including Job Service North Dakota, Rural Minnesota CEP, Inc., North Dakota Vocational Rehabilitation, and several local manufacturing facilities.

"I believe the demand will always be there for welders," Lynnes said. "There aren't enough young welders to replace the generation of welders who will be retiring in the next five to ten years."

Lynnes stays busy with his company and school, and he values having them. "Every day here, it's something new, and it's just a lot of fun and very enjoyable to come to work," he said.

For more information about Lynnes Welding Training, visit *www.learntoweld.com.*◆

Fig. 2 — This is the facility where Dave's Welding and Metal Fabrication is located.

Fig. 3 — Employee Joshua Neumayer gas metal arc welds steel rails.

at a friend's shop, but as he started running out of room, the building next door opened up, and the company moved into a 8000-sq-ft shop — Fig. 2.

Tips on Starting a Weld Shop

"It was a lot of long hours to get my business up and running," Lynnes said, but he did rely on the points listed below.

• **Reading reference materials.** He read numerous books to help out with sales, communicating, and public relations work.

• **Relying on local resources.** He went to Lake Agassiz Development Center in Fargo, where he spoke to business analyst Randy Kingsley. "He's the one who helped a lot as far as the cash flow and getting us advice on how to approach our banks, and what to ask for, setting up line of credits," Lynnes said.

• **Talking with current business owners.** He spoke to a few, and they also discussed cash flows and making sure that the company gets paid on time. "When you've got payroll and everything else coming up, you have to really watch how the cash flow situations are," he said.

• **Devising a plan.** Throughout the years, he had different ideas about starting a company. And, when Lynnes put together a business plan for the weld shop, he wanted to expand on working relationships with customers he already had so he could grow his business.

"If I could give someone advice before starting a business of their own, it would be to do your homework first," Lynnes added. He suggests not getting in over your head, being self motivated and able to multitask, having good communication skills and patience, learning from your mistakes, and be willing to make changes.

Lynnes appreciates the guidance people have given him. "Without their help and my great employees, I wouldn't be where I am today," he said. "I knew how to weld, but had no idea on how to run a successful business."

Fig. 4 — Employee Jason Herfindahl grinds steel rails as part of the finishing process.

Owning a Weld Shop

The company's equipment includes a mandrel pipe bender; nine welding stations and nine different welding machines; two 1-ton overhead cranes; a 10- x 18-in. metal cutting band saw; drill press; track torch for cutting and beveling plate; plasma cutting machine; an iron worker; and 4000-lb-capacity forklift.

It has 18 full-time employees. Lynnes' s sons also hope to work full time for the company when they are finished with school. Adam attends Aakers College at its Fargo campus for business management, and Nathan is going to The Lincoln Electric Co.'s 15-week welding school in Cleveland, Ohio.

Recently, the company received the 2006 "Out on A Limb" Innovative Business award from the West Fargo Chamber of Commerce.

There are challenges to deal with though. "Owning your own business is a lot of work. You don't have regular hours, you're always working. Even when not at work, you're constantly thinking about strategies and the business," Lynnes said. "It has taken a lot of time to get established and to bring in steady customers."

On the other hand, there are advantages that come with owning your own weld shop. "What I like is of all the hard work that's put into it, it's very gratifying to see the growth when everything starts coming together for us," he said.

Jobs to Handle

The company serves some large corporations. It performs manufacturing work for DMI Industries in West Fargo, which makes wind towers. Contract work for this company has consisted of making aluminum platforms and aluminum internal parts that go inside of towers. Also, it works for Case IH in Fargo, which makes tractors and loaders. Here, contract work has consisted from making racks to small parts for the maintenance area. Another main client is Mid-America Steel in Fargo. For it, the shop makes hand railings and staircases for different ethanol plants — Figs. 3, 4.

The company does fabrication work, too. Different welding processes are used depending on the job, type of material, and material thickness. Different metals are used as well, including steel, stainless steel, aluminum, magnesium, and titanium.

In addition, the company gets a lot of walk-in customers. Not long ago, a man came in who needed a repair on his artificial arm. A stainless steel part had broken and the hook was not working anymore. The GTAW process was used to fix this up. "We're still a small enough shop where we'll take in whatever it might be, if we're capable of doing it," Lynnes said.

Expansion on the Horizon

The company is once again running out of room. "We hope to expand in a year or so to a larger facility of about 20,000 sq ft and to add additional staff to include welders and office personnel," he said. He is excited about this upcoming event.

All in all, Lynnes is glad he decided to live out his dream. "It is a tremendous sense of pride and accomplishment owning this business," he said. "The personal gratification is daily."◆

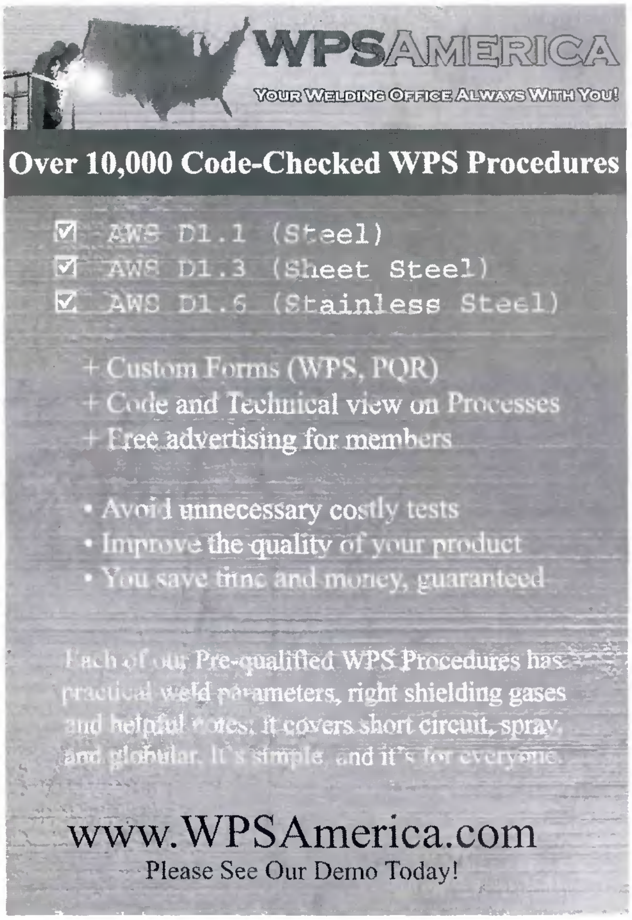

Welding Boiler Tubes

It helps to have a buddy when welding a boiler header 40 ft in the air

BY ROY WILKERSON

Fig. 1 — The 15-ft header is prepped for welding.

Shown is a new economizer inlet header (Fig. 1) for the Haynes Generating Station Unit 1 Boiler located in Long Beach, Calif. The header was prepped for welding on the ground then hoisted up 40 ft through the boiler bay steel — Fig. 2. An opening had to be cut in the hopper to remove the old header and install the new one. The header is a 15-ft piece of Schedule 160 pipe with two 10-in. inlets and 184 2-in., 0.240-in.-thick wall tube stubs to weld.

The gas tungsten arc welding (GTAW) process (Fig. 3) with ER70S weld rod was used for the root, fill, and cover passes. A system called "buddy welding" was used on the tubes. There is a blind spot on the back side where another welder picks up through the center two rows of tubes (Fig. 4) and welds the blind spot; the opposite welder does the same.

Using the GTAW process, the welder will weld as far around the tube as possible, then the opposite welder will put filler rod in front of the arc to make the corner, while the other welder will break his arc to let the other welder continue.

When using the shielded metal arc welding (SMAW) process, the welders will not break their arcs but pass the arc by traveling over the top of the opposite welder's welding electrode. Then the first welder will break and let the other welder continue around the blind side of the tube. The other welder picks up the arc on the other side.

This is a very productive technique and cuts down on repairs due to porosity and pinholing. ♦

Fig. 2 — The header is shown in place after being hoisted 40 ft to the boiler bay.

Fig. 3 — Welder Bryan Gray uses the gas tungsten arc process to join the boiler tubes.

Fig. 4 — Buddy welding in motion — one welder welds as far around the tube as possible, and with a smooth transition at the break, the other welder picks up the welding on the back side.

ROY WILKERSON (roy.wilkerson@ladwp.com) *is mechanical repair general supervisor, Integrated Support Services, Los Angeles Dept. of Water and Power.*

An Enthusiastic Welder: Josie Greek

Welding is a big part of this young woman's life, and she is excited about having a career in the field

BY KRISTIN CAMPBELL

Josie Greek, a 20-year-old welder from Apison, Tenn., likes to show her artistic side with welding — Fig. 1. "I can incorporate art along with physical, working pieces and actually use the things I make," she said. It is this ability that keeps her driven.

Fig. 1 — Josie Greek has enjoyed welding since high school. She is shown above at Litespeed, where she currently works performing gas tungsten arc welding on bicycle frames and in the company's machine shop.

Welding in High School

While attending Harrison Bay Vocational School in Ooltewah, Tenn., Greek wanted to take a vocational course because she liked hands-on work, so in the first semester of her freshman year, she took a graphic arts class. However, she was not very interested in it, and teacher Gary Potter asked if she wanted to try welding.

"I didn't know what to say or think at first, really, because I never even thought about welding," Greek said. She almost said no, but then decided, "I'm going to go ahead and do it, because it's something different, it's something new, and why not?"

Plus, her grandfather, Jake Bohl, is a welder and a blacksmith. Her father, Kevin, enjoys welding, and her uncle, David Bohl, owns his own welding business where his sons work as welders.

Her decision to study welding turned out to be a good idea. Greek learned gas metal arc welding (GMAW), shielded metal arc welding (SMAW), and gas tungsten arc welding (GTAW).

Potter also encouraged Greek to compete in the SkillsUSA competition. "My junior year, I was naturally apprehensive about competing because I had never been in any kind of competitive event before," she said. "That year, I placed in the top five in the region, which meant I was able to compete at the state level in Knoxville."

KRISTIN CAMPBELL (kcampbell@aws.org) *is assistant editor of the* Welding Journal.

Greek continued to study welding throughout high school. "I was pretty much the only girl the whole time," she said, but this did not bother her, and she became friends with most of the boys.

She graduated from high school last year and is thankful to have had a good welding teacher. "I learned, and to this day, attribute everything I know how to do to Mr. Potter," she said. "He also gave me the drive to stick with welding when it was something I had no idea about."

Memorable Projects

During Greek's junior and senior years of high school, she made a queen-size bed frame using mild steel and GMAW. "It's actually pretty heavy," she said. She used a combination of vertical and flat positions on this project.

For the headboard, she decided to cut out a large horse symbol, which was inspired by the 1972 Ford Mustang convertible she drives.

"The project I'm most proud of is a chair I made my mom for Mother's Day," Greek said — Fig. 2. "I love the outdoors, and I made this chair with that in mind. Up both sides, I made it to look like tree branches with real-looking bark and copper leaves at the end of the branches. I also love horses, like my mom, and so I put horseshoes all over it for the arm and foot rests."

Greek made this project in her junior and senior years of high school as well, using scrap metal from her bed frame, which included square tubing, and a flat piece of metal to cut out the seat. To join it all together, she used GMAW. Her mother, Cathie, loves this cherished gift and keeps it at home.

When the chair was on display for Greek's school at a local mall, a woman offered her $500 for it, and when she was told it was not for sale, she offered $1000. "I still couldn't sell it, but it was quite a gesture and it made me feel really good about myself and the quality of my work," Greek said.

She is happy that she had the chance to create these projects. "It was really fun because I knew I could turn my art into actual things that people could see and hopefully enjoy," she said.

Studying at Chattanooga State Technical Community College

In August 2005, Greek began taking welding classes at Chattanooga State Technical Community College in Chattanooga, Tenn. She started out welding beads on a plate, flat, then bringing the plate onto a jig and welding beads horizontal, and doing overlapping and tie ins. Afterward, she moved on to vertical and overhead welding, GMAW, flux cored arc welding, and SMAW.

Fig. 2 — Greek (right) and her mother, Cathie, pose next to the chair she created. Consisting of an outdoor theme, its back rest features a horse.

However, Greek stopped attending school this fall semester. "I actually prematurely ended my college career — one, because I felt I was stretching myself a little too thin with all of my responsibilities, and two, because I found out that my instructor wasn't able to issue welder certification," she said. The primary reason she attended college was to get certified, but when it is more convenient, she will go back to get her diploma. "Also, Mr. Potter told me that he could certify me on our own time, so that works out better for me," she added.

Still, attending college has been beneficial. "I gained more experience in the areas I studied in high school and also learned about flux cored arc welding, something I hadn't done before," she said.

Working at Litespeed

In February, Greek started working part time as a welder at Litespeed, a bike shop in Ooltewah, Tenn. She got the job after her college welding class took a field trip to the company, and her teacher, Larry Ponder, arranged an interview for her. She found out later he put in several good words for her. "I like to think I would have gotten the job anyway, but it's always nice when your superiors think highly enough of you to take the extra time to help you out in a personal matter such as that," she said.

At the company, she performs GTAW on bicycle frames. "Everything I weld is titanium," she said, adding that from time to time, some of the other welders use aluminum.

In addition, Greek works in the company's machine shop. "I put blocks of titanium into a CNC machine to be cut or drilled to whatever setting is needed," she explained. "During the process, the block is moved around in a vise to perform the various cuts and holes that are made."

She is grateful for the opportunity to work there. "I think I was probably one of the first or the very first student they've actually hired, because normally they want somebody more experienced...but for them to sit there and take a chance on me, they've really helped me, and that's what I like about them," she said.

Her days stay busy, and she currently works Monday through Thursday from 6:00 a.m. to 4:30 p.m.

Josie Welds

Ever since Greek started realizing she loved to weld, she thought it would be nice to have her own business. In May, this dream became a reality, and Josie Welds became established.

Her welding facility is located in her father's garage at home. It includes a large bench and several machine tools including a band saw, drill press, SMAW machine, and GMAW machine. Greek is saving up to get a GTAW machine and plasma cutting machine.

"My dad has really helped me out with the whole endeavor and has been nothing but supportive the entire time," she said. Within the past few months, he has even extended the roof line on the back side of the garage almost 10 ft.

"I love it, because I can go home, and if I've got an idea that I want to make something, it's right there," she said.

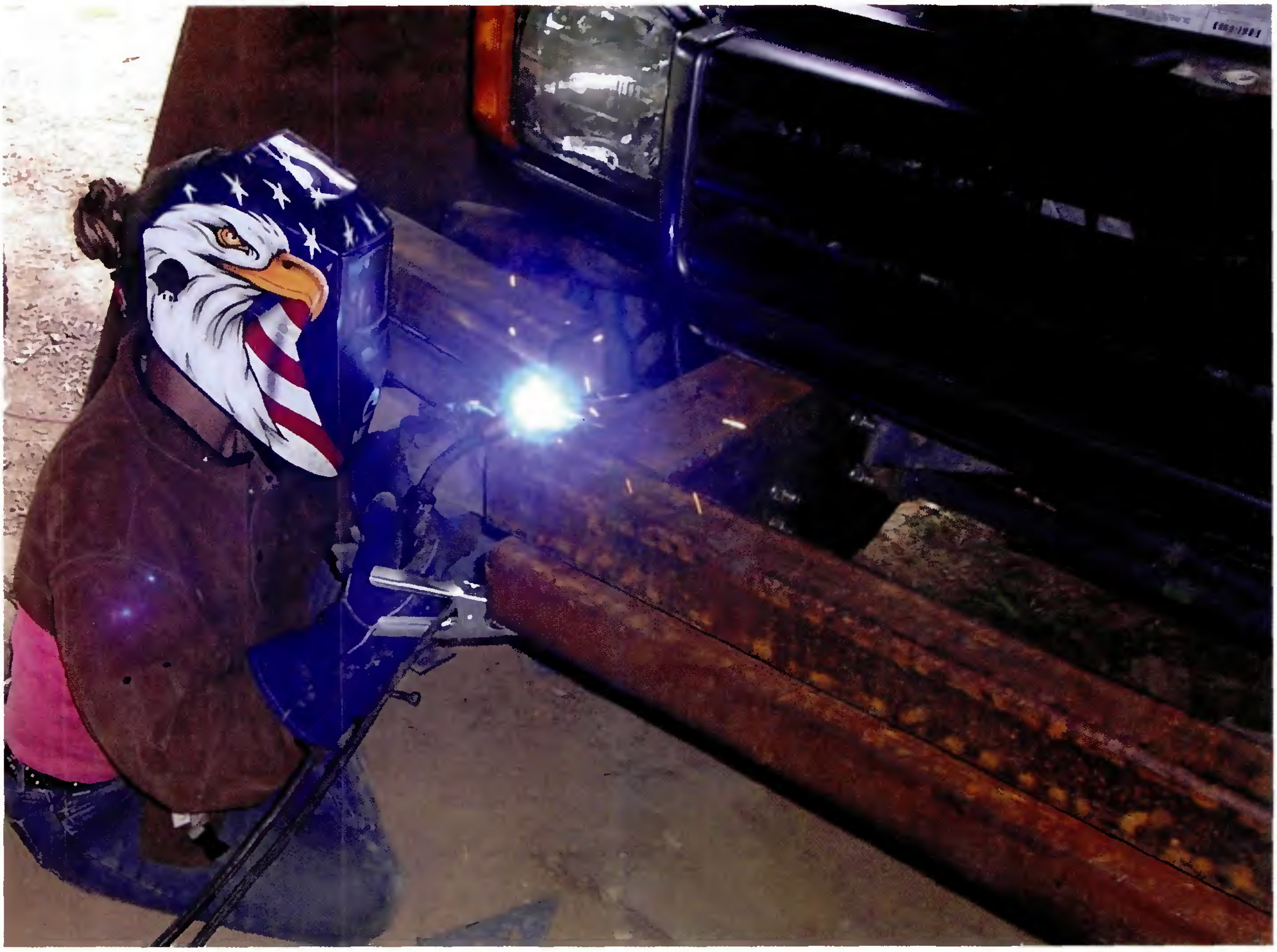

Fig. 3 — Greek is shown performing gas metal arc welding on a bumper for a Land Rover. "I like to be able to do any kind of job I'm confronted with," she said.

For a while, with the help of her fiancé Jeff Hunter, she was working on making a bumper for a Land Rover — Fig. 3. Mild steel, 3 x 3 square tubing, and scrap metal were used for this, and it was assembled with GMA and SMAW.

Unfortunately, work has ceased on it because the customer came upon some difficulties and was not going to be able to pay for the services. "We still plan to finish it the way we had planned, in our own time, and sell it for more profit than we would have made had things gone the way they should have," Greek said.

With help from her father, she recently completed building an inside shell for her aunt and uncle's mailbox. For this, flat plate was used, along with angle iron on the corners of its inside and outside, and GMAW. "My uncle already installed it at his house and had a brick mason cover it," she said. "He says it's working great."

She has a customer who wants a bed frame similar to hers, and after that, she is sure more work will come. People are finding out about her business through word of mouth, but she is hoping to have a Web site set up soon.

With the establishment of Josie Welds, Greek has fulfilled her dream of owning her own business.

"I'm glad because I'm driving myself to have something that I've wanted for a while, and I really enjoy that, knowing that I can do it," Greek said.

Goals for the Future

When Greek is not busy working, she enjoys spending time with her parents and fiancé. She likes drawing and painting, too.

Additionally, she has two horses — Zip, a quarter horse, and Honey, an Arabian. "We're trying real hard to ride them, but they haven't been ridden in quite a while and they don't like the idea of someone on their back anymore," she said. "Hopefully, they will come around."

She is looking forward to her future. "Welding has taught me how to use more of my creative sense than just a simple art class could," Greek said. "It has also taught me perseverance in that, being a woman, it's more difficult to excel in a 'man's' profession, but given time I can and will be accepted for my talents and not my gender."◆

FCAW Electrodes

The flux cored electrode is a composite tubular filler-metal electrode consisting of a metal sheath and a core of various powdered materials. Both the sheath and core contain ingredients that contribute to the highly desirable operating characteristics and weld properties of the process. The use of this electrode differentiates the FCAW process from other arc welding processes.

Much of the versatility of the FCAW process is due to the wide variety of ingredients that can be included in the core of the tubular electrode. For ferrous alloys, the electrode usually consists of a low-carbon steel or an alloy-steel sheath surrounding a core of fluxing and alloying materials. The composition of the flux core varies according to the electrode classification and the particular manufacturer of the electrode.

The primary function of the flux core ingredients is to accomplish the following:

- Provide the mechanical, metallurgical, and corrosion-resistant properties of the weld metal by adjusting the chemical composition.
- Promote weld metal soundness by shielding the molten metal from oxygen and nitrogen in the air or, in the case of self-shielded FCAW, to react with nitrogen or oxygen, or both, in the air and render it harmless.
- Scavenge impurities from the molten metal through the use of fluxing reactions.
- Produce a slag cover to protect the solidifying weld metal from the air.
- Control the shape and appearance of the bead in the different welding positions for which the electrode is suited.
- Stabilize the arc by providing a smooth electrical path to reduce spatter and facilitate the deposition of uniformly smooth, properly sized beads.

Table 1 lists most of the elements commonly found in the flux core, the form in which they are integrated, and the purposes for which they are used.

Table 1 — Common Core Elements in Flux Cored Electrodes

Element	Usually Presented As	Purpose in Weld
Aluminum	Metal powder	Deoxidize and denitrify
Boron	Ferroboron	Grain refinement
Calcium	Minerals such as fluorspar (CaF_2) and limestone ($CaCO_3$)	Provide shielding and form slag
Carbon	Element in ferroalloys such as ferromanganese	Increase hardness and strength
Chromium	Ferroalloy or metal powder	Alloying to improve creep resistance, hardness, strength, and corrosion resistance
Iron	Ferroalloys and iron powder, sheath	Alloy matrix in iron-based deposits, alloy in nickel-based and other nonferrous deposits
Manganese	Ferroalloy such as ferromanganese or as metal powder	Deoxidize; prevent hot shortness by combining with sulfur to form manganese sulfide; increase hardness and strength; form slag
Molybdenum	Ferroalloy	Alloying to increase hardness and strength; in austenitic stainless steels to increase resistance to pitting-type corrosion
Nickel	Metal powder	Alloying to improve hardness, strength, toughness, and corosion resistance
Potassium	Minerals such as potassium-bearing feldspars and silicates in frits	Stabilize the arc and form slag
Silicon	Ferroalloy such as ferrosilicon or silicomanganese; mineral silicates such as feldspar	Deoxidize and form slag
Sodium	Minerals such as sodium-bearing feldspars and silicates in frits	Stabilize the arc and form slag
Vanadium	Oxide or metal powder	Increase strength
Titanium	Ferroalloy such as ferrotitanium; in mineral, rutile (titanium dioxide)	Deoxidize and denitrify; form slag; stabilize carbon in some stainless steels
Zirconium	Oxide or metal powder	Deoxidize and denitrify; form slag

Excerpted from the Welding Handbook, *9th Edition, Vol. 2, Welding Processes, Part 1.*

Guide for Shade Numbers

Process	Electrode Size in.	Electrode Size mm	Current (A)	Minimum Protective Shade	Suggested[a] Shade No. (Comfort)
Shielded metal arc welding (SMAW)	less than 3/32	2.4	less than 60	7	—
	3/32–5/32	2.4–4.0	60–160	8	10
	5/32–1/4	4–6.4	160–250	10	12
	over 1/4	6.4+	250–550	11	14
Gas metal arc and flux cored arc welding (GMAW, FCAW)			less than 60	7	—
			60–160	10	11
			160–250	10	12
			250–500	10	14
Gas tungsten arc welding (GTAW)			less than 50	8	10
			50–150	8	12
			150–500	10	14
Air carbon arc cutting (CAC-A)					
Light			less than 500	10	12
Heavy			500–1000	11	14
Plasma arc welding (PAW)			less than 20	6	6–8
			20–100	8	10
			100–400	10	12
			400–800	11	14
Plasma arc cutting (PAC)			less than 20	4	4
			20–40	5	5
			40–60	6	6
			60–80	8	8
			80–300	8	9
			300–400	9	12
			400–800	10	14
Torch brazing (TB)			—	—	3 or 4
Torch soldering (TS)			—	—	2
Carbon arc welding (CAW)			—	—	14
	Plate Thickness in.	Plate Thickness mm			
Oxyfuel gas welding (OFW)					
Light	under 1/8	under 3			4 or 5
Medium	1/8 to 1/2	3 to 13			5 or 6
Heavy	over 1/2	over 13			6 or 8
Oxygen cutting (OC)					
Light	under 1	under 25			3 or 4
Medium	1 to 6	25 to 150			4 or 5
Heavy	over 6	over 150			5 or 6

a) As a rule of thumb, start with a shade that is too dark to see the weld zone. Then go to a lighter shade which gives sufficient view of the weld zone without going below the minimum . In oxyfuelgas welding, cutting, or brazing where the torch and/or flux produces a high yellow light, it is desirable to use a filter lens that absorbs the yellow or sodium line in the visible light spectrum.

Excerpted from ANSI Z49.1:2005, *Safety in Welding, Cutting, and Allied Processes*

CAREER OPPORTUNITIES

WELDER

Join the Air Products Team!

WELDER/MECHANIC

Air Products and Chemicals, Inc., a Fortune 500 manufacturer of industrial gases and chemicals, has an immediate opening for an experienced Welder/Mechanic to be based out of the **Cleveland, OH** area.

QUALIFICATIONS:

- *Must be able to certify to Air Products procedures per ASME code*
- *5-7 years experience required in welding processes for GTAW & SMAW in carbon and stainless steels*
- *Experience in GTAW & GMAW for aluminum a plus*
- *Pipefitting and blueprint reading a must*
- *High school diploma or GED required. Additional education is a plus*
- *Mechanical ability and willingness to learn about rotating machinery is a must, since when not required to be welding, incumbent will be expected to perform the duties of a mechanic*
- *Must be team player in a team environment*
- *Must be self motivated*
- *Domestic travel throughout the United States required (70-80% travel)*
- *Although limited, international travel may also be required*
- *Willing to travel on short notice; you will be on-call 24/7*
- *Ability to work extended hours - 12 hour days*
- *Must be able to work at heights and in confined spaces*

Air Products (NYSE:APD) serves customers in technology, energy, healthcare and industrial markets worldwide with a unique portfolio of products, services and solutions, providing atmospheric gases, process and specialty gases, performance materials and chemical intermediates. Founded in 1940, Air Products has built leading positions in key growth markets such as semiconductor materials, refinery hydrogen, home healthcare services, natural gas liquefaction, and advanced coatings and adhesives. The company is recognized for its innovative culture, operational excellence and commitment to safety and the environment and is listed in the Dow Jones Sustainability and FTSE4Good Indices. The company has annual revenues of $8.1 billion, operations in over 30 countries, and more than 20,000 employees around the globe. For more information, visit **www.airproducts.com**.

Air Products offers a comprehensive benefits package including paid holidays/vacation, affordable medical, dental, life insurance, pension and 401(k) plans.

To apply for this position, visit the Air Products Career Center at www.airproducts.com/careers. Click on North America, then select Career Center. You can apply specifically to Job Req #24145. If you are a current Air Products employee, please apply via APOnline by clicking on Online Applications, then selecting Career Center.

We thank all applicants in advance for their interest; however, only those applicants who are being considered for an interview, or are currently employed by Air Products, will be contacted.

Air Products is an equal opportunity employer (M/F/D/V) where diversity matters.

AIR PRODUCTS

tell me more
www.airproducts.com/careers

Welders Needed

Colorado Railcar Mfg, LLC, the premiere manufacturer of luxury railcars, has openings for full-time welders at our Fort Lupton, Colorado facility for both 1st and 2nd shift.

Applicants must be able to pass FCAW " 6G tube V-Grove welding test.

Apply in person at:

1011 14th Street
Fort Lupton, CO 80621
or call Garry at 303-857-1066.
You may apply online at
www.coloradorailcar.com

WANTED
Independent Sales Reps

To demonstrate welding alloys to end users.

– Consumables market
– Repeat Customers
– Complements Industrial Rep's present line(s) of products.

Very unique opportunity.

Contact Bob Turner
(800) 642-9885

PETROLOGY
Pipeline Fusion

Petrology Ltd project manages high technology welding pipeline contracts in the UK and Internationally

Welding Engineers / Metallurgists

We require professional engineers who have experience of developing welding proposals to meet technical specifications and to take responsibility from the procedure qualification through to project conclusion.

Replies to Emily Carr, Petrology Limited, Erskine Ferry Road, Old Kilpatrick, Glasgow, G60 5EU or email emily.carr@petrology.com

www.petrology.com

Sr. Technician, Arc Welding

Edison Welding Institute
Columbus, Ohio

Operate state-of-the-art equipment to create high-quality welds using specifications set by our world-class engineers; maintain precise records of parameters and results, and interact with clients. Perform testing, processing, grinding, and material removal using air and electric power tools. 5-10 years welding experience; Certification preferred. U.S. Residents Only. Employer will assist with relocation costs. Salary range of 35K to 55K for most experienced.

See "Careers" at www.ewi.org to apply or call 614-688-5203.

EQUIPMENT FOR SALE OR RENT

CINCINNATI, OHIO
800-288-9414
WELD PLUS
www.weldplus.com
WELD PLUS, INC.
Fax: 513-467-3585
email: melissa@weldplus.com

JUST IN!!
Aronson G1200 Positioner
120,000 lb capacity @ 12" center of gravity.
EXCELLENT CONDITION!!

OVER 50 "BRAND NEW" POSITIONERS IN STOCK!!!

"BRAND NEW 2006" IN OUR STOCK!!!
PANDJIRIS POSITIONERS!!! JETLINE SEAMERS!!
MBC POSITIONERS!!! WEBB TURNING ROLLS!!!

Well Over 150 Positioners Total, Up to 60 Tons!! Head/Tailstocks, Turntables up to 100 Tons. Manipulators up to 14' x 14'. Travel cars, Longitudinal Seamers from 6 in. to 26 ft. Turning Rolls up to 400 Tons. Circular Weld Systems, Welding Lathes, Motoman and Panasonic Welding Robots.

"WE KNOW WELDING"
TALK TO US!! ... COME VISIT US!!
800-288-9414
Pete, Paul, Dennis, Jared or Melissa

SAVE 40%! TURNTABLES

PRESTON EASTIN RFT 25E. We are selling (6) new/almost new two-position turntables for robotic weld cells.
48" x 48" x 1-1/4", aluminum plate, 500 lb. capacity @ 18". A-B PLC control.
$5,900 EACH WITH WARRANTY. Baseplates and robot risers also available.

ANTENEN RESEARCH
800-323-9555
www.antenen.com
Largest inventory of new & used robots in North America

Turning Rolls
Positioners
& Manipulators
New and Used

Joe Fuller LLC
@ www.joefuller.com
or email joe@joefuller.com

Phone: 979-277-8343
Fax: 281-290-6184

We buy and sell
WELDING RODS & WIRE
ALL TYPES ALL SIZES**
ALL QUANTITIES

Excess Welding Alloys, Inc.
A division of Weld Wire Company Inc.

800-523-1266 FAX 610-265-7806
www.weldwire.net

Portable System
Stops Distortion
up to 90% Better
"A natural for welders"

www.Bonal.com
(800) 638-2529

We Buy & Sell Surplus
Welding Rod & Wire
All types, sizes & Quantities

Liberty Alloys INC

Call us first!

800-523-2791
PA: 610-825-1250
FAX: 610-825-1553

BRAND NEW WATSON LABEL EATER

Refurbish aluminum and steel cylinders. Removes plastic, paper and metal labels as well as ADHESIVES and flaking paint.

$2,500
(509) 994-1445

Welding Positioners & Turning Rolls
New and Used

Large selection in stock for immediate delivery.

www.allfabcorp.com

Call, Fax or Email for a free catalog.

All-Fab Corp.
Email: sales@allfabcorp.com
Web: www.allfabcorp.com
Phone: 269-673-6572
Fax: 269-673-1644

RED-D-ARC®
Welderentals
www.red-d-arc.com

All Types of Welding and Positioning Equipment for Rental and Lease

1-800-245-3660
Service Centers Across North America

ATTENTION!!
RETOOLING? CHANGING PRODUCTS?
CLOSING SHOP? GOIN' FISHING?
We pay good prices for used welding machinery!
We are looking for any used welding machinery like: Turning Rolls, Positioners, Manipulators, Seamers, etc.
Send Photos to:
melissa@weldplus.com
or call 800.288.9414
WELD PLUS

SAVE 50%! PLASMA WELDERS

THERMAL ARC ULTIMA-150. We are selling (6) new/almost new plasma power sources with TP100 pulse controls.
$2,900 EACH WITH WARRANTY. Buy all six and we will include a seventh for spares. 3A torches and gas mixers also available.

ANTENEN RESEARCH
800-323-9555
www.antenen.com
Largest inventory of new & used robots in North America

CERTIFICATION & TRAINING

Get REAL Educational Services, Inc.

Call About Courses for 9-Year Renewal

CWI PREPARATORY

Guarantee - Pass or Repeat FREE!

2-WEEK COURSE (10 DAYS)
MORE HANDS-ON/PRACTICAL APPLICATIONS
Pascagoula, MS, Dec. 4–15 Jan. 17–26
Atlanta, GA, Jan. 31–Feb. 9
Houston, TX Feb. 14–23

SAT–FRI COURSE (7 DAYS)
EXTRA INSTRUCTION TO GET A HEAD START
Pascagoula, MS, Dec. 9–15 Jan. 20–26
Atlanta, GA, Feb. 3–9
Houston, TX Feb. 17–23

MON–FRI COURSE (5 DAYS)
GET READY - FAST PACED COURSE
Pascagoula, MS, Dec. 11–15 Jan. 22–26
Atlanta, GA, Feb. 5–9
Houston, TX Feb. 19–23
(Test follows on Saturday at same facility)

SENIOR CWI PREPARATORY
Pascagoula, MS, Dec. 11–15 Jan. 22–26
Atlanta, GA, Feb. 5–9
Houston, TX Feb. 19–23

FOR DETAILS CALL OR E-MAIL:
1-800-489-2890
info@realeducational.com

The AWS Certification Committee

Is seeking the donation of sets of Shop and Erection drawings of highrise buildings greater than ten stories with Moment Connections including Ordinary Moment Resistant Frame (OMRF) and Special Moment Resistant Frame (SMRF) for use in AWS training and certification activities. Drawings should be in CAD format for reproduction purposes. Written permission for unrestricted reproduction, alteration, and reuse as training and testing material is requested from the owner and others holding intellectual rights.

For further information, contact:

Joseph P. Kane
(631) 265-3422 (office)
(516) 658-7571 (cell)
joseph.kane11@verizon.net

CWI Refresher...a fresh approach!

Not only review and learn the most controversial, most often misinterpreted issues facing welding inspectors...now add great quality tools that will enhance your ability to implement true solutions for your clients or your company.

Be a CWQI-continuous workplace quality innovator!

Contact Atema for the 30 hour syllabus comparable to the AWS body of knowledge. Suitable as continuing education for CWIs or for any welding inspection personnel.

Convenient **classes in Chicago**:

312-861-3000
info@atemainc.com
www.atemainc.com/cwi.htm

visit booth #10152 AWS-Atlanta

Atema inc.

Industrial Welding Instruction On-Site and Worldwide

40 years experience
Excellent credentials

Ferrous and nonferrous metals (pipe and plate), GTA, SMA, GMA, underwater welding and burning, and C-4 explosives.

PH: (419) 367-1344
FX: (419) 474-6027

SERVICES

MITROWSKI RENTS

1000 Ton Aronson Tank Turning Rolls

www.mitrowskiwelding.com
sales@mitrowskiwelding.com
800-218-9620
713-943-8032

South Bay Inspection

Visual and Non Destructive Testing Services

Radiography	AWS Certified Weld Inspection
Ultrasonics	API 510 Pressure Inspection
Liquid Penetrant	API 653 Tank Inspection
Magnetic Particle	API 570 Piping Inspection
NDT Training	Level III Services

Turnaround Inspection Staffing
Field and Laboratory Testing

SOUTH BAY INSPECTION
1325 W Gaylord St.
Long Beach, CA 90813
Phone: (562) 983-5505 **Fax:** (562) 983-5237

VISIT US ON THE WEB
www.southbayinspection.com

Cover Gas Problems?

www.weldhugger.com

LITERATAURE

Speciality Welds

A Diver-Welder's Companion

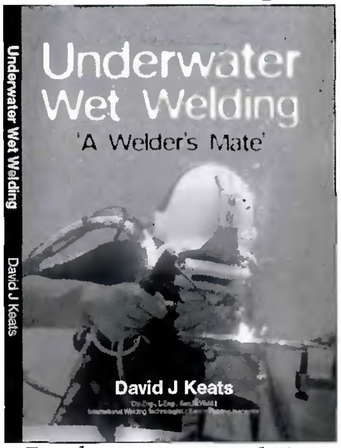

Purchase on our website at www.specialwelds.com

ADVERTISER INDEX

IFC = Inside Front Cover
IBC = Inside Back Cover
OBC = Outside Back Cover
RI = Reader Information Card

Statement of Ownership, Management and Circulation for U.S. Postal Service (Required by U.S.C. 3685)

1. TITLE OF PUBLICATION: Welding Journal — 2. PUBLICATION NO.: ISSN 0043-2296
3 DATE OF FILING: September 26, 2006 — 4. FREQUENCY OF ISSUE: Monthly
5. NO. OF ISSUES PUBLISHED ANNUALLY: 12 — 6. ANNUAL SUBSCRIPTION: $120.00
7. MAILING ADDRESS OF KNOWN OFFICE OF PUBLICATION: 550 N.W. LeJeune Rd., Miami, Dade County, Florida 33126
8. MAILING ADDRESS OF THE HEADQUARTERS OR GENERAL BUSINESS OFFICES OF THE PUBLISHERS:
   550 NW LeJeune Rd., Miami, Dade County, Florida 33126
9. NAMES AND COMPLETE ADDRESS OF PUBLISHER, EDITOR AND MANAGING EDITOR:
   PUBLISHER: Andrew Cullison, AWS, 550 NW LeJeune Rd., Miami, Florida 33126
   EDITOR: Andrew Cullison, AWS, 550 NW LeJeune Rd., Miami, Florida 33126
   MANAGING EDITOR: Zaida Chavez
10. OWNER: NAME: American Welding Society,Inc. ADDRESS: 550 NW LeJeune Rd., Miami, Florida 33126
11. KNOWN BONDHOLDERS, MORTGAGEES, AND OTHER SECURITY HOLDERS OWNING OR HOLDING 1 PERCENT OR MORE OF TOTAL AMOUNT OF BONDS, MORTGAGES OR OTHER SECURITIES: None
12. The purpose, function, and nonprofit status of this organization and the exempt status for Federal income tax purposes: Has not changed during preceding 12 months
13. Publication Title: Welding Journal — 14. Issue date for Circulation Data Below: October 2006
15. EXTENT AND NATURE OF CIRCULATION:

	Average No. Copies Each Issue During Preceding 12 Months	Actual No.Copies of Single Issue Published Nearest to Filing Date
A. Total No. Copies Printed (Net Press Run)	51,933	52,600
B. Paid and/or Requested Circulation		
1. Paid / Requested Outside-County Mail Subscriptions Stated on Form 3541	49,733	49,950
2. Paid In-County Subscriptions Stated on Form 3541	None	None
3. Sales Through Dealers and Carriers, Street Vendor, Counter Sales, and other Non-USPS Paid Distribution	None	None
4. Other Classes Mailed Through the USPS	None	None
C. Total Paid / Requested Circulation	49,733	49,950
D. Free Distribution by Mail (Samples, complimentary and other free)		
1. Outside-County as State on Form 3541	433	433
2. In-County as Stated on Form 3541	None	None
3. Other Classes Mailed Through the USPS	None	None
E. Free Distribution Outside the Mail (Carriers or other means)	None	None
F. Total Free Distribution	433	433
G. Total Distribution	50,166	50,283
H. Copies not Distributed	1,767	2,217
I. Total	51,933	52,600
J. Percent Paid and / or Requested Circulation	99%	99%

16. Statement of Ownership will be printed in the November 2006 issue of this publication.
I certify that the statements made by above are correct and complete:
Andrew Cullison, Publisher

SUPPLEMENT TO THE *WELDING JOURNAL*, NOVEMBER 2006
Sponsored by the American Welding Society and the Welding Research Council

A Genetic Algorithm and Gradient-Descent-Based Neural Network with the Predictive Power of a Heat and Fluid Flow Model for Welding

Six neural networks were developed for gas tungsten arc welding of low-carbon steel, with each network providing one of the six output parameters of GTA welds

BY S. MISHRA AND T. DEBROY

ABSTRACT. In recent years, numerical heat and fluid flow models have provided significant insight into welding processes and welded materials that could not have been achieved otherwise. However, these calculations are complex and time consuming, and are unsuitable in situations where rapid calculations are desired. A practical solution to this problem is to develop a neural network that is trained with the data generated by a numerical heat and fluid flow model. Apart from providing high computational speed, the results of this neural network conform to the basic laws of conservation of mass, momentum, and energy.

In the present study, six feed-forward neural networks have been developed for the gas tungsten arc (GTA) welding of low-carbon steel. Each network provides one of the six output parameters of GTA welds, i.e., depth, width, and length of the weld pool, peak temperature, cooling time from 800° to 500°C, and maximum liquid velocity. The networks require values of 17 input parameters including the welding variables like current, voltage, welding speed, arc efficiency, arc radius, and power distribution factor, and material properties like thermal conductivity and specific heat. The weights of the neural networks were calculated using two optimization schemes, first using the gradient descent (GD) method with various sets of randomized initial weights, and then applying a hybrid optimization scheme where a genetic algorithm (GA) is used in combination with the GD method. The neural networks produced by the hybrid optimization approach gave better results than all the networks based on only the GD method. Unlike the GD method alone, the hybrid optimization scheme could find the significantly better weights, which is illustrated by the good agreement between all the outputs from the neural networks and the corresponding results from the heat and fluid flow model.

S. MISHRA is now with Department of Metallurgical Engineering and Materials Science, Indian Institute of Technology, Bombay, India. Previously he was with Department of Materials Science and Engineering, The Pennsylvania State University, University Park, Pa, as is T. Debroy.

Introduction

In recent decades, systematic correlations between welding variables and weld characteristics have been attempted by numerical modeling of heat and fluid flow (Refs. 1–19) and artificial neural networks (Refs. 20–42). Numerical models of heat and fluid flow have provided significant quantitative insights into welding processes and welded materials. These models have accurately predicted temperature and velocity fields, weld pool geometry, cooling rate, peak temperature, phase transformations (Ref. 20), grain structure (Refs. 6, 7), inclusion structure (Refs. 43, 44), and weld metal composition change owing to both the evaporation of alloying elements and the dissolution of gases (Ref. 8). Although these models are recognized as powerful tools for research, they are not extensively used in the welding industry because these are complex, require specialized training to develop and test, and consume a large amount of computer time to run.

KEYWORDS

Neural Networks
Gas Tungsten Arc Welding (GTAW)
Heat Transfer and Fluid Flow Model
Low-Carbon Steel

Neural network models are powerful nonlinear regression analysis methods (Refs. 20, 21, 45–47) that can relate input variables like welding process parameters and material properties with weld characteristics such as weld pool geometry. The previous efforts to model the GTAW process using a neural network were based on training the network with experimental data (Refs. 27, 32, 38). Since the volume of experimental data required to train a neural network depends on the number of input and output variables, most previous efforts considered only a few input parameters to keep the necessary volume of experimental data tractable (Refs. 27, 32, 38). For example, Tarng et al. (Ref. 27), Andersen et al. (Ref. 32), and Juang et al. (Ref. 38) developed neural network models of the GTA welding process, which considered the effects of process parameters like welding speed, arc current, and voltage as inputs. These neural network models were developed using a limited volume of experimental data, and they could not determine the effect of material properties like thermal conductivity, specific heat, etc., on weld pool geometry. Furthermore, the output variables considered in these neural networks were also limited. For example, the existing neural network models do not provide any information about some of the important parameters such as the cooling rate and peak temperature. A review of previous work indicates that what is needed is a framework for rapid calculation of weld pool

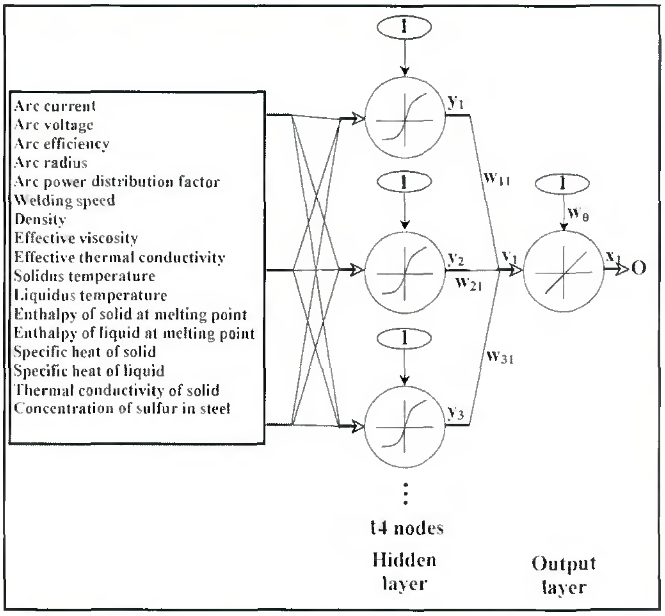

Fig. 1 — Neural network architecture used in this study. The input layer has 17 input variables and the output layer has one of the six output variables, i.e., weld pool depth, weld pool width, weld pool length, peak temperature, cooling time from 800° to 500°C, or maximum liquid velocity in the weld pool.

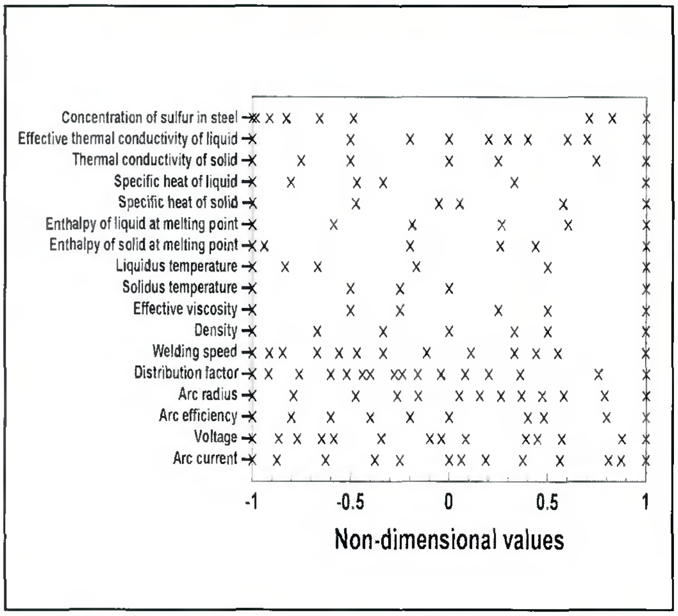

Fig. 2 — The ranges of values of the input variables in the training and testing databases. The normalized values of the variables were obtained using Equation 10 and corresponding minimum and maximum values listed in Table 1.

geometry, cooling rate, and peak temperature for the GTA welding of various materials.

In the present work, a neural network has been trained with the results of a well-tested numerical heat and fluid flow model (Refs. 2, 8, 12). The neural network correlates various output parameters such as weld pool geometry, cooling rate, peak temperature, and maximum liquid velocity with all the major welding variables and material properties. Of these variables, the geometry and cooling rates affect the weld properties. The peak temperature and the velocities are important in understanding the role of convective heat transfer and mixing in the weld pool. Since the training data are made up of results from a reliable numerical heat transfer and fluid flow model, the output of the trained neural network will comply with the basic phenomenological laws of welding physics. This paper seeks to document the problems, issues, and lessons learned in the development of a neural network model from the results of a heat transfer and fluid flow model. The neural network is validated by checking its performance for different sets of material properties and welding conditions, which were not a part of the training data.

The Mathematical Model

Neural Network Model

In the present study, six feed-forward neural networks have been developed for the gas tungsten arc (GTA) welding of low-carbon steel with no filler metal. Partial joint penetration welds with a flat top surface are assumed. Each neural network takes 17 input variables that include various welding variables such as arc current, voltage, welding speed, and material properties such as thermal conductivity, specific heat, and provides a single output, which can be one of the six output parameters, i.e., depth, width, and length of the weld pool, peak temperature, cooling time between 800°C and 500°C, and maximum liquid velocity in the weld pool. The cooling time was calculated on the workpiece surface along the welding direction. The input variables such as arc efficiency, arc power distribution factor, and arc radius determine how heat is absorbed at various locations in the workpiece (Ref. 10). Since temperature-independent thermophysical properties of the solid alloy are used in the model, a question arises as to how to select their values. Since the heat flow in the solid region near the weld pool affects both the size and shape of the weld pool as well as the temperature field in the entire workpiece, it is appropriate to use thermophysical properties at a temperature closer to the melting point than to the ambient temperature. Effective thermal conductivity and effective viscosity are used as input variables because they allow accurate modeling of the turbulence effect in the weld pool. These two variables are system properties, and their values are obtained by enhancing the molecular values of liquid thermal conductivity and viscosity, respectively. Appropriate values of these two variables for GTA welding of low-carbon steel have been determined in the literature (Ref. 5) through reverse modeling.

The structure of each neural network, along with all the input and output variables, is shown in Fig. 1. Each neural network contains an input layer, a hidden layer, and an output layer. The input layer contains all the 17 input variables, which are connected to nodes in the hidden layer, represented by circles in Fig. 1, through the weights assigned for each link. The number of nodes in the hidden layer is found by optimizing the network. Each connection to a node, j, from a node in the previous layer, i, has an adjustable weight, w_{ij}, associated with it. The weights, w_{ij}, embody the nonlinear relationship between the input and the output variables. Also, each node in the hidden and the output layers is given an extra input, which always has a value of 1. The weight of this extra input is called the bias. The net input, v_j, for a node, j, is given as

$$v_j = \sum_i w_{ij} y_i + w_\theta \tag{1}$$

where i is a node in the previous layer, w_{ij} is the weight of the connection between nodes j and i, y_i is the output of node i, and w_θ is the bias weight. Equation 1 is calculated for all the nodes in the hidden layers as well as the output layer.

Now, the output of node j is calculated by using a transfer function. A hyperbolic tangent function (a symmetric sigmoid function), which is a nonlinear function producing output between –1 and 1, is used as transfer function for the nodes in

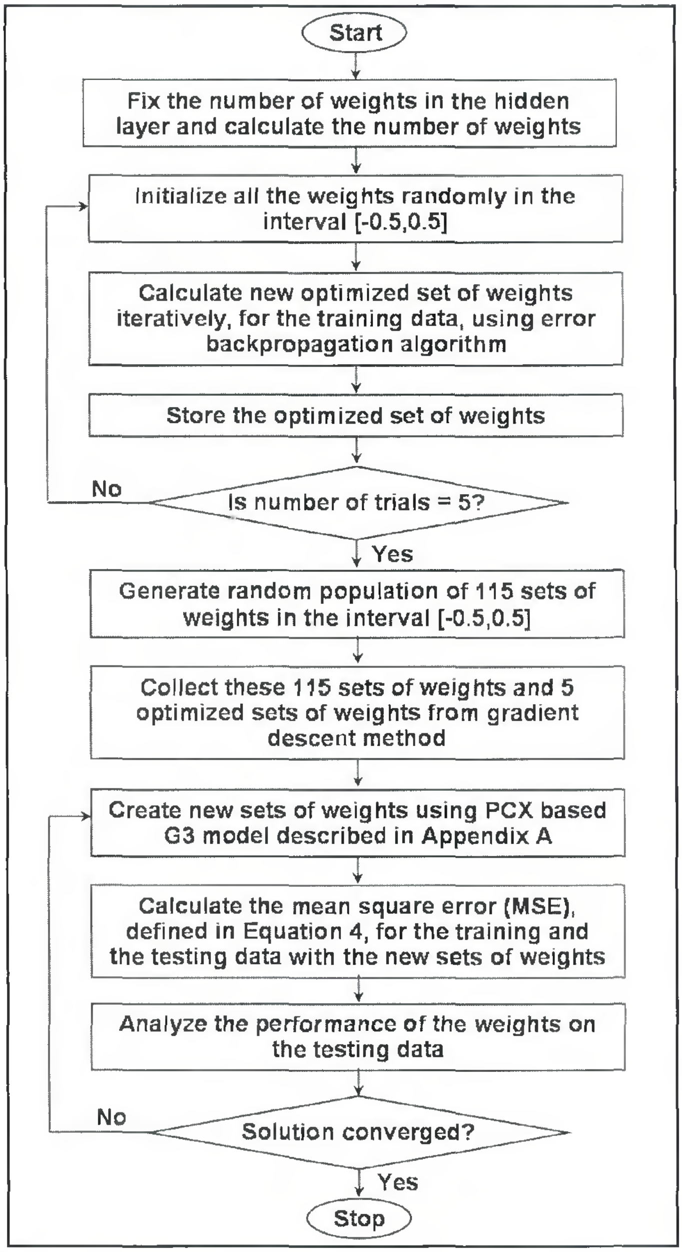

Fig. 3 — Flowchart for training the neural network.

the hidden layer, and a linear transfer function is used for the nodes in the output layer. The use of a nonlinear transfer function in the hidden layer allows the network to learn nonlinear and linear relationships between input and output vectors (Ref. 37), while the use of a linear transfer function in the output layer allows the network to produce values outside the range of –1 to 1. Thus, the output, x_j, of a node j in the hidden layer is given by

(2)

where 'a' is the slope of the sigmoid function. By varying the parameter 'a', sigmoid functions of different slopes can be obtained (Ref. 48). An increase in the value of 'a' increases the slope of the activation function and vice versa. A very high value of the slope makes the curve close to a step function while a low value retards the convergence rate. Based on the findings of previous works, a value of 1.5 was used to achieve rapid convergence (Refs. 49, 50). Furthermore, the use of the tanh function in Equation 2 as the activation function helps in keeping the problem reasonably well conditioned. An attractive feature of the hyperbolic tangent function is that its derivative does not increase computational volume significantly (Ref. 48). The output, x_j, of a node j in the output layer is given by the following:

$$x_j = v_j \tag{3}$$

The training of a neural network implies finding a set of weights that minimize error between the desired output and the output calculated by the neural network. A back-propagation algorithm (Ref. 45) is used for the training of the neural networks. This algorithm tries to minimize the objective function, i.e., the mean square error (MSE) between the desired output and the neural network output. The MSE is defined as (Ref. 45) the following:

$$MSE = \frac{\sum_p \sum_k \left(d_{pk} - o_{pk}\right)^2}{p \times k} \tag{4}$$

where p is the number of training datasets; k represents the number of output nodes, which is one in this work; d_{pk} is the desired output; and o_{pk} is the output produced by the neural network. The desired outputs of the neural network such as weld pool depth, width, and length, cooling rate, peak temperature, and maximum liquid velocity are dependent on input welding conditions, material properties, and the network parameters such as the weights.

The back-propagation algorithm adjusts the weights in the steepest descent direction (negative of the gradient) (Ref. 45). This is the direction in which the error in the value of the output variable, E, decreases most rapidly. For a given set of input-output training data, the partial derivatives of the error with respect to each weight, $\partial E/\partial w$, are calculated in two passes (Ref. 45). The forward pass calculates the output of each node in the hidden layers and the output layer, based on the inputs from the previous layers, as described by Equations 1–3. The backward pass propagates the derivatives from the output layer back to the input layer (Ref. 45). The backward pass is well documented in the literature (Refs. 45, 51) and is not described here. Once $\partial E/\partial w$ are calculated, the weights are changed by an amount proportional to $\partial E/\partial w$ as

$$\Delta w = -\varepsilon \frac{\partial E}{\partial w} \tag{5}$$

where ε is called the learning rate. A large learning rate enables quick convergence, but it can also lead to overstepping of the solution and oscillation of the error (Ref. 24). On the other hand, small learning rate may prevent oscillation of the error, but it requires much more time to reach the solution (Ref. 24). Therefore, in the present study ε was taken as 0.1 during initial iterations, and reduced to 0.01 once the error became very small. A simple method for increasing the rate of learning without oscillation is to include a momentum term in Equation 5 as follows (Ref. 45):

$$\Delta w(n) = -\varepsilon \frac{\partial E}{\partial w} + \alpha \Delta w(n-1) \tag{6}$$

where n is the number of iterations, an iteration being defined as a single sweep through all the input-output pairs in the training dataset, and α is an exponential decay factor between 0 and 1 that determines the relative contribution of the current gradient, $\partial E/\partial w$, and the earlier gradients, $\Delta w(n-1)$, to the weight change. The value of α is set to 0.9 in the present study, based on guidance from previous research (Refs. 37, 51).

The training of the neural network was started with random small weights. It was observed that after the initial rapid decrease in error, further descent became

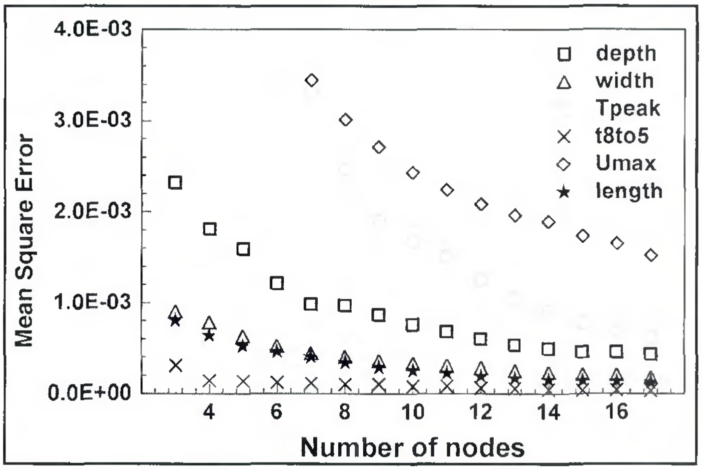

Fig. 4 — Comparison of mean square error (MSE), defined by Equation 4, for different number of nodes in the hidden layer. For each output variable the results are an average of five runs with different sets of initial random weights using the gradient-descent training method.

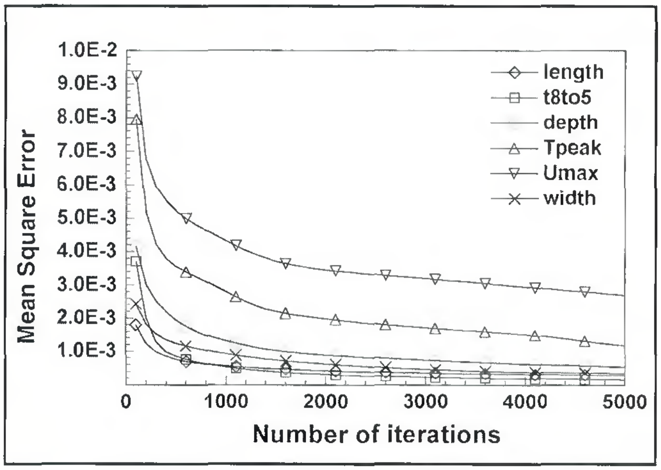

Fig. 5 — Mean square error (MSE), defined by Equation 4, vs. number of iterations for the gradient-descent training method. For each output variable, the results are an average of five runs with different sets of initial random weights.

very sluggish, and the result depended on the initial random weights, which are common problems with gradient-descent algorithms (Refs. 46, 52, 53). Furthermore, for simple two-layer networks (without a hidden layer), the error surface is bowl shaped and using gradient-descent techniques to minimize objective function is not a problem. However, the addition of a hidden layer used to solve more difficult problems like the GTA welding process increases the possibility for complex error surfaces that contain many minima. The gradient-based methods, which are used in the back-propagation algorithm described above, can easily get trapped in such local minima. Stochastic optimization techniques are capable of finding the global minima and avoiding local minima (Refs. 54–56). Therefore, a genetic algorithm (Refs. 54–56) is used along with the gradient-descent method to find the global set of weights in the present work.

The genetic algorithm (GA) used in the present study is a parent centric recombination (PCX) operator-based generalized generation gap (G3) model (Refs. 54–56). This model was chosen because it has been shown to have a faster convergence rate on standard test functions as compared to other evolutionary algorithms and classical optimization algorithms (Ref. 55). Detailed description of this model is available in the literature (Refs. 54–59) and is not repeated here. To start with, many initial sets of randomly chosen values of weights were created. Five of these initial sets of weights were made equal to five different sets of weights calculated by the gradient-descent algorithm. A systematic global search was next undertaken to find the most optimum set of weights that leads to the least mean square error (MSE), given in Equation 4.

Table 1 — The Input Variables and Their Ranges of Values Considered in the Training Dataset

Variables	Minimum value	Maximum value
Arc current, I (A)	9.00E+01	2.50E+02
Voltage, V (V)	9.60E+00	2.60E+01
Arc efficiency, η	3.50E-01	8.50E-01
Arc radius, r (m)	1.00E-03	2.90E-03
Arc power distribution factor, d	5.00E-01	3.00E+00
Welding speed, U (m/s)	1.00E-03	1.00E-02
Density of liquid, ρ (kg/m^3)	6.60E+03	7.80E+03
Effective viscosity of liquid, μ (kg/m-s)	6.00E-02	1.00E-01
Liquidus temperature, T_l (K)	1.730E+03	1.770E+03
Solidus temperature, T_s (K)	1.785E+03	1.845E+03
Enthalpy of solid at melting point, H_s (J/kg)	1.05E+06	1.15E+06
Enthalpy of liquid at melting point, H_l (J/kg)	1.32E+06	1.42E+06
Specific heat of solid, C_{ps} (J/kg-K)	6.27E+02	7.86E+02
Specific heat of liquid, C_{pl}, (J/kg-K)	7.74E+02	8.99E+02
Thermal conductivity of solid, k_s (J/m-s-K)	2.30E+01	3.97E+01
Effective thermal conductivity of liquid, k_l (J/m-s-K)	8.36E+01	5.02E+02
Concentration of surface active species, C_s (wt-%)	0.00E+00	3.50E-01

The mean square error depends on the values of weights:

$$MSE(w) = MSE(w_1, w_2, \ldots, w_q) \qquad (7)$$

where q is the number of weights in the network. The GA produced new individuals, or sets of weights, with iterations based on evolutionary principles (Refs. 20, 55, 56). The specific application of G3-PCX model for obtaining the optimum set of weights is described in Appendix A.

Numerical Heat and Fluid Flow Model for Gas Tungsten Arc (GTA) Welding

The data for the training and testing of the neural network were generated from an extensively tested three-dimensional (3D) numerical heat and fluid flow model for GTA welding (Refs. 1–18). In this model, the transient nature of the problem is transformed to steady-state mode by using a coordinate system moving with the heat source (Refs. 12, 17). The governing equations of conservation of mass, momentum, and energy in three dimensions (3D) are discretized using the power law scheme (Ref. 60). The computational domain is divided into small rectangular control volumes. Discretized equations for the variables are formulated by integrating the corresponding governing equations over the control volumes. The detailed method of discretizing the governing equations is available in the literature (Refs. 12, 17). The discretized equations are solved using the SIMPLE algorithm (Ref. 60) to obtain temperature and velocity fields. The calculated temperature and velocity fields provide the output variables, i.e., weld pool geometry, peak temperature, cooling time between 800° and 500°C, and maximum liquid velocity in the weld pool.

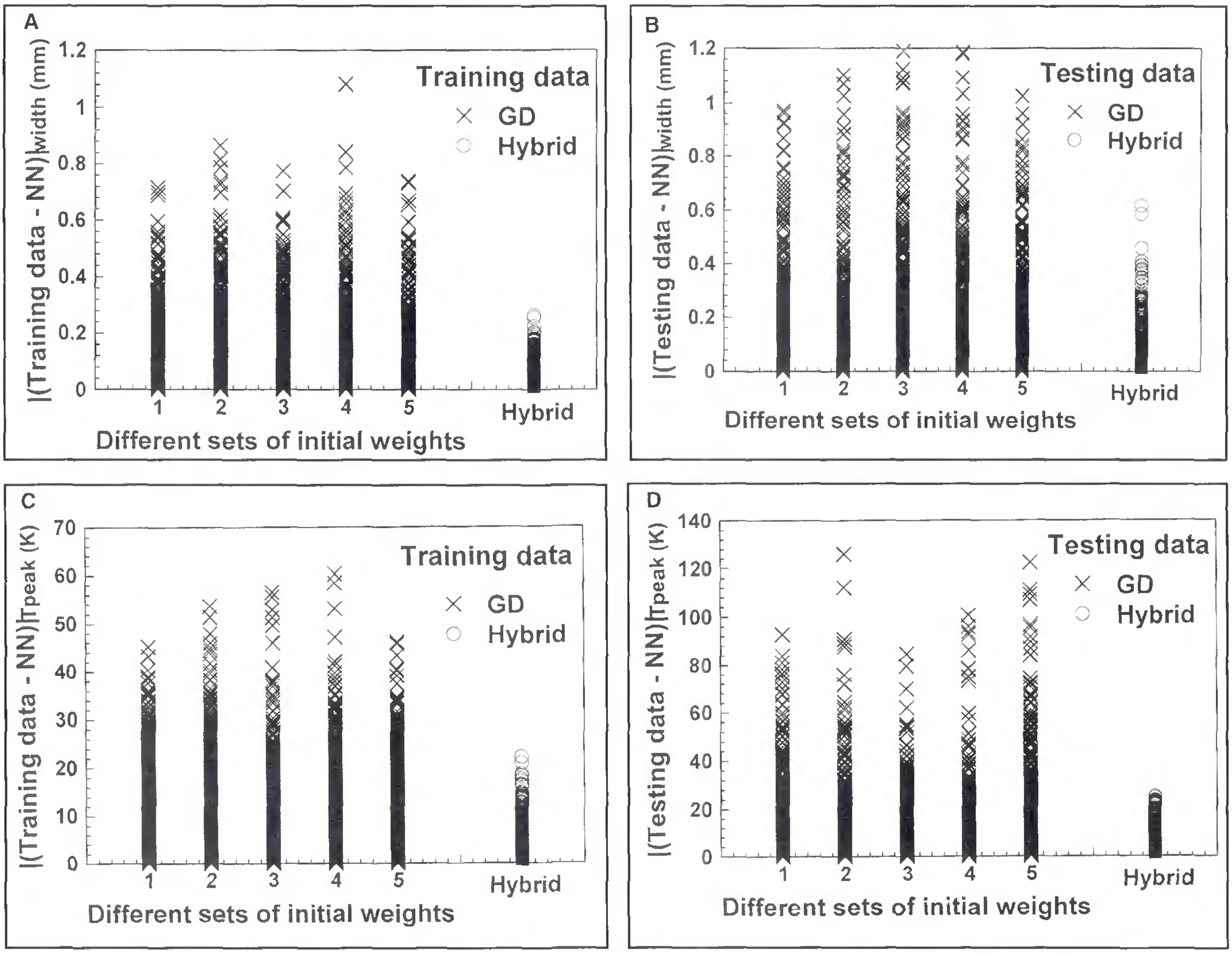

Fig. 6 — Absolute value of the difference between the following: A — The weld pool width in the training data and that calculated from neural network (NN); B — the weld pool width in the testing data and that calculated from neural network; C — the peak temperature in the training data and that calculated from the neural network; and D — the peak temperature in the testing data and that calculated from the neural network. The results are for the five sets of weights calculated by the gradient-descent (GD) method, and the global set of weights calculated by the hybrid approach.

Calculation Procedure

Neural networks require a large database for training and testing. The number of training datasets should be more than the number of weights connecting different nodes. For a single hidden layer network, the number of weights, q, is given as:

$$q = (n_i + 1) \times n_h + (n_h + 1) \times n_o \quad (8)$$

where n_i is the number of input variables, i.e., 17 in the present work, n_h is the number of nodes in the hidden layer, and n_o is the number of output variables, i.e., 1. For a double hidden layer network,

$$q = (n_i + 1) \times n_h + (n_{h1} + 1) \times n_{h2} + (n_{h2}+1) \times n_o \quad (9)$$

where n_{h1} and n_{h2} are the number of nodes in hidden layers 1 and 2, respectively. Since the number of weights increases with the increase in the number of hidden layers, an optimal number of hidden layers are needed.

Number of Hidden Layers in the Network

The number of hidden layers in a neural network depends on the type of problem and the relationships between the input and the output variables represented through the objective function. Theoretically, any continuous variation of output with respect to input can be represented by a single hidden layer (Refs. 61, 62). Two hidden layers are needed when the relationship between the input and the output variables is discontinuous (Refs. 61, 62). The use of more than the optimal number of hidden layers in the network may result in undesirable overfitting of the data (Refs. 48, 61, 62). A single hidden layer was used since the outputs are continuous in nature in GTAW.

Database Generation

A database for training of the neural networks was generated to capture the effects of all the welding parameters and material properties. A well-tested numerical heat transfer and fluid flow model for GTA welding was used to generate the database where the values of various thermophysical properties were assumed to be temperature independent. Out of the 17 input variables in GTA welding, the ten most important variables that affect the output significantly include current, voltage, welding speed, arc radius, arc power distribution factor, arc efficiency, effective

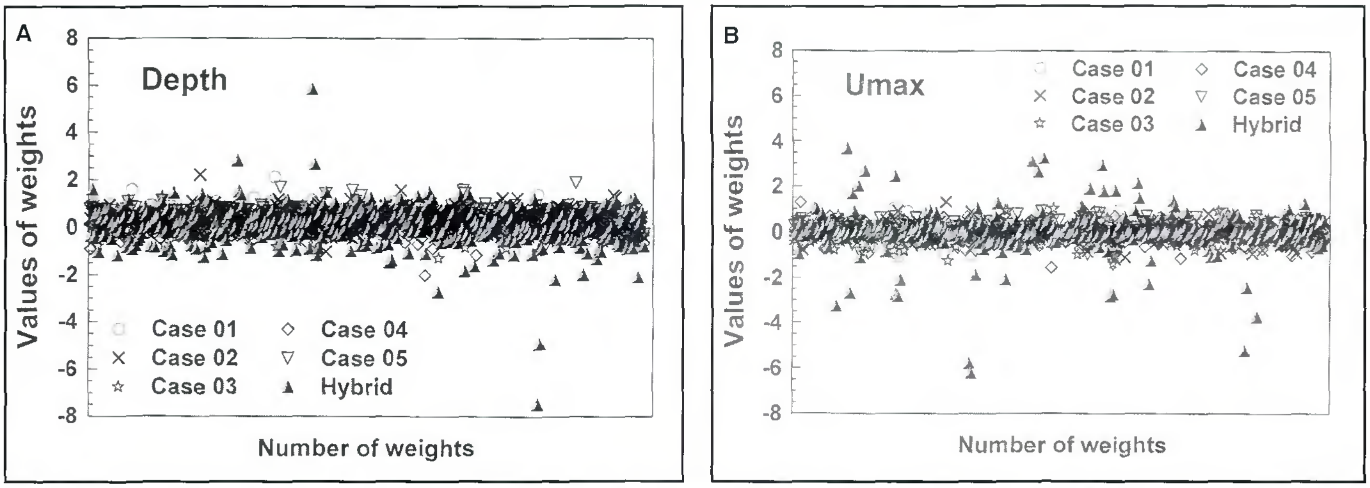

Fig. 7 — Comparison of the values of weights for the gradient-descent and hybrid training approaches for the following: A — Weld pool depth; B — maximum liquid velocity in the weld pool. Cases 01 to 05 are for the five sets of weights obtained from the gradient-descent method when using five different sets of initial random weights.

Table 2 — Comparison of the Mean Square Error (MSE), Defined in Equation 4, for the Gradient-Descent Method and the Hybrid Training Approach. The Results for the Gradient-Descent Method Were Taken after 5000 Iterations

Output variable	MSE Gradient Descent	MSE Hybrid Approach
Weld pool depth (mm)	5.37×10^{-4}	1.50×10^{-4}
Weld pool width (mm)	3.39×10^{-4}	6.77×10^{-5}
Weld pool length (mm)	2.80×10^{-4}	4.00×10^{-5}
Peak temperature (K)	1.17×10^{-3}	1.87×10^{-4}
Cooling time 800° to 500°C (s)	1.50×10^{-4}	3.89×10^{-6}
Maximum velocity (mm/s)	2.69×10^{-3}	9.99×10^{-4}

thermal conductivity of liquid, effective viscosity of liquid, thermal conductivity of solid, and the concentration of sulfur. The complex interactions between these ten variables were captured by making 1250 different runs of the three-dimensional numerical heat and fluid flow model. The effect of the remaining variables such as density, specific heat of the solid, specific heat of the liquid, etc., was captured by making 500 different runs of the numerical heat and fluid flow model. The relative importance of the variables was decided based on their sensitivity on the weld geometry. As described above, more runs of the numerical heat transfer and fluid flow model were made for the variables that have a major influence on the weld geometry. A sufficient number of different values of the variables were considered in order to increase the degrees of freedom and to adequately capture the effect of the variables that have a large influence on the weld geometry and cooling rate. Out of the 1750 total runs conducted, 1250 datasets were chosen randomly and included in the training dataset, and the remaining 500 datasets formed the testing dataset for the validation of the neural network. Thus, the combinations of the values of variables in the testing datasets were completely different from those in the training datasets. The 17 input variables and their ranges of values used for the generation of datasets are shown in Table 1. The ranges of values of the input variables correspond to the GTA welding of low carbon steel (Refs. 12, 54). Furthermore, Fig. 2 shows that the different values considered for each variable are well distributed about the mean value for the variable, which ensures that the effect of almost the entire range of values for each variable can be taken into account in the databases.

Normalizing Inputs and Outputs

There is significant variation in the scales of values of the input and output variables. The vastly different scales of inputs and bias values lead to ill conditioning of the problem (Refs. 48, 49). While large inputs cause ill conditioning by leading to very small weights, large outputs do so by leading to very large weights (Refs. 48, 49). To eliminate the ill-conditioning problem, the data were normalized using the following formula (Ref. 49):

$$x' = 2\times\left(\frac{x - x_{min}}{x_{max} - x_{min}}\right) - 1 \qquad (10)$$

where x is the original value of the variable and x′ is the normalized value, while x_{min} and x_{max} represent the minimum and maximum values of the variable in the entire dataset. Equation 10 normalizes the data in the range of –1 to 1. The range of values of all input and output parameters from –1 to 1 implies that the standard deviation cannot exceed 1, while its symmetry about zero means that the mean will typically be relatively small (Ref. 49).

Selection of Initial Weights

In the back-propagation algorithm, the magnitude of the error propagated backward through the network is proportional to the value of the weights. If all the weights are the same, the back-propagated errors will be the same, and consequently all of the weights will be updated by the same amount (Refs. 48, 49). To avoid this symmetry problem, the initial weights of the network were selected randomly. Furthermore, to avoid the premature saturation of the network, the initial values of the weights were distributed inside a small range of values, i.e., in the interval [–0.5, 0.5]. When the weights are small, the units operate in the linear regions of the transfer function and consequently the transfer function does not saturate.

The calculation starts with the selection of the number of nodes in the hidden layer. The total number of weights in the network depends upon the number of nodes in the hidden layer. The weights are then initialized randomly in the interval [–0.5, 0.5]. In the next step, a back-propagation algorithm is used to minimize the error on the training dataset. The op-

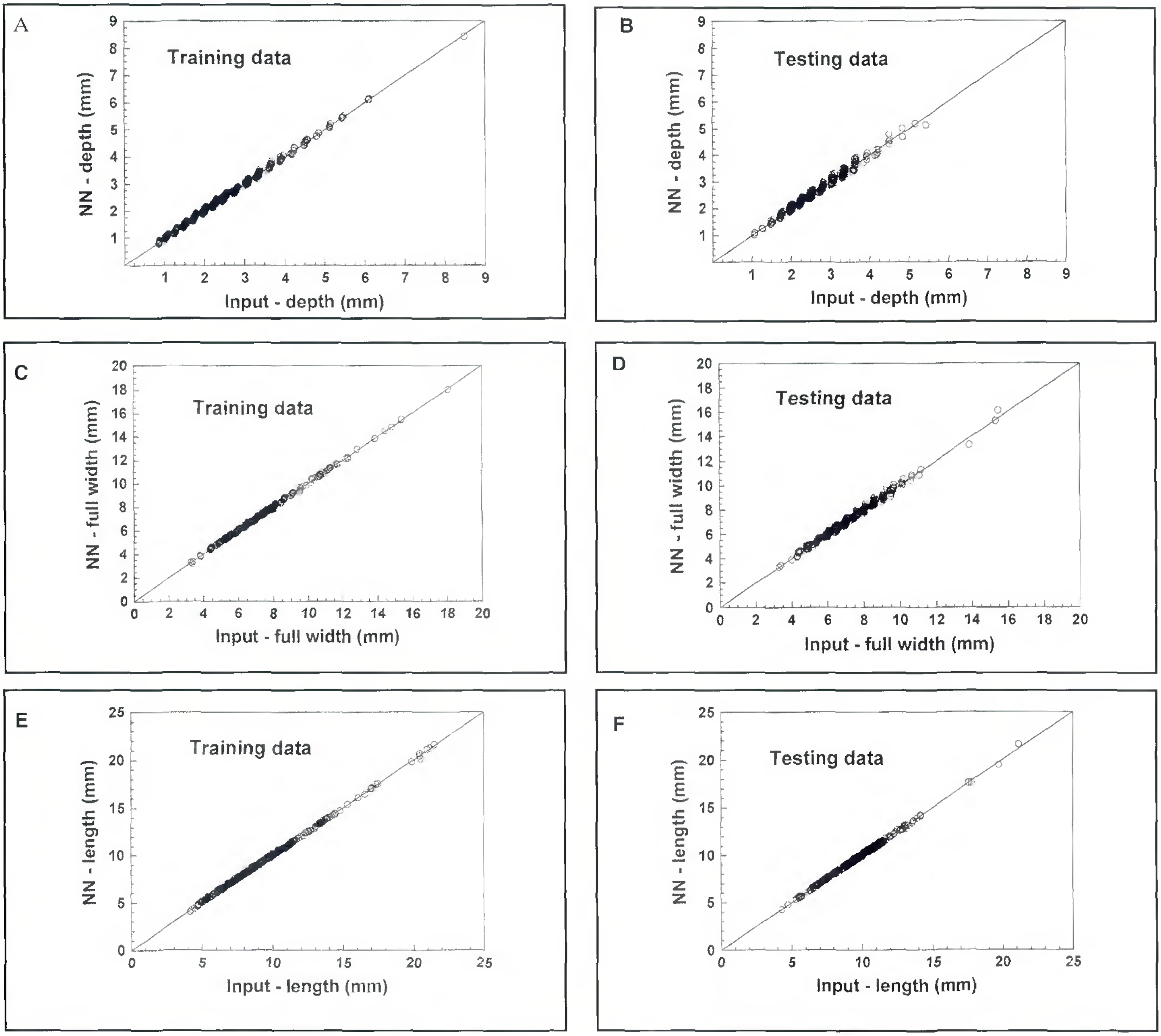

Fig. 8 — Comparison of weld pool dimensions calculated by the respective neural networks and those given in the training and the testing datasets. Top — Depth; Middle — width; Bottom — length.

Table 3 — The Mean Square Error (MSE), Defined in Equation 4, and Mean Error (ME), Defined in Equation 11, for the Results of the Neural Network for the Weld Pool Geometry, Peak Temperature, Cooling Time between 800° and 500°C, and Maximum Liquid Velocity in the Weld Pool. The Results Were Obtained Using the Hybrid Training Approach

Output variable	MSE Training Data	MSI Testing Data	ME Training Data	ME Testing Data	Typical value in the data
Weld pool depth (mm)	1.50 × 10^{-4}	5.00 × 10^{-4}	0.04	0.07	2.3
Weld pool width (mm)	6.77 × 10^{-5}	3.24 × 10^{-4}	0.05	0.09	6.8
Weld pool length (mm)	4.00 × 10^{-5}	1.00 × 10^{-4}	0.05	0.09	8.7
Peak temperature (K)	1.87 × 10^{-4}	6.90 × 10^{-4}	4	8	2237
Cooling time 800° to 500°C (s)	3.89 × 10^{-6}	1.57 × 10^{-5}	0.01	0.01	2.0
Maximum velocity (mm/s)	9.99 × 10^{-4}	3.72 × 10^{-3}	5	10	190

timized weights calculated by the gradient descent method are stored as one possible set of weights. This process is repeated five times with different randomly selected initial weights for fixed values of nodes in the hidden layer. All of these five optimized sets of weight are provided as input to the GA. The final aim of the GA is to find the weights in the network through a systematic global search that will give the least error between the neural network prediction and numerical heat and fluid flow calculations. The flowchart of the calculation scheme is presented in Fig. 3. The convergence is based on the error in training and testing data. When the error during testing starts increasing, the calculation is stopped to avoid overfitting even if the error with

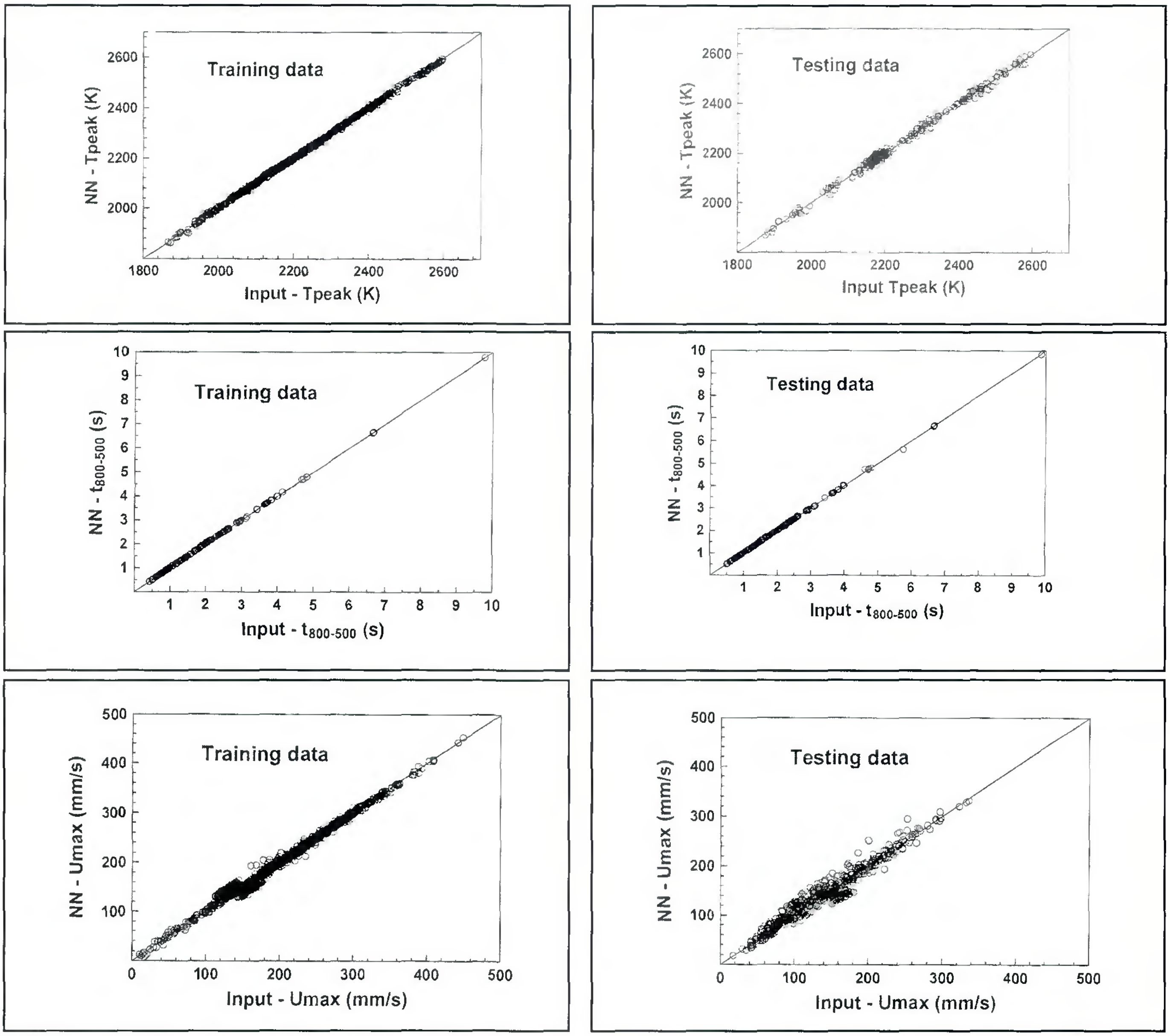

Fig. 9 — Comparison of the following calculated by the respective neural networks and those given in the training and the testing datasets: Top — Peak temperature; Middle — cooling time between 800° and 500°C; Bottom — maximum liquid velocity in the weld pool.

training dataset decreases with further iterations.

Results and Discussion

Structure Chosen for the Neural Networks

The selection of suitable network architecture is important as it affects the network's convergence as well as the accuracy of predictions (Ref. 22). The number of nodes in the hidden layer were varied to get an optimum number of nodes that resulted in minimum mean square error (MSE) defined in Equation 4. The average MSE of five runs made with different initial random weights is plotted in Fig. 4 for different number of nodes in the hidden layer. The results are for all the six neural networks with different output variables, and the runs were conducted using the gradient-descent method. Figure 4 shows that for all the six neural networks, the average MSE decreases with increase in the number of hidden nodes. For the neural networks with depth, width, length, and cooling time from 800° to 500°C, the MSE becomes almost constant for more than 14 hidden nodes in the network. Even for the neural networks with peak temperature and maximum velocity as the output variables, the decrease in MSE on increasing the number of hidden nodes above 14 is rather insignificant. Therefore, networks with 14 nodes in the hidden layer were used in the present study.

Gradient Descent vs. Hybrid Training Approach

As described in the section on mathematical modeling, the neural network model developed in the present study uses a combined gradient descent and genetic algorithm (hybrid) training approach. The initial guidance is provided by a gradient-descent algorithm and then the GA finds the global minimum of the mean square error (MSE) to provide a well-trained network. The neural networks were first trained on the training dataset of 1250 input-output pairs using the gradient-descent method. Since the output of this method depends on the initial set of guessed weights, five sets of initial random

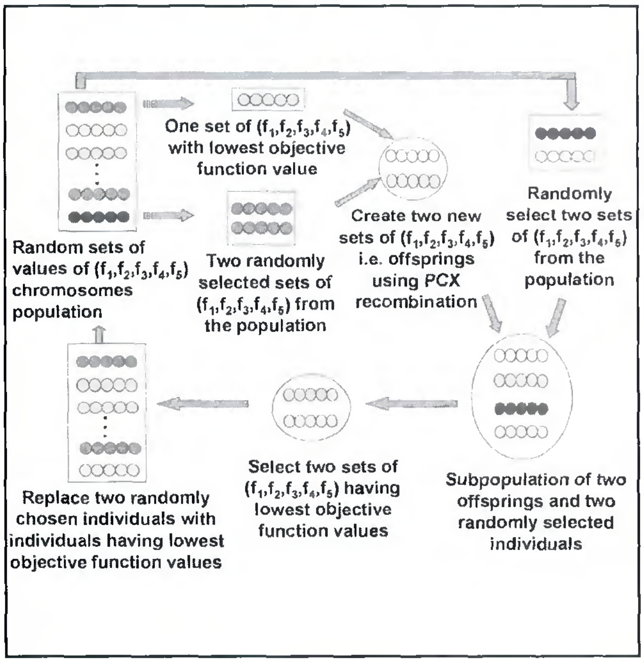

Fig. 10 — *Generalized Generation Gap (G3) model using PCX operator.*

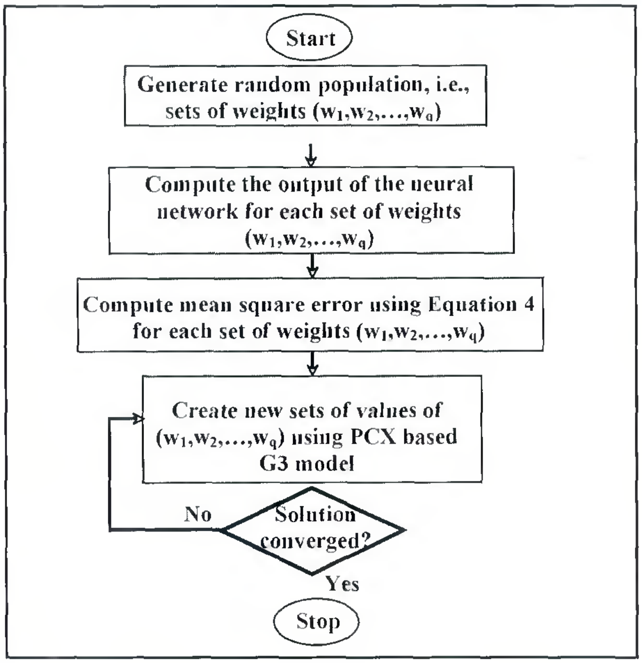

Fig. 11 — *Flow chart of the Generalized Generation Gap (G3) model.*

weights were used. In order to assess the performance of the gradient-descent method, the decrease of MSE with iterations is plotted for all the six neural networks in Fig. 5. Each plot represents an average of five runs with different random initial weights in order to avoid any local optimal solution. It can be seen that in all the cases, the error decreases very rapidly for the first 2000 iterations, but after that, further decrease is very slow. Since further improvement in error was very slow and insignificant, the training of the network using the gradient-descent method was stopped after 5000 iterations. The MSE values for the six neural networks, after training by the gradient-descent method for 5000 iterations, have been listed in Table 2.

Now, to test the performance of the hybrid approach, the five sets of weights calculated after 5000 iterations of the gradient-descent method, were given as inputs to the genetic algorithm (GA). Adding these sets of weights to the initial population of GA ensures the presence of five sets of near-optimum weights within the starting population, and helps in finding the global solutions more efficiently. Two convergence criteria were used. The first criterion required the training to stop if the mean square error became less than 1.0×10^{-6}, which is a low enough acceptable error for the problem at hand. The second criterion was based on the concern of overfitting of the neural network (Refs. 37, 39, 46–48). During training of the neural network, the error on the training data is driven to a very small value, but when new data are presented to the network, the error is large. This means that the network has memorized the training examples, but it has not learned to generalize to new situations (Ref. 37). A common method of avoiding this problem is that while training the network, its performance is simultaneously tested on a set of testing data. The training of the network is stopped as soon as the mean square error in the testing data starts increasing. This was set as the second convergence criterion in the present study in order to avoid overfitting of the neural network. The testing dataset consists of 500 input-output pairs, and the ranges of values of the input and output parameters lie within their ranges of values given in Table 1. The GA found the global set of weights giving much improved mean square errors as listed under the hybrid approach in Table 2. It can be seen that the MSEs for all the neural networks using the hybrid approach are much better than those obtained using the gradient-descent method alone.

To further compare the performance of the gradient-descent and hybrid approaches, the five sets of weights provided by the gradient-descent approach and the global set of weights provided by the hybrid approach were used to calculate the respective output variable values from the neural network for the training and the testing datasets. Figure 6A shows the absolute value of the difference between the training data and the corresponding results from the neural network, for weld pool width as the output variable, while Fig. 6B shows a similar plot for testing data. Figure 6C, D shows similar plots for peak temperature as the output variable. These plots contain results for the five sets of weights obtained using the gradient-descent method and the global set of weights obtained using the hybrid approach. It can be seen that in all the cases the weights from the hybrid approach provide results that fit much better to both the training and the testing data. The results obtained by using the weights from the gradient-descent method have much more scatter as compared to those obtained from the hybrid approach. Similar results were obtained for other output variables as well. Thus, the hybrid approach provides a well-trained network with significantly better weights, where the output from the trained neural network can accurately map the inputs to the outputs.

The values of the five sets of weights from the gradient-descent method and those from the hybrid approach have been plotted in Fig. 7A and B for output variables of weld pool depth and maximum liquid velocity, respectively. It can be seen that the weights from the gradient-descent method are mostly confined to a narrow range of [–1.0, 1.0], which is very close to their initial range of [–0.5, 0.5], while the weights from the hybrid approach are scattered in a much wider area. For example, the global set of weights for weld pool depth lie in the range of [–8.0, 6.0] and those for maximum liquid velocity lie in the range of [–7.0, 4.0]. This means that in the hybrid approach, the genetic algorithm explored a much wider search area, irrespective of the initial guessed values, and was able to find significantly better weights. Thus, the hybrid approach conducts a more thorough search of the possible search space and provides a better trained network.

Evaluating the Predicting Capability of the Neural Networks

Six neural networks have been developed, each providing a specific output, i.e., depth, width, and length of the weld pool, peak temperature, cooling time between 800° and 500°C or maximum liquid velocity in the weld pool. The performance of the neural networks is illustrated in Figs. 8 and 9, which compare the output parameters calculated by the model with their corresponding values provided in the training and the testing datasets. Figures 8A and B compare the weld pool depth calculated by the neural network with that provided in the training and testing datasets, respectively. All points lie on or very close to the diagonal line and the results obtained from the neural network agree well with the values calculated using heat and fluid flow model. The MSE for the training dataset was 1.5 × 10^{-4} mm^2 and that for the testing dataset was 5.0 × 10^{-4} mm^2, which was the least error that could be obtained on the testing dataset. To further evaluate the error in the values of depth provided by the neural network model, the absolute value of mean error, ME, between the target depth, i.e., the one given in the training and the testing datasets, and the depth calculated by the neural network is calculated as

$$ME = \left| \frac{\sum_{i=1}^{p} \left(d_i - o_i \right)}{p \times k} \right| \qquad (11)$$

where i is the index for the input dataset, d_i is the desired output, and o_i is the output produced by the neural network. The ME for depth in the training dataset was 0.04 mm and that in the testing dataset was 0.07 mm, where a typical depth value for GTA welding of low-carbon steel is 2.3 mm. Thus, the error in depth is well within the error limits for the process being considered.

In Fig. 8A, the depth varies from 0.9 to 8.5 mm, depending on the values of the input process parameters and the material properties. This shows that the process parameters and material properties considered in this study have a significant impact on the weld pool depth. The fact that the neural network model could accurately predict the depth values even for the testing data indicates that it is capable of accurately representing the results of the three-dimensional numerical heat and fluid flow model for GTA welding.

Figure 8C, D shows similar results for weld pool width, and Fig. 8E, F shows similar results for weld pool length. Similarly, the results for peak temperature are presented in Fig. 9A, B, those for cooling time between 800° and 500°C in Fig. 9C, D, and those for maximum liquid velocity in the weld pool in Fig. 9E, F. The corresponding MSEs and MEs are listed in Table 3. The MEs for the training data for weld pool width and length, peak temperature, cooling time between 800° and 500°C, and maximum liquid velocity in the weld pool are 0.05 mm, 0.05 mm, 4 K, 0.01 s, and 5 mm/s, respectively. These MEs are quite small compared to the respective magnitudes of these output variables, which are also listed in Table 3. Though the MEs for the testing data were slightly higher than those for the training data in all the cases, the difference was not very significant as can be seen from Table 3. The low values of ME for the testing data indicate that the neural networks can accurately predict different features of weld pool geometry as well as the peak temperature and cooling time, and hence can be used for simulations with predetermined good accuracy.

Summary and Conclusions

Six neural networks were developed for GTA welding of low-carbon steel. Each of these neural networks takes 17 input variables, which include welding process parameters and important material properties, and provides one output variable. The output variables include depth, width, and length of the weld pool, peak temperature, cooling time from 800° to 500°C, and maximum liquid velocity in the weld pool. The networks were trained using a hybrid optimization scheme including the gradient-descent method and a genetic algorithm. The hybrid approach gave lower errors than only the gradient-descent method on both training and testing datasets, and the results did not depend on the initial choice of weights. The training and testing datasets contained results from a reliable numerical heat and fluid flow model for GTA welding. The accurate prediction of these results by the neural networks ensured that the output of these networks complies with the phenomenological laws of welding physics.

Acknowledgments

This research was supported by a grant from the U.S. Department of Energy, Office of Basic Energy Sciences, Division of Materials Sciences, under grant number DE-FGO2-01ER45900. The authors thank Amit Kumar for his interest in this research.

Appendix A

Parent Centric Recombination (PCX) Based Generalized Generation Gap (G3) Genetic Algorithm (GA)

The genetic algorithm used in this study to calculate the optimized set of weights is a parent centric recombination (PCX) operator-based generalized generation gap (G3) model (Refs. 55, 56). This model was chosen because it has been shown to have a faster convergence rate on standard test functions as compared to other evolutionary algorithms. The algorithm for the model is as follows:

1. A population is a collection of many individuals and each individual represents a set of randomly chosen weights. A parent refers to an individual in the current population. The best parent is the individual that has the best fitness, i.e., gives the minimum value of the mean square error, defined by Equation 4, in the entire population. The best parent and two other randomly selected parents are chosen from the population.
2. From the three chosen parents, two offsprings or new individuals are generated using a recombination scheme. PCX-based G3 models are known to converge rapidly when three parents and two offspring are selected (Ref. 56). A recombination scheme is a process for creating new individuals from the parents.
3. Two new parents are randomly chosen from the current population.
4. A subpopulation of four individuals that includes the two randomly chosen parents in step 3 and two new offspring generated in step 2 is formed.
5. The two best solutions, i.e., the solutions having the least values of the mean square error, are chosen from the subpopulation of four members created in step 4. These two individuals replace the two parents randomly chosen in step 3.
6. The calculations are repeated from step 1 again until convergence is achieved.

The above steps, as applied to this study, are shown in Fig. 10. The process of finding the optimum set of weights by minimizing the mean square error is illustrated in Fig. 11. The recombination scheme (step 2) used in the present model is based on the PCX operator. A brief description of the PCX operator, as applied to the present problem of optimum set of weights, is presented below.

The first three parents, i.e.,

$$\left(w_1^0, w_2^0, \ldots, w_q^0\right), \left(w_1^1, w_2^1, \ldots, w_q^1\right), \left(w_1^2, w_2^2, \ldots, w_q^2\right)$$

are randomly selected from the current population. Here, the subscripts represent the q weights of the neural network, while the superscripts denote the parent identification number. The mean vector or centroid,

$$\bar{g} = \left(\frac{w_1^0 + w_1^1 + w_1^2}{3}, \frac{w_2^0 + w_2^1 + w_2^2}{3}, \ldots, \frac{w_q^0 + w_q^1 + w_q^2}{3} \right),$$

of the three chosen parents is computed. To create an offspring, one of the parents, say

$$\bar{x}^{(par)} = \left(w_1^0, w_2^0, \ldots, w_q^0 \right)$$

is chosen randomly. The direction vector,

$$\bar{d}^{(par)} = \bar{x}^{(par)} - \bar{g},$$

is next calculated from the selected parent to the mean vector or centroid. Thereafter, from each of the other two parents, i.e.,

$$\left(w_1^1, w_2^1, \ldots, w_q^1 \right) \text{ and } \left(w_1^2, w_2^2, \ldots, w_q^2 \right),$$

perpendicular distances, D_i, to the direction vector, $\bar{d}^{(par)}$, are computed and their average, $\bar{D}$, is found. Finally, the offspring, i.e.,

$$\bar{y} = \left(w_1', w_2', \ldots, w_q' \right),$$

is created as follows:

$$\bar{y} = \bar{x}^{(par)} + v_\xi \left| \bar{d}^{(par)} \right| + \sum_{i=1, i \neq par}^{q} v_\eta \bar{D} \bar{h}^{(i)} \quad \text{(A1)}$$

where $\bar{h}^{(i)}$ are the orthonormal bases that span the subspace perpendicular to $\bar{d}^{(par)}$, and v_ξ and v_η are randomly calculated zero-mean normally distributed variables. The values of the variables that characterize the offspring,

$$\bar{y} = \left(w_1', w_2', \ldots, w_q' \right),$$

are calculated next. As an example, only the calculation of w'_1 and w'_2 will be described here:

$$w_1' = w_1^0 + w_{11} + w_{12} \quad \text{(A2.a)}$$

$$w_2' = w_2^0 + w_{21} + w_{22} \quad \text{(A2.b)}$$

where,

$$w_{11} = v_\xi \left(\frac{2w_1^0 - w_1^1 - w_1^2}{3} \right) \quad \text{(A3.a)}$$

$$w_{21} = v_\xi \left(\frac{2w_2^0 - w_2^1 - w_2^2}{3} \right) \quad \text{(A3.b)}$$

$$w_{12} = v_\eta \left(\frac{a_2 + b_2}{2} \right) \left[1 - \left(\frac{2w_1^0 - w_1^1 - w_1^2}{3d} \right)^2 \right] \quad \text{(A3.c)}$$

$$w_{22} = v_\eta \left(\frac{a_2 + b_2}{2} \right) \left[1 - \left(\frac{2w_2^0 - w_2^1 - w_2^2}{3d} \right)^2 \right] \quad \text{(A3.d)}$$

The expressions for the variables d, a_2, and b_2 used in Equations A3.c and A3.d, are as follows:

$$d = \sqrt{ \left(\frac{2w_1^0 - w_1^1 - w_1^2}{3} \right)^2 + \left(\frac{2w_2^0 - w_2^1 - w_2^2}{3} \right)^2 + \ldots + \left(\frac{2w_q^0 - w_q^1 - w_q^2}{3} \right)^2 } \quad \text{(A4.a)}$$

$$a_2 = e_1 \times \sqrt{1 - \left(a_1 \right)^2} \quad \text{(A4.b)}$$

$$b_2 = e_2 \times \sqrt{1 - \left(b_1 \right)^2} \quad \text{(A4.c)}$$

$$a_1 = \sum_{i=1}^{q} \frac{ \left(w_i^1 - w_i^0 \right) \left(\frac{2w_i^0 - w_i^1 - w_i^2}{3} \right) }{ d \times e_1 } \quad \text{(A4.d)}$$

$$e_1 = \sqrt{ \left(w_1^1 - w_1^0 \right)^2 + \left(w_2^1 - w_2^0 \right)^2 + \ldots + \left(w_q^1 - w_q^0 \right)^2 } \quad \text{(A4.e)}$$

$$b_1 = \sum_{i=1}^{q} \frac{ \left(w_i^2 - w_i^0 \right) \left(\frac{2w_i^0 - w_i^1 - w_i^2}{3} \right) }{ d \times e_2 } \quad \text{(A4.f)}$$

$$e_2 = \sqrt{ \left(w_1^2 - w_1^0 \right)^2 + \left(w_2^2 - w_2^0 \right)^2 + \ldots + \left(w_q^2 - w_q^0 \right)^2 } \quad \text{(A4.g)}$$

References

1. De, A., and DebRoy, T. 2005. Reliable calculations of heat and fluid flow during conduction mode laser welding through optimization of uncertain parameters. *Welding Journal* 84(7): 101-s to 112-s.

2. Zhang, W., Kim, C.-H., and DebRoy, T. 2004. Heat transfer and fluid flow in welds with complex geometry during gas-metal arc fillet welding, Part I: Numerical model. *Journal of Applied Physics* 95: 5210–5219.

3. Zhang, W., Kim, C.-H., and DebRoy, T. 2004. Heat transfer and fluid flow in welds with complex geometry during gas-metal arc fillet welding, Part II: Application to fillet welding of mild steel. *Journal of Applied Physics* 95: 5220–5229.

4. Zhang, W., DebRoy, T., and Elmer, J. W. 2005. Integrated modeling of thermal cycles, austenite formation, grain growth and decomposition in the heat affected zone of carbon steel. *Science and Technology of Welding and Joining* 10(5): 574–582.

5. De, A., and DebRoy, T. 2004. Probing unknown welding parameters from convective heat transfer calculation and multivariable optimization. *Journal of Physics D* 37: 140–150.

6. Mishra, S., and DebRoy, T. 2004. Grain topology in Ti-6Al-4V welds — Monte Carlo simulation and experiments. *Journal of Physics D* 37: 2191–2196.

7. Mishra, S., and DebRoy, T. 2004. Measurements and Monte Carlo simulation of grain structure in the heat-affected zone of Ti-6Al-4V welds. *Acta Materialia* 52(5): 1183–1192.

8. He, X., Fuerschbach, P., and DebRoy, T. 2003. Probing temperature during laser spot welding from vapor composition and modelling. *Journal of Applied Physics* 94(10): 6949–6958.

9. Mishra, S., Chakraborty, S., and DebRoy, T. 2005. Probing liquation cracking and solidification through modeling of momentum, heat and solute transport during welding of aluminum alloys. *Journal of Applied Physics* 97: 94912–94920.

10. Kumar, A., and DebRoy, T. 2003. Calculation of three-dimensional electromagnetic force field during arc welding. *Journal of Applied Physics* 94(2): 1267–1277.

11. De, A., and DebRoy, T. 2004. A smart model to estimate effective thermal conductivity and viscosity in weld pool. *Journal of Applied Physics* 95(9): 5230–5239.

12. Zhang, W., Roy, G. G., Elmer, J. W., and DebRoy, T. 2003. Modeling of heat transfer and fluid flow during gas tungsten arc spot welding of low carbon steel. *Journal of Applied Physics* 93(5): 3022–3033.

13. Kumar, A., Zhang, W., and DebRoy, T. 2005. Improving reliability of modeling heat and fluid flow in complex gas-metal-arc fillet welding — Part 1: An engineering physics model. *Journal of Physics D* 38: 118–126.

14. Kumar, A., and DebRoy, T. 2005. Im-

proving reliability of modeling heat and fluid flow in complex gas-metal-arc fillet welding — Part II: Application to welding of mild steel. *Journal of Physics D* 38: 127–134.

15. He, X., Elmer, J. W., and DebRoy, T. 2005. Heat transfer and fluid flow in laser microwelding. *Journal of Applied Physics* 97: 84909–84917.

16. Zhang, W., DebRoy, T., Palmer, T. A., and Elmer, J. W. 2005. Modeling of ferrite formation in a duplex stainless steel weld considering nonuniform starting microstructure. *Acta Materialia* 53(16): 4441–4453.

17. Mundra, K., DebRoy, T., and Kelkar, K. 1996. Numerical prediction of fluid flow and heat transfer in welding with a moving heat source. *Numerical Heat Transfer* 29: 115–129.

18. Kumar, A., and DebRoy, T. 2004. Guaranteed fillet weld geometry from heat transfer model and multivariable optimization. *International Journal of Heat and Mass Transfer* 47(26): 5793–5806.

19. Lancaster, J. F. 1986. *The Physics of Welding*, 2nd Edition, Pergamon: Oxford, UK.

20. Vitek, J. M., Iskander, Y. S., and Oblow, E. M. 2000. Improved ferrite number prediction in stainless steel arc welds using neural networks — Part 1: Neural network development. *Welding Journal* 79(2): 33-s to 40-s.

21. Vitek, J. M., Iskander, Y. S., and Oblow, E. M. 2000. Improved ferrite number prediction in stainless steel arc welds using neural networks — Part 2: Neural network results. *Welding Journal* 79(2): 41-s to 50-s.

22. Kim, I. S., Son, J. S., Lee, S. H., and Yarlagadda, P. K. D. V. 2004. Optimal design of neural networks for control in robotic arc welding. *Robotics and Computer-Integrated Manufacturing* 20: 57–63.

23. Kim, I. S., Son, J. S., and Yarlagadda, P. K. D. V. 2003. A study on the quality improvement of robotic GMA welding process. *Robotics and Computer-Integrated Manufacturing* 19: 567–572.

24. Nagesh, D. S., and Datta, G. L. 2002. Prediction of weld bead geometry and penetration in shielded metal-arc welding using artificial neural networks. *Journal of Materials Processing Technology* 123: 303–312.

25. Bhadeshia, H. K. D. H., Mackay, D. J., and Svensson, L. E. 1995. The impact toughness of C-Mn steel arc-welds — A Bayesian neural network analysis. *Materials Science and Technology* 11: 1046–1051.

26. Li, P., Fang, M. T. C., and Lucas, J. 1997. Modelling of submerged arc weld beads using self-adaptive offset neutral networks. *Journal of Materials Processing Technology* 71: 288–298.

27. Tarng, Y. S., Tsai, H. L., and Yeh, S. S. 1999. Modeling, optimization and classification of weld quality in tungsten inert gas welding. *International Journal of Machine Tools & Manufacture* 39: 1427–1438.

28. Jeng, J.-Y., Mau, T.-F., and Leu, S.-M. 2000. Prediction of laser butt joint welding parameters using back propagation and learning vector quantization networks. *Journal of Materials Processing Technology* 99: 207–218.

29. Srikanthan, L. T., and Chandel, R. S. 1988. Neural network based modeling of GMA welding process using small data sets. *Proceedings of the 5th International Conference on Control, Automation, Robotics and Vision*. Singapore, pp. 474–478.

30. Metzbower, E. A., Deloach, J. J., Lalam, S. H., and Bhadeshia, H. K. D. H. 2001. Analysis of strength and ductility of welds in shipbuilding steels. *Science and Technology of Welding and Joining* 6: 116–124.

31. Kim, I. S., Jeong, Y. J., Lee, C. W., and Yarlagadda, P. K. D. V. 2003. Prediction of welding parameters for pipeline welding using an intelligent system. *International Journal of Advanced Manufacturing Technology* 22: 713–719.

32. Andersen, K., Cook, G. E., Karsai, G., and Ramaswamy, K. 1990. Artificial neural networks applied to arc welding process modeling and control. *IEEE Transactions on Industry Applications* 26(5): 824–830.

33. Cook, G. E., Barnett, R. J., Andersen, K., and Strauss, A. M. 1995. Weld modeling and control using artificial neural networks. *IEEE Transactions on Industry Applications* 31(6): 1484–1491.

34. Tsuei, H., Dunne, D., and Li, H. 2003. Neural network analysis of impact properties of flux cored arc weld metals for structural steels. *Science and Technology of Welding and Joining* 8(3): 205–212.

35. Gao, J., and Wu, C. 2003. Neurofuzzy control of weld penetration in gas tungsten arc welding. *Science and Technology of Welding and Joining* 8(2): 143–148.

36. Kim, I. S., Lee, S. H., and Yarlagadda, P. K. D. V. 2003. Comparison of multiple regression and back propagation neural network approaches in modeling top bead height of multipass gas metal arc welds. *Science and Technology of Welding and Joining* 8(5): 347–352.

37. Demuth, H., and Beale, M. 1998. *Neural network tool box user's guide — Version 3.0*. Mathworks, Inc., Mass.

38. Juang, S. C., Tarng, Y. S., and Lii, H. R. 1998. A comparison between the backpropagation and counter-propagation networks in the modeling of the TIG welding process. *Journal of Materials Processing Technology* 75: 54–62.

39. Vitek, J. M., David, S. A., Richey, M. W., Biffin, J., Blundell, N., and Page, C. J. 2001. Weld pool shape prediction in plasma augmented laser welded steel. *Science and Technology of Welding and Joining* 6: 305–314.

40. Eguchi, K., Yamane, S., Sugi, H., Kubota, T., and Oshima, K. 1999. Application of neural network to arc sensor. *Science and Technology of Welding and Joining* 4(6): 327–334.

41. Li, X., Simpson, S. W., and Rados, M. 2000. Neural networks for online prediction of quality in gas metal arc welding. *Science and Technology of Welding and Joining* 5(2): 71–79.

42. Metzbower, E. A., Deloach, J. J., Lalam, S. H., and Bhadeshia, H. K. D. H. 2001. Analysis of the toughness of welds in shipbuilding steels. *Science and Technology of Welding and Joining* 6: 368–374.

43. Hong, T., Pitscheneder, W., and DebRoy, T. 1998. Quantitative modeling of inclusion growth in the weld pool by considering their motion and temperature gyrations. *Science and Technology of Welding and Joining* 3(1): 33–41.

44. Hong, T., and DebRoy, T. 2001. Effects of time, temperature and steel composition on the growth and dissolution of inclusions in liquid steels. *Ironmaking and Steelmaking* 28(6): 450–454.

45. Rumelhart, D. E., Hinton, G. E., and Williams, R. J. 1986. Learning representations by back-propagating errors. *Nature* 323: 533–536.

46. Burke, L., and Ignizio, J. P. 1997. A practical overview of neural networks. *Journal of Intelligent Manufacturing* 8(3): 157–165.

47. Fausett, L. 1994. *Fundamentals of Neural Networks*. Englewood Cliffs, N.J.: Prentice-Hall.

48. Haykin, S. 2001. *Neural Networks – A Comprehensive Foundation*, 2nd Edition. Singapore: Pearson Education.

49. Masters, T. 1993. *Practical Neural Network Recipes in C++*. Boston, Mass.: Academic Press.

50. Kalman, B. L., and Kwasny, S. C. 1992. Why tanh? Choosing a sigmoidal function. *Proceedings of the International Joint Conference on Neural Networks - Volume 4*. Baltimore, Md. pp. 578–581.

51. Bose, N. K., and Liang, P. 1996. *Neural Network Fundamentals with Graphs, Algorithms, and Applications*. New York, N.Y.: McGraw-Hill.

52. Yarlagadda, P. K. D. V. 2001. Prediction of processing parameters for injection moulding by using a hybrid neural network. *Proceedings of the Institution of Mechanical Engineers B Journal of Engineering Manufacture* 215(10): 1465–1470.

53. Huang, S. H., and Zhang, H. C. 1995. Neural-expert hybrid approach for intelligent manufacturing: A survey. *Computers in Industry* 26: 107–126.

54. Kumar, A., Mishra, S., Elmer, J. W., and DebRoy, T. 2005. Optimization of Johnson Mehl Avarami equation parameters for α-ferrite to γ-austenite transformation in steel welds using a genetic algorithm. *Metallurgical and Materials Transactions A* 36: 15–22.

55. Deb, K., Anand, A., and Joshi, D. 2002. A computationally efficient evolutionary algorithm for real-parameter optimization. *Evolutionary Computation* 10(4): 371–395.

56. Deb, K. 2001. *Multi-Objective Optimization Using Evolutionary Algorithms*, 1st Edition, New York, N.Y.: Wiley.

57. Mishra, S., and DebRoy, T. 2005. A computational procedure for finding multiple solutions of convective heat transfer equations. *Journal of Physics D* 38: 2977–2985.

58. Mishra, S., and DebRoy, T. 2005. A heat transfer and fluid flow based model to obtain a specific weld geometry through multiple paths. *Journal of Applied Physics* 98: 044902-1 to 044902-10.

59. Kumar, A., and DebRoy, T. 2005. Tailoring complex weld geometry through reliable heat transfer and fluid flow calculations and a genetic algorithm. *Metallurgical and Materials Transactions A* 36: 2725–2735.

60. Patankar, S. V. 1980. *Numerical Heat Transfer and Fluid Flow*. New York, N.Y.: Hemisphere.

61. Lippmann, R. P. 1987. An introduction to computing with neural nets. *IEEE Acoustics, Speech, and Signal Processing Magazine* 3(4): 4–22.

62. Makhoul, J., El-Jaroudi, A., and Schwartz, R. 1989. Formation of disconnected decision regions with a single hidden layer. *Proceedings of the International Joint Conference on Neural Networks* — Vol. 1. Washington, D.C., pp. 455–460.

Looking at the Sensitization of 11–12% Chromium EN 1.4003 Stainless Steels during Welding

Using a range of heat inputs and welding speeds, two steel grades with different austenite potentials were welded, and they were found to be sensitized when lower heat inputs and faster cooling rates suppressed austenite nucleation during cooling

BY M. L. GREEFF AND M. du TOIT

ABSTRACT. The susceptibility of 11–12% chromium type EN 1.4003 ferritic stainless steels to sensitization during continuous cooling after welding at low heat input levels was investigated. These steels transform partially to austenite in the high-temperature heat-affected zone (HTHAZ) during cooling, with the austenite transforming to martensite at lower temperatures. Two steel grades with different austenite potentials were welded using a range of heat inputs (30 to 450 J/mm) and welding speeds (2.36 to 33.3 mm/s). The steels were found to be sensitized when lower heat inputs and faster cooling rates suppressed austenite nucleation during cooling, resulting in almost fully ferritic heat-affected zones and continuous networks of ferrite-ferrite grain boundaries in the HTHAZ. With an increase in heat input, the cooling rate was reduced, and more martensite formed in the HTHAZ. The ferrite-martensite boundaries were generally observed to be unsensitized. The results suggest that if enough austenite forms in the HTHAZ during cooling, it acts as a carbon sink to dissolve excess carbon. This prevents supersaturation of the ferrite phase and subsequent carbide precipitation that could lead to sensitization of the ferrite grain boundaries. Excessive welding speeds appear to promote sensitization during low heat input welding.

Introduction

Low-carbon, 11 to 12% chromium ferritic stainless steels are used extensively in South Africa as low cost, utility stainless steels. These steels conform in composition to grades S41003 (ASTM A240) and 1.4003 (EN 10088-2 and EN 10028-7), with the specified chemical composition limits for these grades shown in Table 1. The EN 1.4003- type alloys perform well in many wet sliding abrasion applications and in aqueous environments, often replacing mild and galvanized steel in mildly corrosive surroundings (Refs. 1–3), and are widely used in the petrochemical, metallurgical, pulp, paper, coal, and sugar industries in materials handling and structural applications. The past few years have also seen a marked increase in the use of these steels in the transport, mining, and agricultural sectors, with successful application in passenger vehicles, coaches, buses, trucks, freight and passenger wagons, and rail infrastructure (Refs. 2, 3).

The EN 1.4003 ferritic stainless steels are designed to transform partially to austenite on cooling, passing through the dual-phase (austenite + ferrite) phase field on the Fe-Cr equilibrium phase diagram (shown in Fig. 1 for carbon contents below 0.01%). This partial solid-state phase transformation of ferrite to austenite during cooling improves the weldability and as-welded toughness of these steels by restricting heat-affected zone grain growth (Refs. 4, 5). The alloys are usually supplied in the fully annealed and desensitized condition. During annealing (normally at temperatures between 700° and 750°C (Refs. 1, 2)), any austenite formed on cooling through the dual-phase region transforms completely to ferrite. Due to its low solubility in ferrite, the majority of the carbon precipitates as chromium-rich carbides or carbonitrides during annealing, but any chromium-depleted zones formed in the ferrite are healed through rapid chromium back-diffusion from the grain interiors.

The rapid cooling rates associated with welding, however, prevent the transformation of austenite to ferrite at lower temperatures, and any austenite formed on cooling through the dual-phase ($\delta + \gamma$) region transforms to low-carbon martensite below the M_s temperature (Ref. 4). The microstructure of the high-temperature heat-affected zone (HTHAZ) adjacent to the weld interface after cooling therefore usually consists of ferrite grains surrounded by grain boundary martensite. Despite the partial solid-state phase transformation from ferrite to austenite on cooling, the HTHAZ is normally characterized by grain growth. This is in contrast to the much finer grain size of the low-temperature heat-affected zone(LTHAZ) further removed from the weld interface.

Austenitic consumables are generally preferred for welding the EN 1.4003 alloys. Although this leads to a property mismatch between the weld and the surrounding base metal, the tough austenitic weld metal improves the overall toughness of the weld by absorbing some of the impact that the joint may be exposed to during service. A matching welding electrode is commercially available (classified as

KEYWORDS

EN 1.4003
High-Temperature Heat-Affected Zone (HTHAZ)
Ferrite-Ferrite Grain Boundaries
Stress Corrosion Cracking
Austenite

M. L. GREEFF is a graduate student and M. du TOIT (mtoit@postino.up.ac.za) *is an associate professor with the Department of Materials Science and Metallurgical Engineering, University of Pretoria, Pretoria, South Africa.*

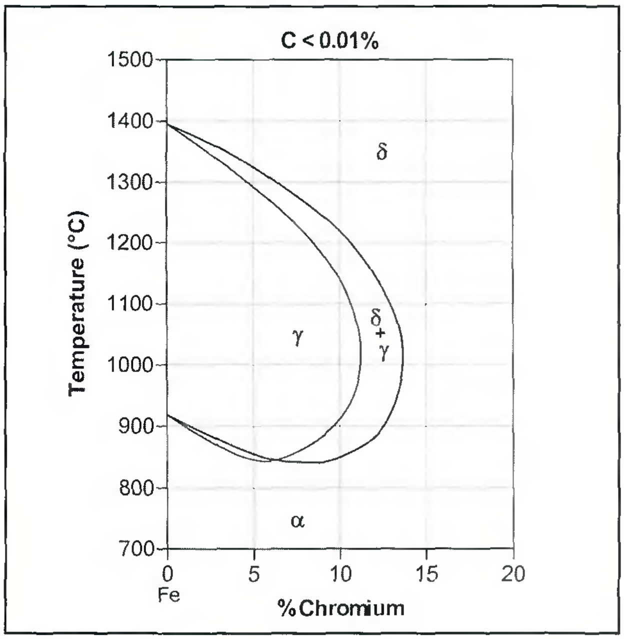

Fig. 1 — Vertical section of the ternary Fe-Cr-C system at carbon contents below 0.01%. Although the steels in this investigation contain more than 0.01% carbon, this phase diagram illustrates the general shape of the austenite and (austenite + ferrite) phase fields. An increase in carbon content is expected to enlarge these phase fields at the expense of ferrite (Ref. 6).

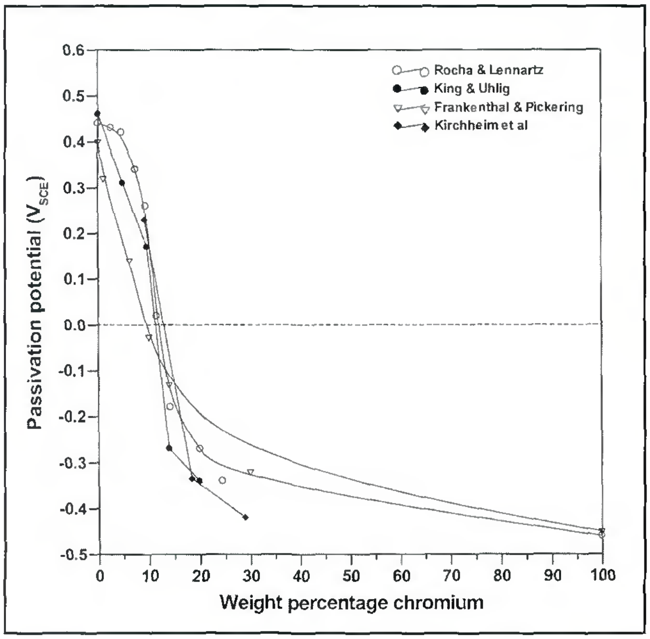

Fig. 2 — Passivation potential of binary iron-chromium alloys in 0.5 M H_2SO_4 at room temperature (Ref. 18), with data from Rocha and Lennartz (Ref. 19), King and Uhlig (Ref. 20), Frankenthal and Pickering (Ref. 21), and Kirchheim et al. (Ref. 22).

Table 1 — Specified Chemical Composition Limits for Grades S41003 (ASTM A240) and 1.4003 (EN 10088-2 and EN 10028-7) (% by mass, balance Fe)

Grade	C	Cr	Mn	Si	Ni	P	S	N
S41003	0.030 max.	10.5–12.5	1.50 max.	1.00 max.	1.50 max.	0.040 max.	0.030 max.	0.030 max.
1.4003	0.030 max.	10.5–12.5	1.50 max.	1.00 max.	0.30–1.00	0.040 max.	0.015 max.	0.030 max.

E410NiMo, with modified chromium content), but it is not recommended in applications where impact, shock, fatigue, or any other form of nonstatic loading is anticipated. This electrode is only specified in applications where matching corrosion resistance is essential.

A number of in-service failures of EN 1.4003 welds due to stress corrosion cracking in the high-temperature heat-affected zone adjacent to the weld interface have been reported in recent years (Ref. 7). Although it is frequently claimed that nickel-free stainless steels are immune to stress corrosion cracking, such failures have been reported in both nickel-free ferritic and martensitic stainless steels with corrosion potentials within the passive range (Refs. 8–10). The stress corrosion cracking of these stainless steels is generally believed to be associated with some degree of sensitization. Even though various sensitization models have been proposed for stainless steels, chromium depletion is the most widely accepted mechanism (Ref. 11). This theory states that sensitization is caused by intergranular precipitation of chromium-rich $M_{23}C_6$-type carbides, resulting in chromium depletion of the matrix surrounding the precipitated particles. If chromium depletion reduces the chromium level in the affected areas to below the concentration required to maintain passivation, the steel becomes sensitized to intergranular corrosion.

It was originally believed that the typical dual-phase heat-affected zone microstructure that develops during welding renders the EN 1.4003-type steels largely immune to sensitization. The cooling rates during welding are generally considered to be too fast to cause sensitization of the austenite phase, whereas the ferrite phase is rapidly desensitized by chromium back-diffusion into depleted regions during cooling. This mechanism is similar to that proposed for the enhanced sensitization resistance observed in duplex austenitic-ferritic stainless steels (Ref. 12). It has, however, since been confirmed that the EN 1.4003 steels are susceptible to sensitization under very specific conditions. The majority of the failures associated with stress corrosion cracking and sensitization in these steels were caused by a two-step thermal cycle. The first step involves heating the steel to a temperature within the ($\gamma + \delta$) phase field above the carbide dissolution temperature (approximately 950°C). During this heating cycle, carbon liberated through the dissolution of the carbide precipitates is absorbed by the austenite phase. On cooling after welding, the austenite transforms to unsensitized martensite. If this martensite is subsequently heated to a temperature within the carbide precipitation range of approximately 550° to 850°C (the second step in the thermal cycle), sensitization of the martensite phase may occur. In the heat-affected zone, these conditions may be satisfied by an isothermal heat treatment above 950°C (step 1), followed by rapid cooling and welding (step 2), or by overlapping heat-affected zones in the case of multipass or closely spaced welds (Ref. 7).

The chromium depletion mechanism for sensitization in the EN 1.4003 steels has been confirmed using transmission electron microscopy with electron energy loss (EELS) image filtering. Sensitized material displays chromium enrichment along the grain boundaries, as well as distinctive chromium-depleted zones adjacent to the boundaries (Ref. 13). The in-

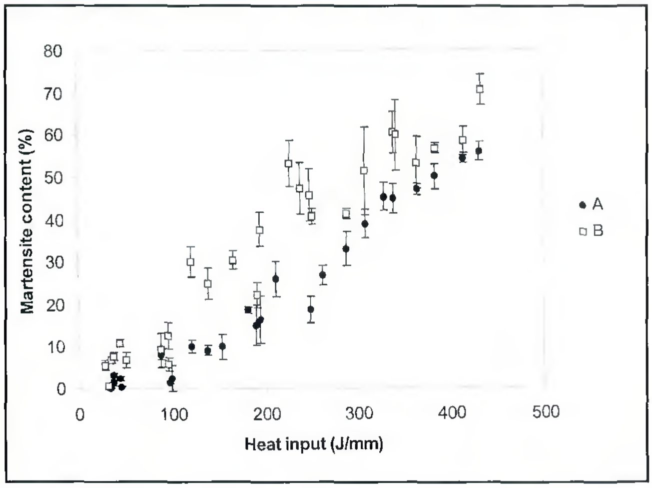

Fig. 3 — Measured HTHAZ martensite content of steels A and B as a function of heat input during welding.

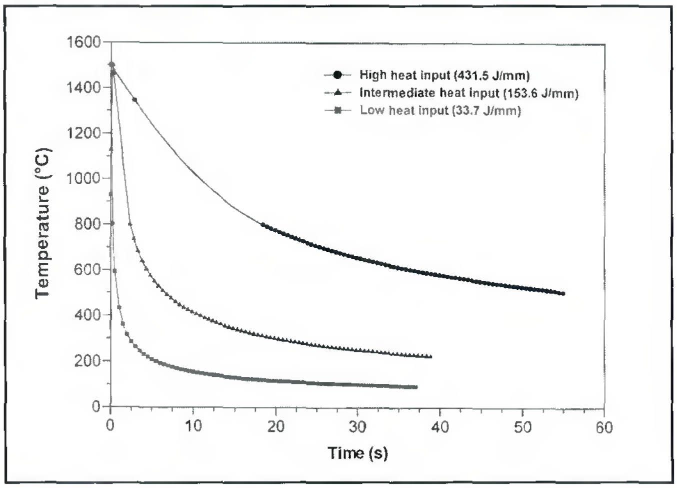

Fig. 4 — Calculated temperature-time profiles experienced by a point located on the weld interface for a "low" heat input weld (33.7 J/mm or 856 J/in., with a cooling time from 1500° to 800°C, Δt_{15-8} of 0.22 s), an "intermediate" heat input weld (153.6 J/mm or 3901 J/in., with a Δt_{15-8} of 2.08 s), and a "high" heat input weld (431.5 J/mm or 10960 J/in., with a Δt_{15-8} of 18.40 s).

Table 2 — The Chemical Compositions of the Two Type EN 1.4003 Alloys Examined during the Course of This Investigation (% by mass, balance Fe)

Steel	C	Cr	Mn	Si	Ni	Ti	N	KFF
A	0.018	11.61	0.56	0.70	0.33	0.032	0.0213	12.05
B	0.012	11.57	0.49	0.38	0.55	0.014	0.0177	9.59

Table 3 — Material Constants Supplied by Columbus Stainless for the EN 1.4003 Steels

Thermal diffusivity, a	$1.10819.10^{-5}$ m^{2}s^{-1}
Thermal conductivity, λ	41.0 Jm^{-1}s^{-1}K^{-1}

tergranular precipitation of chromium-rich carbides with associated grain boundary chromium depletion in dual-phase ferritic-martensitic 12 and 13% chromium steels has also been reported by Tomari et al. (Ref. 14) and Frangini et al. (Ref. 15).

A number of recent fillet weld failures attributed to stress corrosion cracking and sensitization suggested, however, that sensitization can also occur during continuous cooling after welding, without recourse to the two-step thermal cycle described above. These failures were associated with fast welding speeds and excessive fillet weld overlap, implying that low heat inputs play a role in promoting sensitization under these conditions. This investigation aimed to show that it is possible for the EN 1.4003-type steels to sensitize during continuous cooling after welding. The project also attempted to identify the mechanism of sensitization during low heat input welding, and to relate this phenomenon to the cooling rate and the heat-affected zone microstructure that develops during the weld thermal cycle.

Experimental Procedure

The chemical compositions of the EN 1.4003-type steels examined during the course of this investigation, designated steels A and B, are shown in Table 2. Both steels conform in chemical composition to the specifications shown in Table 1 for grades S41003 and 1.4003. The Kaltenhauser ferrite factor (KFF), calculated from Equation 1 (Ref. 16), is included in Table 2 for both alloys. This factor quantifies the ratio of ferrite- to austenite-forming elements in the steel. As shown in Table 2, steel B has a lower ferrite factor, and consequently a higher austenite potential, than steel A. More austenite is therefore expected to form in the high-temperature heat-affected zone of steel B during cooling. The steels were supplied in the form of fully annealed and homogenized plate with a thickness of 3 mm.

$$KFF = Cr + 6Si + 8Ti + 4Mo + 2Al - 40(C+N) - 2Mn - 4Ni \quad (1)$$

In order to examine the influence of the welding parameters, and in particular the heat input and the welding speed on the microstructure and sensitization resistance of the high-temperature heat-affected zone adjacent to the weld interface, the alloys shown in Table 2 were welded autogenously using heat inputs ranging from about 30 to 450 J/mm (762 to 11430 J/in.) and welding speeds from 2.36 to 33.3 mm/s (5.6 to 78.7 in./min). Direct current gas tungsten arc welding (GTAW) was used with argon shielding gas and electrode negative polarity. The welding parameters selected to produce the experimental welds are given in Tables I and II in the Appendix for alloys A and B, respectively. All the experimental welds were pickled and passivated using commercially available solutions.

Sensitization was evaluated using the 10% oxalic acid electrolytic etch described in Practice W of ASTM 763-93 (Ref. 17). In order to classify the resulting microstructures as ditched (possibly sensitized), dual (unsensitized), or step (unsensitized), the etched samples were examined using an optical microscope. The oxalic acid etch reveals the presence of any chromium-rich carbides in the microstructure, but only serves as a screening test for sensitization. In order to confirm that a sample with ditched grain boundaries after oxalic acid etching is in the sensitized condition, additional tests are required. The boiling acid tests described in ASTM 763-93 were found to be too aggressive for the 12% chromium EN 1.4003 steels, and confirmation of whether the heat-affected zones were in the sensitized condition was therefore obtained using a potentiostatic chromium depletion test performed in 0.5 M H_2SO_4 at 0 V_{SCE} (relative to a saturated calomel electrode)

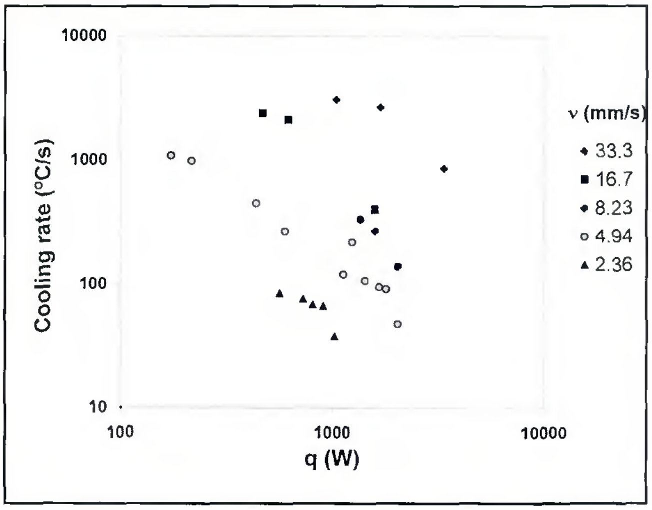

Fig. 5 — The influence of welding parameters on the cooling rate from 1500° to 800°C.

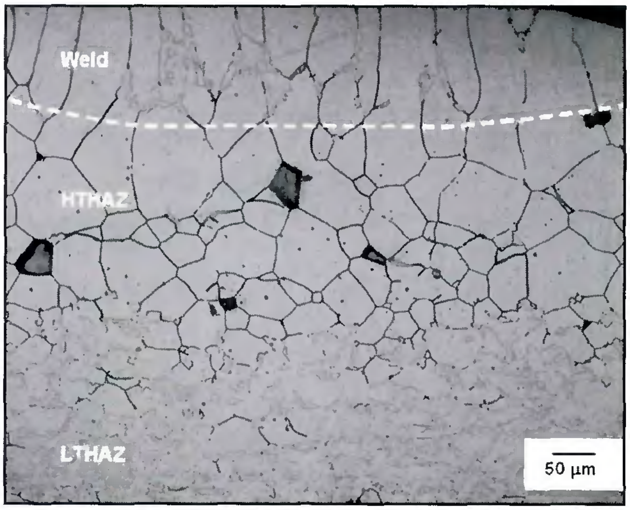

Fig. 6 — Optical photomicrograph of autogenous bead-on-plate weld A2, welded at a heat input of 31.2 J/mm (792 J/in.), and etched electrolytically in 10% oxalic acid. A continuous network of ditched ferrite-ferrite grain boundaries is visible in the high-temperature heat-affected zone.

Table 4 — Summary of the Microstructures Observed in the High-Temperature Heat-Affected Zones of the Experimental Welds after Oxalic Acid Etching

Group	Microstructure	Oxalic acid etch results
1	Predominantly ferritic, with less than half of all grain boundaries containing some martensite	All ferrite-ferrite grain boundaries ditched; ferrite-martensite phase boundaries largely unattacked
2	Predominantly ferritic, with at least half of all grain boundaries containing some martensite	All ferrite-ferrite grain boundaries ditched; ferrite-martensite phase boundaries intermittently attacked
3	Ferritic, with most of the grain boundaries covered in martensite	Localized carbide precipitation on any remaining ferrite-ferrite grain boundaries; ferrite-martensite phase boundaries largely unaffected

for a period of 300 seconds (Ref. 18). At a potential of 0 V_{SCE}, any regions of the microstructure containing more than 10% chromium will be passive, whereas any regions with less than 10% chromium will corrode actively (as shown in Fig. 2). Any chromium-depleted regions will therefore dissolve preferentially. Since it is difficult to accurately measure the area covered by the narrow high-temperature heat-affected zone, a current density value could not be calculated. A microstructural examination of the samples subjected to the test, using optical and scanning electron microscopes, was therefore preferred as a method of evaluation.

In order to determine the influence of welding parameters on the microstructure of the high-temperature heat-affected zone adjacent to the weld interface, point count methods were used to estimate the room-temperature martensite content of each weld. Point counting was performed by randomly moving a grid with four intersecting lines on a series of photomicrographs of the HTHAZ of each weld, counting all the intersection points located within the martensite phase (counted as one), or on a ferrite-martensite phase boundary (counted as half). A total of eighty counts was performed for each weld. The cooling rate experienced by a point located on the weld interface of each weld as a function of the welding parameters was then calculated using Rosenthal's conduction-driven heat flow model (Ref. 23).

Results and Discussion

Weld Thermal Cycles and HTHAZ Microstructures

Equation 2 can be used to calculate the heat input, HI, of each experimental weld from the welding parameters, where V is the arc voltage, I is the welding current, v is the travel speed, and q is the weld heat flux. The arc efficiency factor, η, was estimated by comparing the actual q/v required to produce a weld with a given weld pool diameter (measured experimentally), with the heat input calculated from the welding parameters (without considering the arc efficiency factor).

$$HI = \frac{\eta VI}{v} = \frac{q}{v} \quad (2)$$

The average arc efficiency was calculated as 47.76%. This value approaches the upper limit of the range normally quoted for gas tungsten arc welding (between approximately 22 and 48%) (Ref. 24). Electrode negative polarity was used for welding, which focuses the majority of the heat generated by the power source into the workpiece and restricts electrode heating, thereby limiting heat losses through the tungsten electrode and the water-cooled welding torch. The actual heat input during welding, taking into consideration the measured welding parameters and the average arc efficiency factor, was then calculated from equation 2 for each experimental weld. These heat input values are shown in Tables 1 and II for alloys A and B, respectively.

The martensite content measured in the high-temperature heat-affected zone of each weld is presented graphically in Fig. 3 as a function of the actual heat input during welding. From this figure, it is evident that alloy B formed more martensite than alloy A at corresponding heat input levels. This can be attributed to the higher austenite potential of steel B, denoted by the lower Kaltenhauser ferrite factor listed in Table 2. Figure 3 also shows that the heat-affected zone martensite content of both steels decreases as the heat input during welding is reduced. This reduction in the martensite content of the high-temperature heat-affected zone with de-

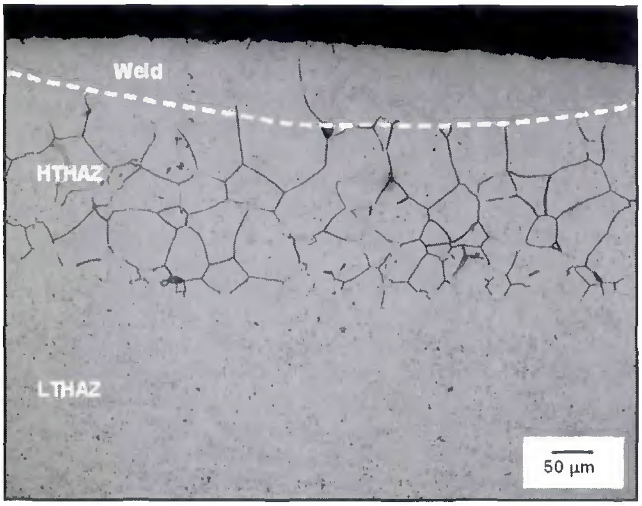

Fig. 7 — Optical photomicrograph of autogenous bead-on-plate weld B2, welded at a heat input of 28.1 J/mm (714 J/in.), and etched electrolytically in 10% oxalic acid. A continuous network of ditched ferrite-ferrite grain boundaries is visible in the high-temperature heat-affected zone.

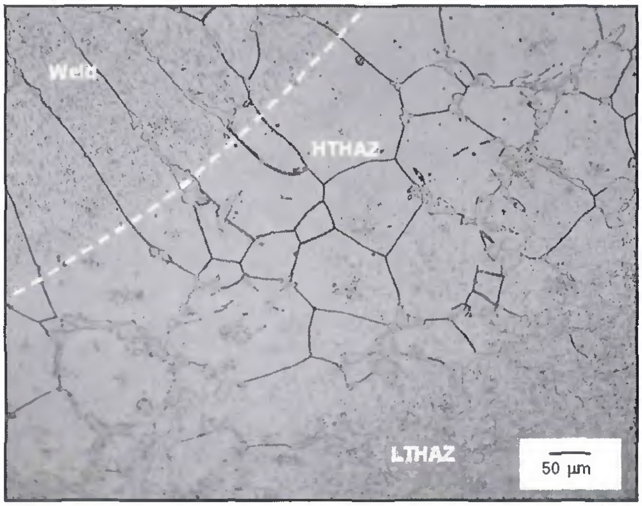

Fig. 8 — Optical photomicrograph of autogenous bead-on-plate weld A13, welded at a heat input of 190.9 J/mm (4849 J/in.), and etched electrolytically in 10% oxalic acid. More grain boundary martensite is present. The ferrite-ferrite grain boundaries are ditched, whereas the ferrite-martensite phase boundaries are largely unattacked.

creasing heat input can be attributed to an increase in the cooling rate after welding.

In order to quantify the influence of the welding parameters, and in particular the heat input, welding speed, and heat flux or power, q, on the cooling rate, Rosenthal's conduction-driven model for heat flow was used to estimate the thermal cycle experienced by a point located on the weld interface during welding. The two-dimensional heat flow model developed by Rosenthal was selected after calculation of the critical thickness for the range of heat inputs used. The weld interface forms between the weld metal and the high-temperature heat-affected zone, and therefore represents the edge of the HTHAZ adjacent to the weld bead. In equation 3, T is the temperature at a radial distance r from the heat source (K), T_0 is the original temperature of the plate prior to welding (K), λ is the thermal conductivity ($Jm^{-1}s^{-1}K^{-1}$), d is the plate thickness (m), a is the thermal diffusivity (m^2s^{-1}), ξ is the distance from the moving point heat source in the direction of travel of the arc ($\xi > 0$ for points in front of the heat source, and $\xi < 0$ for points behind the heat source), and r is the radial distance from the heat source (m). The material constants, λ and a, used in the calculation were supplied by the steel producer and are shown in Table 3.

$$T - T_0 = \frac{q}{2\lambda d\sqrt{\pi v r / a}} \exp\left(-\frac{-v(\xi + r)}{2a}\right) \quad (3)$$

The time required for a point located on the weld interface to cool from 1500° to 800°C, Δt_{15-8}, after welding was then estimated from the calculated temperature-time curves for each experimental weld. The temperature interval from 1500° to 800°C represents the approximate temperature range from the liquidus to a temperature just below the austenite phase field on the phase diagram in Fig. 1, and therefore includes the interval over which the solid-state transformation of ferrite to austenite takes place.

Examples of the calculated temperature-time curves are shown in Fig. 4 for "low," "intermediate," and "high" heat inputs, respectively. These thermal cycles illustrate that an increase in heat input leads to more gradual cooling and a longer cooling time from 1500° to 800°C after welding. Since the solid-state transformation of ferrite to austenite during cooling is nucleation and growth controlled, it is postulated that the faster cooling rates experienced by the high-temperature heat-affected zone during welding at low heat input levels may suppress the transformation to austenite, resulting in lower room-temperature heat-affected zone martensite contents (as illustrated in Fig. 3).

The influence of welding speed, v, and heat flux, q, on the cooling rate experienced by the high-temperature heat-affected zone is presented graphically in Fig. 5, which demonstrates that at comparable values of q, the cooling rate increases with an increase in welding speed.

Sensitization Tests

The Oxalic Acid Electrolytic Etch

The results of the oxalic acid electrolytic etch (Practice W of ASTM 763-93) are summarized in Table 4. In order to simplify the subsequent discussion of these results, the high-temperature heat-affected zone microstructures revealed by the etch are divided into three groups based on observed similarities in microstructure.

Group 1 refers to as-etched high-temperature heat-affected zone microstructures consisting predominantly of ferrite, with less than half of all grain boundaries containing some martensite. All the ferrite-ferrite grain boundaries are ditched, implying that these boundaries may be in the sensitized condition. The ferrite-martensite phase boundaries are largely unaffected, suggesting that these boundaries are not sensitized. Figures 6 and 7 display optical micrographs of as-etched heat-affected zones with almost no grain boundary martensite. A continuous network of ditched ferrite-ferrite grain boundaries is visible, and etching resulted in isolated incidences of grain dropping. Very little martensite is present in the high-temperature heat-affected zone, and the martensite shows little or no evidence of grain boundary attack during oxalic acid etching.

Group 2 welds contain high-temperature heat-affected zones with at least half of the grain boundaries covered in martensite. In the case of steel A, up to 65%, and in the case of steel B, up to 100% of all the boundaries contain some martensite, as shown in the micrographs in Figs. 8 and 9. The ferrite-ferrite grain boundaries are ditched, but only sporadic attack is visible on the ferrite-martensite phase boundaries. Ditching of the ferrite-ferrite grain boundaries in group 2 indicates that sensitization is possible, but additional tests are required to confirm this. The ferrite-martensite phase boundaries

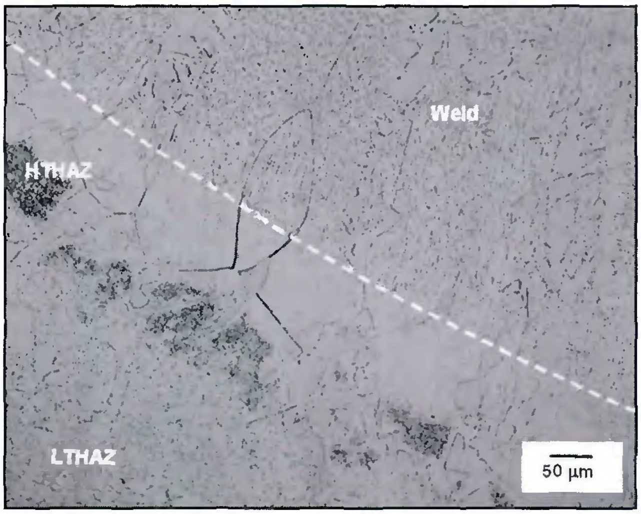

Fig. 9 — Optical photomicrograph of autogenous bead-on-plate weld B13, welded at a heat input of 191.7 J/mm (4869 J/in.), and etched electrolytically in 10% oxalic acid. The majority of the grain boundaries are covered in martensite. Any remaining ferrite-ferrite boundaries are ditched.

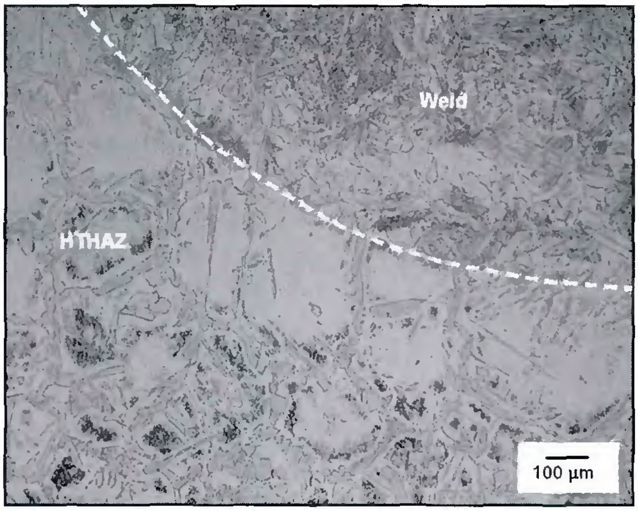

Fig. 10 — Optical photomicrograph of autogenous butt joint weld A25, welded at a heat input of 414.2 J/mm (10521 J/in.), and etched electrolytically in 10% oxalic acid. No ferrite-ferrite grain boundaries are visible.

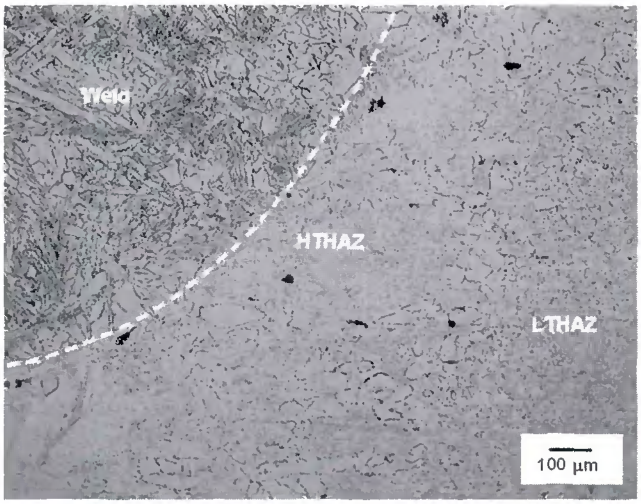

Fig. 11 — Optical photomicrograph of autogenous butt joint weld B25, welded at a heat input of 414.2 J/mm (10521 J/in.), and etched electrolytically in 10% oxalic acid. No ferrite-ferrite grain boundaries are visible.

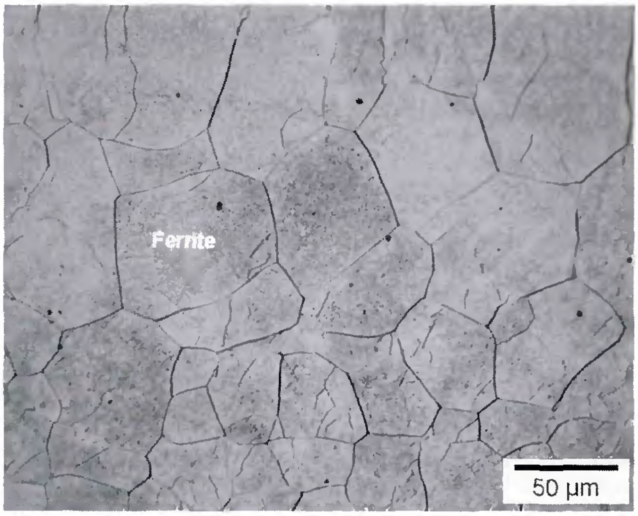

Fig. 12 — Optical photomicrograph of autogenous bead-on-plate weld A2, welded at a heat input of 31.2 J/mm (792 J/in.), after the potentiostatic chromium depletion test. A continuous network of ditched ferrite-ferrite grain boundaries is visible.

are not continuously ditched, and are therefore assumed to be unsensitized.

The high-temperature heat-affected zone grain boundaries of welds in group 3 are not continuously ditched, as illustrated in Figs. 10 and 11. Most of the grain boundaries contain martensite, with martensite covering between 65 and 100% of the total grain boundary area in steel A heat-affected zones, and almost all the grain boundaries in steel B. The absence of continuously ditched grain boundaries indicates that none of these heat-affected zones is sensitized. The potentiostatic chromium depletion test will be used to confirm that the high-temperature heat-affected zone grain boundaries in these samples are in the unsensitized condition.

Potentiostatic Chromium Depletion Test

The results of the potentiostatic chromium depletion test were found to be in excellent agreement with those of the 10% oxalic acid etch, i.e., the ferrite-ferrite grain boundaries that were ditched during the oxalic acid etch generally also contain continuous chromium-depleted zones. Some of the results are considered below.

At very low heat inputs, where almost no martensite forms in the high-temperature heat-affected zone during cooling, all the ferrite-ferrite grain boundaries were etched during the potentiostatic scan. An example of such a high-temperature heat-affected zone is shown in Fig. 12. The presence of etched chromium-depleted zones at the ferrite-ferrite grain boundaries confirms that carbide precipitation during cooling resulted in sensitization of the high-temperature heat-affected zone.

Figure 13 shows the high-temperature heat-affected zone of a weld produced at a slightly higher heat input level, resulting in an increased volume-fraction of grain boundary martensite. The ferrite-ferrite grain boundaries are attacked (and therefore in the sensitized condition), while the phase boundaries between the ferrite and

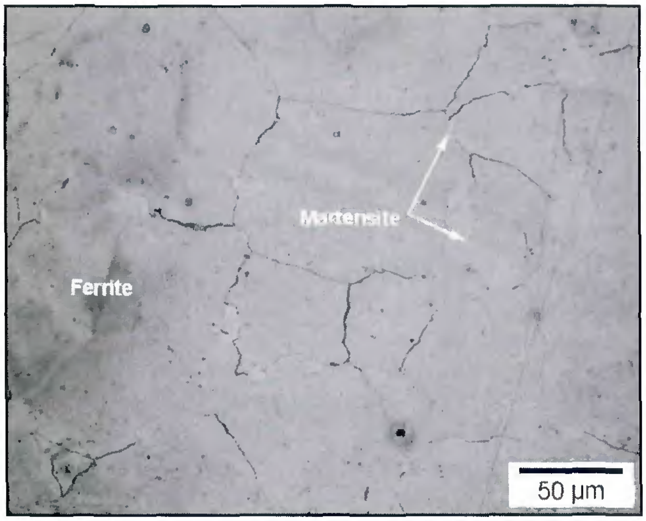

Fig. 13 — Optical photomicrograph of autogenous bead-on-plate weld A11, welded at a heat input of 153.6 J/mm (3901 J/in.), after the potentiostatic chromium depletion test. A discontinuous network of ditched ferrite-ferrite grain boundaries is visible, whereas the ferrite-martensite phase boundaries are largely unattacked.

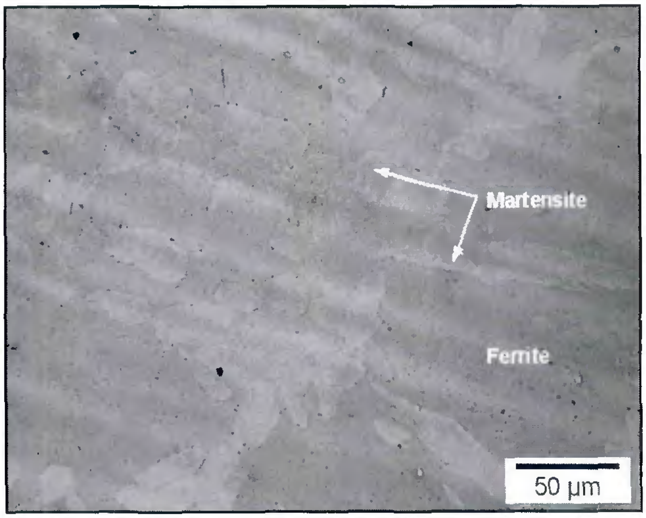

Fig. 14 — Optical photomicrograph of autogenous butt joint weld A18, welded at 262.7 J/mm (6673 J/in.), after the potentiostatic chromium depletion test. No ferrite-ferrite grain boundaries are present.

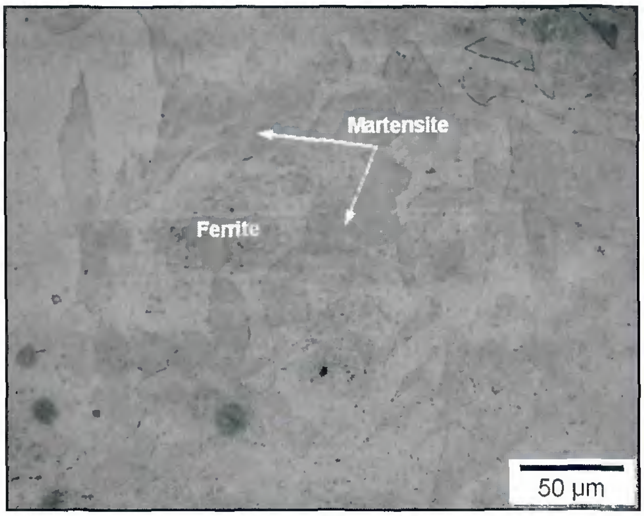

Fig. 15 — Optical photomicrograph of autogenous butt joint weld B15, welded at 250.6 J/mm (6365 J/in.), after the potentiostatic chromium depletion test. No ferrite-ferrite grain boundaries are present.

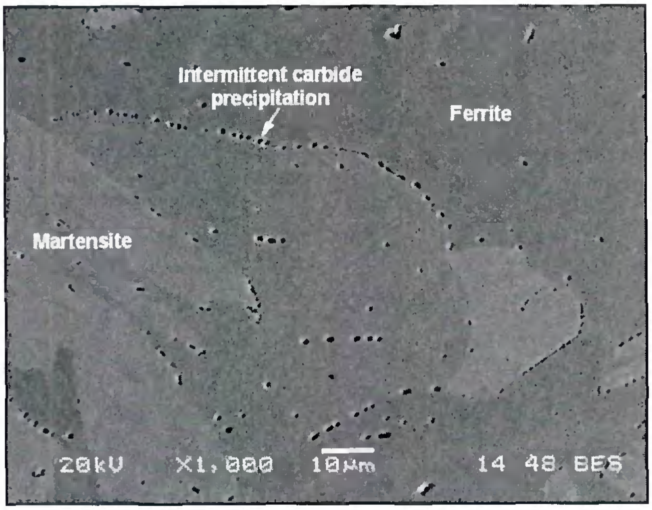

Fig. 16 — SEM photomicrograph of autogenous butt joint weld A18, welded at 262.7 J/mm (6673 J/in.), after the potentiostatic etch. A ferrite-ferrite grain boundary is visible, but it is not continuously ditched.

the lighter martensite phase are largely unattacked, and therefore assumed to be unsensitized.

In welds where the high-temperature heat-affected zone grain boundaries are completely or almost completely covered in martensite, no chromium depletion is evident, as shown in Figs. 14 and 15. This was confirmed by examining these samples using a scanning electron microscope (SEM). The SEM photomicrographs of the heat-affected zones of welds A18 and B13 are shown in Figs. 16 to 19. These welds represent the lowest heat input levels where continuous ferrite-ferrite grain boundaries did not form in the high-temperature heat-affected zones of steels A and B. Note that in these figures the lighter phase is martensite and the darker phase is ferrite.

Figures 16 and 17 show various regions of weld A18 after the potentiostatic etch. Some evidence of localized chromium depletion is evident in Fig. 16, but attack is not continuous. Most of the grain boundaries in Fig. 17 are covered in martensite and display little evidence of chromium depletion. Two ferrite-ferrite grain boundaries close to the weld interface display evidence of chromium depletion, but it should be noted that a continuous network of ditched ferrite-ferrite grain boundaries is not present in this sample.

Figure 18 shows a large area of weld B13, including the high-temperature heat-affected zone and part of the low-temperature heat-affected zone. No ferrite-ferrite grain boundaries are visible. Figure 19 displays the high-temperature heat-affected zone at a higher magnification. Only ferrite-martensite phase boundaries are visible, and no chromium depletion is evident in the vicinity of any of these boundaries.

The objective of this investigation was to demonstrate that a single weld can sensitize during continuous cooling after welding. The results described above suggest that this occurs when low heat input welding results in very fast cooling rates. Rapid cooling after welding can suppress

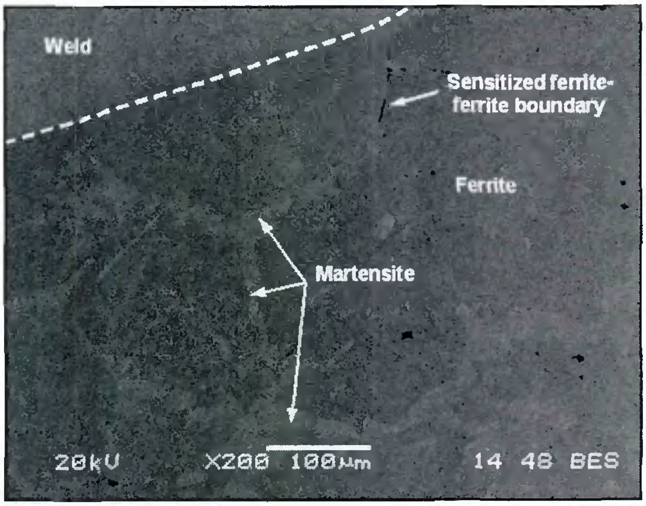

Fig. 17 — SEM photomicrograph of the HTHAZ of autogenous butt joint weld A18, welded at 262.7 J/mm (6673 J/in.), after the potentiostatic etch. Note the isolated ditched ferrite-ferrite grain boundaries close to the weld interface (top, center).

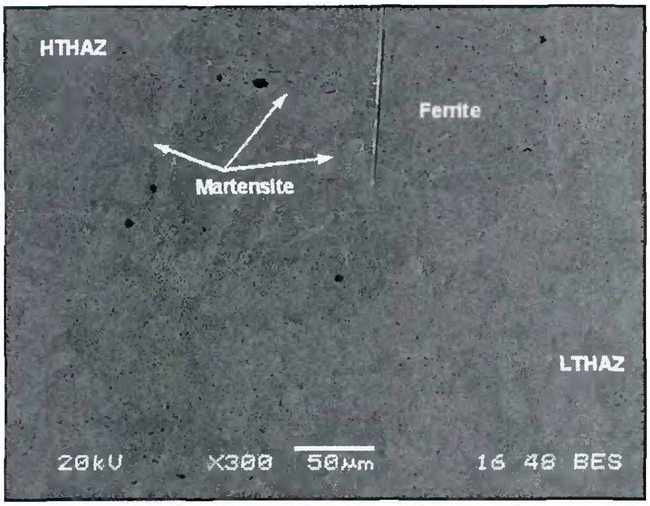

Fig. 18 — SEM photomicrograph of the HTHAZ and the LTHAZ (low-temperature heat-affected zone) of autogenous butt joint weld B13, welded at 191.7 J/mm (4869 J/in.), after the potentiostatic etch. No ferrite-ferrite grain boundaries are present.

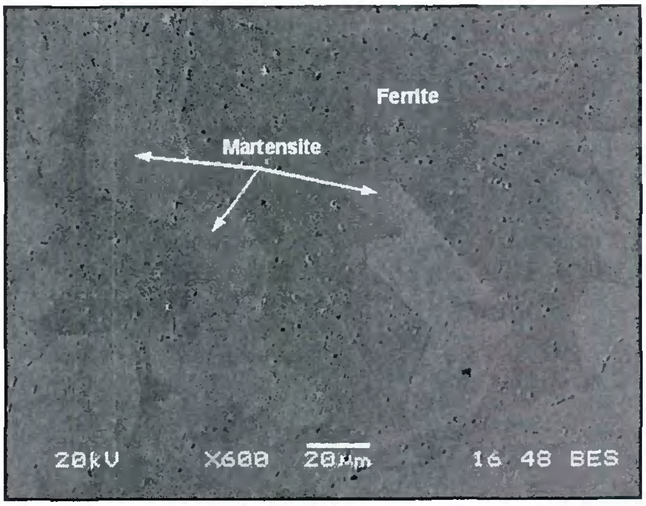

Fig. 19 — SEM photomicrograph of the HTHAZ of autogenous butt joint weld B13, welded at 191.7 J/mm (4869 J/in.), after the potentiostatic etch. No ferrite-ferrite grain boundaries are present.

austenite nucleation as the heat-affected zone cools through the dual-phase (austenite+ferrite) phase field, resulting in almost fully ferritic high-temperature heat-affected zone microstructures. The ferrite phase becomes supersaturated in carbon, and extensive carbide precipitation occurs at the ferrite-ferrite grain boundaries during cooling. The fast cooling rate also prevents the back-diffusion of chromium to the depleted regions adjacent to the chromium-rich carbides, resulting in a continuous network of sensitized ferrite-ferrite grain boundaries. As the heat input increases, the cooling rate is reduced and more austenite forms in the heat-affected zone. This austenite transforms to martensite at lower temperatures and is retained down to room temperature as a grain boundary martensite network within the ferritic heat-affected zone. If enough austenite forms on cooling to absorb excess carbon (austenite has a higher carbon solubility than ferrite), a continuous network of chromium-depleted zones does not form and sensitization is prevented. Slower cooling after welding at higher heat input levels also allows the ferrite phase to desensitize through diffusion of chromium from the grain interiors into any chromium-depleted zones.

Due to its higher austenite potential, steel B formed more martensite in the high-temperature heat-affected zone than steel A after welding at comparable heat input levels. In steel B almost continuous networks of martensite were observed on the high-temperature heat-affected zone grain boundaries of all welds produced at heat inputs of 192 J/mm (4877 J/in.) or higher, corresponding to cooling rates of 293°C/s or less. In steel A, continuous ferrite-ferrite grain boundaries were only eliminated at heat inputs of 263 J/mm (6680 J/in.) (corresponding to a cooling rate of 85°C/s) or higher. In welds produced at higher heat input levels, continuous ferrite-ferrite grain boundaries were virtually eliminated, and the heat-affected zones were shown to be unsensitized.

Conclusions

This investigation studied the sensitization of two type EN 1.4003 ferritic stainless steels during continuous cooling after welding. Based on the results obtained, the following conclusions can be drawn:

- Sensitization of type EN 1.4003 ferritic stainless steels during continuous cooling after welding is possible if low heat input levels are used.
- Welding at low heat inputs can suppress the transformation of ferrite to austenite as the heat-affected zone cools through the (austenite+ferrite) dual-phase region during welding. This results in largely ferritic high-temperature heat-affected zones.
- Carbon supersaturation of the ferrite phase occurs in the absence of sufficient austenite during cooling, resulting in extensive carbide precipitation on the ferrite-ferrite grain boundaries. Chromium back-diffusion is prevented by rapid cooling, and the ferrite-ferrite grain boundaries are sensitized to intergranular corrosion.
- With an increase in heat input, the cooling rate after welding is reduced, and more austenite forms in the high-temperature heat-affected zone. Sensitization is prevented by the presence of enough austenite to eliminate continuous ferrite-ferrite grain boundaries.
- Due to its higher austenite potential, steel B contained more martensite than steel A in the high-temperature heat-affected zone after welding at comparable heat input levels. A sufficiently high austenite potential should be maintained in these steels to promote austenite formation during cooling. In this respect, a reduction in carbon content or an increase

in the amount of ferrite-forming elements in type EN 1.4003 steels needs to be balanced by the addition of austenite-forming elements such as nickel.

- Excessive welding speeds appear to exacerbate sensitization during low heat input welding.

In addition to specifying a maximum heat input for welding the EN 1.4003 steels (to limit heat-affected zone grain growth), guidelines supplied to fabricators should include a minimum recommended heat input level. This minimum heat input will be a function of the plate thickness and chemistry, but 300 J/mm appears to be an appropriate limit for 3-mm plate. Heat flow modeling can be used for different chemistries to calculate appropriate minimum heat input levels for various plate thicknesses. A maximum weld interface cooling rate of 80°C/s (Δt_{15-8} = 8.75 s) can be used as a preliminary guideline to distinguish between heat inputs likely to cause sensitization, and those where cooling after welding is slow enough to prevent the formation of continuous chromium-depleted zones. Guidelines should also emphasize the harmful effect of fillet weld overlap (most welding standards limit the amount of allowable overlap) and excessive welding speeds.

Acknowledgments

The authors would like to thank Columbus Stainless and THRIP for sponsoring the project and the University of Pretoria for providing laboratory facilities. The assistance of Prof. P. C. Pistorius and Prof. G. T. van Rooyen is also gratefully acknowledged.

References

1. *3CR12 - The Utility Stainless Steel*. 1997. Technical manual published by Columbus Stainless.

2. *3CR12 – Technical Data*. 2004. Technical manual published by Columbus Stainless.

3. Maxwell, D. K., Warrington, J., and Dewar, K. 1993. From niche to commodity, 3CR12 – a ten-year scenario. *Corrosion Reviews* 11(3-4): pp. 17–32.

4. Grobler, C. 1987. Weldability studies on 12% and 14% chromium steels. PhD dissertation, University of Pretoria, South Africa.

5. Meyer, A. M. 2000. Interstitial diffusion from the weld metal into the high temperature heat affected zone in 11 – 12 percent chromium steel welded joints. MEng thesis, University of Pretoria, South Africa.

6. Folkhard, E. 1988. *Welding Metallurgy of Stainless Steels*. Springer-Verlag, Vienna: p. 11.

7. Matthews, L. M., Griesel, B., Longman, P. T., Van Rooyen, G. T., and Prozzi, J. M. 1999. Sensitisation in low-carbon 12% chromium containing stainless steels. *Proceedings of the 14th International Corrosion Congress*. Cape Town, South Africa: p. 332.

8. Bavarian, B., Szklarska-Smialowska, Z., and MacDonald, D. D. 1982. Effect of temperature on the stress corrosion cracking of tempered type 403 martensitic stainless steel in sodium sulfate solution. *Corrosion* 38(12): pp. 604–608.

9. Nishimura, R. 1992. Stress corrosion cracking of type 430 ferritic stainless steel in chloride and sulfate solutions. *Corrosion* 48(11): pp. 882–890.

10. Frangini, S. 1994. Sensitivity to stress corrosion cracking of type 405 stainless steel in high-temperature aqueous environments. *Corrosion* 50(6): pp. 447–456.

11. Cíhal, V. 1984. Intergranular Corrosion of Steels and Alloys. *Material Science Monographs*, 18. Elsevier: pp. 79–83.

12. Solomon, H. D., and Devine, T. M. 1984. Duplex stainless steels – A tale of two phases. *Proceedings of Duplex Stainless Steels*. St. Louis, Mo.: pp. 693–756.

13. Tuling, A. 2001. EELS study of sensitisation in 12% chromium steel. *Proceedings of the Microscopy Society of Southern Africa* 31: p. 26.

14. Tomari, H., Fujiwara, K., Shimogori, K., Fukuzuka, T., and Kanda, M. 1982. Intergranular stress corrosion cracking of 13% Cr and 18% Cr ferritic steels in high temperature high purity water. *Corrosion* 38(5): pp. 283–294.

15. Frangini, S., and Mignone, A. 1992. Modified electrochemical potentiokinetic reactivation method for detecting sensitisation in 12 wt-% chromium ferritic stainless steels. *Corrosion* 48(9): pp. 715–726.

16. Kaltenhauser, R. H. 1982. *Source Book on the Ferritic Stainless Steel*. ASM Engineering Bookshelf: pp. 212–218.

17. ASTM A763-93 (2004). *Standard Practices for Detecting Susceptibility to Intergranular Attack in Ferritic Stainless Steels*. ASTM International.

18. Pistorius, P. C., and Coetzee, M. 1996. Sensitization of 430 ferritic stainless steel during continuous annealing. *Journal of the South African Institute of Mining and Metallurgy* 96(3): pp. 119–125.

19. Rocha, H. J., and Lennartz, G. 1955. The activation potential of iron-chromium alloys and its relationship to the sulfur content of these alloys. *Archives of Eisenhüttenwese* (26): pp. 117–123.

20. King, P. F., and Uhlig, H. H. 1959. Passivity in the iron-chromium binary alloys. *Journal of Physical Chemistry* 63: pp. 2026–2032.

21. Frankenthal, R. P., and Pickering, H. W. 1973. Intergranular corrosion of a ferritic stainless steel. *Journal of the Electrochemical Society* 120: pp. 23–26.

22. Kirchheim, R., Heine, B., Fischmeister, H., Hofmann, S., Knote, H., and Stolz, U. 1989. The passivity of iron-chromium alloys. *Corrosion Science* 29: pp. 889–917.

23. Rosenthal, D. 1946. The theory of moving sources of heat and its application to metal treatments. *Transactions of the AIME* 68: pp. 849–866.

24. Easterling, K. 1992. *Introduction to the Physical Metallurgy of Welding*. 2nd Edition, Butterworth-Heinemann: p. 19.

Appendix

Table I — Welding Parameters Measured for Steel A during Autogenous Gas Tungsten Arc Welding

Weld number	Welding current A	Arc voltage V	Welding speed mm/s	Heat input J/mm
A1	168	14	33.3	33.7
A2	109	10	16.7	31.2
A3	38	10	4.94	36.7
A4	222	14	33.3	44.6
A5	130	10	16.7	37.2
A6	50	9	4.94	43.5
A7	355	19	33.3	96.7
A8	223	15	16.7	95.7
A9	91	10	4.94	88.0
A10	301	16	16.7	137.7
A11	189	14	8.23	153.6
A12	125	10	4.94	120.9
A13	272	17	11.57	190.9
A14	210	16	8.23	195.0
A15	144	13	4.94	181.0
A16	252	17	8.23	248.6
A17	168	13	4.94	211.1
A18	118	11	2.36	262.7
A19	199	15	4.94	288.6
A20	127	12	2.36	308.4
A21	219	16	4.94	338.8
A22	135.5	12	2.36	329.1
A23	236	16	4.94	365.1
A24	146	13	2.36	384.1
A25	252	17	4.94	414.2
A26	164	13	2.36	431.5

Table II — Welding Parameters Measured for Steel B during Autogenous Gas Tungsten Arc Welding

Weld number	Welding current A	Arc voltage V	Welding speed mm/s	Heat input J/mm
B1	168	13	33.3	31.3
B2	109	9	16.7	28.1
B3	38	9.5	4.94	34.9
B4	222	16	33.3	50.9
B5	130	10	16.7	37.2
B6	50	9	4.94	43.5
B7	352	20	33.3	101.0
B8	223	15	16.7	95.7
B9	91	10	4.94	88.0
B10	301	16	16.7	137.7
B11	190	15	8.23	165.4
B12	125	10	4.94	120.9
B13	273	17	11.56	191.7
B14	210	16	8.23	195.0
B15	144	18	4.94	250.6
B16	252	17	8.23	248.6
B17	168	14	4.94	227.4
B18	118	10	2.36	238.8
B19	199	15	4.94	288.6
B20	127	12	2.36	308.4
B21	219	16	4.94	338.8
B22	135.5	12.5	2.36	342.8
B23	236	16	4.94	365.1
B24	246	13	2.36	647.2
B25	252	17	4.94	414.2
B26	165	13	2.36	434.1

Development of an Explosive Welding Process for Producing High-Strength Welds between Niobium and 6061-T651 Aluminum

Thin interlayers of Nb and Al were used to improve the joining of thicker plates

BY T. A. PALMER, J. W. ELMER, D. BRASHER, D. BUTLER, and R. RIDDLE

ABSTRACT. An explosive welding procedure for joining 9.5-mm-thick niobium plate to 203-mm-thick 6061-T651 Al plate has been developed in order to maximize the weld tensile and impact strengths and the amount of welded material across the surface of the plate. This procedure improves upon previous efforts, in which the 9.5-mm-thick niobium plate is welded directly to 6061-T4 Al plate. In this improved procedure, thin Nb and Al interlayers are explosively clad between the thicker niobium and aluminum plates. Welds produced using these optimized parameters display a tensile strength of approximately 255 MPa and an impact strength per unit area of approximately 0.148 J/mm^2. Specialized mechanical testing geometries and procedures are required to measure these weld properties because of the unique weld geometry. In order to ensure that differences in the thermal expansion coefficients of aluminum and niobium do not adversely affect the weld strength, the effects of thermal cycling at temperatures between –22° and 45°C on the mechanical properties of these welds have also been investigated by testing samples in both the as-received and thermal cycled conditions. Based on the results obtained from this series of mechanical tests, thermal cycling is shown to have no adverse effect on the resulting tensile and impact strengths of the welds produced using the optimized welding parameters.

Introduction

A preliminary investigation of the feasibility of explosively welding niobium to aluminum has been previously published (Ref. 1). In that study, 9.5-mm-thick commercially pure Nb is welded to a 178-mm-thick 6061 Al plate in the T4 condition. These initial welds are produced in a conventional manner with the detonator placed at the edge of the plate. The aluminum plate is required to be in the softened (T4) heat treated condition to facilitate the explosive welding process. In order to transform the 6061-T4 Al to the desired T6 heat treated condition, a postwelding heat treatment is required. An ultrasonic evaluation of these welded plates shows that areas of disbonding are present on the side of the plate directly opposite from the detonator.

Radially symmetric welding across the weld interface can be achieved by moving the detonator to the center of the plate. A divot, surrounded by a small area of nonwelded material, is produced at the detonator location in the center of the plate. Additional areas of disbonding, as confirmed by ultrasonic scans, tend to be isolated near the edges of the plate, far from the locations where well-welded material is required. A ring of well-welded material extends radially outward more than 430 mm from the nonwelded region in the center of the plate.

In order to eliminate the postweld heat treatment and to directly weld the niobium to the 6061 Al plate in the hardened (T6) condition, explosively welded niobium and aluminum interlayers are introduced between the aluminum and niobium plates. Smaller explosive charges can be used to weld these interlayers to the thick aluminum plate, thus making it much easier to work with the aluminum plate in the hardened condition. The effects of the introduction of these interlayers on the resulting mechanical properties of the explosive weld are also investigated in this study.

The tensile properties of the initial welds produced with the detonator located at the edge of the plate were investigated using conventional tensile tests with a dog-bone geometry (Ref. 1). In order for the samples to have a sufficient length to place the Al-Nb weld interface in the center of the gauge length of the tensile bar, niobium extension bars were electron beam welded to the niobium-clad plate. During testing, these samples failed in the explosively clad niobium at locations near the weld interface, but not at the weld interface, showing that the strength of the weld exceeds that of the niobium. Additional mechanical tests, using sample geometries optimized for testing the tensile, shear, and impact strengths of the welds, have also been performed on samples taken from both the edge-detonated and center-detonated welds. These procedures are discussed further in a following section.

Table 1 provides a summary of the mechanical properties of the edge-detonated (Ref. 1) and center-detonated explosive welds. For both sets of welds, failure occurs at the Al-Nb weld interface, and the notched (268 ± 14.5 MPa and 287 ± 35.4 MPa, respectively) and unnotched (351 ± 17 and 268 ± 9 MPa, respectively) tensile strengths compare favorably with the ultimate tensile strengths of both niobium (310 MPa) and 6061-T6 Al (312 MPa) (Ref. 1). The measured shear strengths

KEYWORDS

Aluminum
Initiation Point
Explosive Welding
Mechanical Properties
Niobium
Solid State
Dissimilar Metal Joining
Impact Strength

T. A. PALMER, J. W. ELMER, and R. RIDDLE are with Lawrence Livermore National Laboratory, Livermore, Calif. D. BRASHER and D. BUTLER are with High Energy Metals, Inc., Sequim, Wash.

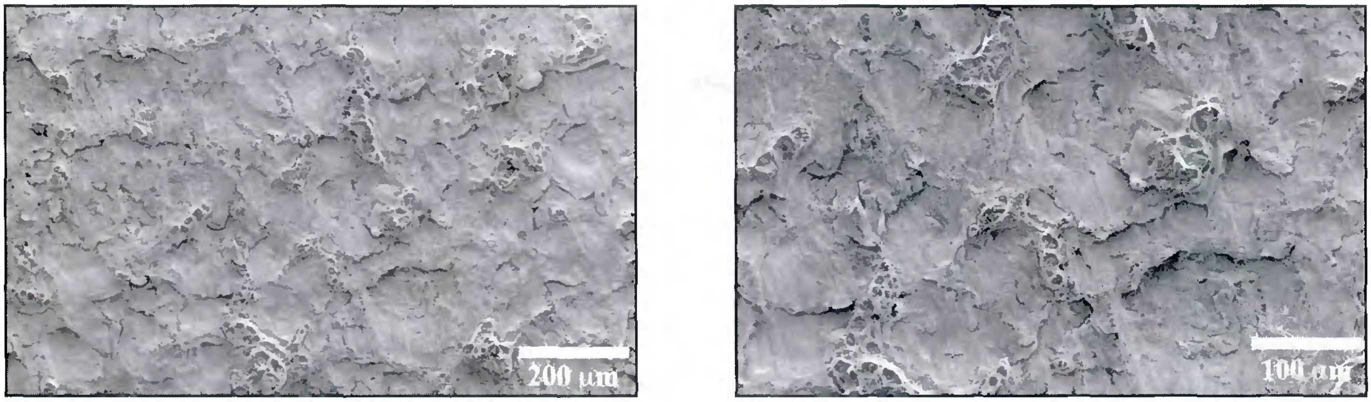

Fig. 1 — SEM micrographs of the fracture surface on one of the edge-detonated Izod samples.

Table 1 — Summary of Mechanical Properties of Preliminary Single-Welded Al-Nb Clad Plates

	Edge-Detonated Plates			Center-Detonated Plates		
	Number of Tests	Average	Standard Deviation	Number of Tests	Average	Standard Deviation
Tensile Strength (MPa)						
Unnotched	6	350.6	17.0	5	266.8	10.07
Notched	3	265.6	14.5	3	287.3	35.4
Shear Strength (MPa)	4	224.3	6.76	3	180.4	5.38
Impact Strength (J)	2/7	0.8/1.5[a]	0.1/0.1[a]	12	1[b]	0.2[b]
Impact Energy/Unit Area (J/mm2)	2/7	0.020/0.023	0.003/0.002	12	0.015	0.003

(a) Impact strength sample geometries are varied from a cross section of 3.2 x 10.2 mm to one of 6.4 x 10.2 mm.
(b) Impact strength sample geometry has a cross section of 12.7 x 10.2 mm.

(224 ± 7 MPa and 180 ± 5, respectively) are approximately 72% and 58%, respectively, of the measured tensile strength of the 6061-T6 Al. These measured shear strengths are consistent with the von Mises ductile failure criteria, which predict that the shear strength should be approximately 58% of the ultimate tensile strength (Ref. 2). It is also in line with the reported shear strength of 6061-T6 Al plate (207 MPa).

On the other hand, there are significant concerns about the impact strength of the resulting welds. As shown in Table 1, the measured impact strengths of the edge- and center-detonated weld samples are low (≥0.02 J/mm^2). All of the samples failed along the Al-Nb weld interface, and the majority of the fracture surface displays a rather flat appearance, indicative of a brittle fracture mode. Figure 1A and B shows micrographs taken of typical areas on a fracture surface obtained from an edge-detonated impact sample. While the majority of the fracture surface is characteristic of a brittle failure mode, there are small areas interspersed on the fracture surface displaying features similar to those more commonly associated with a more desirable ductile failure mode.

These low impact strengths and the brittle failure mode can be correlated with characteristics of the weld interface morphology. An examination of the weld cross section, which is shown in Figs. 4 and 5 in Ref. 1, shows regions of intermixing of the Al and Nb (Ref. 1). These regions consist primarily of submicron-sized Nb-rich particulates mixed with larger fragments of Nb in an Al-rich matrix. This behavior is consistent with the formation of Al-Nb intermetallic phases at the weld interface caused by the melting of the Al during the explosive welding process. It appears that these regions of Al and Nb intermixing result in a brittle weld being formed over a large area of the interface between the Al and Nb plates.

Changes to the welding process are thus required in order to produce welds with the desired tensile and impact strengths. In the current study, a three-step explosive welding process is developed to join Grade 1 (Reactor) niobium directly to 6061-T651 Al plate, thus removing the follow-on heat treatment. These welds must meet minimum criteria for tensile, shear, and impact strengths, which are measured using specialized mechanical testing geometries and procedures. In addition to meeting these mechanical property requirements, the amount of well-welded material across the surface of the thick Al plate must be maximized. In order to meet these requirements, a procedure involving the explosive welding of thin sheets of Al and Nb between the thicker Al and Nb plates, has been developed. The introduction of these thin interlayers not only produces welds with the required tensile, shear, and impact strengths, but also allows the thick Al plate to be welded in the high-strength (T-651) condition, thus removing the requirement for a postweld heat treatment of the clad material.

Experimental

Explosive Welding

The explosive welding (EXW) process is a solid-state joining process used to join a wide variety of materials that cannot be joined using traditional fusion welding processes (Ref. 3). A schematic diagram showing the basic components of this process (the explosive charge, a base metal, and a clad metal) is shown in Fig. 2. Prior to welding, the clad metal is offset a given distance above the base metal, and a predetermined amount of explosive is placed on top of the clad metal. A controlled explosive detonation is used to accelerate this clad metal into the base metal at a sufficient velocity that the collision

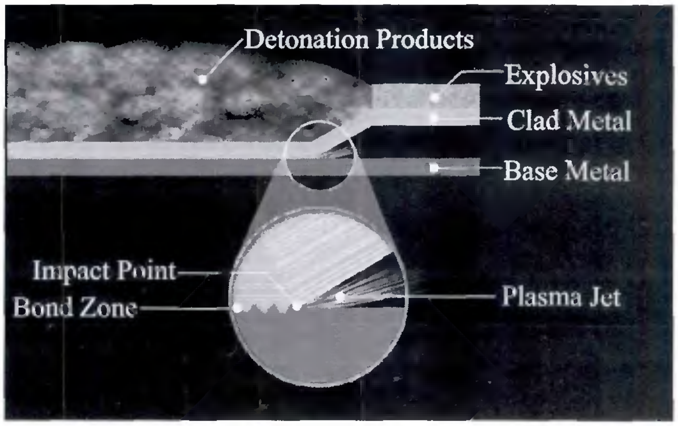

Fig. 2 — Schematic figure showing the basic features of the explosion welding process and the properties of the resulting weld.

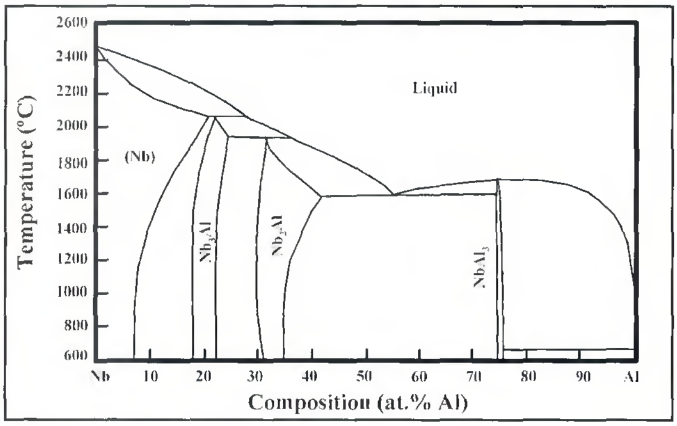

Fig. 3 — Plot showing the Al-Nb phase diagram (Ref. 5).

Table 2 — Summary of Explosion Welding Parameters Used during the Development of the Al-Nb Weld

Welding Parameter Identification	Detonator Location	Material Thickness (mm) Al Plate	Al Interlayer	Nb Interlayer	Nb Plate	Explosive Energy (MJ) Al-Al Bond	Al-Nb Bond	Nb-Nb Bond
Single Welds								
1[a]	Edge	203	—	—	9.5	—	3.1	—
2[a]	Center	203	—	—	9.5	—	3.1	—
Multiple Welds								
0.8-mm Al Interlayer								
3a	Center	203	0.8	0.33	9.5	0.9	1.0	3.08
3b	Center	203	0.8	0.33	9.5	1.01	0.95	3.76
3c	Center	203	0.8	0.33	9.5	0.82	1.0	3.08
1.0-mm Al Interlayer								
4a	Center	203	1.0	0.33	9.5	1.37	1.54	3.08
4b	Center	203	1.0	0.33	9.5	1.37	1.54	3.08

(a) A postweld heat treatment is required to convert the 6061 Al plate from the T4 heat treatment condition to the T6 heat treatment condition.

causes the two metals to fuse together. The force of the explosion sets up an angular collision, which produces a plasma phase, which is ejected ahead of the leading edge of the weld interface. Since the plasma jet is located in front of the collision point, it is inferred that melting is not necessarily part of the welding occurring behind it. This plasma jet removes impurities from the surfaces of both the base and clad plates, thus leaving clean metal surfaces for joining. The pressures at the collision point (690 to 4137 MPa) are enough to cause the metals to behave like viscous fluids. This behavior is responsible for the wave-like weld pattern produced at the interface of the two materials and shown in the figure (Refs. 3, 4).

The joining of niobium to aluminum is hindered by the potential formation of several intermetallic phases, as shown in the Al-Nb phase diagram in Fig. 3 (Ref. 5). The presence of these intermetallic phases can lead to significant decreases in the weld strength, thus making the use of fusion welding techniques to join these two materials impractical. Therefore, a solid-state joining process, where no melting or significant intermixing of the Al and Nb occurs, is required. Explosive welding is preferable to other solid-state joining processes in this case because of the thickness of the niobium plate (9.5 mm) and the large surface area, approximately 508 × 508 mm, to be welded.

In the development of this explosive weld, a number of different materials are used. These materials include a 203-mm-thick 6061-T651 Al plate, a thin (0.8/1.0 mm) 6061-O Al sheet, a thin (0.33-mm) Nb sheet, and a thick (9.5-mm) Nb plate. The 6061-T651 Al base plate meets the chemistry and mechanical property requirements in ASTM B209M-02a (Ref. 6) and AMS-QQ-A-250/11 (Ref. 7), while the Nb sheet and plate materials meet the requirements for R04200-Type 1 Reactor Grade material, which appears in ASTM B393-03 (Ref. 8).

Because of the nature of the weld development process, which evolved over an extended period of time, a number of different heats have been used for each of the materials defined in Table 2. Changes in material heats are made between Welds #1 and #2, which encompass the initial development work on single welds. The first multiple welds with a 0.8-mm-thick Al interlayer in Welds #3a through #3c use a single heat of each material. Different heats of each material are used when the 0.8-mm Al interlayer is replaced by a 1.0-mm-thick Al interlayer in Welds #4a and #4b. Compositional variations between the different heats are not considered significant since the weld parameters play a much more dominant role than the material chemistry in producing an explosive weld with suitable properties.

The explosive welding operations described here have been performed by High Energy Metals, Inc. All welds are made using an ammonium nitrate-fuel oil (ANFO)-based explosive mixture. In the explosive welding process, there are several essential parameters that must be tightly controlled and monitored as part of the welding process. These parameters include the surface finish and cleanliness of the welded face of each material, the placement of the detonator, and the ex-

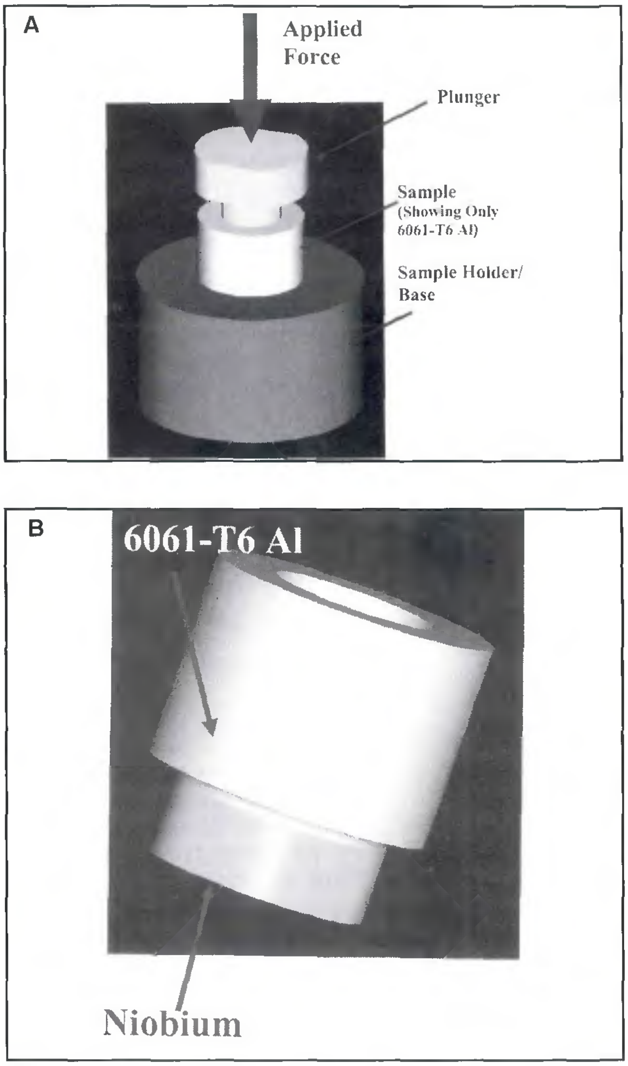

Fig. 4 — Schematic diagrams. A — The tensile testing setup used to measure the tensile strength of the Al-Nb explosion weld; B — the ram tensile specimen.

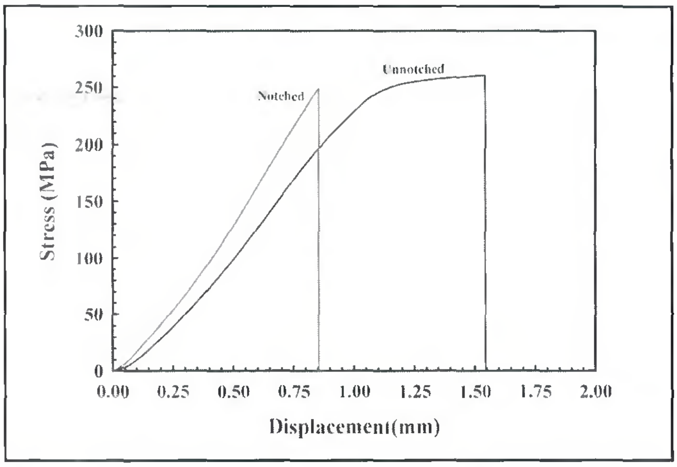

Fig. 5 — Typical stress-strain curve obtained during the tensile testing of an explosively welded sample in the unnotched and notched configurations.

plosive energy. The explosive energy is defined as the kinetic energy of the impacting plate for a given explosive detonation velocity, which is controlled by mixing the ANFO-based explosive with fine silica, and stand-off distance between the two plates. The explosive velocity of a small portion of the explosive mixture is measured before the welding operation by timing the speed of the explosive wave front over a distance of approximately 305 mm.

The surfaces to be welded are ground to a surface finish of 3.2 μm root mean square (RMS) or better and cleaned in order to remove any oxide, dirt, or other foreign objects. Each of the plates, which are all 508 × 508 mm in size, must also meet a flatness tolerance, of at least 0.2 mm over its length, in order to maintain a uniform stand-off distance between the clad and base metals. The development of a set of suitable welding parameters has involved a number of iterations. Table 2 provides a summary of the various welding parameters for both the preliminary single welds, as well as the multiple welds. The location of the detonator and the explosive energy are varied in an attempt to produce a weld with acceptable properties. The stand-off distances used in each of the welds is approximately equal to the thickness of the sheet or plate being welded. Smaller-capacity detonators are used to weld the thin interlayers, which require lower explosive energies (approximately 1 MJ) during the welding operation. A higher-capacity detonator is used to weld the 9.5-mm-thick Nb plate, which requires a higher explosive energy (> 3 MJ) during welding.

Nondestructive and Metallographic Evaluation of Weld Integrity

The quality of each explosive weld is examined in the as-welded condition using an ultrasonic evaluation technique to inspect the integrity of the Al-Nb weld region. The ultrasonic evaluation of each explosive weld is performed by immersing the welded plates into a water tank and using a pulse echo ultrasonic examination technique (Refs. 9–11) to detect indications of voids, defects, and areas of disbonding in the explosive weld. A 5-MHz, 12.7-mm-diameter, 32-mm spherical focus transducer, which has a theoretical spot size of 0.76 mm, is used. During each scan, the transducer is automatically rastered over the surface of the plate with a maximum step size of 0.5 mm in order to provide a complete picture of the weld region across the entire plate. The results of each scan are used to judge the extent of well-welded material on each plate and as a means of determining whether any defects are present in the region where mechanical testing samples are removed.

An ultrasonic calibration standard, fabricated from a piece of explosively clad Al-Nb weld, is used to calibrate the equipment prior to each scan and to ensure that the system is able to detect defects of a given size. Known reflectors, in the form of flat bottomed holes and rectangles with a minimum area of 0.79 mm^2, are placed in the standard at the Al-Nb weld interface and are used to establish the primary reference responses of the equipment. The sizes of the individual defects in the calibration standard are chosen to ensure that the system is able to detect defects smaller than the maximum allowable defect size in the final part.

Metallographic examination of the cross section of the explosively welded material is typically performed in the as-polished condition. In this condition, the different weld regions are visible. More detailed information about the weld regions can be obtained by etching the sample in a chemical bath containing 20 mL of glycerol, 10 mL of hydrofluoric acid, and 10 mL of nitric acid. Because the aluminum etches at a more rapid rate than the niobium, care must be taken to ensure that the aluminum is not overetched. With etching, the microstructure of the weld region is better revealed, making it much easier to identify areas of intermixing between the dissimilar metals. This examination of the weld cross section al-

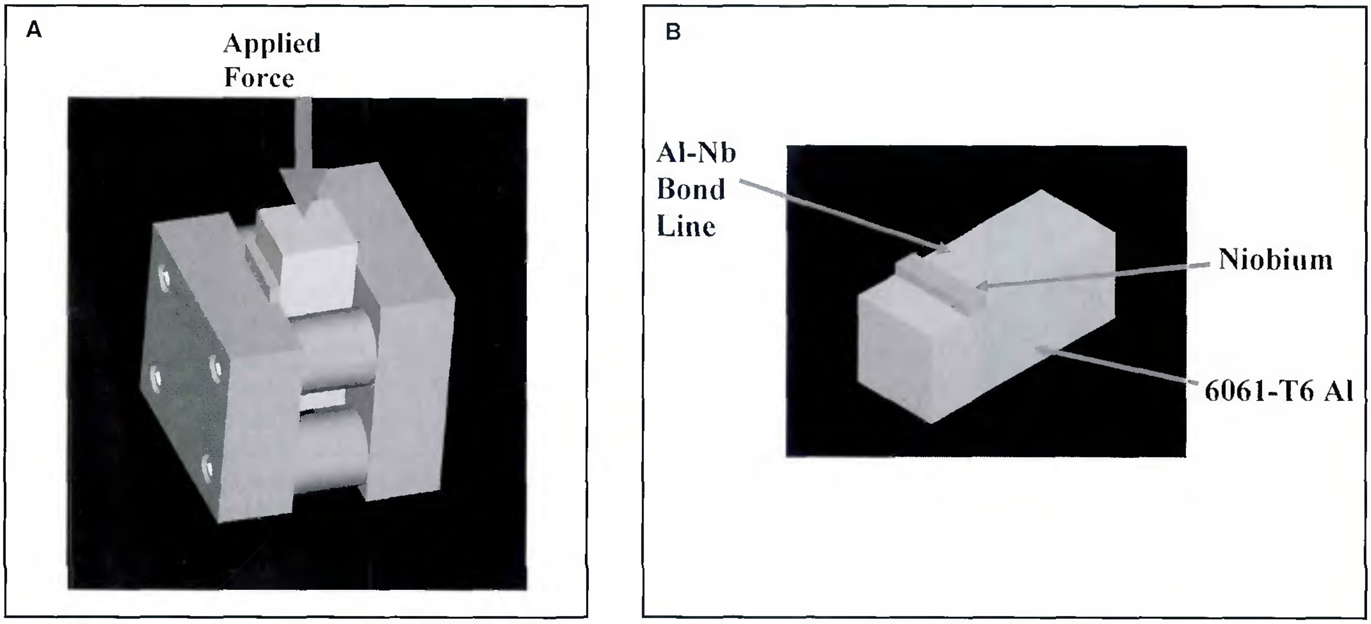

Fig. 6 — Schematic diagrams. A — The shear testing setup used to measure the shear strength of the Al-Nb explosion weld; B — the shear strength specimen.

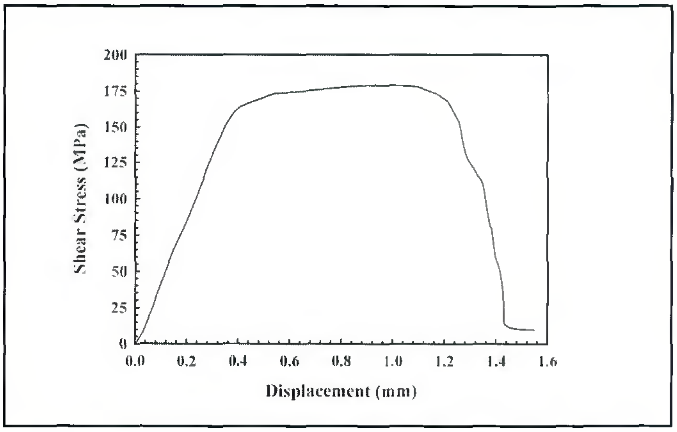

Fig. 7 — Typical stress-strain curve obtained during the shear testing of an explosion welded sample.

lows the weld wave pattern to be evaluated and determine if any changes to the welding parameters are required in order to produce the most desirable weld pattern morphology.

Mechanical Testing

The mechanical properties of the explosive welds produced during each welding iteration are measured to ensure that the welds produced during the explosive welding process have the maximum possible strength. Mechanical test samples are removed from specific locations in each welded plate. The samples taken from Welds #1 and #3a are removed from the center region of the welded plate. Samples taken from Weld #2 are removed from locations at the corners of the plate. Those samples used to test the mechanical properties of Welds #3b, #3c, and #4(a and b) are also taken from the center region of the welded plate outside the center defect area. In these plates, though, the samples are removed from better defined radial locations, 152 mm from the center of the plate. The locations where the samples are removed in each plate have been ultrasonically scanned to ensure that only properly welded material is used in the mechanical testing samples. The results reported for Welds #3a–c and #4a include results from only a single welded plate, while those reported for Weld #4b are an average of results taken from three different Al-Nb clad plates welded using identical procedures.

Modifications to traditional mechanical test geometries and procedures are required to test the strength of the weld. Typical tensile and Charpy impact specimen geometries would require an extension be welded onto the rather thin niobium clad layer, as done in the previous study (Ref. 1). Because the addition of these welded extensions introduces an additional level of complexity to the testing, a set of modified mechanical testing geometries and procedures, based on existing standard techniques, are employed to test the tensile, shear, and impact strength of the Al-Nb weld (Refs. 12–14).

The tensile strength of the weld is measured using the tensile testing setup and corresponding ram tensile specimen schematically shown in Fig. 4 A and B (Ref. 12). This test specimen, shown in Fig. 4B, can be divided into two components. The first component encompasses the 6061-T651 Al side of the weld and has an outer diameter of 33.3 mm and a height of 25.4 mm. An internal hole with a diameter of 19.1 mm is machined through the height of the aluminum and into the niobium-clad layer. The second component of the ram tensile specimen consists of the niobium- clad layer, which is machined to a diameter of 25.4 mm. In the design of these specimens, the niobium portion of the specimen in contact with the plunger is made thick enough (8.89 mm) so that the niobium does not yield during testing. Samples with and without a notch machined at the Al-Nb weld interface are tested. In the notched samples, a 60-deg ± 2 deg notch with a depth of 0.635 ± 0.127 mm is used. During testing, a plunger is inserted into the center hole, and a compressive force is exerted while the Al portion of the sample is held in place. As a result, the strength of the weld is measured in tension.

All of these ram tensile tests are performed on an Instron electromechanical test machine, equipped with an 89-kN load cell. The load (N)-displacement (mm) behavior of the tensile sample is monitored at a constant crosshead speed of 0.5 mm/min during each test. After test-

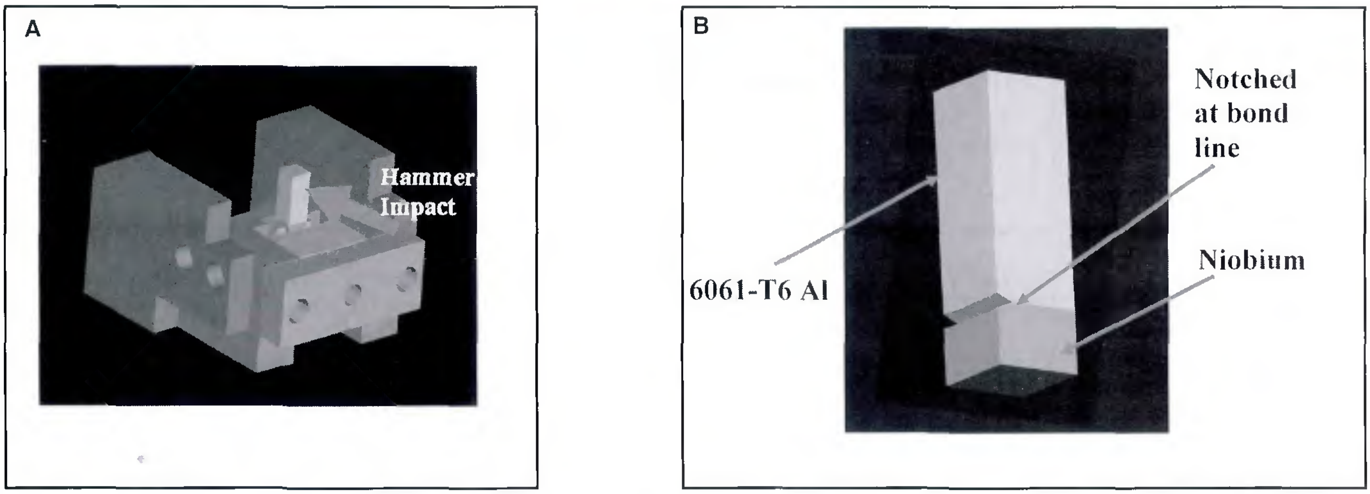

Fig. 8 — Schematic diagrams. A — The Izod impact testing setup used to measure the impact strength of the Al-Nb explosion weld; B — the modified Izod specimen.

Table 3 — Summary of the Base Metal Room-Temperature Mechanical Properties for Niobium and Aluminum Demonstrating Their Differences in Mechanical Properties (Refs. 15–16)

	Youngs' Modulus (GPa)	Poisson's Ratio	Coefficient of Thermal Expansion (K^{-1})	Yield Strength (MPa)	Ultimate Tensile Strength (MPa)
Niobium	104.9	0.397	7.20×10^{-6}	207	585
6061-T6 Al	70.6	0.345	2.36×10^{-5}	280	310
6061-O Al	70.6	0.345	2.36×10^{-5}	48.3	117

ing, the load is then converted to stress by dividing the measured load by the initial annular cross-sectional area at the weld interface. Figure 5 shows typical stress-displacement curves for tensile tests performed on explosively welded samples in both the unnotched and notched configurations. The tensile tests continue until the sample fails, and the tensile strength of each weld is equivalent to the maximum stress measured during each test.

The shear strength of the weld is measured using the testing setup and shear strength sample shown in Fig. 6A and B (Ref. 12). In order to test the shear strength of the weld, a rectangular sample is fabricated from the explosively clad Al-Nb weld material by removing a majority of the niobium-clad layer, leaving only a small nub of niobium measuring 6.35 mm wide. The aluminum portion of the sample is 63.5 mm in length by 12.7 mm in width and 25.4 mm high. When the sample is placed in the fixture, it is supported by this niobium nub, which is located 19.05 mm from the end of the sample and extends across the 12.7 mm width of the sample.

With the niobium nub restrained by the fixture, a compressive force is applied to the top of the sample placing the Al-Nb explosive weld region in shear. The test continues, measuring load vs. sample displacement, until the sample fails. The load-displacement behavior of the shear sample is monitored at a crosshead speed of 0.5 mm/min on the Model 4400R1225 Instron electromechanical test machine. After testing, the load is converted to stress by dividing the measured load by the cross-sectional area at the weld interface, as defined by the weld interfacial area between the aluminum and the niobium nub on the shear specimen. Figure 7 shows a typical stress-strain curve for a shear strength test performed on an explosively welded sample. The resulting shear strength of the weld corresponds to the maximum shear stress measured during this test.

In order to measure the impact strength of the Al-Nb explosive weld, a modified Izod impact testing procedure and sample, which are shown in Fig. 8A and B have been developed (Refs. 13, 14). The holding fixture of the Izod tester has been modified to grasp the undersized niobium-clad layer, which is 8.89 mm thick. The 6061-T651 aluminum portion of the sample is 31.75 mm in length, which allows the hammer to strike the sample in the appropriate location, as defined by the governing standards (Refs. 13, 14). A 45-deg ± 5 deg angled notch with a depth of 2.54 mm ± 0.05 mm is machined into the Izod sample at the Al-Nb weld interface using a slitting saw to minimize potential machining damage.

During testing, the notch is positioned so that it points in the direction of hammer impact, thus placing the weld in tension during testing and subsequent failure of the sample. Different sample sizes, ranging from 3.2 × 12.7 mm to 12.7 ×12.7 mm, are tested. All of the Izod impact tests are performed on a Tinus Olsen Charpy-Izod impact test machine, Model 66, with a maximum capacity of 22.6 J. The resulting fracture surfaces of selected samples have been examined using an FEI Model XL30 S FEG scanning electron microscope in order to identify the prevailing failure modes and mechanisms.

Thermal Cycling of Al-Nb Explosion Welds

A comparison between several pertinent mechanical properties of niobium and 6061 Al is shown in Table 3. (Refs. 15, 16). Since niobium and aluminum have significantly different thermal expansion properties, as shown by the differences in their respective coefficients of thermal expansion (7.20×10^{-6} K^{-1} for niobium and 2.36×10^{-5} K^{-1} for aluminum), thermal

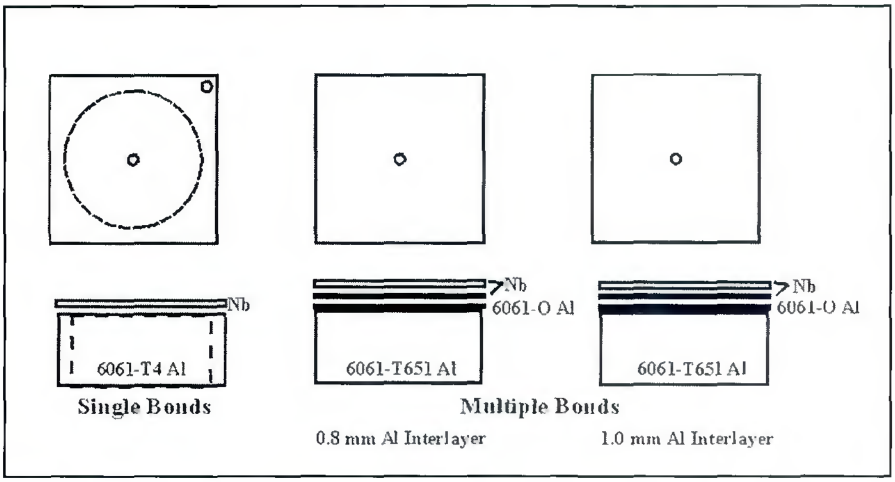

Fig. 9 — Schematic diagram summarizing the evolution of the explosion weld development. The circles on the top view of the explosion weld schematics indicate the locations of the detonators. In the single bonds shown in part A, the dotted lines indicate the circular shape of the Al plate during welding with the detonator placed at the edge of the niobium plate.

stresses can develop across the weld interface with changes in temperature. As a result, residual stresses of a magnitude sufficient enough to affect the long-term weld integrity can build between the Al and Nb. In order to examine the effects of changes in temperature on the explosion weld properties, selected ram tensile and Izod specimens are subjected to a series of ten thermal cycles.

In each thermal cycle, the samples are first placed in a bath heated to a temperature of 49°C. The temperature of the samples is monitored by a thermocouple attached to one of the samples. After the samples are immersed in the bath, the samples are allowed five minutes to reach the desired temperature. At the completion of this time period, the samples are then held in the bath for a period of 15 minutes. After this 15-minute hold is complete, the samples are removed from the bath and immediately placed in a second bath cooled to a temperature of –22°C. The sample temperature is again allowed to equilibrate for five minutes, after which the samples are held in the bath for 15 minutes. This process is repeated until a total of ten hot/cold cycles are completed on each sample. After the completion of the thermal cycling of these samples, the tensile and impact strengths of the welds are then tested in the same manner as those samples in the as-received condition.

Results and Discussion

Development of Multiple-Layer Welds

An explosive charge of 3.1 MJ is originally used to clad the 9.5-mm-thick Nb plate directly to the 203-mm-thick 6061-T4 Al plate in the initial weld development study discussed previously (Ref. 1). With such a large explosive charge, temperatures at the weld interface can become high enough to melt the aluminum, which then reacts with the niobium to form brittle intermetallic phases. Visual confirmation for intermixing of the aluminum and niobium at the weld interface has been previously discussed (Ref. 1). Since the impact strength of the weld produced using these procedures is not acceptable, improvements to the process are required in order to significantly increase the impact strength of the welded material while maintaining the tensile and shear strengths at or near their current levels. In order to achieve this goal, a means for avoiding melting and intermetallic formation during welding must be developed.

Figure 9 provides an overview of the ensuing weld development process undertaken in an attempt to produce explosion welds with the desired mechanical properties. In this figure, the evolution of the welding process from the single weld procedure described previously (Ref. 1) to the ensuing multiple weld procedures is summarized. These multiple welds are produced using a three-step welding process based on the addition of thin sheets or interlayers of aluminum and niobium between the 9.5-mm-thick niobium and the 203-mm-thick aluminum plates. The welding of each thin interlayer requires a smaller explosive charge, thus decreasing the likelihood for melting and intermetallic formation and allowing the explosion welds to be made directly on the 6061-T651 Al plate, thus removing the final heat treating step. A summary of the explosion energies required to join these interlayers is provided in Table 2.

Welds #3a–c utilize a 0.8-mm-thick 6061-O Al sheet, which is welded directly to the 6061-T651 Al plate. Since the Al sheet is in an annealed condition, it is much more ductile than the Al plate, allowing it to be welded with a rather low explosive energy (0.8 to 1.0 MJ). After the

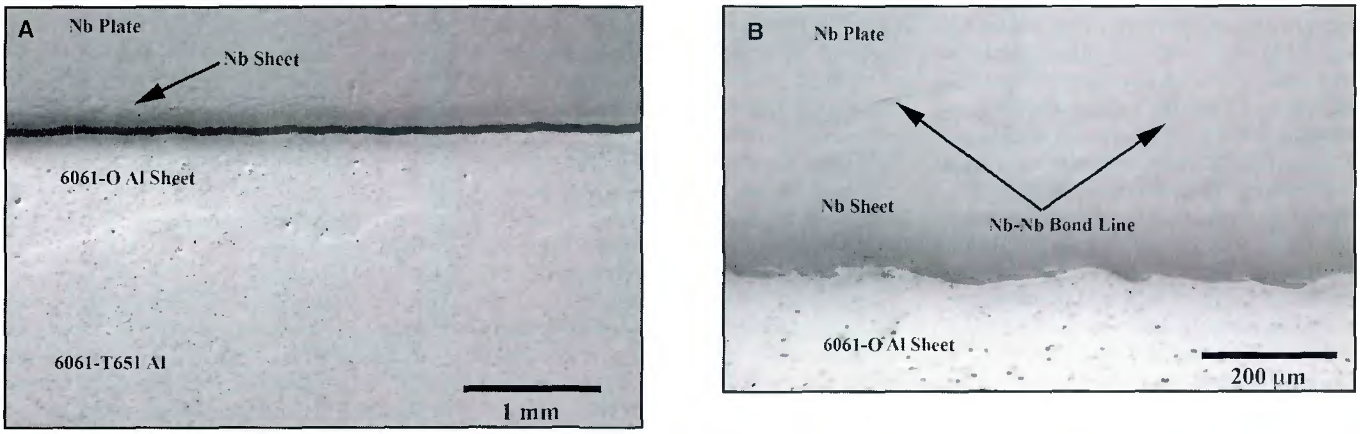

Fig. 10 — Micrographs of the weld cross section taken at an orientation perpendicular to the explosive wave. A — The overall weld, including the Al-Al, Al-Nb, and Nb-Nb weld interfaces. B — a closer view of the Al-Nb and Nb-Nb weld interfaces.

welding of this thin Al interlayer, a 0.25-mm-thick niobium sheet is welded directly on top of it. Since a low explosive energy (0.95 to 1.0 MJ) is used to make this weld, the possibility of intermixing between the Al and Nb is significantly decreased. As a final step, the 9.5-mm-thick niobium plate is welded onto this thin niobium interlayer using a much larger explosive energy (3.08 to 3.76 MJ). By joining the thick niobium plate (9.5 mm) to the thin niobium sheet, the possibility of creating conditions under which any melting can occur is nearly eliminated because the niobium has a high melting point (2468°C).

Figure 10A and B provides views of a typical weld cross section taken at an orientation perpendicular to the explosive wave front in Weld #3a. In Fig. 10A, the entire weld region, including the Al-Al, Al-Nb, and Nb-Nb interfaces, is shown. In this figure, the Al-Nb weld interface appears as a dark line. This feature is a remnant of the metallographic preparation of the sample and results from the difference in the height of the niobium and 6061-T651 Al after polishing, caused by the difference in hardness of the two materials. Each weld interface displays a wavy appearance, which is typical of explosive welds. Of the three weld interfaces shown in this figure, the Al-Al interface displays the most prevalent wavy weld interface appearance. The Al-Nb weld interface, which is highlighted in Fig. 10B, is also much wavier in appearance than that observed with the single-layer welds. There is also no visual evidence of melting, intermetallic formation, or a mixed zone along the Al-Nb interface, which is an improvement over the weld interface observed in the previous work (Ref. 1).

Results from the tensile and shear strength testing for Welds #3a–c are summarized in Table 4. Taking an average of the results from these three welds, average tensile strengths of 243 ± 20 MPa and 231 ± 25 MPa are observed for the unnotched and notched conditions, respectively. The tensile strengths of the multiple welds in both the unnotched and notched conditions are approximately 9% and 20%, respectively, lower than those observed in the single-welded plates. In addition, failure in the ram tensile specimens in the multiple welds (Welds #3a–c) occurs within the thin Al interlayer, as compared with the Al-Nb weld interface in the single welds (Welds #1 and #2).

Welds #3a–c also display lower shear strength values (112 ± 22 MPa) than those observed in the edge- and center-detonated plates (224 ± 7 MPa and 180 ± 5 MPa, respectively). Results of the shear strength testing of these welds are also summarized in Table 4. This decrease in measured shear strength is due, in part, to the addition of the interlayers between the aluminum and niobium plates. In the sin-

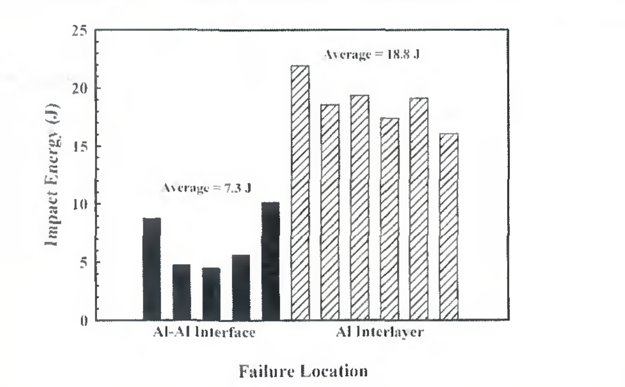

Fig. 11 — Summary of measured impact strengths for the multiple weld plate made using parameters #3a, showing the effects of differences in failure location on the measured impact strength.

Table 4 — Summary of Tensile and Shear Strengths Measured in Each Al-Nb Explosion Weld

Welding Parameter Identification	Number of Tests	Tensile Strength (MPa) Unnotched Average	Unnotched Standard Deviation	Notched Average	Notched Standard Deviation	Shear Strength (MPa) Number of Tests	Average	Standard Deviation
0.8-mm Al Interlayer								
3a	3/3	264	9	246	26	3	88	39
3b	3/1	225	8	202	—	3	128	5
3c	3/3	240	52	244	52	3	12	1
1.0-mm Al Interlayer								
4a	3/—	251	21	—	—	3	127	2
4b	6/6	255	13	284	25	—	—	—

Table 5 — Summary of Impact Strengths Measured in Each Al-Nb Explosion Weld

Welding Parameter Identification	Number of Tests	Impact Energy (J) Average	Impact Energy (J) Standard Deviation	Impact Energy/Unit Area (J/mm^2) Average	Impact Energy/Unit Area (J/mm^2) Standard Deviation
0.8-mm Al Interlayer					
3a[(a)]	11	6.8/19.2	2.6/1.7	0.052/0.148	0.020/0.013
3b	10	16.8	3.6	0.130	0.028
3c[(a)]	10	9.2/13.3	0.8/1.0	0.071/0.103	0.006/0.008
1.0-mm Al Interlayer					
4a	3	21.2	2.6	0.164	0.020
4b	19	19.2	3.5	0.148	0.027

(a) Two distinct failure modes (Al-Al interface and Al interlayer) are observed.

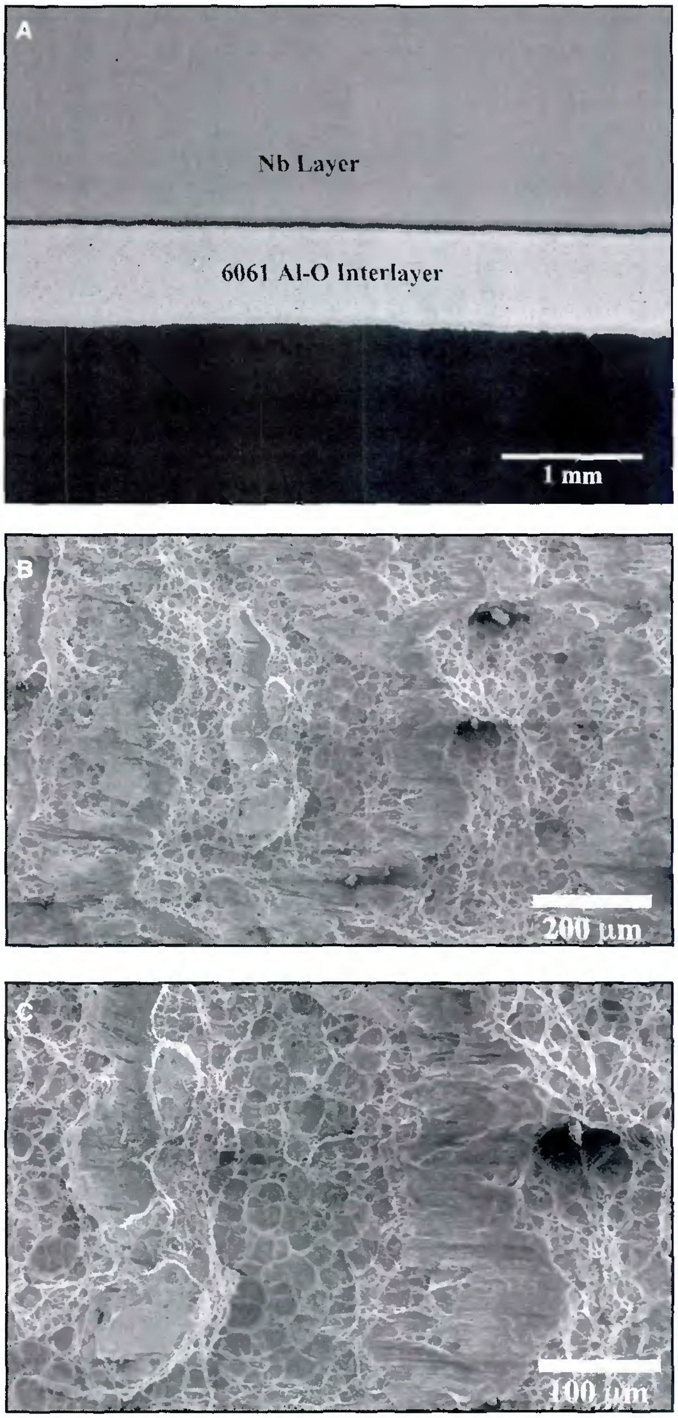

Fig. 12 — Micrographs. A — Showing the cross section; B and C — fracture surface of an Izod impact sample, which fails at the Al-Al weld interface.

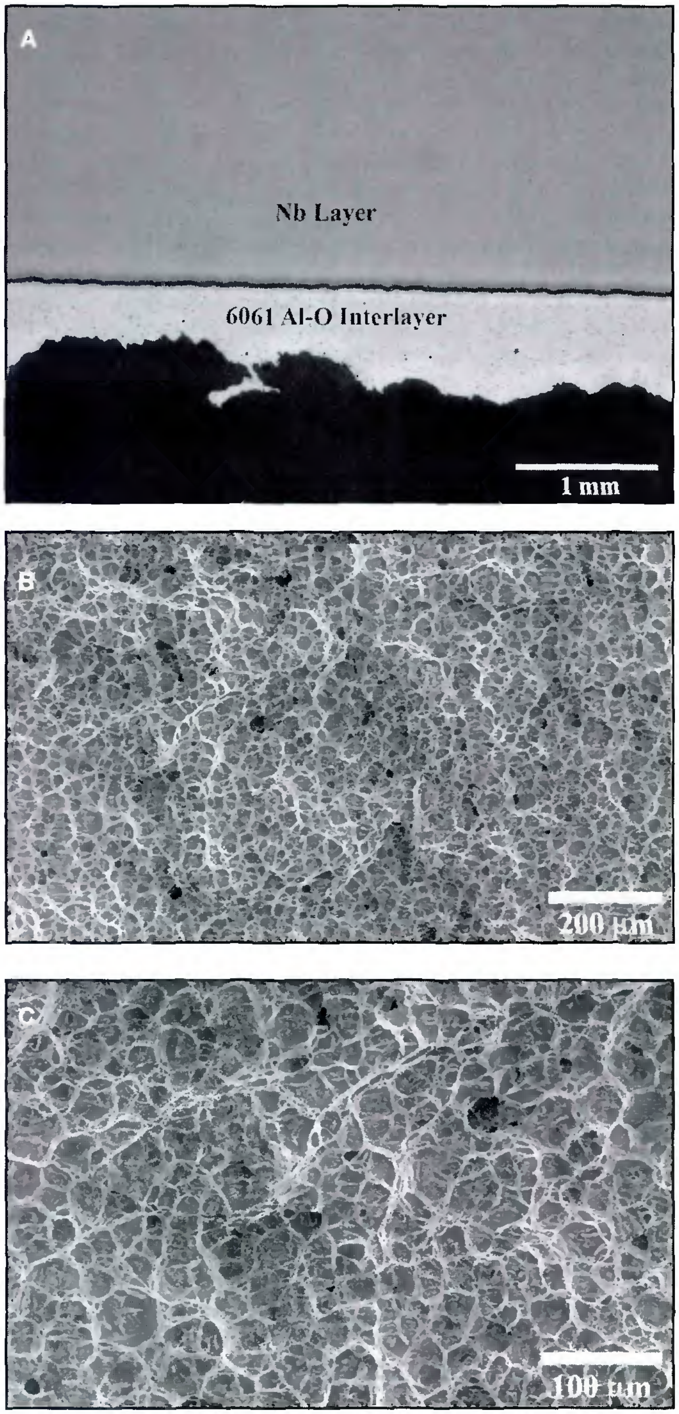

Fig. 13 — Micrographs. A — Showing the cross section; B and C — fracture surface of an Izod impact sample, which fails in the Al interlayer.

gle-weld plates, a distinct failure surface at the Al-Nb interface is observed in the shear strength samples after testing. The multiple welds display no such clear failure mode. Rather, during testing, the thin Al interlayer yields, causing the explosively clad niobium layer on the shear strength sample to only be displaced and not be removed from the Al plate during testing.

Even though the tensile and shear strengths are lower than those observed in Welds #1 and #2, this decrease in weld strength is not a concern because the tensile and shear strengths are still acceptable. Most importantly, though, these multiple welds display significant enhancements in the measured impact strength when compared with the edge- and center-detonated plates. As shown in Table 5, the impact strength of the multiple weld plates increases to a level of 19 J (0.147 J/mm^2), which is much higher than that observed in the single weld plates (0.020 J/mm^2). Based on these results, it is clear that the use of a 0.8-mm-thick Al interlayer in the explosion welding process has dramatically increased the impact strength of the Al-Nb weld, while maintaining desirable levels of tensile and shear strength. However, there is a rather wide range of impact strength values observed in the welds produced using the 0.8-mm-thick Al interlayer. In Weld #3a, in particular, a bimodal distribution in impact strengths, as shown in Fig. 11, is observed. The average values of the two lev-

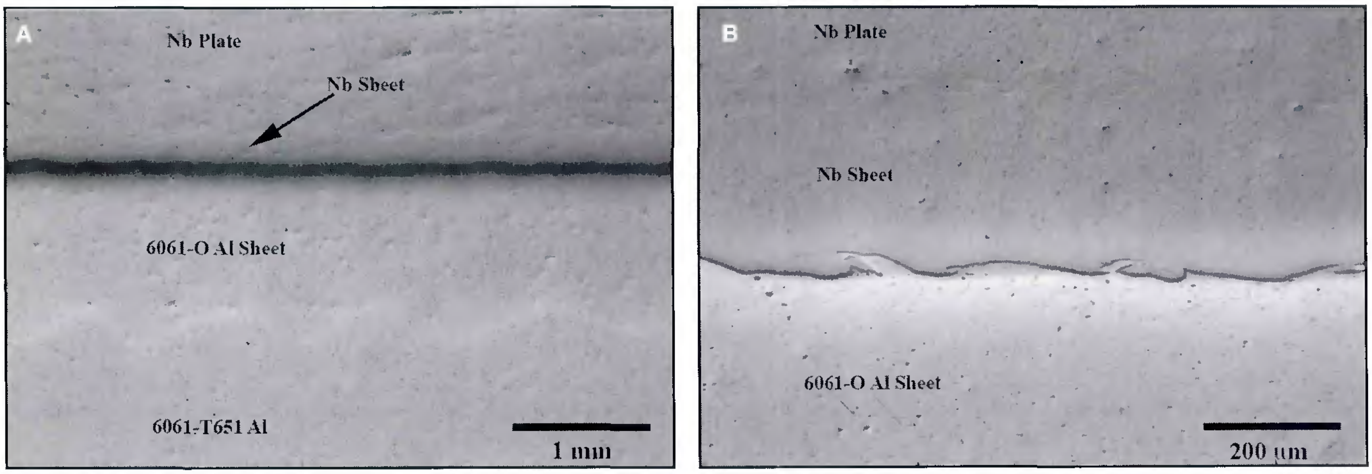

Fig. 14 — Micrographs. A — Showing the entire weld cross section; B — the Al-Nb and Nb-Nb welds taken at an orientation perpendicular to the explosive wave front for a multiple weld plate with a 1.0-mm Al interlayer.

Table 6 — Summary of Tensile and Impact Strengths Measured in Thermal Cycled Samples

		Tensile Strength (MPa)				Impact Strength (J)		
Welding Parameter Identification	Number of Tests	Unnotched Average	Unnotched Standard Deviation	Notched Average	Notched Standard Deviation	Number of Tests	Average	Standard Deviation
0.8mm Al Interlayer								
3a[(a)]	4/4	175	50	256	65	9	4.3	1.6
1.0mm Al Interlayer								
4a[(b)]	3/—	243	17	—	—	3	17.3	8.4
4b[(b)]	13/6	267	28	277	38	19	19.4	2.9

(a) Izod impact samples display failure at the Al-Al interface.
(b) Izod impact samples display failures within the Al interlayer.

els vary by nearly a factor of three (0.052 and 0.148 J/mm^2).

The bimodal distribution of impact strengths, which appears in Fig. 11, is attributed to the presence of two distinct failure modes. In the first failure mode, which results in low weld impact strength, the weld failure occurs very close to the Al-Al weld interface. Figure 12A–C displays the cross section and fracture surface of an Izod impact sample with low impact strength taken from Weld #3a. In this figure, the Al-Nb weld interface appears as a single dark line, as a result of the differences in the heights of the aluminum and niobium in the as-polished specimen, resulting from the metallographic preparation. It is apparent in the cross section shown in Fig. 12A that the 0.8-mm Al interlayer remains nearly intact, and the resulting fracture surface is generally flat. Figure 12B and C shows images of the same fracture surface at different magnifications. In this figure, the fracture surface displays a mixed mode fracture appearance with areas exhibiting both brittle and ductile fracture modes present.

In the second failure mode, which is observed in the welds with the higher impact strength, failure occurs within the 6061-O Al interlayer. As shown in the cross-section view in Fig. 13A, the region of failure displays a tortuous morphology across the width of the Al interlayer. Micrographs of the fracture surface, shown in Fig. 13B and C, display a dimpled morphology, indicative of a ductile fracture mode. No regions indicative of brittle fracture are observed, and the dimpled morphology covers the entire fracture surface. This failure mechanism is desirable.

A closer examination of the cross sections of the two fracture surfaces in Figs. 12A and 13A provides evidence that the explosion welding pattern is playing a role in the formation of these two distinct failure mechanisms. In Fig. 13A, it appears that the tortuous fracture surface morphology correlates with the wavy weld pattern observed in the weld cross section in Fig. 10A. On the other hand, the failure mechanism shown in Fig. 12A for the low-impact strength sample indicates that the explosion welding pattern at this location in the welded plate does not develop the clearly defined waves observed in Fig. 10A. These differences in failure mechanism can thus be correlated with corresponding differences in weld morphology.

The formation of the characteristic wavy weld interface morphology in explosion welds is known to be controlled by the flyer plate collision velocity (Ref. 17). In order for this preferred weld interface morphology to form, the interface kinetics governing the welding of the two plates must be controlled by a turbulent flow mechanism. Sufficient collision velocities are required in order for this mechanism to dominate and for the preferred weld line morphology to be formed. If the collision velocity becomes excessive, the turbulence can become extreme, leading to very large waves, which can result in a mixing and melting of the constituent metals at the wave crests and troughs, and the formation of either voids or brittle zones, resulting in a decrease in strength. This condition dominates in Welds #1 and #2, where evidence for melting at the Al-Nb weld interface is observed. On the other hand, at collision velocities below the threshold value where turbulent flow dominates, the resulting interface kinetics is controlled by laminar flow. When laminar flow dominates, the resulting weld interface morphology is devoid of the wave patterns characteristic of turbulent flow.

In the case of Weld #3a, it can be assumed that the collision velocity, driven by the explosive energy, is in a transition region, where both laminar and turbulent flows are present. As a result, both flat and wavy weld interface morphologies are observed. The presence of this nonuniform welding pattern across the surface of the

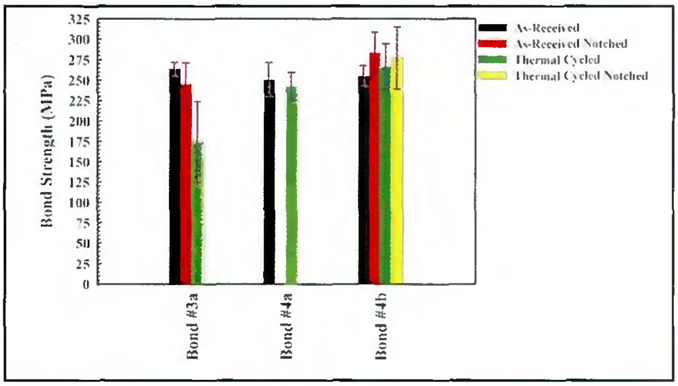

Fig. 15 — Comparison between measured tensile strengths in the as-received and thermal cycled multiple welded plates.

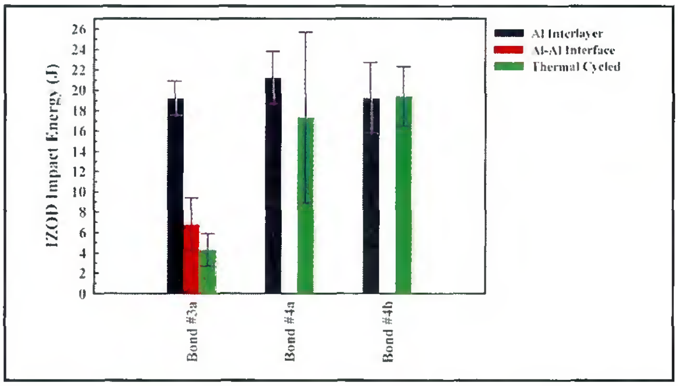

Fig. 16 — Comparison between measured Izod impact strengths in the as-received and thermal cycled multiple welded plates.

welded plate also creates a large degree of uncertainty in the weld strength and subsequent performance. Therefore, changes in the explosive energies used to weld the thin Al interlayer to the thick Al plate are made in an attempt to produce more uniform weld properties and to promote the desired failure mechanism within the Al interlayer during impact testing.

There is an optimization point at which the turbulent flow is sufficient to produce a wavy weld interface morphology without the appearance of either a flattened weld interface morphology or intermixed regions resulting from excessive turbulent flow. By increasing the explosive energy, a collision velocity can be attained where the entire welded area consists of a wavy interface. Table 2 shows that Weld #3b uses a higher explosive energy to weld the 6061-O Al sheet to the 6061-T651 Al plate than Welds #3a and #3c. With this higher explosive energy, the collision velocity is now of a sufficient magnitude to produce turbulent flow across the entire weld interface. As a result, the bimodal distribution of impact strengths and multiple failure modes are not observed in this weld.

On the other hand, Weld #3b does not contain an adequate region of acceptable welding, thus prohibiting the use of these welding parameters. The increase in explosive energy required to achieve the wavy interface when using the 0.8-mm 6061-O sheet in Weld #3b not only decreases the amount of well-welded material but also leaves a roughened top surface on the thin aluminum sheet. Because of the small thickness of the Al sheet (0.8 mm), the associated surface roughness nearly reaches the depth of the explosion wave pattern through the thickness of the sheet. Changes to the welding procedures are therefore required in order to produce welds with the desired wave pattern weld interface morphology and resulting high impact strength levels.

In order to use higher explosive energies to weld the 6061-O Al interlayer to the 6061-T651 Al plate, a thicker Al interlayer is used. The combination of the thicker Al interlayer and the increased explosive energy is expected to produce a stronger weld between the 6061-O and 6061-T651 Al and allow for an enhanced amount of acceptable welding area across the surface of the plate. Welds #4a and #4b, as summarized in Table 2, utilize a 1.0-mm-thick Al interlayer, allowing an explosive energy, on the order of nearly 50% higher than those used in Welds #3a through #3c, to be used for both the Al-Al and Al-Nb welds.

Figure 14A shows a micrograph of the weld cross section at an orientation perpendicular to the explosion wave front taken from Weld #4a, which utilizes the 1.0-mm-thick Al interlayer and higher explosion welding energies. When compared with the weld formed using a thinner Al interlayer, which is shown in Fig. 10A and B, the increased thickness of the Al interlayer is apparent, as is the desired wavy weld pattern. In Fig. 14B, the Al-Nb and Nb-Nb welds are shown at a higher magnification. Both welds display the desired wavy weld pattern, and the Al-Nb weld shows no evidence of a mixed region or intermetallic formation.

The use of a 1-mm-thick 6061-O Al interlayer does not adversely affect either the tensile or shear strength of the weld, as summarized in Table 4. In general, the tensile and shear strengths are equivalent to those observed in the welds that use the 0.8-mm-thick Al interlayer. During the testing of the impact strengths of these welds, as summarized in Table 5, the welds with the thicker Al interlayer display a significantly higher impact energy, approaching 21 J for a 12.7 × 10.2 mm cross-sectional area in Weld #4a, than the welds formed with the thinner Al interlay. This impact energy corresponds to a value for the impact energy per unit area of 0.119 J/mm^2. In addition, only a single failure mode, occurring in the Al interlayer, is observed in all of the tests. The resulting fracture surfaces exhibit only features that indicate a ductile fracture mode, similar to that shown in Fig. 13C.

Even though the results of the mechanical testing of Weld #4a are a significant improvement over those observed in Welds #3a–c, additional changes are made to the welding procedures. These changes are primarily related to how the Al and Nb sheets and Nb plate are fixtured during the explosion welding process in order to achieve more uniform welding properties across the surface of the Al-Nb clad plate. They are also meant to minimize any potential plate-to-plate variations in the properties of the Al-Nb explosion welds during the manufacture of many clad plates. With these changes in place, the tensile and impact strengths of Weld #4b are similar to those observed in Weld #4a.

In summary, the development of an explosion welding process for joining a 9.5-mm-thick Nb plate to a 203-mm-thick 6061-T651 Al plate has been successful in producing welds with high tensile and impact strengths. In this process, thin 6061-O Al and Nb sheets have been utilized to produce a weld having a tensile strength (255 ± 13 MPa) approximately 80% of the 6061-T6 Al base metal ultimate tensile strength (312 MPa). The impact strength of the welds produced using this process (19.2 ± 3.5 J or 0.148 ± 0.0027 J/mm^2) exceed the impact strength of the 6061-T6 Al base metal (9.8 ± 0.5J or 0.076 ± 0.004 J/mm^2) by nearly a factor of two. The explosive energies and fixturing of the individual layers during the welding process have also been optimized to maximize the area of acceptable welding across the surface of the 203 × 203 mm 6061-T651 Al plate.

Effects of Thermal Cycling on Weld Properties

Thermal cycling tests have been performed in order to determine if the mechanical properties of the welds are affected by exposures to extremes of temperature. Notched and unnotched ram tensile and Izod impact samples taken from multiple welds with both 0.8- and 1.0-mm-thick Al interlayers have been tested. Table 6 provides a summary of the tensile and impact strength measurements made on samples exposed to the thermal cycling sequence described above. Tests have been performed on samples taken from Weld #3a, which has a 0.8-mm- thick Al interlayer, and Welds #4a and #4b, which both have a 1.0-mm-thick Al interlayer. In general, the welds made with the thicker Al interlayer display significantly higher tensile and impact strengths after thermal cycling than the weld with the thinner Al interlayer.

Comparisons of these results with those obtained from the testing of similar samples in the as-received condition are given in Figs. 15 and 16, respectively, for the tensile and impact strengths of the welds. In the case of the thinner Al interlayer, there is an evident decrease in the tensile (175.3 ± 49.5 MPa) and impact energy per unit area (0.027 J/mm^2) after thermal cycling, with the most prominent decrease occurring in the impact strength. This decrease in impact strength can be traced to the appearance of only a single failure mode at the Al-Al interface for all of the samples tested in the thermal cycled condition.

On the other hand, the welds made using a thicker Al interlayer (1.0 mm) display no such decrease in impact strength after thermal cycling. In both of the welds tested with the thicker Al interlayer, the tensile and impact strengths measured after thermal cycling basically match those measured in the as-received condition. In fact, Weld #4b shows the highest mechanical property values of all of the welds tested. Failure in each weld is observed within the Al interlayer, with the resulting fracture surfaces showing evidence of ductile failure, similar to that observed in the as-received samples.

Weld #4b displays unnotched and notched tensile strengths of 267 ± 28 MPa and 277 ± 38 MPa, respectively, in the thermal cycled condition. Both values fall within 6% of the as-received values. The measured impact strength for the thermal cycled samples taken from Weld #4b is 19.4 ± 2.9 J (0.150 ± 0.22 J/mm^2). This value varies from that measured in the as-received condition by only 1%. Based on these results, it is thus apparent that the explosive welds produced with the 1.0-mm-thick Al interlayer are unaffected by the thermal cycling.

Summary and Conclusions

An explosion welding procedure was developed to clad 9.5-mm-thick niobium plate to 203-mm-thick 6061-T651 Al plate using a three-step procedure. This weld consists of three separate explosively clad layers: a 1.0-mm-thick 6061-O Al sheet, a 0.33-mm-thick Nb sheet, and a 9.5-mm-thick Nb plate. The introduction of the thin 6061-O Al and niobium sheets allows the 9.5-mm-thick niobium plate to be welded to the Al plate in the high-strength (T-651) condition, thus removing the need for a postwelding heat treatment required in earlier welds. Metallographic examination of the multiple weld region also shows no evidence of melting or intermetallic formation.

In the final welding process, the detonator is located in center of plate, and different explosive energies are used to make the three welds. For the weld between the 6061-O Al sheet and the 6061-T651 Al-plate, an explosive energy of 1.37 MJ is used. An explosive energy of 1.54 MJ is used to weld the Nb sheet to the 6061-O Al sheet, and an explosive energy of 3.08 MJ is used to weld the thick Nb plate to the thin Nb sheet. The resulting weld displays a tensile strength of approximately 255 ± 13 MPa in the unnotched and 284 ± 25 MPa in the notched condition. These values are approximately 80% of the ultimate tensile strength of the 6061-T6 Al. The impact strength of the welds, which is 19.2 J ± 3.5 J (0.148 ± 0.027 J/mm^2) is also three times that of the high-strength aluminum.

Selected tensile and impact strength samples were also exposed to accelerated thermal cycling treatments between –22° and 45°C to determine if the significant differences in the coefficients of thermal expansion for the niobium and aluminum cause the weld to be weakened over time. After being exposed to these extremes of temperature, the tensile and impact strength samples were tested and compared with results from as-welded samples. These thermally cycled samples showed no degradation in mechanical properties when compared with the as-received material. For example, the unnotched tensile strength of the thermal cycled samples is 267 ± 28 MPa, the notched tensile strength is 277 ± 38 MPa, and the impact strength is 19.4 ± 2.9 J (0.150 ± 0.22 J/mm^2). In each case, the differences between the tensile and impact strengths of the as-welded and thermally cycled welds are insignificant.

Acknowledgments

This work has been performed under the auspices of the U.S. Department of Energy, by the University of California, Lawrence Livermore National Laboratory under Contract No. W-7405-ENG-48. Additional thanks go to Dennis Freeman for his extensive support during the mechanical testing, Edwin Sedillo (LLNL) for providing the scanning electron microscopy support, Robert Vallier (LLNL) and Jackson Go (LLNL) for their metallography support, Robert Huber (LLNL), Trung Le (LLNL), and Paul Souza for their ultrasonic evaluation support, and Mark Gauthier (LLNL) for material handling and movement.

References

1. Elmer, J. W., Terrill P., Brasher, D., and Butler, D. 2002. Joining depleted uranium to high-strength aluminum using an explosively clad niobium interlayer. *Welding Journal* 81(8): 167-s to 173-s.

2. Juvinall, R. C. 1967. *Engineering Considerations of Stress, Strain, and Strength.* New York, N.Y.: McGraw Hill.

3. *Welding Handbook*, Vol. 2, Welding Processes. 1991. Miami, Fla.: American Welding Society.

4. ASM *Metals Handbook* Vol. 6: Welding Brazing, and Soldering. 1993. Materials Park, Ohio, ASM International.

5. Massalski, T. B. 1990. *Binary Alloy Phase Diagrams*, Vol. 3, 2nd ed. Materials Park, Ohio: ASM International.

6. ASTM B209M-02a, *Standard Specification for Aluminum and Aluminum-Alloy Sheet and Plate* (Metric).

7. AMS-QQ-250/11, *Aluminum Alloy 6061, Plate and Sheet.*

8. ASTM B393-03, *Standard Specification for Niobium Alloy Strip, Sheet, and Plate.*

9. ASTM A578M-96, *Standard Specification for Straight Beam Ultrasonic Examination of Plain and Clad Steel Plates for Special Applications.*

10. ASTM E214-01, *Standard Practice for Immersed Ultrasonic Examination by the Reflection Method Using Pulsed Longitudinal Waves.*

11. ASTM E1001-99a, *Standard Practice for Detection and Evaluation of Discontinuities by the Immersed Pulse-Echo Ultrasonic Method Using Longitudinal Waves.*

12. ASTM B898-99, *Standard Specification for Reactive and Refractory Metal Clad Plate.*

13. ASTM D256-02, *Standard Test Methods for Determining the Izod Pendulum Impact Resistance of Plastics.*

14. ASTM D4812-99, *Standard Test Method for Unnotched Cantilever Beam Impact Resistance of Plastics.*

15. Brandes, E. A. ed. 1992. *Smithells Metals Reference Book*, 7th Edition. London, Butterworth and Heinemann.

16. *Metals Handbook*, 1990. Vol. 2, Properties and selection: Nonferrous alloys and special-purpose materials, 10th Ed. Materials Park, Ohio: ASM International.

17. Cowan G. R., Bergman O. R., and Holtzman A. H. 1971. Mechanism of weld zone formation in explosion clad metals. *Metallurgical Transactions.* 2 (11): 3145–3155.

Effect of Defects on Fatigue Strength of GTAW Repaired Cast Aluminum Alloy

Fatigue test data were analyzed to determine the relationship between defects and fatigue performance of weld repaired aluminum castings

BY L. LI, Z. LIU, AND M. SNOW

ABSTRACT. The effect of porosity on the fatigue life of weld repaired D357 aluminum cast alloy was investigated. Investment cast D357 aluminum alloy was repaired with gas tungsten arc (GTA) welding using a matching filler metal. The repaired alloy underwent a postweld heat treatment involving solutioning and artificial aging. The number of cycles to failure of the welded specimens showed a much wider distribution band than those of the as-cast specimens. Crack-like shrinkage porosity was identified to be the predominant factor leading to the inconsistent fatigue strength of the welded specimens. The relationship between defects in the fusion zone and fatigue failure cycles was statistically analyzed. Crack-like shrinkage porosity in the welds was found to have the most significant effect in decreasing the fatigue life of the welded specimens. Spherical pores also contributed to decreasing the fatigue life of welded specimens, although not as significant as the crack-like pores.

Introduction

Welding repair is occasionally a necessary process in fabrication of cast aluminum structures. Properly repaired aluminum castings may have equivalent static strength, ductility, fracture toughness, and fatigue strength levels as the as-cast structures. For cast structures designed to be used for aerospace applications, fatigue property is a critical performance parameter. Past experience and published literature on this issue indicate that casting defects (cracking, porosity, inclusions) and microstructure (coarse second phases) decrease the fatigue strength of aluminum castings (Refs. 1–4). Welding and weld repair may introduce further complications due to not only additional metallurgical defects, but also geometric discontinuity and residual stresses (Refs. 5, 6). Some researchers advised against repair welding (Ref. 7), citing the possibility of additional residual stresses and defects. Some researchers suggest a tighter control of defect sizes. For instance, Nordmark et al. (Ref. 5) suggested that incomplete fusion and porosity in the repair welds did not lower the fatigue strength if the defects were smaller than a certain size. While ways to avoid weld cracking and porosity defects have been actively investigated (Refs. 8–10), remedial methods to increase the weld fatigue strength are widely used. Shot peening and heat treating (Ref. 11) have been used to increase the fatigue properties of welded aluminum joints.

The causes for the degraded fatigue property in an industrial setting can be many and complicated, ranging from base materials composition, melting and casting procedures, heat treatment, weld repair procedures, and quality control process. This study reports an attempt to analyze and interpret more than 200 sets of fatigue testing data, gathered over two years from as-cast and weld repaired D357 alloy, in order to find out the relationship between defects and the fatigue performance of weld-repaired D357 aluminum castings.

L. LI is an assistant professor in the Department of Mechanical and Aerospace Engineering at Utah State University, Logan, Utah. Z. LIU is a visiting researcher from Zhengzhou University, China. M. SNOW is a metallurgical engineer with GSC Foundries Inc., Ogden, Utah.

KEYWORDS

Aluminum Casting
Weld Fatigue
Repair Weld
Weld Defects

Experimental Procedure

Specimens for fatigue tests were prepared as part of the actual investment casting of D357 aluminum alloy, as specified by the aerospace material specification AMS 4249, with the nominal composition (in wt-%) of Si 6.50–7.50, Mg 0.55–0.60, Ti 0.10–0.20, Be 0.04–0.07, Fe 0–0.12, Mn 0–0.10, Al balance. The fatigue specimens were cut from the castings and underwent a simulated repair welding. The welding was done with the manual gas tungsten arc (GTA) spot welding process, for simulating the repair of casting defects during the actual production. The welding filler metal, 1.575-mm- (0.062-in.-) diameter R-357 specified by AWS A5.10-99, was of the same nominal composition of the casting alloy except that the welding filler metal did not contain Be. The welding current was 22 A for the spot welding on the 3.175-mm (⅛- in.-) thick specimens, with the current ratio of direct current electrode negative (DCEN) to direct current electrode positive (DCEP) set to 5.9:1, with a frequency of variable polarity of 50 Hz. A gas mixture of 24% Ar, 76% He was used for the arc and pure (99.998%) Ar was used for back shielding. A total of 150 s of welding was conducted on a spot. Approximately 110 s of welding was conducted on the front side of the sample. The sample was flipped over, and about 40 s of welding was conducted on the backside of the sample. Following welding, the welded area was ground flush with the base metal. Heat treating for both the as-cast specimens and weld-repaired specimens involved a 549°C (1020°F) solution treatment (72 h with Glycol quench) followed by 171°C (340°F) aging (5.5 h with air cooling).

The geometry and dimensions of the fatigue specimen were designed according to ASTM E 466 with a 2.54-mm- (0.1-in.-) diameter though-hole machined at the center of the weld spot that was located at the center of the specimen — Fig. 1. The

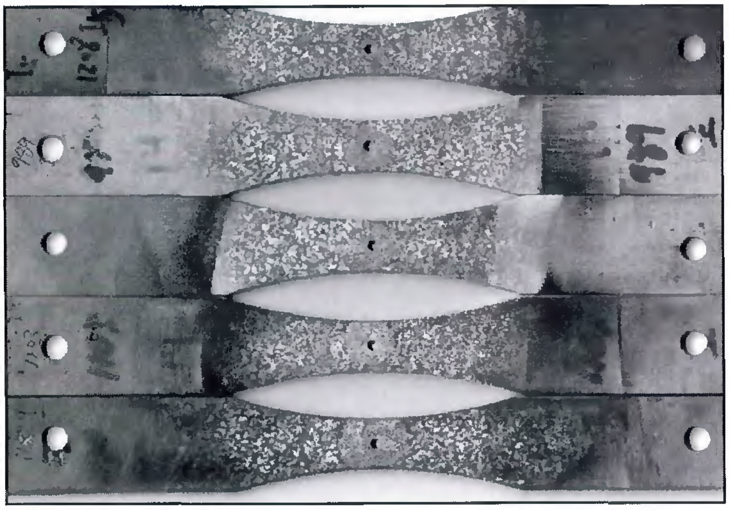

Fig. 1 — Fatigue test specimens of GTA welding repaired D357 alloy. A stress-concentration hole is located at the center of the weld. Specimens were etched after fatigue testing to show the location of welds and the grain size.

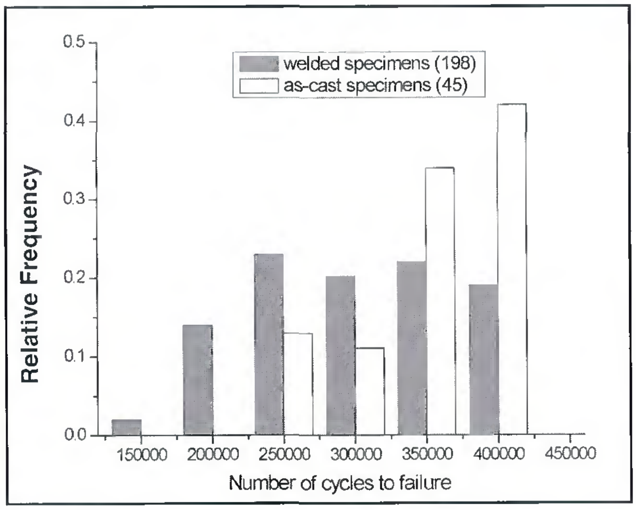

Fig. 2 — Distribution of fatigue failure cycles for 198 repair-welded specimens and 45 as-cast specimens.

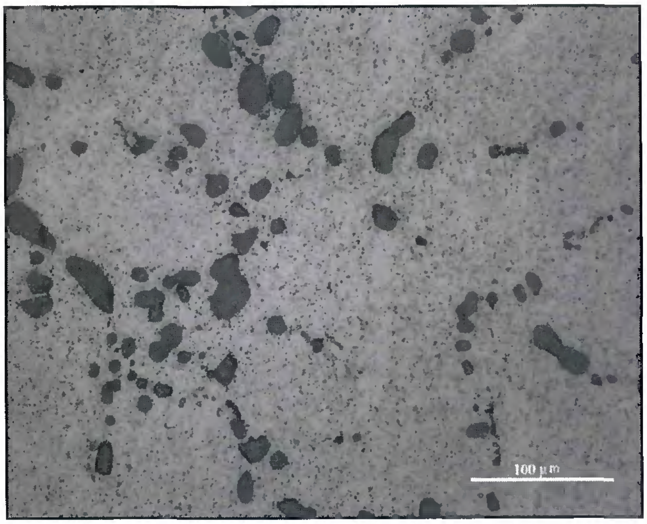

Fig. 3 — Microstructure of the base material following solutioning and aging.

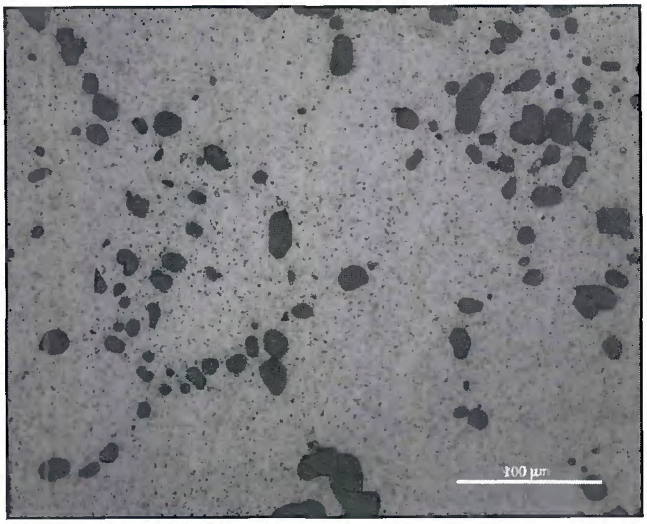

Fig. 4 — Microstructure of the fusion zone following solutioning and aging.

specimen has a thickness of 3.175 mm (⅛ in.), with either the as invest-cast surface finish for the cast specimens, or the ground surface finish for the weld-repaired specimens. The fatigue testing was conducted in accordance with ASTM E 466 at a loading frequency of 15 Hz. The maximum stress was 103.4 MPa (15 ksi) at a stress ratio of 0.1 and stress concentration factor of 2.5. The average fatigue life was recorded. The fatigue tests were stopped at 400,000 cycles if the specimens had not failed. A total of 198 weld-repaired specimens and 45 as-cast specimens were tested in this study.

All fatigue-tested specimens were analyzed with a stereographic binocular microscope. The macroscopic observation provided information on bulk behavior of the specimens, including the existence of defects, degree of plastic deformation, origin of the fatigue crack and propagation path. Digital images were taken and recorded for further analysis. Following the macroscopic analysis, specimens were mounted in the longitudinal orientation of fatigue-tested specimens, and prepared for microscopic observation. The microstructure was recorded using the PaX-IT™ digital imaging system mounted on a Zeiss metallurgical microscope. The mounted and fractured specimens were observed under a Hitachi scanning electron microscope. The quantitative analysis of porosity in the welds was conducted on samples in the as-polished condition (without etching). For microstructure observation, the specimens were etched with 2% HF in water. Digital images of the entire weld area of each sample were captured under the microscope at 350× magnification. An image-processing software was used to measure the size, shape, and area fraction of the porosity. Statistical methods were used to process the measured data.

Results

Fatigue failure cycles of weld-repaired and as-cast specimens in the heat-treated condition are shown in Fig. 2. The weld-repaired specimens exhibited a much wider distribution of fatigue cycles than

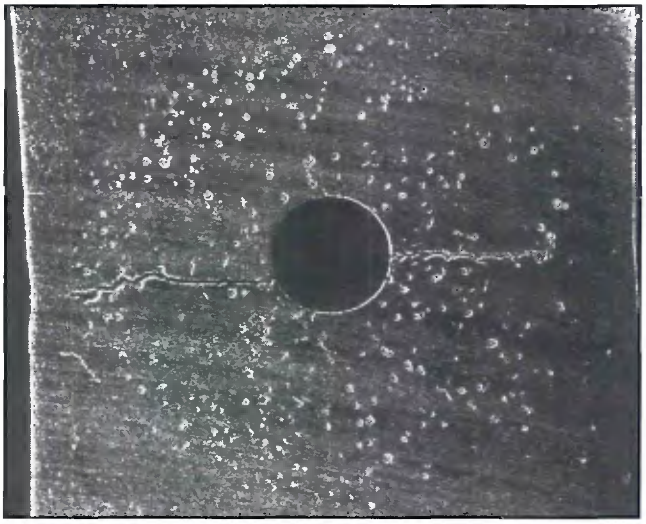

Fig. 5 — The as-polished surface of a typical sample with low fatigue cycle. Shrinkage porosity is observed in the weld zone.

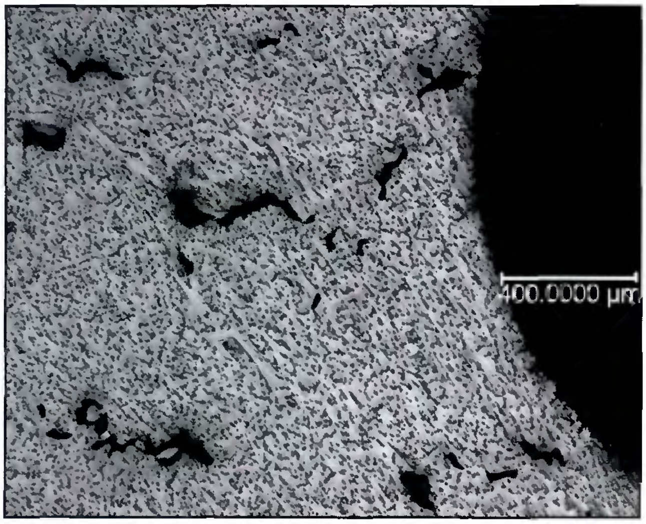

Fig. 6 — Crack-like shrinkage porosity with the length/width ratio of 0.1397/0.0396 near the weld center, where the stress-concentration hole (right of the photomicrograph) is located.

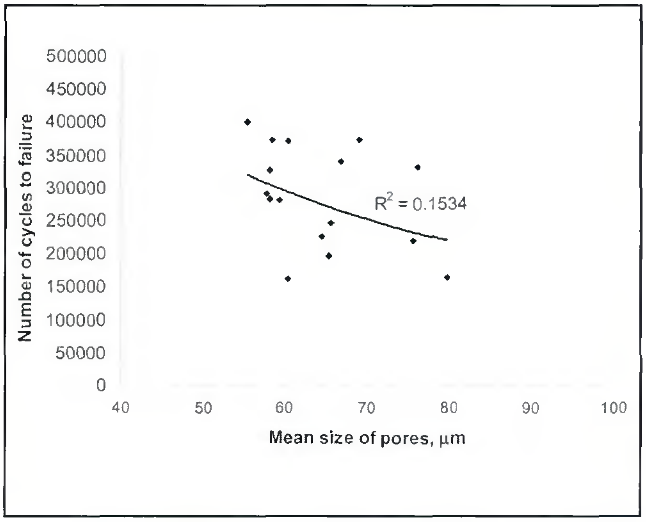

Fig. 7 — Fatigue failure cycles as a function of mean size of pores in welds.

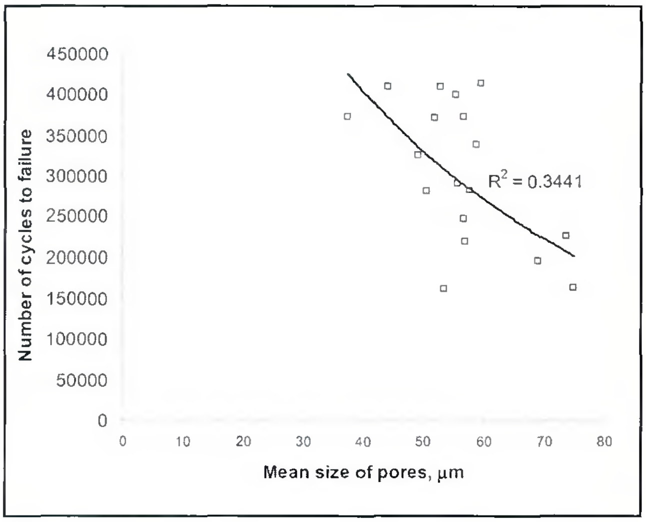

Fig. 8 — Fatigue failure cycles as a function of mean size of pores in the 0.5-mm-thick ring-shaped region around the stress-concentration hole.

the as-cast specimens. About 20% of the welded specimens had achieved 400,000 fatigue cycles, and there were about 20% of the welded specimens to have less than 200,000 fatigue cycles. The remaining welded specimens were approximately evenly distributed between 250,000 and 350,000 fatigue cycles. In comparison, all of the as-cast specimens had fatigue failure cycles greater than 250,000, and about 45% of the as-cast specimens had fatigue cycles no less than 400,000.

The microstructure of the base material following solutioning and aging is shown in Fig. 3. The rounded, dark gray, Si particles are distributed along the grain boundaries, while smaller precipitates are dispersed intragranularly upon the aging treatment. The microstructure of weld-repaired specimens, shown in Fig. 4, is almost the same as the cast specimens, except the grain size for the weld is smaller. Specimens with high fatigue failure cycles generally had some common features, including the fine-grain-sized microstructure in the weld fusion zone, the shape of the grains was nearly equiaxed following heat treatment; and, most importantly, there were no significant crack-like porosity defects.

Specimens with low-fatigue failure cycles invariably contained different levels of defects. The predominant defect was porosity in the weld fusion zone, as shown in Fig. 5 for a severe case. The fatigue fracture originated from the stress-concentration hole at the center of the weld, propagated in both directions perpendicular to the longitudinal axis (the fatigue loading direction) of the sample. Some specimens fractured completely and some specimens fractured partially, in which case the fatigue cracking was constrained within the weld fusion zone, i.e., the cracking was arrested at the weld boundary. Crack-like voids were generally found near the center of the weld (Fig. 6), while the spherical pores tend to be distributed over the entire weld.

Measurements of spherical porosity and crack-like porosity from the fatigue-tested samples confirmed quantitatively the above observations. These measurements are presented here in the order of

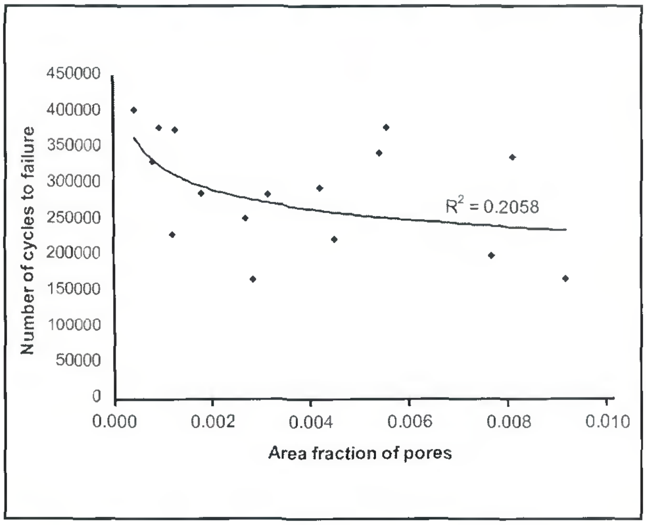

Fig. 9 — Fatigue failure cycles as a function of the area fraction of pores in welds.

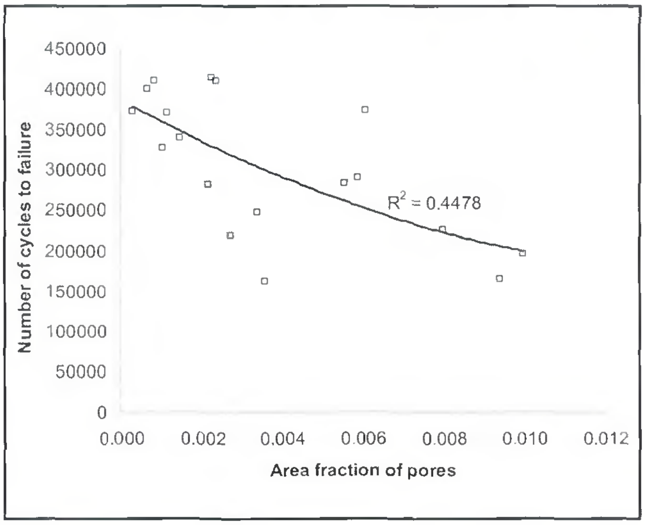

Fig. 10 — Fatigue failure cycles as a function of the area fraction of pores in the 0.5-mm-thick ring-shaped region around the stress-concentration hole.

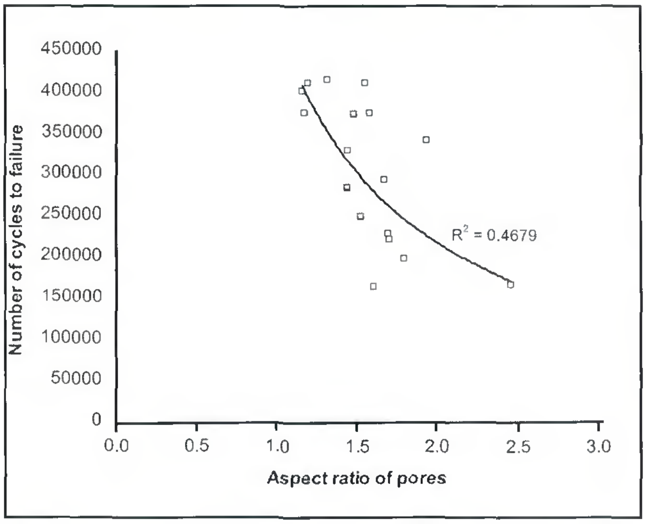

Fig. 11 — Fatigue failure cycles as a function of the aspect ratio of pores in the 0.5-mm-thick ring-shaped region around the stress-concentration hole.

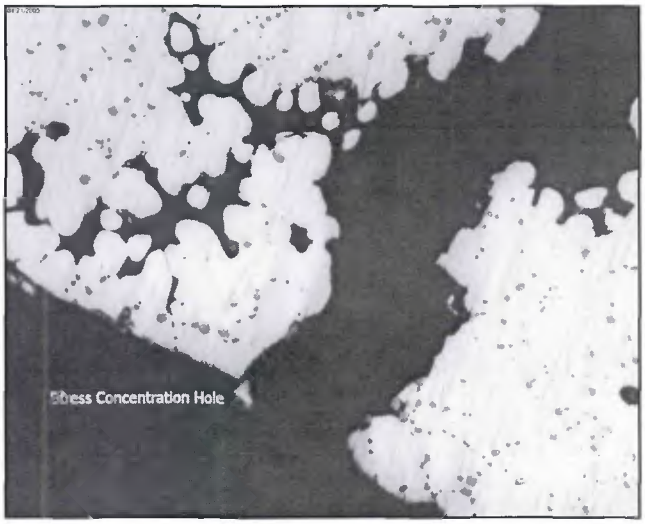

Fig. 12 — The role of crack-like shrinkage porosity in fatigue cracking initiation and propagation. The stress-concentration hole is shown at the lower left of the micrograph.

mean size, total amount, and shape (aspect ratio of length to width) of the porosity defects. The distinction between the spherical and crack-like pores was represented by the shape (aspect ratio). It was observed that the variation from spherical pores to microcracks was almost continuous, making it difficult to clearly define a microcrack. Therefore, for the statistical analysis, the term "pores" is used to include both the spherical and crack-like pores.

Figure 7 shows the fatigue failure cycles as influenced by the mean size of pores in the welded specimens. With much scatter, a weak correlation (R^2 = 0.153) was observed between the fatigue failure cycles and the mean size of pores. The general trend was that the greater the mean size of pores, the lower the fatigue cycles. It was believed that pores that were distributed near the region where the fatigue crack initiated should have more significant effects on the fatigue life (Ref. 2). When the pores that were distributed within a ring of 500 μm around the stress-concentration hole were counted, the mean size indicated a more obvious correlation (R^2 = 0.344) with the failure cycles — Fig. 8. The increased correlation confirmed the more significant effect of pores at the fatigue initiation sites. For the samples with lower fatigue cycles, the mean size of pores was up to about 75 μm; for the samples with higher fatigue cycles, the mean size of pores was within a 40 to 60 μm range.

The total amount of porosity in terms of the area fraction of pores, defined as ratio of the area of pores to the area of weld, was plotted against fatigue failure cycles — Fig. 9. The scatter of data was still significant, with the correlation factor R^2 = 0.206 between the area fraction of pores and the fatigue cycles. It seems the total amount of porosity in welds had a similar, but more pronounced effect on fatigue cycles than the mean size of pores in

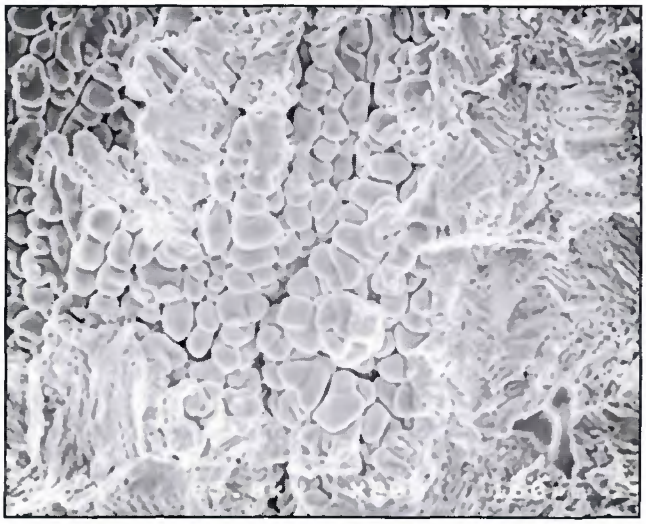

Fig. 13 — Fracture surface of a crack-like shrinkage porosity, showing dendrite surfaces.

Fig. 14 — Fractography of a porosity-containing, fatigue-tested specimen.

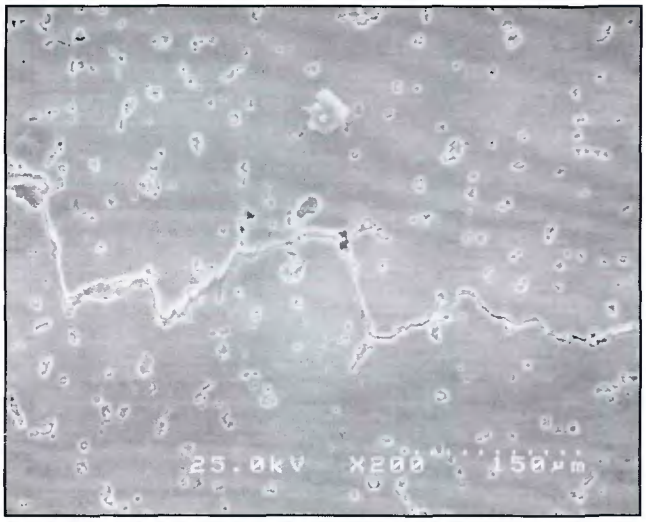

Fig. 15 — Fatigue crack propagation along the grain/interdendritic boundaries in the weld fusion zone. The Si-rich particles are distributed at the grain/interdendritic boundaries.

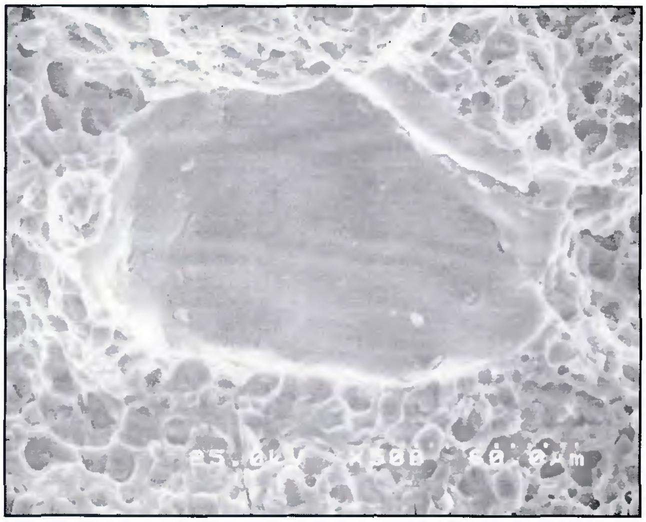

Fig. 16 — Magnified region A in Fig. 14. The fracture mechanism appears to be microvoid coalescence (dimples) along the grain/interdendritic boundaries.

welds. When the pores that were distributed within a ring of 500 μm around the stress-concentration hole were counted, the amount of porosity showed a more definite correlation (R^2 = 0.448) to the number of cycles to failure — Fig. 10. For the samples with 400,000 failure cycles, the area faction of porosity was lower than 0.001. For the samples with failure cycles lower than 200,000, the area fraction of porosity was higher than 0.008.

The shapes of porosity defects ranged from spherical pores to elongated shrinkage cavities and cracks. To describe the shape of these porous defects, the average aspect ratio of length to width was measured from the tested specimens. The plot of fatigue cycles against the aspect ratio for the pores that were distributed within a ring of 500 μm around the stress-concentration hole showed a clear trend: the higher the aspect ratio (or the more "crack-like" for the pore shape), the lower the fatigue cycles. Specimens with high fatigue cycles generally contained pores that were more spherical, with the aspect ratio less than 1.5 — Fig. 11.

All the above statistical data seemed to indicate that the amount and shape of the porosity near the stress-concentration hole had a greater effect on the failure cycles than the porosity distributed in other areas of the weld. This observation confirmed the role of defects close to the surface on decreasing the fatigue life, as observed in other studies (Refs. 2, 12). Among the parameters that describe the porosity defects, the aspect ratio seemed to have the highest degree of correlation to fatigue life, indicating the crack-like defects to be more potent in decreasing the fatigue life. The amount of porosity, measured by fraction of porosity area, seemed to have the second-highest degree of correlation with fatigue life. The average size of the porosity seemed to have the least degree of correlation to fatigue life. Apparently, the probability for a porosity to

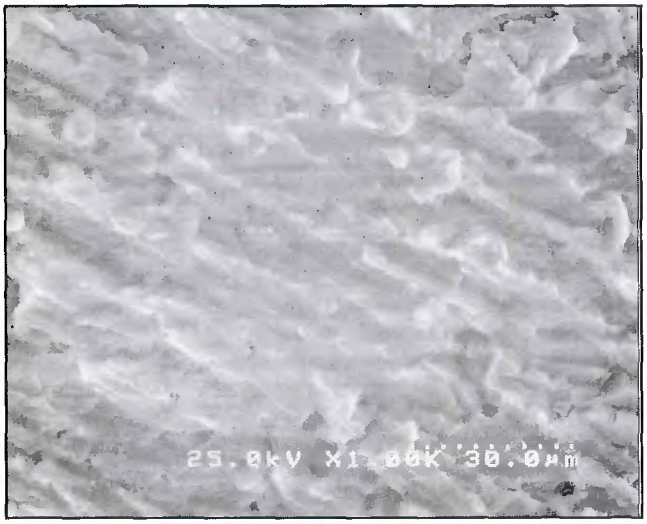

Fig. 17 — Magnified region B in Fig. 14. Fatigue striations are clearly seen.

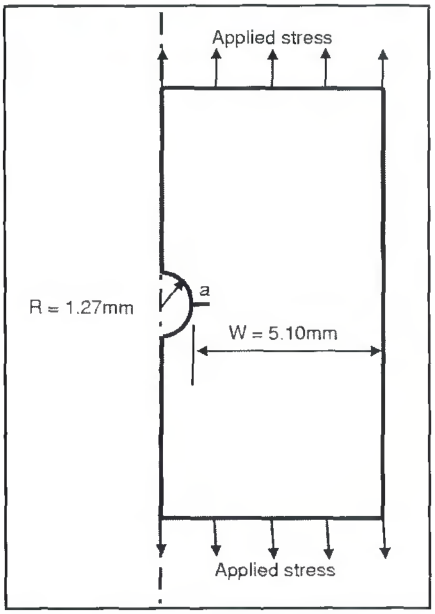

Fig. 18 — The model for stress intensity factor calculations. Due to symmetry, only half of the fatigue specimen is considered in this model.

be right at the crack initiation site was mainly determined by the amount of porosity.

Discussion

The existence of crack-like porosity exposed to the stress-concentration hole, which was located near the center of the weld, might have provided the initiation sites for the fatigue failure. An example of such accelerated formation of fatigue fracture is shown in Fig. 12. Welded specimens that showed the lowest fatigue cycles almost always contained a significant amount of crack-like porosity. The fracture surface of a typical crack-like pore is shown in Fig. 13. Dendritic features and shrinkage cavities indicated a typical solidification hot cracking mechanism for the formation of the crack-like porosity. Having a crack-like geometry, and a minute crack tip radius, these pores effectively acted as preformed fatigue cracks. Consequently, there was an absence of crack nucleation period, explaining the premature fatigue failure for the specimens containing crack-like porosity.

Porosity defects in the repair welds also accelerated the fatigue crack propagation. An example is shown in Fig. 14, in which the fatigue crack is seen to have propagated through the pores as a low-resistance path. The fatigue crack propagated intergranularly along the grain/interdendritic boundaries that are delineated by silicon particles — Fig. 15. The propagation connected the pores and bypassed or cut through the silicon particles, which were dispersed in the interdendritic boundaries. The fracture surfaces revealed micromechanisms for the fatigue failure. The separation was mostly through the "dimple" or micro microvoid coalescence along the grain/interdendritic boundaries — Fig. 16. Because of the existence of defects, the specimens did not fail by typical fatigue failure mechanism, but rather by a fast fracture mechanism. In areas that are free of defects, small regions created by a typical fatigue failure mechanism could be seen. In Fig. 17, the fatigue striations and transgranular propagation path are clearly visible. It seems the fatigue specimens tested in this study involved a mixed fracture mechanism: fast fracture around defects and fatigue striations in pockets of defect-free regions.

Fatigue crack growth rate has been characterized in fracture mechanics as a function of the stress intensity factor. Depending on the stress intensity factor range (ΔK), the growth rate (da/dN) measured by the crack extension (da) per fatigue cycle (dN) can be 1) no growth, if ΔK is less than a threshold value for propagation ΔK_{th}, 2) Region I growth, if ΔK is greater than ΔK_{th}, 3) Region II (steady state) growth, and 4) Region III (fast) growth, if ΔK is greater than the fracture toughness K_{IC}. The Paris-Erdogen power law for the Region II fatigue crack propagation has been used by many researchers to estimate the entire fatigue life (Refs. 2, 4, 12). However, to account for Region I fatigue crack propagation, the equation proposed by Klesnil can be used (Ref. 13)

$$N_f = \int_{a_i}^{a_f} \frac{da}{C\left(\Delta K^m - \Delta K_{th}^m\right)} \quad (1)$$

where N_f represents fatigue life, C and m are material constants, ΔK is the stress-intensity factor range, ΔK_{th} is the threshold stress intensity factor range, and a_i and a_f are the initial and final crack lengths, respectively. The value of a_f is dependent on the fracture toughness of the material; a_i is dependent on the crack-initiating spherical or crack-like pores.

Since the present study deals with fatigue testing of specimens with preexisting defects, the stress intensity factor range ΔK may be higher than the threshold ΔK_{th}. Therefore, the fatigue propagation in the present study may have bypassed the Region I and directly entered the Region II (or steady-state) growth. While this study is not aimed at fatigue crack growth rate (da/dN), a discussion of the effect of defect size on ΔK will help understand the role of defects on fatigue life.

The stress intensity factor K_I for the defect-containing fatigue specimens was estimated for both types of pores that were exposed to the surface of the stress-concentration hole. For the specimen with multiple defects, the fatigue crack always starts from a defect that is located close to the region of maximum stress concentration and propagates along the horizontal diameter of the hole, and be perpendicular to the loading direction — Fig. 5. A model for such crack propagation is given in Fig. 18. Since the material had significant ductility, the stress intensity factor had been corrected for crack-tip plasticity using the second-order estimate. The plasticity-corrected effective stress intensity factor K_{eff} was calculated according to the following (Ref. 14):

$$K_{eff} = Y\left(a_{eff}\right)\sigma\sqrt{\pi a_{eff}} \quad (2)$$

where $Y(a_{eff})$ was a geometrical parameter defined as

$$Y\left(a_{eff}\right) = \sqrt{\frac{W}{\pi a}} \frac{\sqrt{2\tan\frac{\pi a}{2W}}}{\cos\frac{\pi a}{2W}} \left[0.752 + 2.02\left(\frac{a}{W}\right) + 0.37\left(1-\sin\frac{\pi a}{2W}\right)^3 \right] \quad (3)$$

in which the effective crack length was $a_{eff} = a + r_y$, and the plastic zone size was estimated by

$$r_y = \frac{1}{\pi}\left(\frac{K_I}{\sigma_{YS}}\right)^2 \quad (4)$$

The peak load during fatigue tests was 108 MPa, the measured yield strength (σ_{YS}) of the material was 290 MPa, plate width (W) was 5.1 mm, crack length (a) for the average crack-like porosity was 0.4 mm, crack length (a) for the average pore depth was 0.05 mm. These values were put into the above equations and K_{eff} values were iteratively solved. The calculated maximum K_{eff} for the specimen with 0.05-mm pore exposed to the surface was 4.37 $MPa\sqrt{m}$; the calculated maximum K_{eff} for the specimen with 0.4-mm crack-like pores exposed to the surface was 12.79 $MPa\sqrt{m}$. The observed crack-like pores were estimated to produce a stress intensity factor value at about three times of that for the case of the pores. The threshold for fatigue crack propagation for cast aluminum Alloy 357 is not available, but the threshold ΔK_{th} for Alloy 356, which is similar to Alloy 357 in the present study, has been calculated by Yi et al. (Ref. 2). Their estimated threshold ΔK_{th} value is 6.1 $MPa\sqrt{m}$. From this, it can be suggested that a specimen with spherical pores would have a ΔK lower than the critical value for crack propagation; a specimen containing crack-like defects, however, would have a ΔK greater than the critical value for crack propagation. This analysis is qualitatively supported by the fatigue data reported in Figs. 7-11. Although this discussion only considered the peak load condition and the worst location and orientation of the defects, it did provide a quantitative insight into the relative effects of the shape and size of pores on fatigue crack initiation and propagation.

Conclusions

The major factors that decreased fatigue life for the welded specimens were the existence of welding defects. Crack-like shrinkage porosity in the welds had the most significant effect in decreasing the fatigue life of the welded specimens. Spherical pores also contributed to decreasing the fatigue life of welded specimens, although not as significant as the crack-like pores. Fatigue cracking propagated intergranularly in the welded sample, connecting the pores along its path. With increasing effects on fatigue life were mean size, area fraction, and aspect ratio of pores. Defects located near the fatigue initiation sites were more effective in decreasing the fatigue cycles. To improve fatigue cycles, elimination of crack-like defects (those with greater aspect ratios) was suggested to be more effective than decreasing the total amount of porosity, which in turn to be more effective than decreasing the average size of pores.

References

1. Evans, W. J., Lu, Z.-J., Spittle, J. A., and Devlukia, J. 1997. Fatigue crack development from defects in a cast aluminum alloy. *Proceedings of the High Cycle Fatigue of Structural Materials*, p. 445–457, TMS Fall Meeting.

2. Yi, J. Z., Gao, Y. X., Lee, P. D., Flower, H. M., and Lindley, T. C. 2003. Scatter in fatigue life due to effects of porosity in cast A356-T6 aluminum-silicon alloys. *Metallurgical and Materials Transactions* A 34(9): 1879–1890.

3. Byczynski, G. E. 2004. A study of crack initiation sites in high cycle fatigue of 319 aluminum alloy castings. JOM 56(11): 188.

4. Skallerud, B., Iveland, T., and Harkegard, G. 1993. Fatigue life assessment of aluminum alloys with casting defects. *Engineering Fracture Mechanics* 44(6): 857–874.

5. Nordmark, G. E., Herbein, W. C., Dickerson, P. B., and Montemarano, T. W. 1987. Effect of weld discontinuities on fatigue of aluminum butt joints. *Welding Journal* 66(6): 162-s to 173-s.

6. El-Soudani, S. M., and Pelloux, R. M. 1975. Anisotropy of fatigue crack propagation in aluminum alloy butt welded joints. *Welding Journal* 54(5): 144-s to 152-s.

7. Shankar, K., and Wu, W. 2002. Effect of welding and weld repair on crack propagation behaviour in aluminium alloy 5083 plates. *Materials and Design* 23(2): 201–208.

8. Matsuda, F., Nakata, K., Shimokusu, Y., Tsukamoto, K., and Arai, K. 1983. Effect of additional element on weld solidification crack susceptibility of Al-Zn-Mg alloy (report 1) Results of ring casting cracking test. *Transactions of JWRI* (Japanese Welding Research Institute) 12(1): 81–87.

9. Kearney, A. L. 1974. Avoiding cracks in weld repair of aluminum. *Foundry* 102(4): 65–67.

10. Ghosh, P. K., and Ghosh, A. K. 2004. Control of residual stresses affecting fatigue life of pulsed current gas metal-arc weld of high-strength aluminum alloy. *Metallurgical and Materials Transactions* A 35A(8): 2439–2444.

11. Bertini, L., Fontanari, V., and Straffelini, G. 1998. Influence of postweld treatments on the fatigue behavior of Al-alloy welded joints. *International Journal of Fatigue* 20(10): 749–755.

12. Wang, Q. G., Apelian, D., and Lados, D. A. 2001. Fatigue behavior of A356-T6 aluminum cast alloys. Part I. Effect of casting defects. *Journal of Light Metals* 1(1): 73–84.

13. Klesnil, M., and Lukas, P. 1972. Influence of strength and stress history on growth and stabilization of fatigue cracks. *Engineering Fracture Mechanics, Vol.* 4, pp. 77–92.

14. Anderson, T. L. 2005. *Fracture Mechanics — Fundamentals and Applications*, 3rd Edition, p. 52, Taylor & Francis.

se these convenient, postage-aid inquiry cards to request ee information about the roducts or services dvertised in this issue of *Velding Journal.*

or information about specific dvertisements: Circle the ey number on the card that natches the number on the ottom of the ad.

FREE INFORMATION • FREE INFORMATION

For faster processing, please FAX this card to (630) 739-9700. Type or print the information and copy before faxing. This fax number is for the service bureau only, not AWS.

Please send literature on items circled at right:

November 2006 — Card void after May 1, 2007

Name ____________ Title ____________

Company ____________

Address ____________

City ____________ State ________ Zip ________

Phone: ____________ Fax: ____________

E-mail ____________

Please circle an entry for each category:

I. TYPE OF BUSINESS
1. Construction
2. Primary Metal Products
3. Fabricated Metal Products
4. Transportation
5. Petrochemical
6. Misc. Repair Services
7. Educational Services
8. Utilities
9. Other

II. JOB FUNCTION/TITLE
1. Corp. Management
2. Plant Mgmt.
3. Engineer
4. Welding or Cutting Oper.
5. Quality Control
6. Sales
7. Purchasing
8. Education
9. Other

III. PURCHASING AUTHORITY
1. Recommend
2. Specify
3. Approve

IV. NUMBER OF EMPLOYEES
1. Under
2. 50 to 99
3. 100 to 499
4. 500 to 999
5. 1000 to 2499
6. 2500 to more

V. ANNUAL DOLLAR VOLUME
1. Under $1 Million
2. $1 Million to 5 Million
3. Over $5 Million

VI. THIS INQUIRY IS FOR
1. Immediate Purchase
2. Future Project
3. General Information

1	35	69	103	137	171	205	239	273
2	36	70	104	138	172	206	240	274
3	37	71	105	139	173	207	241	275
4	38	72	106	140	174	208	242	276
5	39	73	107	141	175	209	243	277
6	40	74	108	142	176	210	244	278
7	41	75	109	143	177	211	245	279
8	42	76	110	144	178	212	246	280
9	43	77	111	145	179	213	247	281
10	44	78	112	146	180	214	248	282
11	45	79	113	147	181	215	249	283
12	46	80	114	148	182	216	250	284
13	47	81	115	149	183	217	251	285
14	48	82	116	150	184	218	252	286
15	49	83	117	151	185	219	253	287
16	50	84	118	152	186	220	254	288
17	51	85	119	153	187	221	255	289
18	52	86	120	154	188	222	256	290
19	53	87	121	155	189	223	257	291
20	54	88	122	156	190	224	258	292
21	55	89	123	157	191	225	259	293
22	56	90	124	158	192	226	260	294
23	57	91	125	159	193	227	261	295
24	58	92	126	160	194	228	262	296
25	59	93	127	161	195	229	263	297
26	60	94	128	162	196	230	264	298
27	61	95	129	163	197	231	265	299
28	62	96	130	164	198	232	266	300
29	63	97	131	165	199	233	267	301
30	64	98	132	166	200	234	268	302
31	65	99	133	167	201	235	269	303
32	66	100	134	168	202	236	270	304
33	67	101	135	169	203	237	271	
34	68	102	136	170	204	238	272	

Please mail:
- ❏ 305- List of AWS publications
- ❏ 306- Information on AWS Membership

NO POSTAGE NECESSARY IF MAILED IN THE UNITED STATES

BUSINESS REPLY MAIL
FIRST CLASS PERMIT NO. 11992 MIAMI, FL

POSTAGE WILL BE PAID BY ADDRESSEE

WELDING *Journal*

C/O CREATIVE DATA
519 E BRIARCLIFF RD
BOLINGBROOK IL 60440-9882

NO POSTAGE NECESSARY IF MAILED IN THE UNITED STATES

BUSINESS REPLY MAIL
FIRST CLASS PERMIT NO. 11992 MIAMI, FL

POSTAGE WILL BE PAID BY ADDRESSEE

WELDING *Journal*

C/O CREATIVE DATA
519 E BRIARCLIFF RD
BOLINGBROOK IL 60440-9882

Use these convenient, postage-paid inquiry cards to request free information about the products or services advertised in this issue of *Welding Journal*.

For information about specific advertisements: Circle the key number on the card that matches the number on the bottom of the ad.

FREE INFORMATION • FREE INFORMATION

Please send literature on items circled at right:

November 2006 Card void after May 1, 2007

Name ______________________ Title ______________________

Company ______________________

Address ______________________

City ______________________ State __________ Zip __________

Phone: ______________________ Fax: ______________________

E-mail ______________________

Please circle an entry for each category:

I. TYPE OF BUSINESS
1. Construction
2. Primary Metal Products
3. Fabricated Metal Products
4. Transportation
5. Petrochemical
6. Misc. Repair Services
7. Educational Services
8. Utilities
9. Other

II. JOB FUNCTION/TITLE
1. Corp. Management
2. Plant Mgmt.
3. Engineer
4. Welding or Cutting Oper.
5. Quality Control
6. Sales
7. Purchasing
8. Education
9. Other

III. PURCHASING AUTHORITY
1. Recommend
2. Specify
3. Approve

IV. NUMBER OF EMPLOYEES
1. Under
2. 50 to 99
3. 100 to 499
4. 500 to 999
5. 1000 to 2499
6. 2500 to more

V. ANNUAL DOLLAR VOLUME
1. Under $1 Million
2. $1 Million to 5 Million
3. Over $5 Million

VI. THIS INQUIRY IS FOR
1. Immediate Purchase
2. Future Project
3. General Information

1	35	69	103	137	171	205	239	273
2	36	70	104	138	172	206	240	274
3	37	71	105	139	173	207	241	275
4	38	72	106	140	174	208	242	276
5	39	73	107	141	175	209	243	277
6	40	74	108	142	176	210	244	278
7	41	75	109	143	177	211	245	279
8	42	76	110	144	178	212	246	280
9	43	77	111	145	179	213	247	281
10	44	78	112	146	180	214	248	282
11	45	79	113	147	181	215	249	283
12	46	80	114	148	182	216	250	284
13	47	81	115	149	183	217	251	285
14	48	82	116	150	184	218	252	286
15	49	83	117	151	185	219	253	287
16	50	84	118	152	186	220	254	288
17	51	85	119	153	187	221	255	289
18	52	86	120	154	188	222	256	290
19	53	87	121	155	189	223	257	291
20	54	88	122	156	190	224	258	292
21	55	89	123	157	191	225	259	293
22	56	90	124	158	192	226	260	294
23	57	91	125	159	193	227	261	295
24	58	92	126	160	194	228	262	296
25	59	93	127	161	195	229	263	297
26	60	94	128	162	196	230	264	298
27	61	95	129	163	197	231	265	299
28	62	96	130	164	198	232	266	300
29	63	97	131	165	199	233	267	301
30	64	98	132	166	200	234	268	302
31	65	99	133	167	201	235	269	303
32	66	100	134	168	202	236	270	304
33	67	101	135	169	203	237	271	
34	68	102	136	170	204	238	272	

Please mail:
- ❑ 305- List of AWS publications
- ❑ 306- Information on AWS Membership

NOTE:
To speed the processing of your inquiry, please provide ALL the information requested on the card. This will make it easier for the companies to follow up on your request as soon as possible.

WANT TO IMPROVE YOUR ALUMINUM WELDING?

Ask Lincoln How!℠

Lincoln Electric's exclusive **Pulse-On-Pulse®** MIG welding process has what you need when welding aluminum.

- Uniform bead appearance
- Excellent penetration
- Outstanding arc heat control
- Better surface oxide cleaning
- More forgiving operation
- Less operator skill required

Ask the Experts at Lincoln if Pulse-On-Pulse welding can improve your productivity and keep you ahead of the competition.

LINCOLN ELECTRIC NEXTWELD® ℠

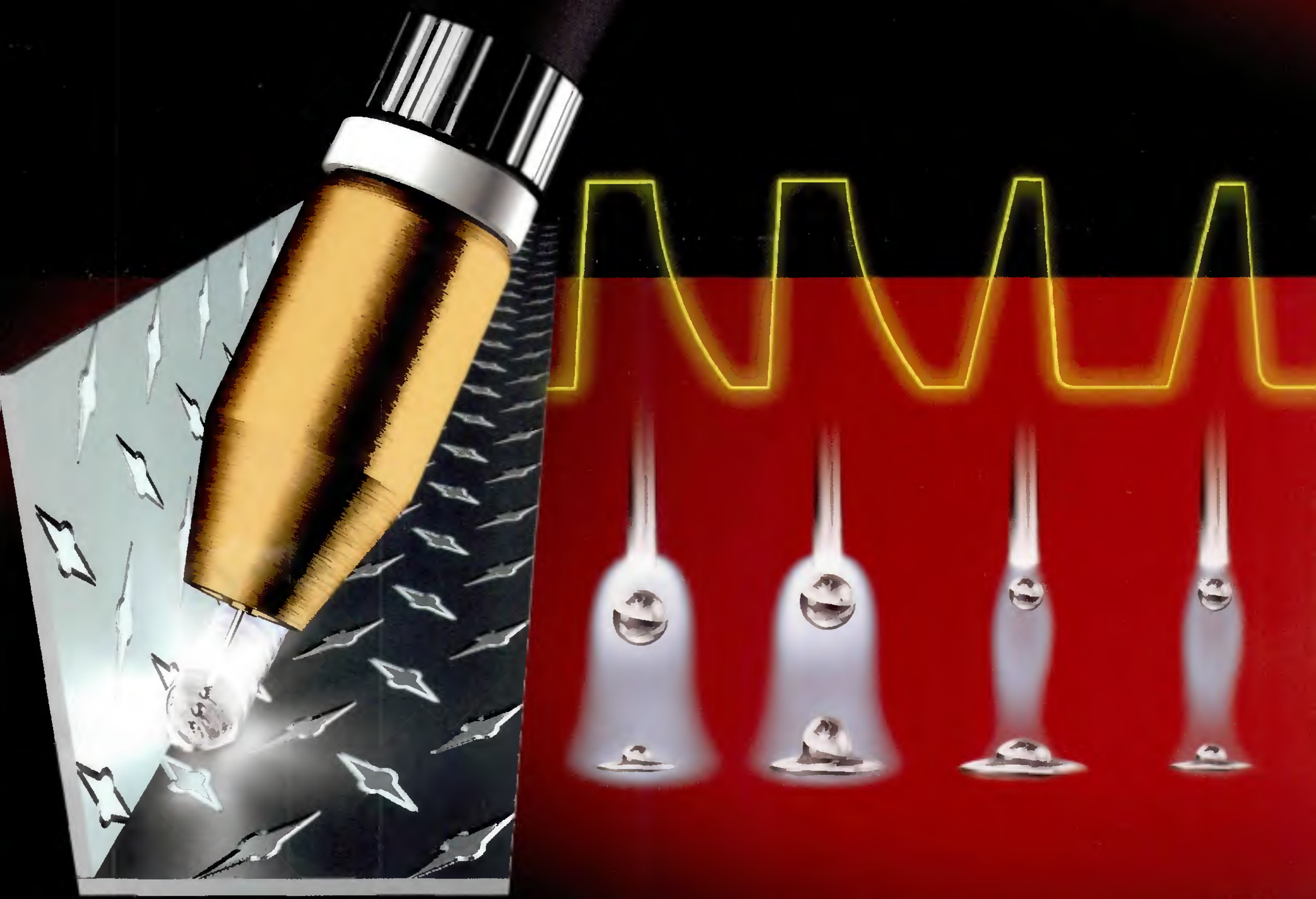

AR05-16

Automation Tech Support Consumables Equipment

Ask Lincoln How!℠

www.lincolnelectric.com/askhow

Circle No. 32 on Reader Info-Card

LINCOLN® ELECTRIC

THE WELDING EXPERTS®